DOE/NASA/0035-1
NASA CR-165226

TRACTION CONTACT PERFORMANCE EVALUATION AT HIGH SPEEDS

Joseph L. Tevaarwerk
Transmission Research Inc.

September 1981

Prepared for
NATIONAL AERONAUTICS AND SPACE ADMINISTRATION
Lewis Research Centre
Under Contract DEN 3-35

for
U.S. DEPARTMENT OF ENERGY
Conservation and Renewable Energy

DOE/NASA/0035-1
NASA CR-165226

TRACTION CONTACT PERFORMANCE EVALUATION AT HIGH SPEEDS

Joseph L. Tevaarwerk
Transmission Research Inc.

September 1981

Prepared for
National Aeronautics and Space Administration
Lewis Research Centre
Cleveland, Ohio 44135
Under Contract DEN 3-35

for
U.S. DEPARTMENT OF ENERGY
Conservation and Renewable Energy
Washington, D.C. 20545
Under Interagency Agreement EC-77-A-31-1011

1. Report No.	2. Government Accession No.	3. Recipient's Catalog No.
NASA CR-165226		

4. Title and Subtitle	5. Report Date
TRACTION CONTACT PERFORMANCE EVALUATION AT HIGH SPEEDS	September, 1981
	6. Performing Organization Code

7. Author(s)	8. Performing Organization Report No.
Dr. J.L. Tevaarwerk, APPLIED TRIBOLOGY LTD. BOX 866, New Hamburg, Ontario, Canada.	
	10. Work Unit No.

9. Performing Organization Name and Address	11. Contract or Grant No.
Transmission Recearch Inc. 10823 Magnolia Dr, Cleveland, Ohio 44106	DEN-3-35
	13. Type of Report and Period Covered
12. Sponsoring Agency Name and Address U.S. Department of Energy Conservation and Renewable Energy Office of Vihicle and Engine R & D	Contractor Report
	14. Sponsoring Agency Code Report No. DOE/NASA/0035-1

15. Supplementary Notes

Interim Report. Prepared under Interagency Agreement EC-77-A-31-1011. Project Manager, D.A. Rohn, Bearing Gearing and Transmission Section, NASA Lewis Research Center, Cleveland, Ohio 44135.

16. Abstract

This report contains the results of traction tests performed on two fluids. These tests covered a pressure range of 1.0 to 2.5 GPa, an inlet temperature range of 30 'C to 70 'C, a speed range of 10 to 80 m/sec, aspect ratios of .5 to 5 and spin from 0 to 2.1%. The test results are presented in the form of two dimensionless parameters, the initial traction slope and the maximum traction peak . With the use of a suitable rheological fluid model the actual traction curves measured can now be reconstituted from the two fluid parameters. More importantly, the knowledge of these parameters, together with the fluid rheological model allow the prediction of traction under conditions of spin, slip and any combination thereof. Comparison between theoretically predicted traction under these conditions and those measured in actual traction tests shows that this method gives good results.

17. Key Words (Suggested by Author(s))	18. Distribution Statement
Traction drives; Traction; Traction fluid; Traction lubricant; Traction drive design; High speed traction; Traction drive performance	Unclassified-unlimited STAR Category 37 DOE Category UC-96

19. Security Classif. (of this report)	20. Security Classif. (of this page)	21. No. of Pages	22. Price*
Unclassified	Unclassified	V + 193pp	

* For sale by the National Technical Information Service, Springfield, Virginia 22161

TABLE OF CONTENTS

LIST OF FIGURES FIG.

SUMMARY

High speed traction tests were performed on two traction fluids, Santotrac 50 and TDF-88, commonly employed. Traction data on these fluids is required for traction drive design optimization techniques. These techniques will allow for the best possible design of a given drive configuration.

To obtain this data, two twin discs traction machines were used. These machines were in existence at the University of Waterloo, Ontario, Canada, and were modified to accommodate the range of test variables. The majority of the data reported was obtained under conditions of side slip, a technique whereby only low power levels are required to simulate real traction drive contacts. The second machine was modified so that it operated under actual traction transfer conditions as encountered on real drives. This was done to investigate the ability of fluid rheological models to predict the actual traction performance of these contacts.

The range of the test variables were; contact pressure from 1 to 1.9 GPa, disc surface velocity from 10 to 80 m/sec, fluid inlet temperature from 30 to 70 'C and contact spin from 0 to 2.1%. The resulting traction curves were reduced to two dimensionless parameters by using the Johnson and Tevaarwerk isothermal traction model. The two dimensionless parameters are the initiall zero spin traction curve slope and the peak traction coefficient. These data were then correlated with regression equations to facilitate their use in design programs and to reduce the invariably present experimental errors.

Also the theoretical traction prediction technques of the Johnson and Tevaarwerk model were tested against data obtained in this investigation. These predictions were based on simple side slip traction curves, longitudinal slip traction curves, side slip with spin traction and combinations of side slip,spin and longitudinal slip. The resulting comparison showed that the theoretical predictions are good provided that thermal effects can be kept to a minimum.

The correlated traction data obtained under this investigation can be used, together with the Johnson and Tevaarwerk model, to give reasonable theoretical traction predictions for the two fluids investigated.

NOMENCLEATURE

a,b	Semi Hertzian contact size in the x and y direction	(m)
A,B	Hertzian shape factor for x and y direction	(-)
Ai	Regression constants	
C	Contact size calculation constant	(m/Pa)
C"	Spin calculation constant	(GPa^{-1})
Ci	Regression constants for traction properties	(-)
e	Curvature offsett from the rolling axis	(mm)
E'	Composite elastic modulus for the disc material	(Pa)
Fx	Contact force in the x direction	(N)
Fy	Contact force in the y direction	(N)
Fz	Normal force on the contact	(N)
G	Local fluid shear modulus	(Pa)
G	Average fluid shear modulus over the contact	(Pa)
h	EHL filmthickness of the fluid in the Hertzian contact	(m)
J2	Dimensionless side slip variable	(-)
J3	Dimensionless spin variable	(-)
J5	Dimensionless side slip traction variable	(-)
k	Contact aspect ratio =b/a	(-)
K	Calibration constant in side slip measurement	(m^{-1})
m	Initial slope of the zero spin traction curve	(-)
Po	Hertzian contact pressure	(Pa)
Rx	Radius of curvature in x direction	(m)
Ry	Radius of curvature in y direction	(m)
Re	Equivalent radius of curvature for discs	(-)
S	Dimensionless spin grouping	(-)
	or dimensionless slip grouping	(-)

U	Rolling speed of the discs	(m/sec)
Δv	Side slip velocity of the discs	(m/sec)
Δx	Small displacement of the displacement transducer	(m)

GREEK SYMBOLS

α	Angle of tilt of the toroidal axis	(rads)
β	Side slip angle	(rads)
μ	Peak traction coefficient for a given test	(-)
ω	Angular spin velocity on the contact	(rad/sec)
Θ	Temperature of the inlet fluid	('C)
τ	Shear stress	(Pa)
τ_c	Critical or limiting shear strength of fluid	(Pa)
ν	Poissons ratio	(-)

SUBSRIPTS OR SUPERSCRIPTS

	Denotes upper (+) or lower (-) body
x,y,z	Denotes x or y or z direction
'	Nondimensional regression variable
-	Denotes averaged variables
c	Denotes critical on the shear stress

1. INTRODUCTION

Traction drives have a rather checkered history of existence. After a brief period of acceptance in the automotive market during the first quarter of this century, they disappeared in rapid fashion. The main reason for their initial acceptance was the simplicity with which a variable speed output can be obtained from a nearly constant speed input. Their rapid demise was due the fact that while simple in concept, the average life expectancy was very low indeed. With the advent of a more demanding motoring public this short life expectancy became unacceptable and other solutions were found to the speed match problem. In recent years traction drives have had a resurgence because of the energy crisis and the fact that a lot of the initial problems have now been, partially at least, solved.

In simple terms the traction drives basic elements are two rollers, pressed into nominal contact and rolled about their respective axis. Power is transmitted in the form of a shear stress across the contact area. A fluid is present to prevent initial surface scuffing damage and to provide for some form of cooling. The rolling motion of the discs draws this fluid into the contact zone and a thin layer of this fluid will separate the actual contact area. It is also in this region where the torque is transmitted from one roller to the next and therefore the performance of a traction drive depends to a large extent upon the rheological properties of the fluid. Close examination of the fluid history as it passes through the contact gap reveals that it experiences a sudden pressure pulse from atmospheric to possibly several Giga Pascal in a time period of 1 to .1 msec. The shear stress that is transmitted from one disc to the other (about 10% of the normal stress) passes through this layer of fluid "trapped" in the contact and causes a shear. This in turn will lead to heat generation and from simple calculations, temperatures in the centre of the film can easily reach several hundred degrees Centigrade.

To the designer of traction drives, the traction behaviour of the fluid under the severe conditions is of utmost importance because of the direct influence that it has on the efficiency, size and life of a given drive. Besides a good rheological model for the fluid, he must have at his disposal pertinent rheological properties of the fluid that he proposes to use. It is in this area where this report addresses itself.

1-1 PRIOR TRACTION INVESTIGATIONS

To study the rheological properties of the fluid under the severe conditions as described above precludes the use of most of the conventional instruments used for steady state measurements. In fact the only suitable type of instrument for the study is a disc machine where most of conditions are the same or similar to those in traction drives. From the resulting traction tests, certain models are inferred and it is in this area where there has been a lot of activity recently. Notable contributions have come from Clark et al (1), Hewko (2), Smith (3), Smith et al (4), Johnson and Cameron (5), Niemann (6), and more recently Johnson and Roberts (7) and Johnson and Tevaarwerk (8). Some of these investigations were strictly experimental in nature, and aimed at obtaining traction drive design data, while others were aimed at understanding the traction phenomena so that rheological models could be formulated. This latter research is ofcourse ultimately aimed at relating fluid molecular properties to traction properties. Research by Johnson and Tevaarwerk (8), Daniels (9), Hirst and Moore (10) and Alsaad et al (11) is directed specifically towards this purpose. The reader is refered to an exellent review by Johnson (12) for further aspects of this topic.

Many of the rheological models derived so far have been isothermal in nature. This is not so much due to the level of understanding of traction but rather because of the degree of complexity that thermal analysis introduces. This is not to say however that thermal effects are not important, a simple method is required however to include them in the analysis.

Current understanding of traction has led to traction models that describe the fluid shear behaviour in terms of an elastic and a dissipative element. For purposes of mathematical tractability this dissipative element is taken to be plastic like in nature. This gives an adequate discription of the fluid behaviour at conditions such as those encountered in traction drives. An analysis of traction drive performance using such a model was done by Tevaarwerk (13). It showed that under certain conditions the prediction technique by Hagi (14) can be used. This work has now been further expanded by developing a simple method to correct for thermal effects due to spin, Tevaarwerk (15), and an overall thermal traction study, Tevaarwerk (16).

As with all models however, their usefullness is severely restricted if inadequate input traction data is available to the designer. This is especially so if new high traction fluids are used that were not tested previously for use under conditions that exist in modern highly advanced traction drives.

1-2 TRACTION DATA RESEARCH PROGRAM

Several novel and new forms of traction drives have recently been developed and tested by Loewenthal et al (17). These particular drives are suitable for the high speed applications area where gears in their current form would not suffice. For purposes of design of these drives, adequate fluid rheological data is needed under the operating speeds, pressures and

temperatures encountered. For this reason, and for traction drive optimization in general, a program was undertaken to obtain traction contact data under a variety of conditions. Variables studied to determine their influence on traction included surface speed, contact pressure, temperature, contact area, aspect ratio, spin and side slip. Additionaly, the data could be tested against an existing traction model to validate its traction performance predictions.

This project was undertaken as a part of the Highway Vehicle Systems Program of the U.S. Department of Energy to provide basic traction technology information for traction drive design. The work was in support of automotive applications of traction drives, but certainly not limited to that field. It was managed by the Bearing, Gearing and Transmission Section of the NASA Lewis Research Center. All experimental and theoretical work was done through the Waterloo Research Institute of the University of Waterloo, Ontario, Canada. The author wishes to thank Mr. Blair Bruce , Mr A. Blahey and Mr. J Devaal, all from the U.of W., for their assistance in this research program.

2-0 EXPERIMENTS

The various traction experiments were carried out on two existing twin disc machines. These machines are known as the high speed machine, capable of speeds up to 80 m/sec, and the low speed machine with speeds up to 30 m/sec. These two machines are shown in figure 2-1a and 2-1b. Traction curves were obtained by using the side slip technique; a technique whereby large traction transfer can be measured without the need for a large motor-generator set. The principal difference between the high speed and low speed is the fact that the low speed machine has the ability to measure traction under longitudinal power transfer as well as side slip conditions. This feature is useful if some of the predictions of the fluid rheological model are to be checked against experimental results.

2-1 DESCRIPTION OF TWIN DISC MACHINES

For an extensive description of twin disc traction testers the reader is refered to the literature; Smith (3) and Johnson and Roberts (7). Basically the machines consists of two discs, called the upper and lower disc. The lower disc is the driver, powered by an electric motor through timing belts. The upper disc is the driven and is loaded against the lower disc through a dead weight system. This lower disc is shaft mounted in rolling element bearings and the only degree of freedom is one of rotation about the drive axis. The lower disc always has a transverse radius of curvature of infinity. To avoid problems with gravity forces the axis of rotation of this disc should be horizontal to within a few milliradians. The upper disc is shaft mounted in bearings contained in the upper assembly. This upper assembly is suspended with elastic hinges such that only direct normal motion or axial motion is possible. The assembly will however always stay horizontal. The upper disc (or toroid) has curvatures such that the desired contact geometry is arrived at. The upper assembly is constructed such that the rotational axis can be tilted relative to the horizon so as to introduce spin on the contact. It can also be turned about the normal to the contact so as to introduce a side slip velocity. A straingage load cell restrains axial motion of the upper assembly, thereby permitting the direct measurement of the axial force. Furthermore, by employing a dynamic brake on the upper toroid, longitudinal slip can be introduced. This latter feature allows for the measurements of traction under conditions of power transmission.

In order to achieve the various aspect ratios a number of special discs with varying crown curvatures were employed as shown in figures 2-2 and 2-3. Table 2-1 lists the actual curvatures used. All the discs were made of AISI-01 steel, hardened to 7.00 GPa, ground and polished to a surface finish of less than .05 μm RMS and with an out of roundness error of less than 5 μm. Between tests the discs were inspected for surface damage and if needed, reground and polished to bring them back up to original specifications.

Aspect Ratio	High Speed Machine				Low Speed Machine				Re	
	Upper		Lower		Upper		Lower		HS	LS
k	Rx	Ry	Rx	Ry	Rx	Ry	Rx	Ry		
.5	-	-	-	-	25.0	4.3	25.0	∞	-	3.2
1.0	33.0	22.6	71.4	∞	25.0	12.5	25.0	∞	11.3	6.25
2.0	-	-	-	-	25.0	36.5	25.0	∞	-	9.3
5.0	33.0	270	71.4	∞	25.0		25.0	∞	20.8	11.5

TABLE 2-1: Disc curvatures as used in the investigation. (Dimensions are all in millimeters.)

Figure 2-2 shows the various discs as employed on the low speed machine. The required normal load, obtained by dead loading techinques for both machines, can be calculated from the Hertz theory for elastic bodies in contact. The maximum pressure is given by;

(1) $$Po = (1/2\pi AB) * \sqrt[3]{(3\ Fz\ E'^2/Re^2)}$$

where Fz= contact normal load (N)

E'= composite elastic modulus (Pa)

$$= \tfrac{1}{2}\ ((1-\nu^2/E^+) + (1-\nu^2/E^-))^{-1}$$

Re= equivalent disc radius (m)

$$= (1/Rx^+ + 1/Rx^- + 1/Ry^+ + 1/Ry^-)^{-1}$$

A,B= Hertzian contact shape factors (-)

(NOTE; The superscripts refer to the upper disc (+) and lower disc (-)).

It is often desirable to calculate the contact dimension directly from the normal pressure Po. This may be done by using a factor C where C is derived from the Hertzian contact theory.

(2) $$a = C\ Po$$

where $$C = 2\ \pi A^2 B\ Re/E'$$

The constants A,B and C are shown in Table 2-2 below (using E' for steel).

k	A	B	C ($*10^{12}$m/Pa)	
.5	1.46	.725	.135	-
1.0	1.0	1.0	.170	.307
2.0	.725	1.46	.194	-
5.0	.511	2.55	.208	.376
			low speed machine	high speed machine

TABLE 2-2:Contact size for various aspect ratios. (m/Pa Hertzian pressure)

From this table it can be seen that the contact size varies

considerably between the two machines even at the same pressures and contact aspect ratio.

2-2 TRACTION MEASUREMENTS

By suitable instrumentation of the disc machines the side slip traction curves may be obtained. For both machines a load cell was used to measure the side slip force of the upper toroid assembly. The electrical signal from the load cell was then filtered to remove noise and applied to the vertical axis of an X-Y recorder. The skew angle was measured by using a displacement transducer on the upper assembly and thereby measuring the rotation angle of this assembly. This skew angle gives the amount of side slip/roll ratio through the relationship;

(3) $$\Delta v/U = \tan(\beta)$$

where β= side slip angle (rad.)
v= side slip velocity (m/sec)
U= rolling velocity (m/sec)

By measuring the amount of skew with the displacement transducer the side slip/roll ratio is obtained directly through;

(4) $$\Delta v/U = \Delta x\ K$$

where Δx is the displacement of the transducer and K a scale factor. The electrical output of the displacement transducer was filtered and applied to the horizontal axis of the X-Y recorder. Calibration of both the load cell and the displacement transducer were checked on the average for every 5-10 traction tests. Calibration of the load cell was by a deadweight loading technique while the displacement transducer was calibrated by rotating the upper assembly through a known angle and then calculating the amount of side slip for this angle. The distance traced on the X-Y recorder for this given angle was then noted and the scale factor calculated.

Traction curves were obtained by the slow rotation of the upper assembly from a positive value of side slip/roll ratio to a negative value. The X-Y recorder would then automatically trace the force versus slip curve on graph paper. By reversing the direction of rotation of the machine, a duplicate set of curves can be obtained. For the zero spin traces, this curve should be completely symmetric about the origin. Typical traction curves thus obtained are shown in figures 2-4 through 2-11. The horizontal slip scale and vertical traction scale were added after the test from the calibration results. The expected range of accuracy of these traction measurements was +/- 5% of the true traction force.

These typical curves shown in figures 2-4 to 2-11 cover almost the entire range of traction curves measured in this investigation. The various independent parameters are listed in Table 2-3.

Fluid type (-)	test number (-)	inlet temp ('C)	Hertz press. (GPa)	speed U (m/sec)	aspect ratio (-)	normal load (N)
SANTO 50	790531-01	32	1.45	20	5	5000
"	790126-03	69	1.0	80	5	1500
"	790329-04	29	1.9	20	1	1400
"	790311-06	69	1.0	80	1	200
TDF-88	791119-04	30	1.9	10	1	416
"	791130-06	70	1.45	30	1	185
"	791130-04	70	1.0	30	5	460
"	791103-11	33	1.45	10	5	1400

TABLE 2-3:Typical traction test conditions.

2-3 TRACTION WITH SPIN

Spin may be introduced on the contact by tilting the upper assembly relative to the horizontal through an angle α . This angle is refered to as the spin angle, however it is not a direct measure of the spin itself because it does not consider contact geometry. A more suitable measure of spin is given by the dimensionless variable J3 (see appendix IV).

(5) $$J3 = 3/8\ m/\mu\ (\omega\sqrt{ab}/U)\sqrt{k}$$

where
- m = initial traction slope (-)
- μ = peak traction coefficient (-)
- ω = spin velocity on contact (rad/sec)
- k = aspect ratio b/a (-)
- U = contact rolling velocity (m/sec)
- a,b = contact sizes (m)

Most of the variables in equation (5) are known from the traction curves and from the contact geometry. The grouping $\omega\sqrt{ab}/U$ provides for a measure of the spin intensity on the contact and it will be used here to indicate spin as such. The angular spin velocity on the contact can be related to the angle of tilt through the following:

(6) $$\omega/U = \sin(\alpha)/(Ry\cos(\alpha) + e)$$

where
- α= spin angle (rad)
- e= center of curvature offset (m)

In some instances the distance e has a negative value ;i.e., the centre of Ry is above the axis of rotation as shown in figure 2-3a. Tnis is the case for example in the 6° spin test on the low speed machine and for the 15° and 30° spin tests on the nigh speed machine (k=5).

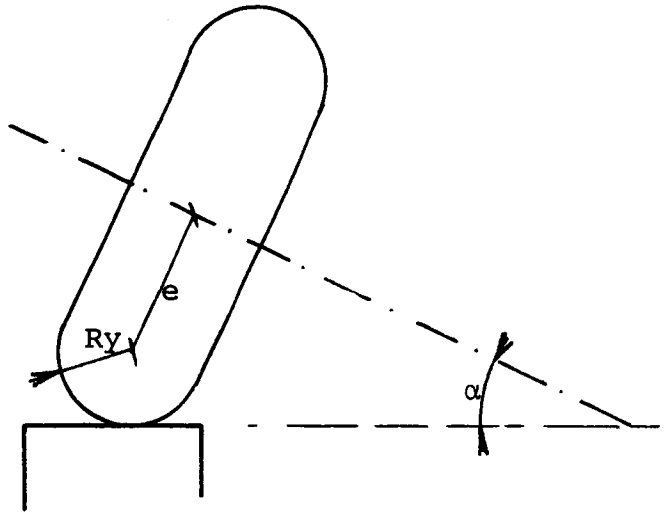

Figure 2-3a: General disc arrangement for spin tests.

Equation (6) still applies provided that the sign of the distance e is taken into account. Figure 2-3b shows the actual discs tilted to introduce spin.

For the toroids as used in this investigation the values of e and Ry are given in Table 2-4.

Aspect ratio	Low Speed Machine		High Speed Machine	
b/a	e(mm)	Ry (mm)	e(mm)	Ry(mm)
.5	20.7	4.3	-	-
1.0	12.5	12.5	10.4	20.6
2.0	-11.5	36.5	-	-
5.0	-125(6°)	150.4	-230(15°)	270
			-205(30°)	270

TABLE 2-4: Toroid dimensions for the spin tests.

When the toroids are tilted a slight change takes place in the curvatures, this was kept small however by the proper selection of the radii.

The spin tests were performed at specific angles only for the two machines. These angles were 6° for the low speed machine and 15° and 30° for the high speed machine. A further simplification in the spin factor calculation can therefore be made by employing the relationship between contact size and pressure as indicated in Table 2-2. In simple terms we may write;

$$\omega\sqrt{ab}/U = C'' \, Po \qquad (7)$$

where $C'' = \omega \, C\sqrt{k} \, /U$

Values for C" are indicated in Table 2-5 below.

k	Low Speed (6^0)	High Speed (15^0)	High Speed (30^0)
.5	$.399 \times 10^{-3}$	----	----
1.0	$.713 \times 10^{-3}$	2.46×10^{-3}	5.12×10^{-3}
2.0	1.15×10^{-3}	----	----
5.0	1.98×10^{-3}	7.06×10^{-3}	14.6×10^{-3}

TABLE 2-5: Spin factors for the various test conditions.

Traction curves with imposed spin were obtained in the same manner as described for the zero spin traction curves. Typical curves obtained are shown in figure 2-12 to 2-19 for a variety of spin conditions. Table 2-6 lists the various independent parameters for these traces.

fluid type	test number	Θ 'C	press. GPa	speed m/sec	aspect ratio	spin angle	$\omega\sqrt{ab}/U$
SANTO 50	79072704	73	1.45	80	5	30^0	.021
SANTO 50	79072601	32.5	1.22	20	1	15^0	.003
SANTO 50	80062306	70	1.90	20	1	6^0	.00135
SANTO 50	8006201	70	1.00	20	5	6^0	.00198
TDF-88	79100403	50	1.0	20	5	15^0	.0071
TDF-88	79100403	50	1.0	80	5	15^0	.0071
TDF-88	79111902	29	1.45	30	1	6^0	.00103
TDF-88	80051402	70	1.00	20	1	6^0	.00135

TABLE 2-6: Typical range of the conditions for the spin tests.

3-0 TRACTION CURVE PARAMETERS

The typical traction curves shown may be fitted to the Johnson & Tevaarwerk (8) traction model. This model consists of an elastic element coupled in series with a viscous element. In the limit, when pressures are high, speeds high and temperature low, this elastic/viscous model may be approximated by an elastic/plastic model. Conditions in traction drives are such that this approximation is almost always valid, certainly for the fluids with high traction coefficients. The advantage of the model is that only two parameters are needed to describe the isothermal portion of the curves. When thermal effects set in, one more parameter is needed besides the externally known fluid thermal properties, see Tevaarwerk (15, 16).

Based on the elastic/plastic model, Tevaarwerk (13) and Tevaarwerk and Johnson (18) made several predictions about the traction behaviour of such fluids in typical traction contacts. The simple side slip traction curve for such a fluid is given as: (For an explanation see also Appendix V)

$$(8) \qquad J5 = \left(\pi/2 - \sin^{-1}\left((1-S^2)/(1+S^2)\right) + 2S/(1+S^2)\right)/\pi$$

$$(9) \quad \text{where} \quad S = (2/3)\, J2/\sqrt{k} = (\pi/4)(m/\mu)(\Delta v/U)$$

$$(10) \quad \text{and} \quad J5 = Fy/(Fz\ \mu)$$

This equation may now be used to see how well the shape of the traction curves shown in figures 2-4 to 2-11 is predicted by this theory. Firstly, the traces snown in figure 2-4 to 2-11 are replotted on a traction force vs. slip velocity graph as shown in figures 3-1. Using the symmetry relationship of the traction curve, only the trace in the upper quadrant is graphed although the results from all the four quadrants were used in obtaining the average traction curve for the fluid. Generally speaking the symmetry of the traces is nearly perfect. The calculated traction data for these traces is shown in Appendix I under the columns labelled DV and Fy.

The range on the traction forces and the slip velocity may be reduced somewhat by plotting the results in the more conventional fashion of traction coefficient Fy/Fz and side slip/roll ratio $\Delta v/U$. Replotting the results from figure 3-1 in this form produces figure 3-2. While the ranges have been reduced somewhat, the shapes, though similar, are still not identical. The traction coefficient and slide roll ratio are indicated as Fy/Fz and $\Delta v/U$ in Appendix I.

By using equation (8) and the slope and the peak traction coefficient of the traction traces, the entire group of 8 traces can now be presented as a simple single curve, see figure 3-3. The completely reduced traction data is shown in Appendix I under Js for the slip parameter and J5 as the side slip traction. Also indicated are the traction coefficient and the traction slope used to reduce the data. The two parameters that completely specify the entire isothermal traction curve therefore are the initial traction slope $m=(Fy/Fz)/(\Delta v/U)$ when slip is small, and the peak traction coefficient $\mu = (Fy/Fz)_{peak}$. These two parameters are related to the fluid elastic shear modulus and the limiting shear strength of the fluid (as described in Chapter 4). Only the "isothermal" portion of the

traction curve is predicted by this model. This however, is often adequate because operation of traction drives is very often in this regime.

The fact that the traction curve can be described by two parameters makes for a very easy recording of all the traction tests performed in this investigation. The initial traction slope m and peak traction coefficient μ results thus obtained on the side slip traction measurements are recorded in Appendix II for both the fluids and all the aspect ratios tested. Also listed in this Appendix are the peak traction coefficients for the side slip with spin experiments. The traction slope is not recorded for these traces because it has no direct meaning in terms of fundamental fluid properties.

3-1 TRACTION DATA CORRELATION

Examination of the traction coefficients in Appendix II reveals that there are certain trends when one of the external parameters such as pressure, speed, inlet fluid temperature or aspect ratio is varied. The trends are;

--Traction coefficient increases with increasing pressure.
--Traction coefficient decreases with increasing speed.
--Traction coefficient decreases with increasing temperature.
--Traction coefficient decreases with increasing aspect ratio.

By linearization of these trends the following equations may be written;

$$\begin{aligned} \mu &\propto A1 + A2*Po \\ \mu &\propto A3 + A4*U \\ \mu &\propto A5 + A6/\Theta \\ \mu &\propto A7 + A8*k \end{aligned} \qquad (11)$$

where; Po=Hertz contact pressure
U =rolling speed of the discs
Θ =fluid inlet temperature
k =contact aspect ratio (b/a)

These equations can be used directly for correlation purposes, however, to reduce the influence of weighting because of the physical magnitude of the variables, nondimensional variables should be used. These can be obtained quite easily by using the following;

$$U'=(U-\bar{U})/\bar{U} \; ; \; P'=(Po-\overline{Po})/\overline{Po} \; ; \; \Theta=(\Theta-\bar{\Theta})/\bar{\Theta}; \; k'=(k-\bar{k})/\bar{k} \qquad (12)$$

,where the prime indicates the transformed variable and the barred variables the average magnitude. Because the trends are all equally likely for a given condition of speed, temperature, pressure and aspect ratio, the following general equation for the traction coefficient may be expected;

$$\mu=(A1+A2*P')*(A3+A4*U')*(A5+A6/\Theta')*(A7+A8*k') \qquad (13)$$

Multiplication yields the following expression;

$$(14)\quad \mu = C1 + C2*k' + C3*P' + C4*(P'k') + C5/\theta' + C6*(k'/\theta') + C7*(P'/\theta') + C8*(k'P'/\theta') + C9*U' + C10*(U'k') + C11*(U'P') + C12*(U'P'k') + C13*(U'/\theta') + C14*(k'U'/\theta') + C15*(P'U'/\theta') + C16*(k'P'U'/\theta')$$

Where the coefficient C1-C16 are directly related to the coefficients A1-A8. Equation (14) may now be used on the data to obtain the coefficients C1-C16 by a least squares regression. All the data for a given fluid can be combined provided that there is no spin or longitudinal slip present on the traction test.

In the regression reported herein all the results in a certain class were nondimensionalized by using equation (12). Before one can now use the regression coefficients to predict the traction coefficient the variables need to be transformed according to this equation. This requires the knowledge of the average quantities of the variables and these are given for each regression.

Appendix IIIA -IIID contains the regression results for the two fluids used on both the traction coefficient and the initial traction slope. (The analysis for traction slope is identical to that for traction coefficient). Also listed in these appendices are the average quantities $\bar{U}, \bar{\theta}, \bar{k}$ and $\bar{P}$, the mean of the percent error and the standard deviation of the percent error. In the far right columns are listed the estimate of the regressed variable and the mean percent error between the predicted and the actual regressed variable.

The listing of the coefficients C in the Appedices is as follows;

C1	C2	C2	C4
C5	C6	C7	C8
C9	C10	C11	C12
C13	C14	C15	C16

When spin is present on the contact then a further variation in the traction coefficient is possible. A similar treatment to the spin traction results gives the following expression for the traction coefficient;

$$(15)\quad \mu = C1 + C2*Z' + C3*k' + C4*(k'Z') + C5*P' + C6*(P'Z') + C7*(P'k') + C8*(P'k'Z') + C9/\theta' + C10*(Z'/\theta') + C11*(k'/\theta') + C12*(k'Z'/\theta') + C13*(P'/\theta') + C14*(P'Z'/\theta') + C15*(k'P'/\theta') + C16*(k'P'Z'/\theta') + C17*U' + C18*(U'Z') + C19*(U'k') + C20*(U'k'Z') + C21*(U'P') + C22*(U'P'Z') + C23*(U'P'k') + C24*(U'P'k'Z') + C25*(U'/\theta') + C26*(U'/\theta') + C27*(k'U'/\theta') + C28*(U'k'Z'/\theta') + C29*(P'U'/\theta') + C30*(U'P'Z'/\theta') + C31*(k'P'U'/\theta') + C32*(U'k'P'Z'/\theta')$$

where $Z = \omega\sqrt{\bar{a}\bar{b}}/\bar{U}$

and $Z' = (Z - \bar{Z})/\bar{Z}$

These coefficients are given in Appendix IIIE and IIIF in the following order:

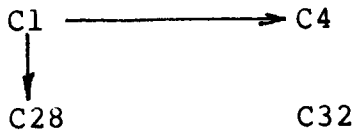

It could be argued that a regression of the above type is not desirable because of the large number of coefficients involved. This is certainly true and it is hoped that at some future time all the data can be reduced to two or three fundamental fluid parameters. However such a model has not been sufficiently developed for inclusion here.

4-Ø TRACTION CURVE PREDICTIONS

The main purpose in this investigation was to obtain traction data from two fluids that can and may be used for the prediction of traction contact performance. It is of course, not practical to experimentally measure the traction under every variation of contact kinematic conditions. These conditions may consist of longitudinal slip, side slip and spin.

With the knowledge of a few of the fluid rheological parameters, it is however possible to calculate the fluid traction curves under widely differing contact conditions. Present day models take into account the fluid and disc elasticity effects as well as the dissipative behaviour of the fluid film. The model that will be used here is that due to Johnson and Tevaarwerk (8). This model can be simplified for purposes of traction drive analysis to a simple linear elastic spring in series with a Coulomb friction model.

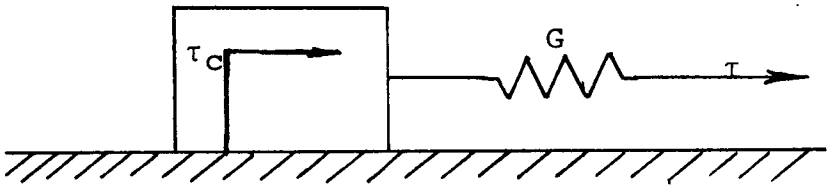

Figure 4-1: Schematic of the elastic/plastic traction model.

The method of operation of this model is as follows; upon the application of a shear force the linear spring element will extend. This extension or strain is directly proportional to the stress at all levels of stress until a certain critical stress τ_c is reached. At this point the Coulomb friction is insufficient and the extension in the elastic element remains constant. Sliding will now take place provided that the stress is maintained at τ_c. Upon a reduction or reversal of stress the elastic element will retract and recover the energy stored in it. The frictional work is however lost. (This frictional work will result in heat generation which in turn results in a local temperature rise. This temperature rise influences the level of stress τ_c in a complicated manner but always reduces it. It can therefore happen that the initial stress level required to get the friction element moving is higher than to keep it moving. Such nonlinear effects are very common in fluid rheology.) The modulus G of the elastic element is related to the initial traction slope through contact geometry and the kinematic conditions.

For simple slip traction curves m and G are related as follows;

(16) $$\bar{G} = (3/8)\, m\, Fz\, h/a^2 b$$

where h=average filmthickness (m)
a,b=semi contact dimension (m)
Fz=contact normal load (N)

The quantity $\bar{G}$ is indicated here rather than G. This is to signify that we only deduce an average shear modulus. The reason for this is that we do not know exactly how the fluid shear modulus is influenced by the local pressure in the contact. (The extraction of G for the fluid is further complicated by the fact that in the traction slope a certain amount of elastic creep of the disc material is invariably present, see also section 4-2). The frictional stress c is directly related to the peak traction coefficient u through the following equation;

(17) $$\tau c = \mu Fz/\pi ab$$

Again we are only extracting the average guantity τc because of the lack of knowledge about the variation of τc with pressure. (This limiting stress is temperature dependent and the temperature of the fluid is not constant but rises as more and more slip occurs on the contact. For simplicity however we often use the peak traction coefficient if such a peak exists.)

To apply the above concept to the analysis of traction in an EHL contact that is subjected to spin and slip is more complicated and a two dimensional model is now required. A much more detailed description of how this model can be used to predict traction under conditions of spin, side slip and the usual longitudinal slip is given in Appendix IV and Appendix V. The analysis described in these Appendices is entirely isothermal in nature.

4-1 TRACTION WITH SPIN ONLY

Side slip traction tests with spin taken on both the high speed and low speed machine were compiled into the traction data presented. Typical traces obtained are shown in figures 12 to 19

In order to predict these spin traction curves from theory, it was decided that the correlated data would be used to obtain the two fluid input parameters m(initial slope of zero spin curve) and μ (the zero spin traction peak). It was also possible to use the correlated data for a corrected spin traction peak so as to allow for possible thermal effects. For the treatment of thermal effects in traction, the reader is referred to Tevaarwerk (15) and Tevaarwerk (16). The analysis of traction including thermal effects is however outside the scope of this investigation.

The table below indicates the values used for the prediction of the spin traction curves.

trace #	slope m (-)	traction peak μ (-)	spin traction peak μ (-)
79072704	35	.075	.035
79100403a	33.3	.051	.044
79100403b	40.9	.081	.080
79072601	53.5	.083	.084
79111902	35.9	.085	.084
80051402	59.6	.098	.091
80062306	53.9	.096	.0955
80062801	41.2	.082	.082

TABLE 4-1: Experimental values of m and μ used in the spin traction prediction.

The results of the theoretical calculations are shown in Appendix VI for both the positive and negative rolling directions. The theoretical curves thus obtained are shown in figures 4-1 to 4-8. In general the prediction is very good except for some of the very high spin/high speed results where the thermal effects are not negligable.

4-2 TRACTION WITH SPIN, SIDE SLIP AND LONGITUDINAL SLIP

The low speed traction machine used in this investigation has the ability to impose the three general forms of slip on the fluid in the contact: a) side slip, imposed by skewing of the two discs relative to each other, b) spin imposed by tilting the axis of rotation of the upper disc, and c) longitudinal slip, imposed by retarding the rolling velocity of the upper disc. The advantage of being able to apply the three forms of slip is that the rheological models can now be tested out under various conditions of the forms of the imposed slip. A disadvantage of this system is that only relatively low speeds can be employed because of the power levels involved. Unlike the side slip traction tests, one now requires a drivemotor and braking system that is capable of generating and absorbing the entire power that can be transmitted through the fluid in the contact. For the high speed tests that were performed under conditions of side slip these power levels would have reached 15 to 20 kW if done in longitudinal form.

To see how well the traction under the combined kinematic conditions of spin, slip and side slip are predicted, a number of traction curves were obtained with these conditions imposed on the contact. To be sure that the possible difference between experiment and theory are not due to the correlation error contained in the correlated side slip traction results, it was decided to use the traction slope and traction peak from a side slip test under otherwise identical conditions to the longitudinal traction test.

Four such traces were taken for different aspect ratios. Table 4-2 indicates the resulting traction data from these curves.

fluid	Po	U	k	Θ	μ	m
Santotrac 50	2.53	20	.5	70	.0935	64.06
Santotrac 50	1.96	20	1.0	70	.0956	57.60
Santotrac 50	1.45	20	2.0	70	.100	54.40
Santotrac 50	1.22	20	5.0	70	.089	52.40

Table 4-2: Raw experimental data obtained from the four side slip traction measurements.

The traction traces, together with the theoretical curves fitted to them, are shown in figure 4-9 to 4-12 and the corresponding data calculation sheets are shown in Appendix VII-A.

Next this data was used to calculate the longitudinal slip traction curves with imposed side slip. The side slip was increased in four steps. In order to use the data from the side slip traction curves for the longitudinal traction prediction, two corrections have to be made. The first correction is for the slope of the traction curve because of possible disc compliance effects. This comes about because even though the modulus of the disc material is much higher than that for the fluid(by about two orders of magnitude), we can only measure the elastic creep of the series combination of thin film and two discs. Because the fluid film is so thin relative to the amount of disc material that is strained, it presents a rather stiff spring in this system. In fact as much as 70% of the total elastic creep may take place in the discs. Also the amount of elastic creep that takes place in the discs depends on the direction in which the stress is acting. Since side slip data is to be used for longitudinal traction prediction a correction has to be made for this effect. (This correction is described in detail by Tevaarwerk (13) see Appendix IV). The other correction is for the reduction in the traction peak due to the rolling traction component. At high speed this can be a significant amount(anywhere from 1 to 10% of the traction coefficient). In the analysis and calculations performed here, this correction was omitted because of the uncertainty in the magnitude of the film thickness. Table 4-3 contains the corrected values of the slope used for the prediction of the longitudinal slip traces.

fluid	Po	U	k	Θ	m	μ
Santotrac 50	2.53	20	.5	70	66.74	.0935
Santotrac 50	1.96	20	1.0	70	65.19	.0956
Santotrac 50	1.45	20	2.0	70	62.78	.100
Santotrac 50	1.22	20	5.0	70	61.10	.089

TABLE 4-3: Corrected experimental traction data for longitudinal traction predictions.

As can be seen, the slope correction can be quite substantial for the higher aspect ratio traction curves.

Appendix VII-B contains the experimental and theoretical results for these longitudinal traction predictions and the results are shown in figures 4-13 to 4-16. These figures show that the predictions compare favourably with the experimental results at the lower side slip results. When the side slip increases, thermal effects set in and a significant discrepancy becomes apparent.

To examine the influence of spin alone on the side slip, four tests were performed with side slip and spin present. The former side slip test results were now used to predict the results with spin traction. This prediction is similar to the one done above, except that the correlated traction data was used. Figures 4-17 to 4-20 shows the comparison between observed and predicted spin traction results, The calculation results are shown in Appendix VII-C.

Finally, the combined spin, side slip and longitudinal slip traction curves are predicted and compared with theory in figures 4-21 to 4-24. The calculation for this case is shown in Appendix VII-D. Generally speaking, the predictions are good except for the high side slip traction traces where a significant amount of thermal effect is present. This is especially clear from figure 4-24 where the observed traction is on a downward trend at increased longitudinal slip while the theoretical predictions indicate an upward trend. It is expected that with the inclusion of a correct thermal analysis, the predicted traction curves would be closer to the observed. The remainder of the longitudinal traction data obtained under combinations of spin and or side slip are reported in Appendix VII-E. This data shows the corresponding traction peak observed under the various conditions of spin and side slip.

5-Ø CONCLUSION

Traction tests were conducted on two twin disc traction machines. These machines are known as the high speed machine, capable of surface velocities of up to 8Ø m/sec, and the low speed machine. The low speed machine was instumented such that all these conditions of slip could be introduced and their effects on traction measured. The high speed machine could only be operated under conditions of side slip and spin. Two fluids were investigated for their traction properties, TDF-88 and Santotrac-5Ø. The traction data obtained were reduced to two variables per test. These variables were the initial traction slope and the maximum traction coefficient. The resulting data from all the test were then reduced to 32 regression constants for further use in traction drive design. To verify the theoretical traction predictions as given by the Johnson and Tevaarwerk model, a series of combined slip, side slip and spin tests were performed on the low speed machine and the results were compared to the predictions. These comparisons showed that the isothermal predictions by the above model are in good agreement with the experimental observations in the region where thermal effects in the fluid can be kept to a minimum.

Also comparison of the data generated with TDF-88 and Santotrac-5Ø fluids show that they have comparable performance.

6-0 REFERENCES

1) Clark, O.H., Woods, W.W. and White, J.R. "Lubrication at Extreme Pressure with Mineral Oil Films". J. Appl. Phys., vol. 22, no. 4, Apr. 1951, pp. 474-483

2) Hewko, L.O., "Contact Traction and Creep of Lubricated Cylindrical Rolling Elements at Very High Surface Speeds". ASLE Trans., vol. 12, 1969, pp. 151-161

3) Smith, F.W. "The Effect of Temperature in Concentrated Contact Lubrication". ASLE Trans., vol. 5, no. 1, Apr. 1962, pp. 142-148

4) Smith, R.L., Walowit, J.A. and McGrew, J.M. "Elastohydrodynamic Traction Characteristics of 5P4E Polyphenyl Ether". ASME Jolt., July 1973, pp. 353-362

5) Johnson, K.L. and Cameron, R. "Shear Behaviour of Elastohydrodynamic Oil Films at High Rolling Contact Pressures". Proc. Inst. Mech. Eng. (London), vol. 182, pt. I, no. 14, 1967, ppl 307-319

6) Niemann, G. and Stoessel, K. "Reibungszahlen bei elasto-hydrodynamisher Schmierung in Reibrad- und Zahnradgetrieben". Konstruktion, vol. 23, number 7, 1971, pp. 245-260

7) Johnson, K.L. and Roberts, A.D. "Observations of Viscoelastic behaviour of an Elastonydrodynamic Oil Film", Proc. Roy. Soc. (London), A, vol. 337, no. 1609, Mar. 19, 1974, pp. 217-242.

8) Johnson, K.L. and Tevaarwerk, J.L. "Shear behaviour of Elastohydrodynamic Oil Films". Proc. Roy. Soc. (London), Series A, vol. 356, no. 1685, Aug. 24, 1977, pp. 215-236.

9) Daniels, B.K. "Non-Newtonian thermo-viscoelastic EHD Traction from combined slip and spin" ASME Preprint 78-LC-2A-2. ASLE/ASME Lubrication Conference, Minneapolis, Minnesota, October 24-26,1978.

10) Hirst, W. and Moore, A.J. "The effect of temperature on traction in elastohydrodynamic lubrication". Phil. Trans. Roy. Soc. of London, Sept. 1980, vol. 298, number 1438, pp. 183-208

11) Alsaad, M., Bair, S., Sandorn, D.M. and Winer, W.O. "Glass Transition in Lubricants: Its Relation to Elastohydrodynamic Lubrication". Trans. ASME, Journal of Lubrication Technology, 100 (July 1978) 404-417.

12) Johnson, K.L., "Introductory Review of Lubricant Rheology and Traction". Proc. of the Leeds-Lyon Conference, Leeds 1978, pp. 155-161

13) Tevaarwerk, J.L. "Traction Drive Performance Prediction for the Johnson and Tevaarwerk Traction Model". NASA Technical Paper 1530 (1979) (see also Appendix IV)

14) Magi, Mart, "On Efficiencies of Mechanical Coplanar Shaft Power Transmissions". Chalmers University of Technology, Gothenburg, 1974

15) Tevaarwerk, J.L. "A Simple Thermal Correction for Large Spin Traction Curves" A.S.M.E. paper 80-C2/DET-60 (1980).

16) Tevaarwerk, J.L. "Thermal Influence on the Traction behaviour of an Elastic/Plastic model" Proceedings of the Leeds/Lyon Conference, Leeds (1980).

17) Loewenthal, S,H., Anderson, N.H. and Nasvytis, A.A. "Performance of a Nasvytis Multiroller Traction Drive." NASA TP 1378. (1978).

18) Tevaarwerk, J.L. and Johnson, K.L. "The Influence of Fluid Rheology on the Performance of Traction Drives", Trans. Am. Soc. Mech. Engrs. (J.O.L.T.) Vol. 101, p 266, (1979) (see also Appendix V).

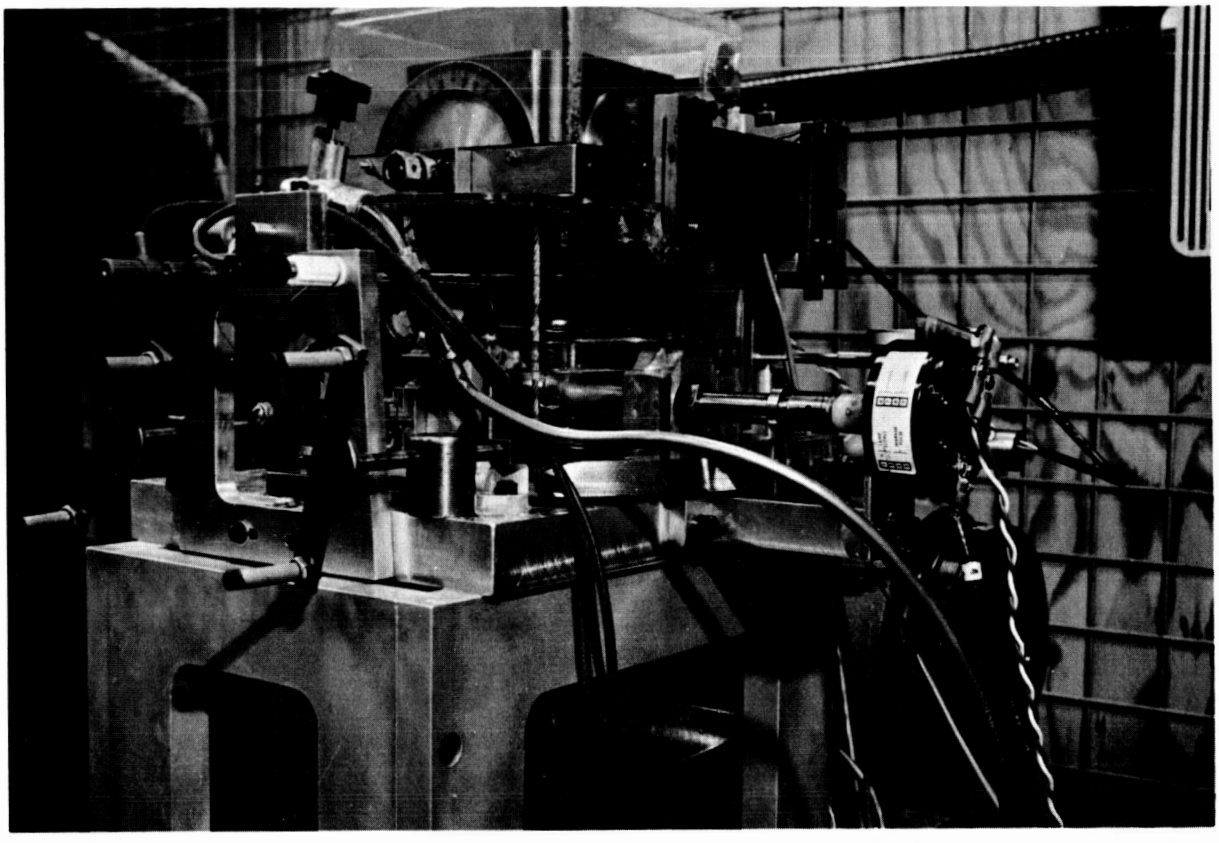

Fig.2-1a Photograph of the high speed traction machine.

ORIGINAL PAGE
BLACK AND WHITE PHOTOGRAPH

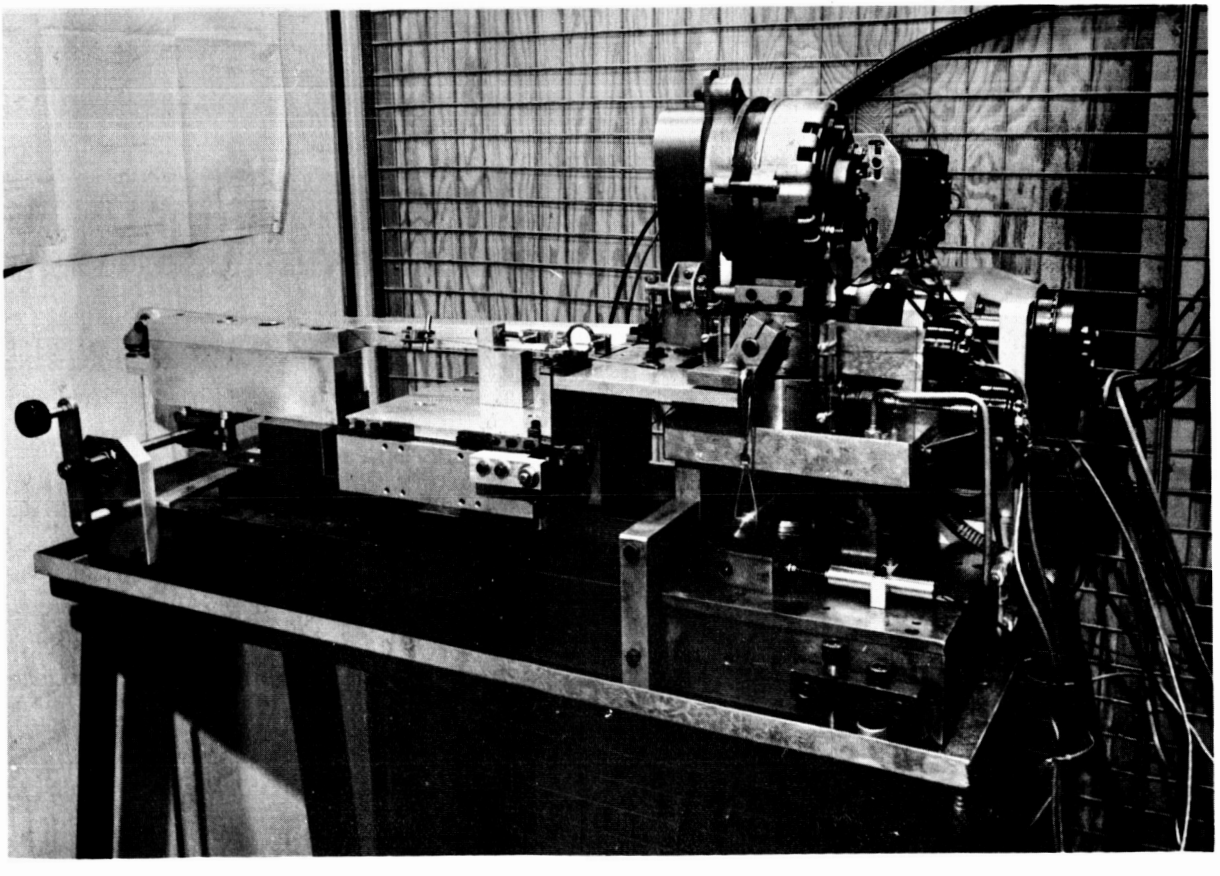

Fig.2-1b Photograph of the low speed traction machine.

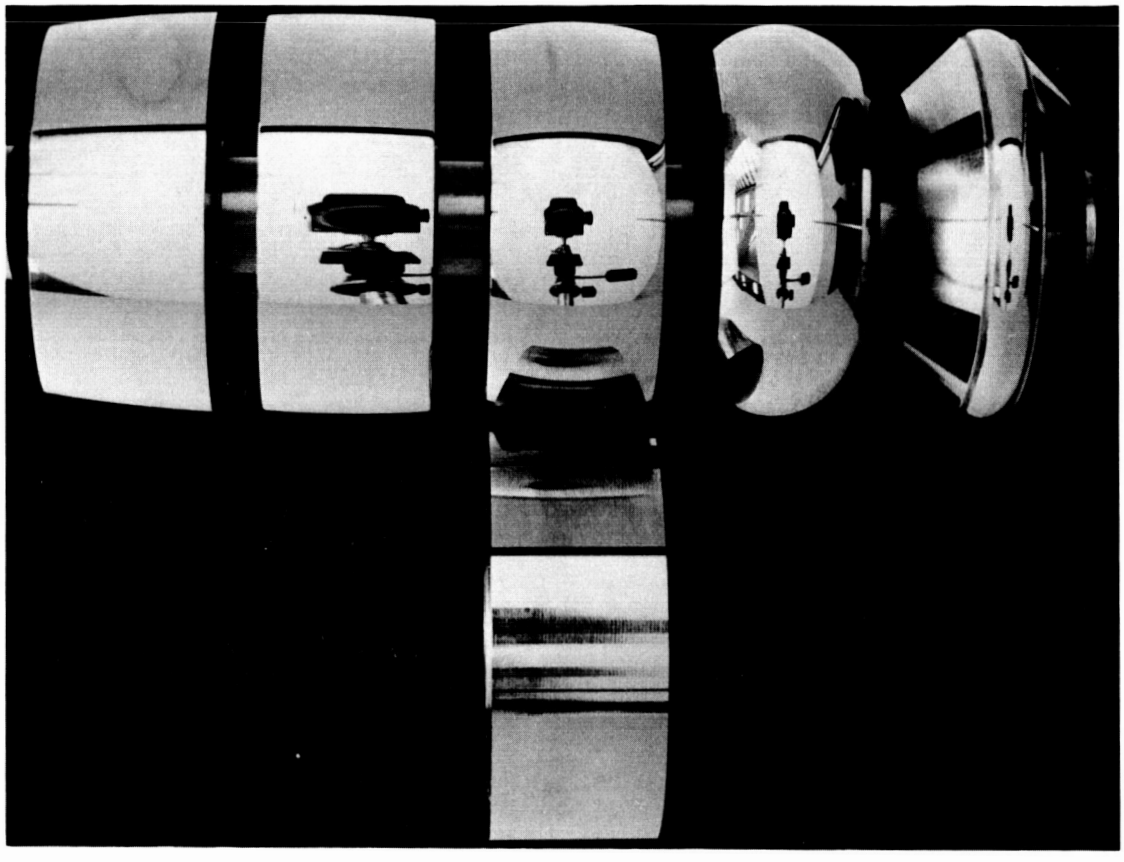

Fig.2-2a Photograph of discs used for the low speed traction tester.

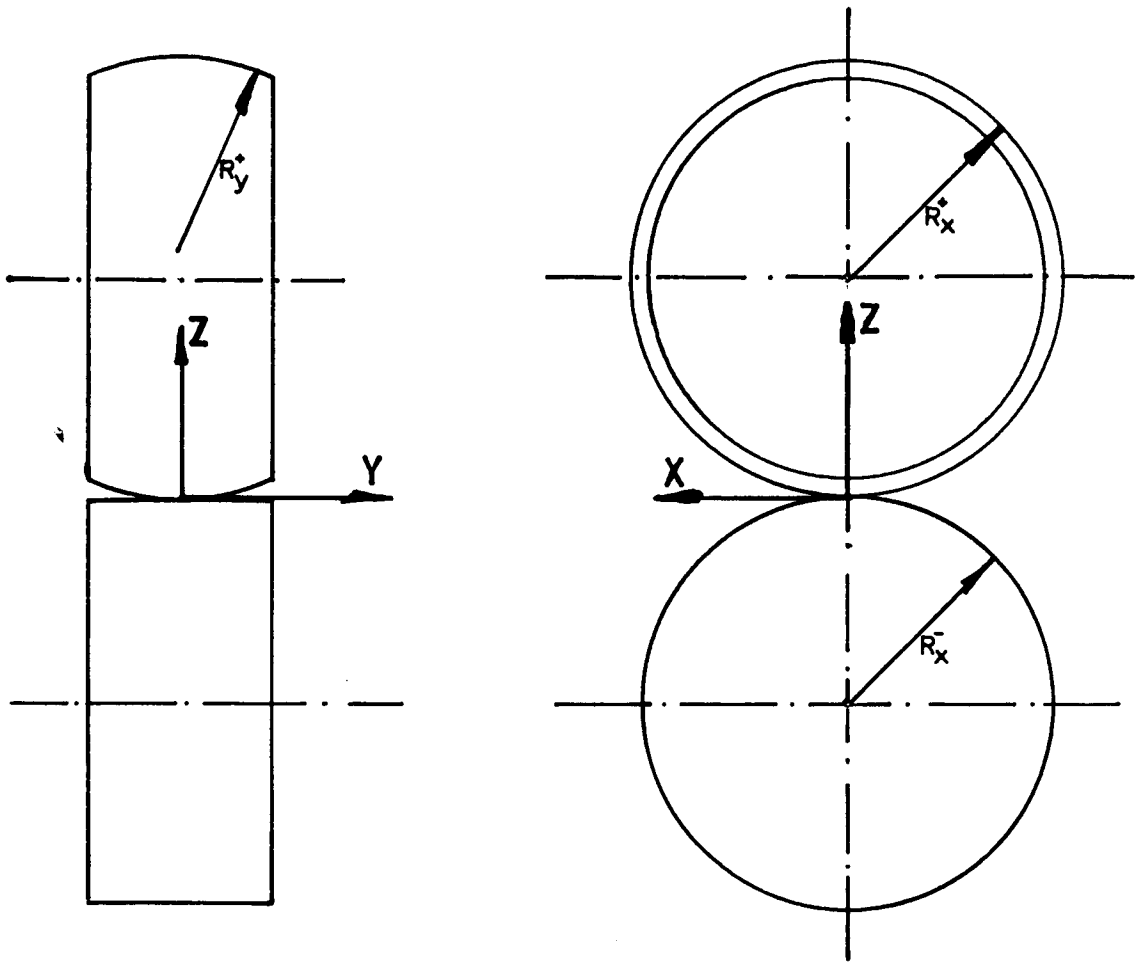

Figure 2-2b: Curvature conventions as used on the toroids for the two disc machines.

Fig 2-3b Photograph of the tilted disc to introduce spin.

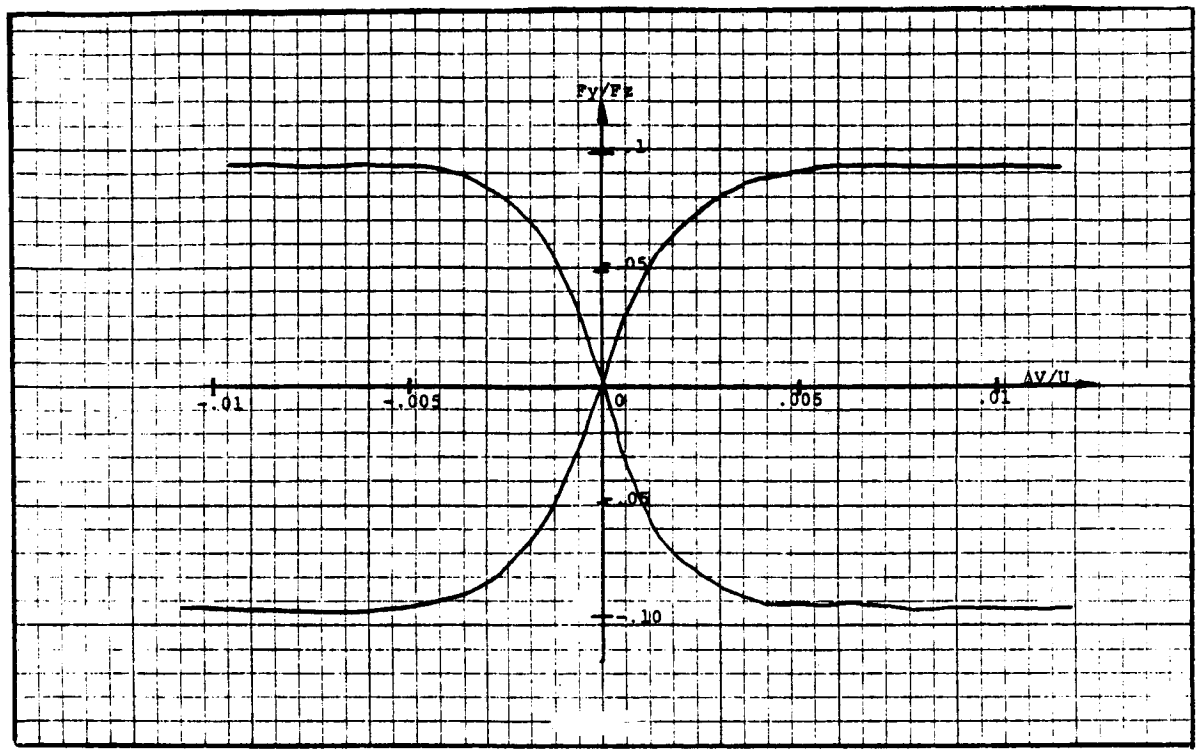

Figure 2-4: Side slip traction curve for TDF-88 under the following conditions; speed =30 m/sec; Hertz pressure =1.45 GPa; inlet temperature =70 'C; aspect raio k=1.0 and spin angle =0. The curve was obtained on the low speed traction tester.

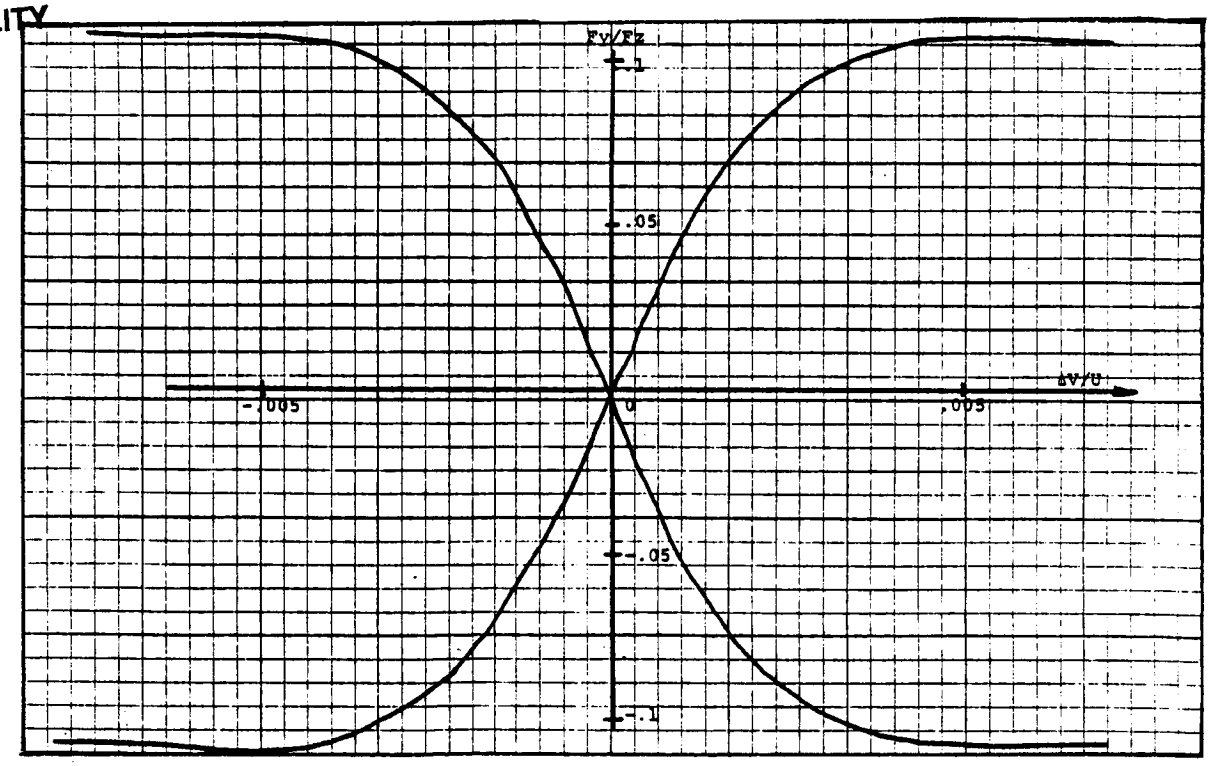

Figure 2-5: Side slip traction curve for SANTO-TRAC 50 under the following conditions; speed =20 m/sec; Hertz pressure =1.9 GPa; inlet temperature =29 'C; aspect ratio k=1.0 and spin angle =0. The curve was obtained on the high speed traction tester.

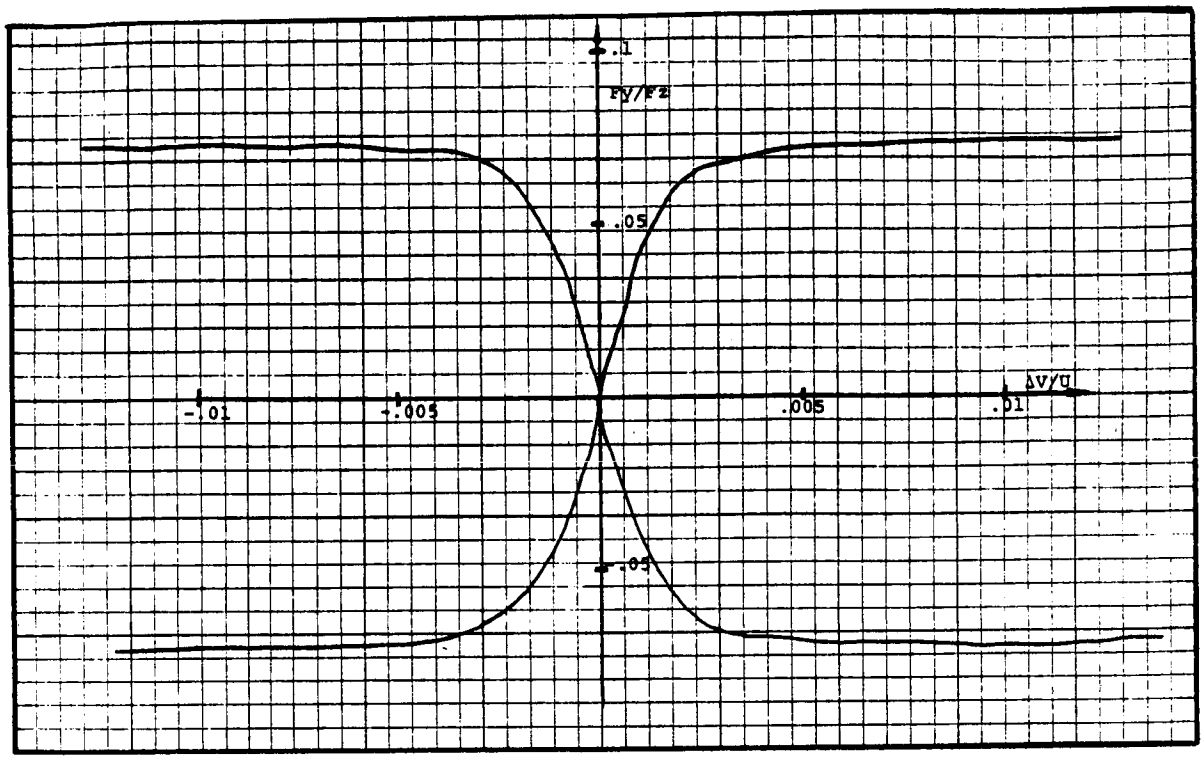

Figure 2-6: Side slip traction curve for TDF-88 under the following conditions; speed =30 m/sec; Hertz pressure =1.45 GPa; inlet temperature =70 'C; aspect ratio k=1.0 and spin angle =0. The curve was obtained on the low speed traction tester.

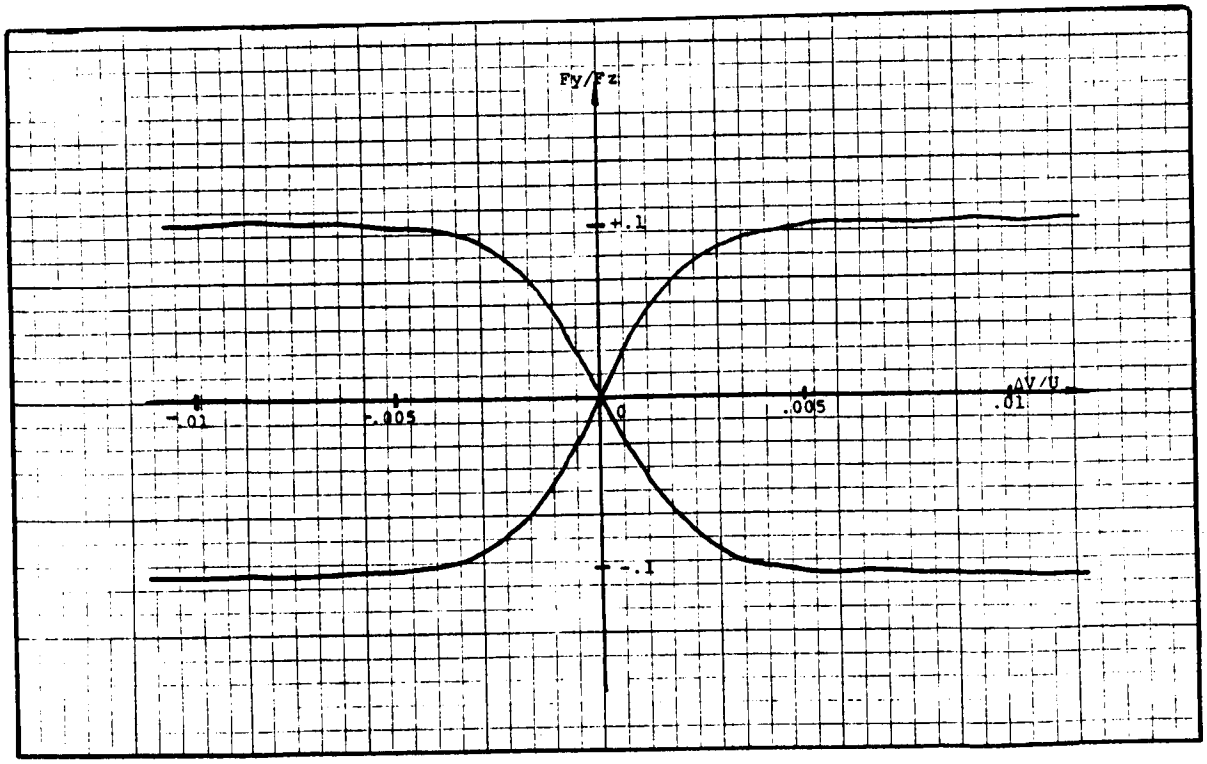

Figure 2-7: Side slip traction curve for TDF-88 under the following conditions; speed =10 m/sec; Hertz pressure =1.9 GPa; inlet temperature =30 'C; aspect ratio k=1.0 and spin angle =0. The curve was obtained on the low speed traction tester.

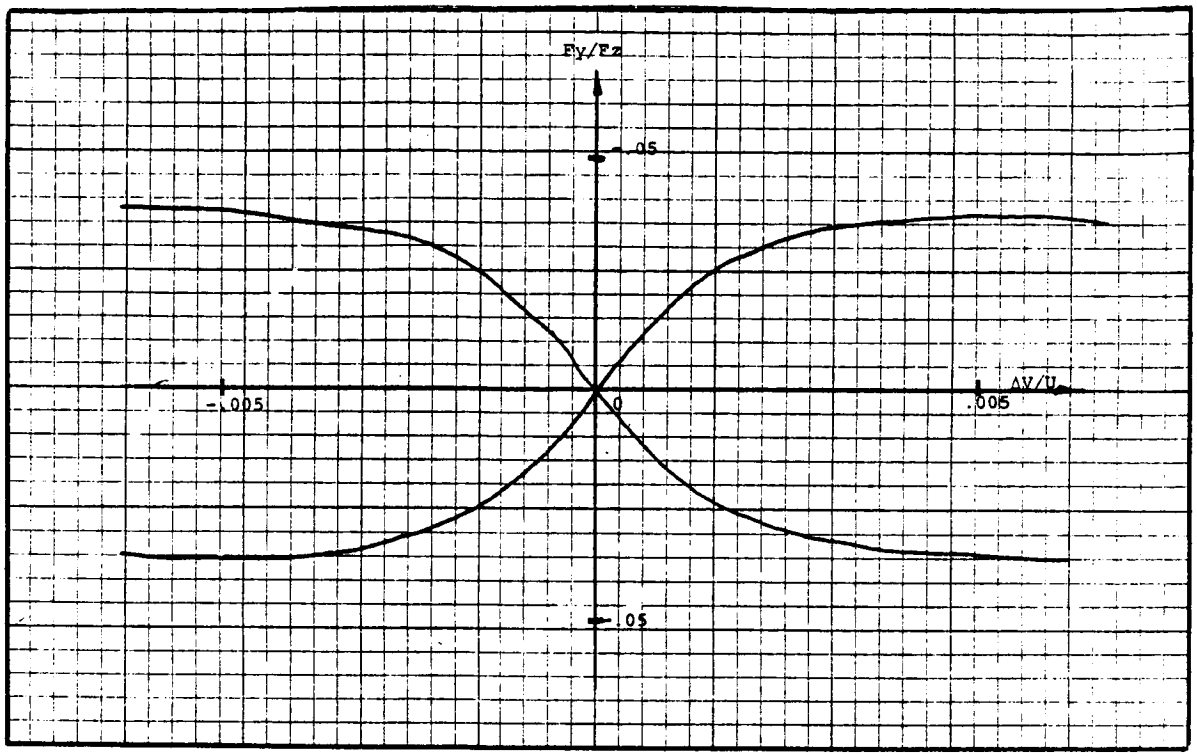

Figure 2-8: Side slip traction curve for SANTO-TRAC 50 under the following conditions; speed =80 m/sec; Hertz pressure =1.0 GPa; inlet temperature =69 'C; aspect ratio k=5.0 and spin angle =0. The curve was obtained on the high speed traction tester.

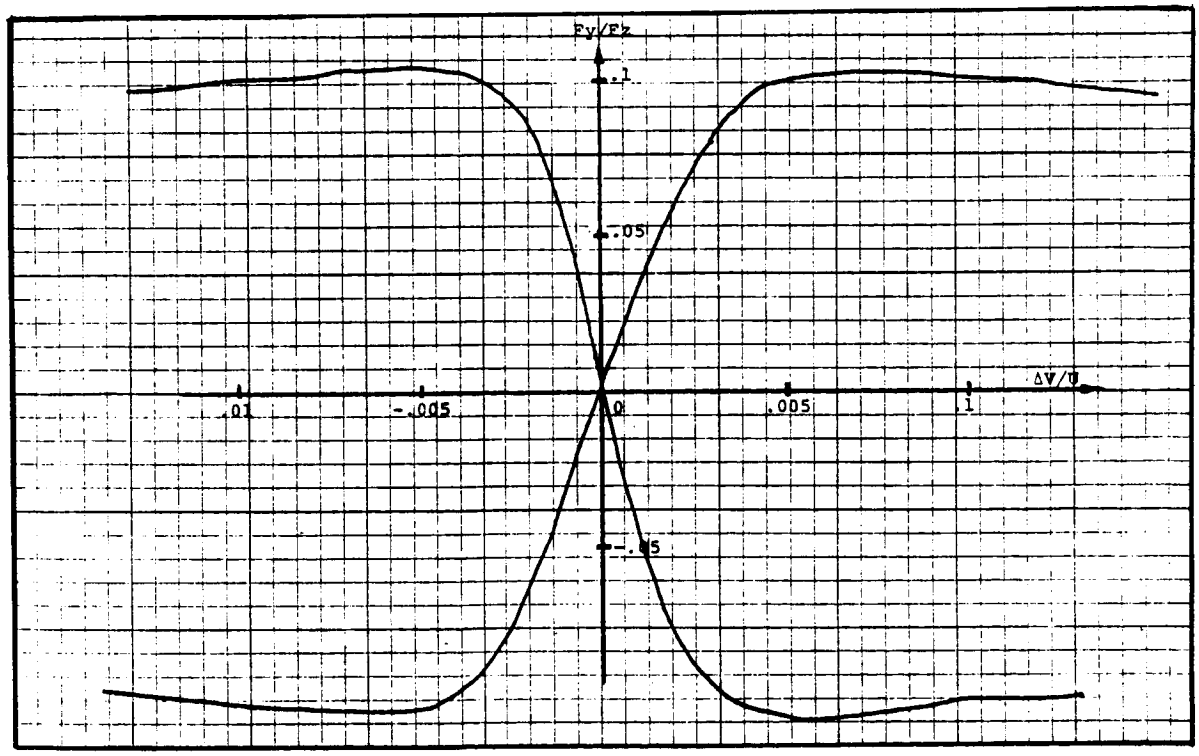

Figure 2-9: Side slip traction curve for SANTO-TRAC 50 under the following conditions; speed =20 m/sec; Hertz pressure =1.45 GPa; inlet temperature =32 'C; aspect ratio k=5.0 and spin angle =0. The curve was obtained on the high speed traction tester.

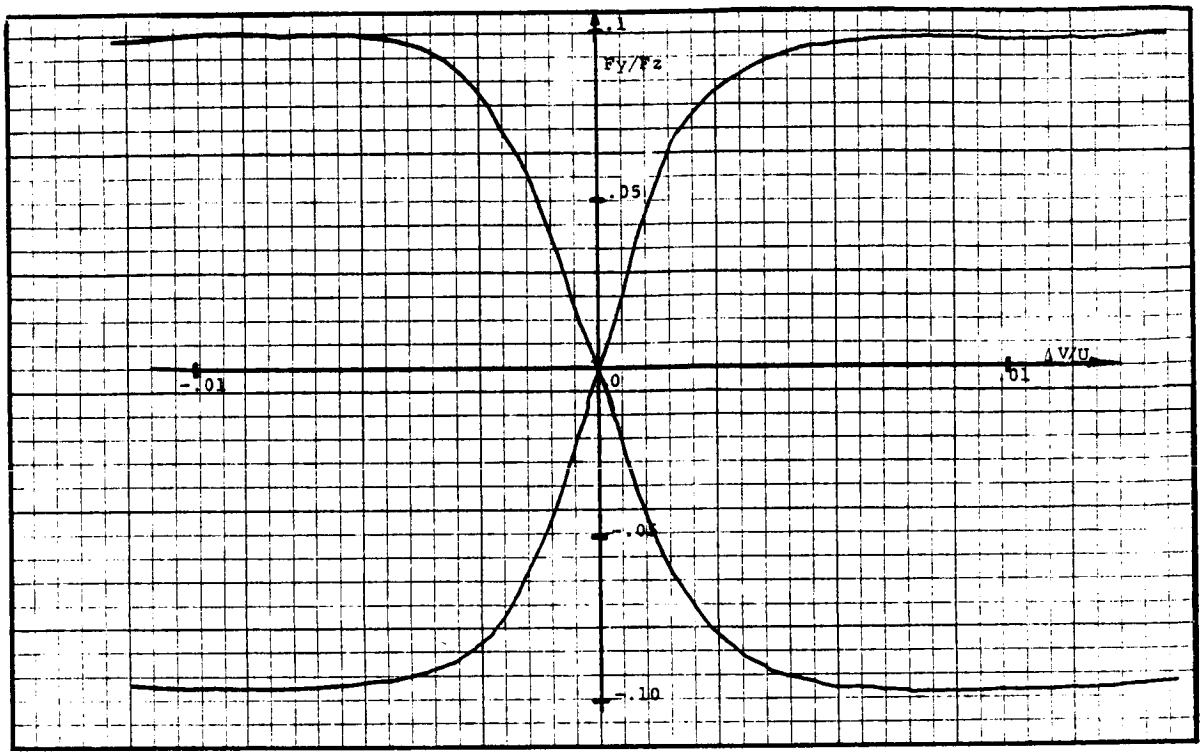

Figure 2-10: Side slip traction curve for TDF-88 under the following conditions; speed =10 m/sec; Hertz pressure =1.45 GPa; inlet temperature =33 'C; aspect ratio k=5.0 and spin angle =0. The curve was obtained on the low speed traction tester.

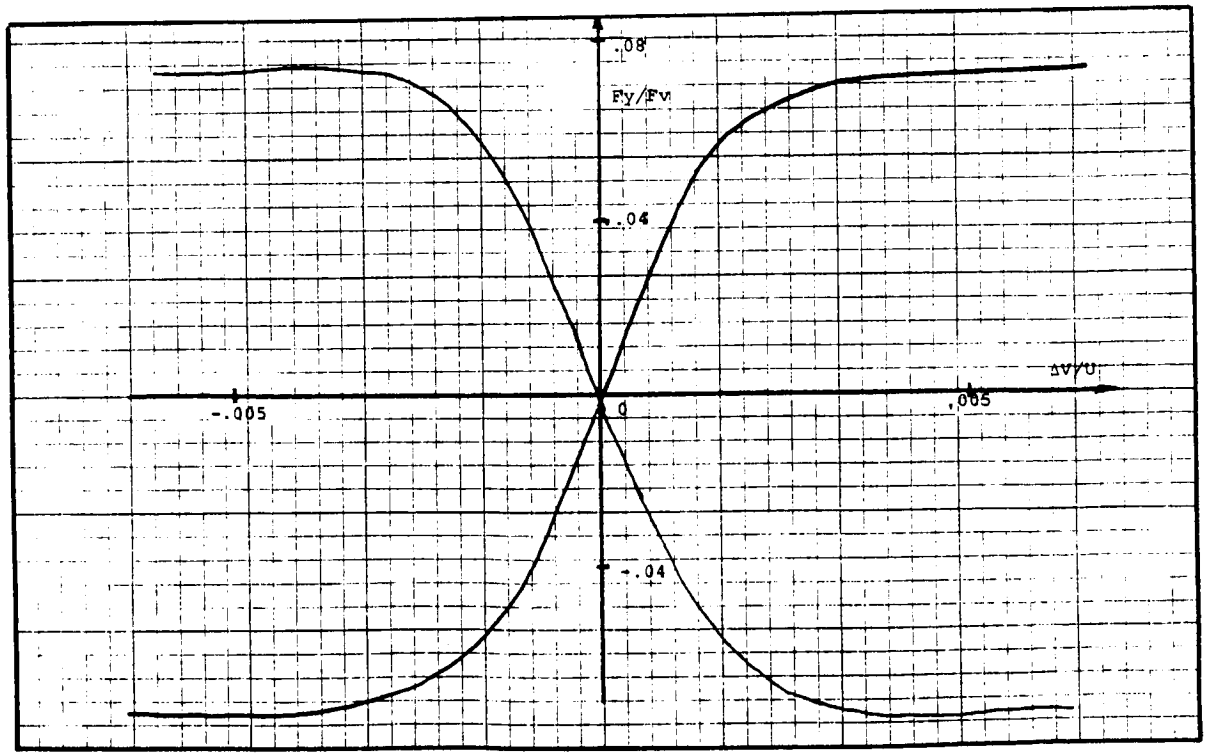

Figure 2-11: Side slip traction curve for SANTO-TRAC 50 under the following conditions; speed =80 m/sec; Hertz pressure =1.0 GPa; inlet temperature =69 'C; aspect ratio k=1.0 and spin angle =0. The curve was obtained on the high speed traction tester.

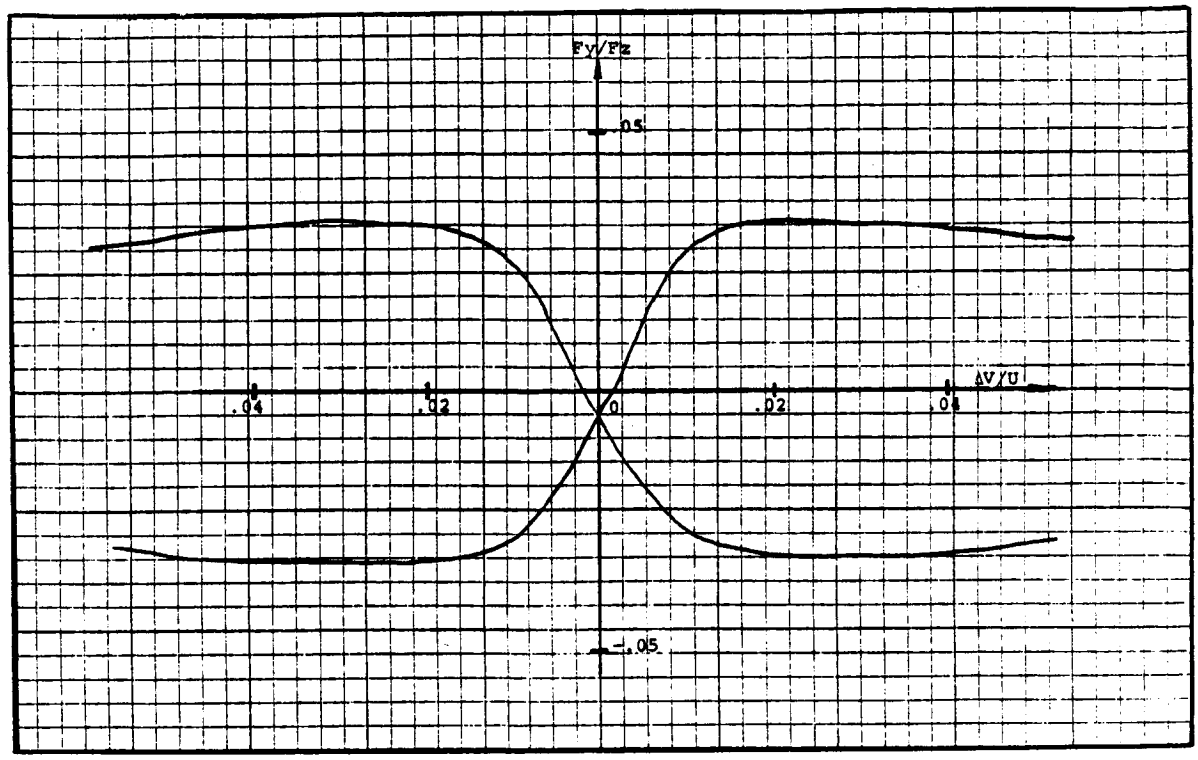

Figure 2-12: Side slip traction curve for SANTO-TRAC 50 under the following conditions; speed =80 m/sec; Hertz pressure =1.45 GPa; inlet temperature =73 'C; aspect ratio k=5.0 and spin angle =30 degrees. The curve was obtained on the high speed traction tester.

ORIGINAL PAGE IS OF POOR QUALITY

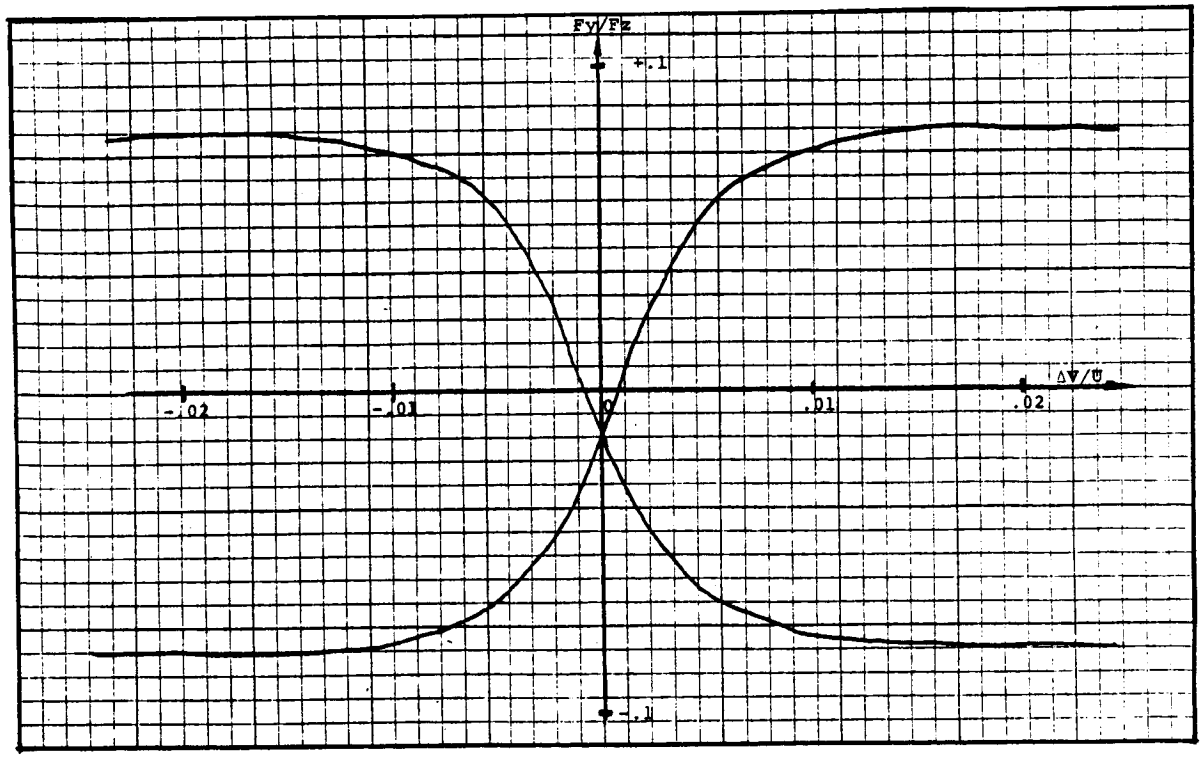

Figure 2-13: Side slip traction curve for TDF-88 under the following conditions; speed =20 m/sec; Hertz pressure =1.0 GPa; inlet temperature =50 'C; aspect ratio k=5.0 and spin angle =15 degrees. The curve was obtained on the high speed traction tester.

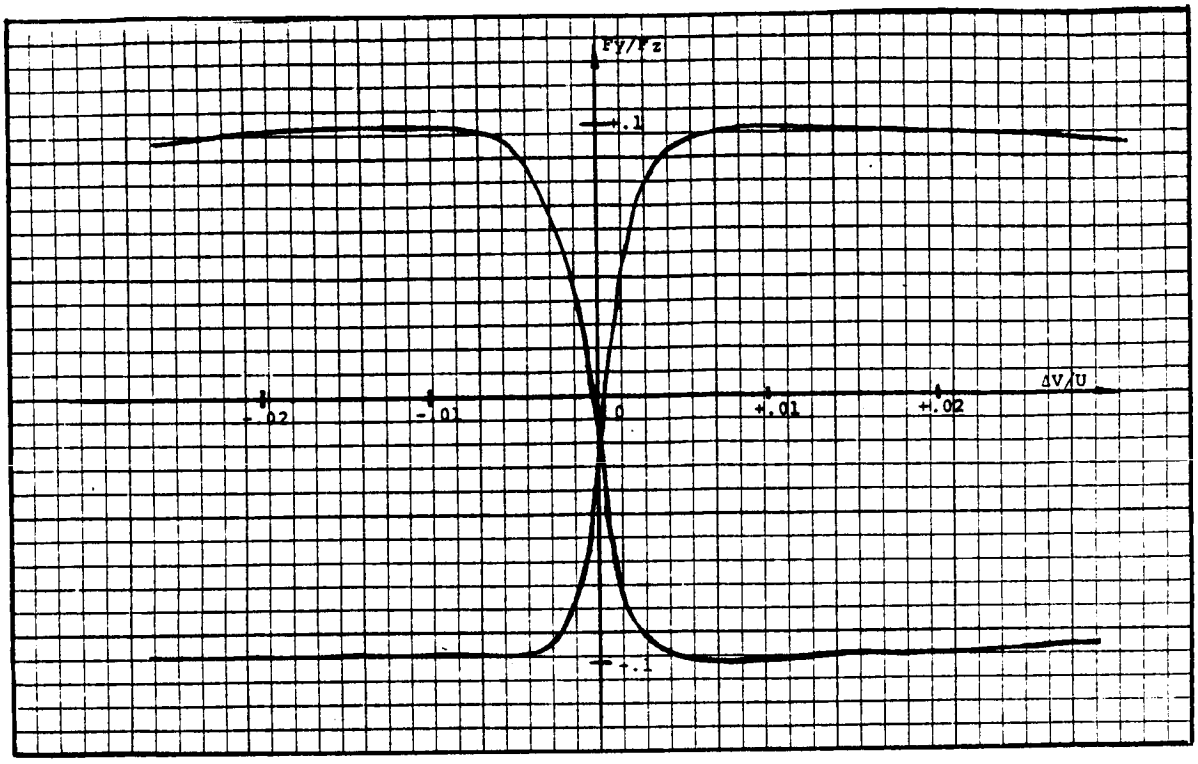

Figure 2-14: Side slip traction curve for SANTO-TRAC 50 under the following conditions; speed =20 m/sec; Hertz pressure =1.9 GPa; inlet temperature =70 'C; aspect ratio k=1.0 and spin angle =6 degrees. The curve was obtained on the low speed traction tester.

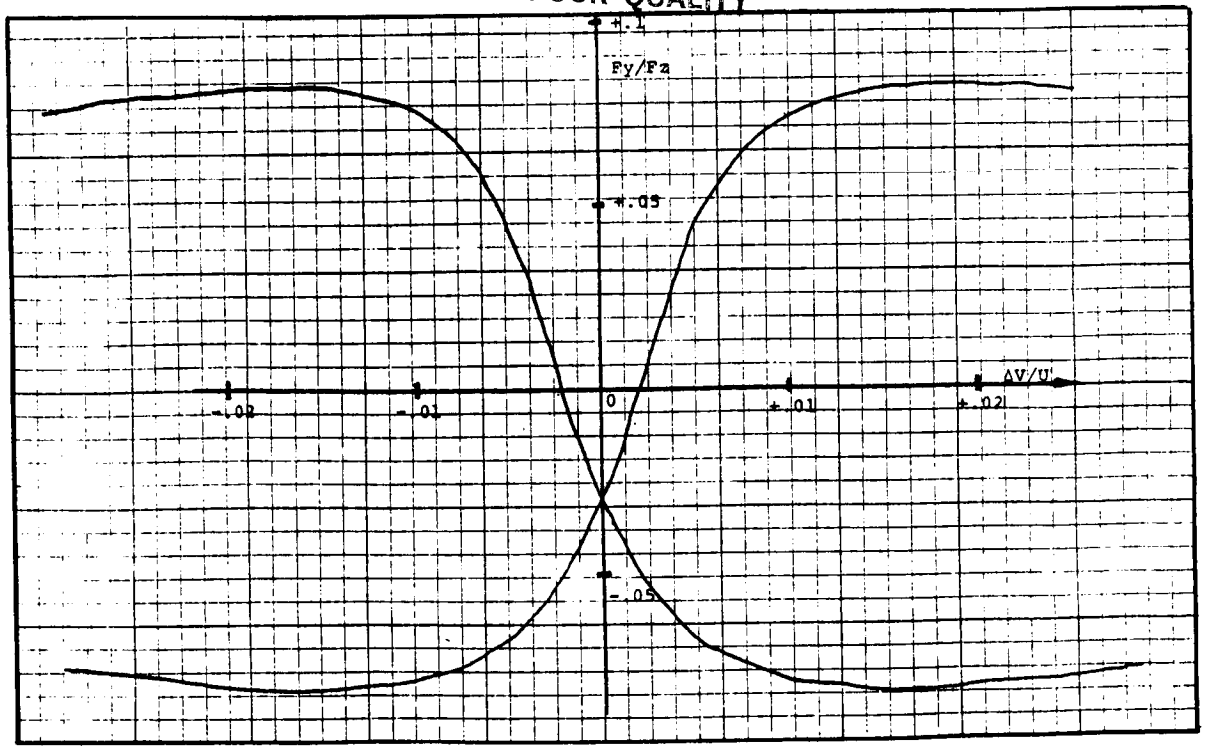

Figure 2-15: Side slip traction curve for SANTO-TRAC 50 under the following conditions; speed =20 m/sec; Hertz pressure =1.22 GPa; inlet temperature =32.5 'C; aspect ratio k=1.0 and spin angle =15 degrees. The curve was obtained on the high speed traction tester.

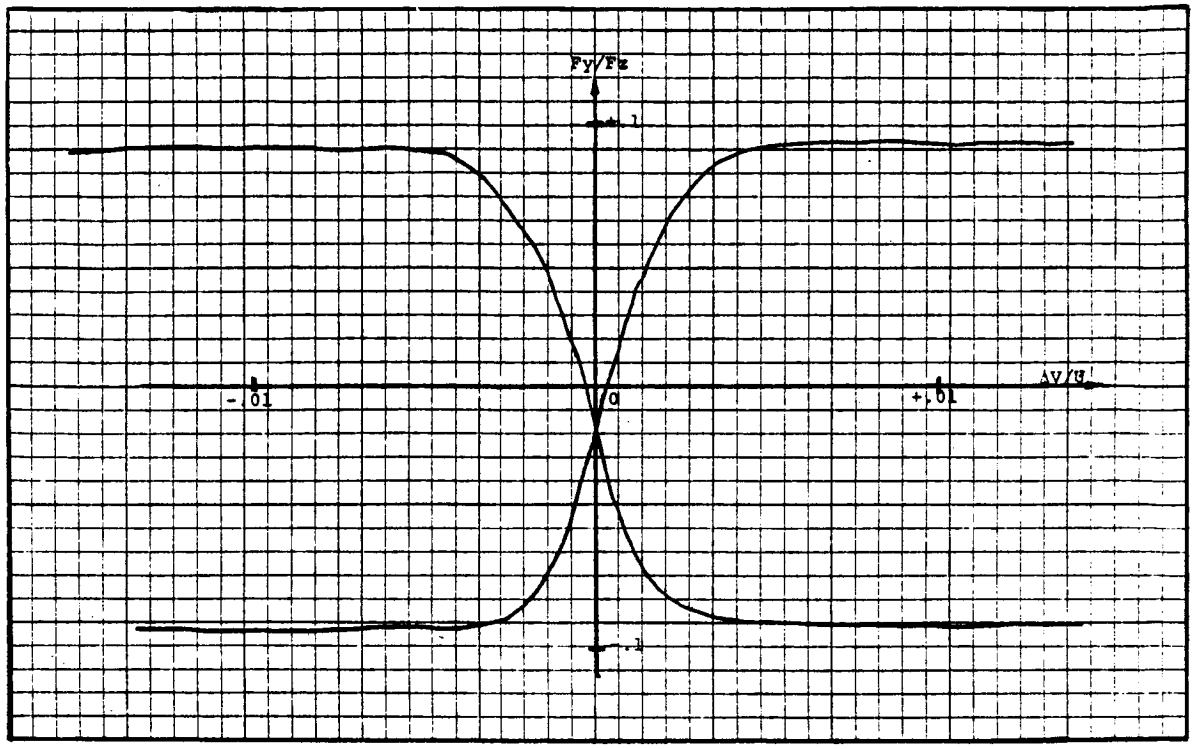

Figure 2-16: Side slip traction curve for TDF-88 under the following conditions; speed =20 m/sec; Hertz pressure =1.9 GPa; inlet temperature =70 'C; aspect ratio k=1.0 and spin angle =6 degrees. The curve was obtained on the low speed traction tester.

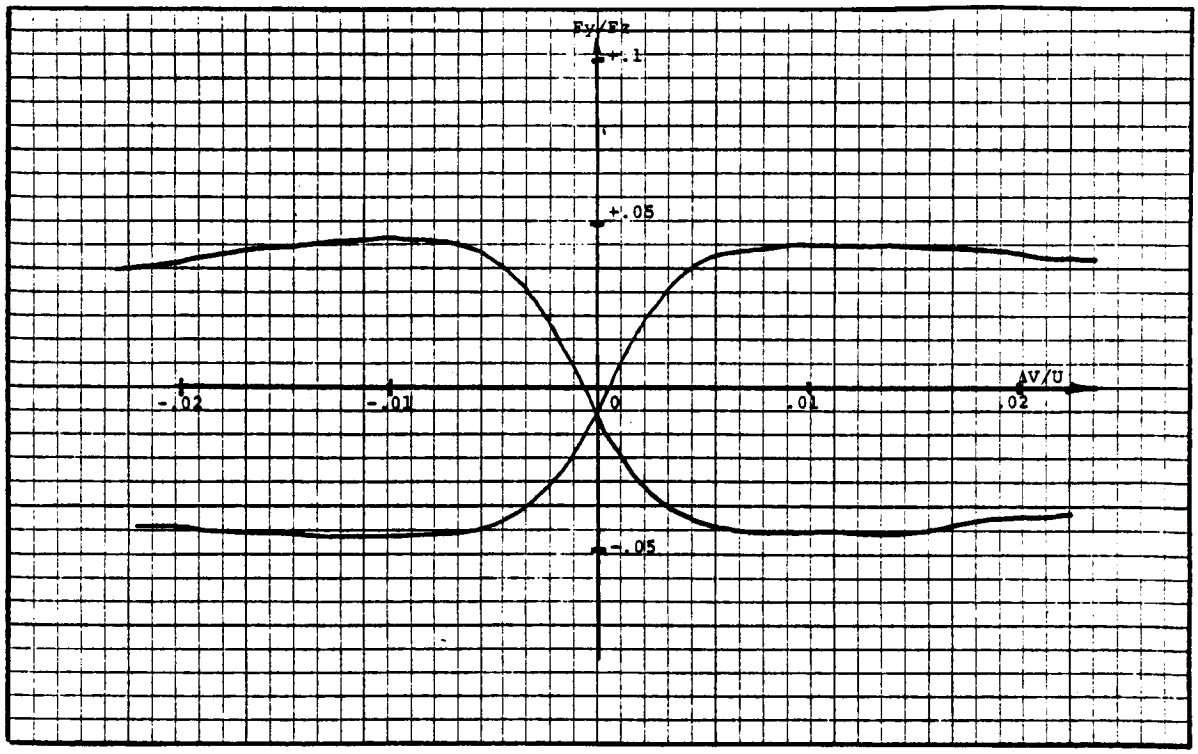

Figure 2-17: Side slip traction curve for TDF-88 under the following conditions; speed =80 m/sec; Hertz pressure =1.0 GPa; inlet temperature =50 'C; aspect ratio k=5.0 and spin angle =16 degrees. The curve was obtained on the high speed traction tester.

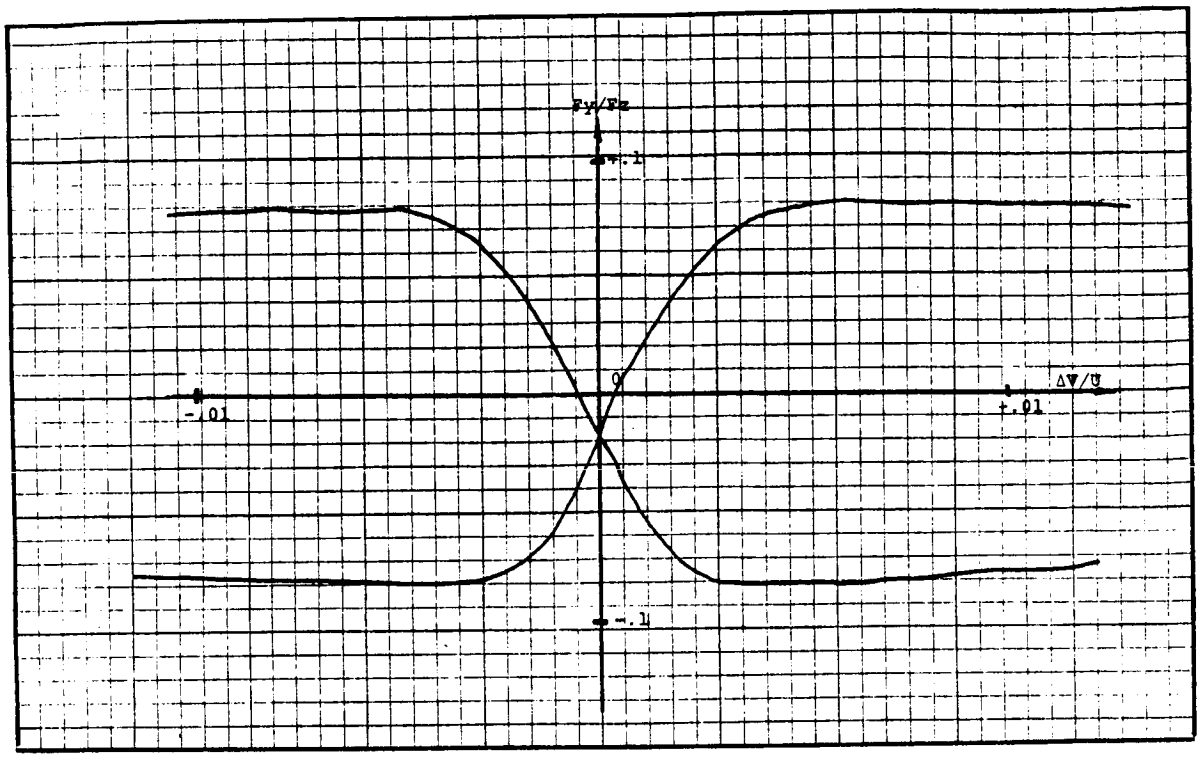

Figure 2-18: Side slip traction curve for TDF-88 under the following conditions; speed =30 m/sec; Hertz pressure =1.45 GPa; inlet temperature =29 'C; aspect ratio k=1.0 and spin angle =6 degrees. The curve was obtained on the low speed traction tester.

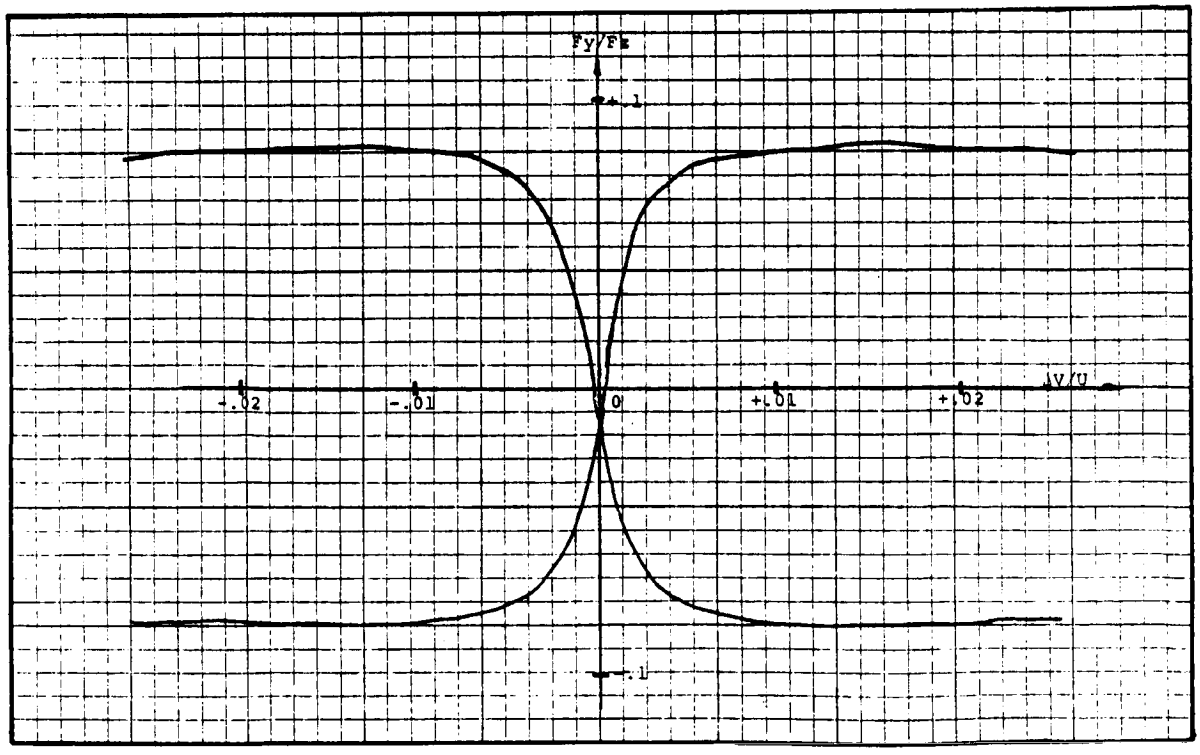

Figure 2-19: Side slip traction curve for SANTO-TRAC 50 under the following conditions; speed =20 m/sec; Hertz pressure =1.0 GPa; inlet temperature =70 'C; aspect ratio k=5.0 and spin angle =6 degrees. The curve was obtained on the low speed traction tester.

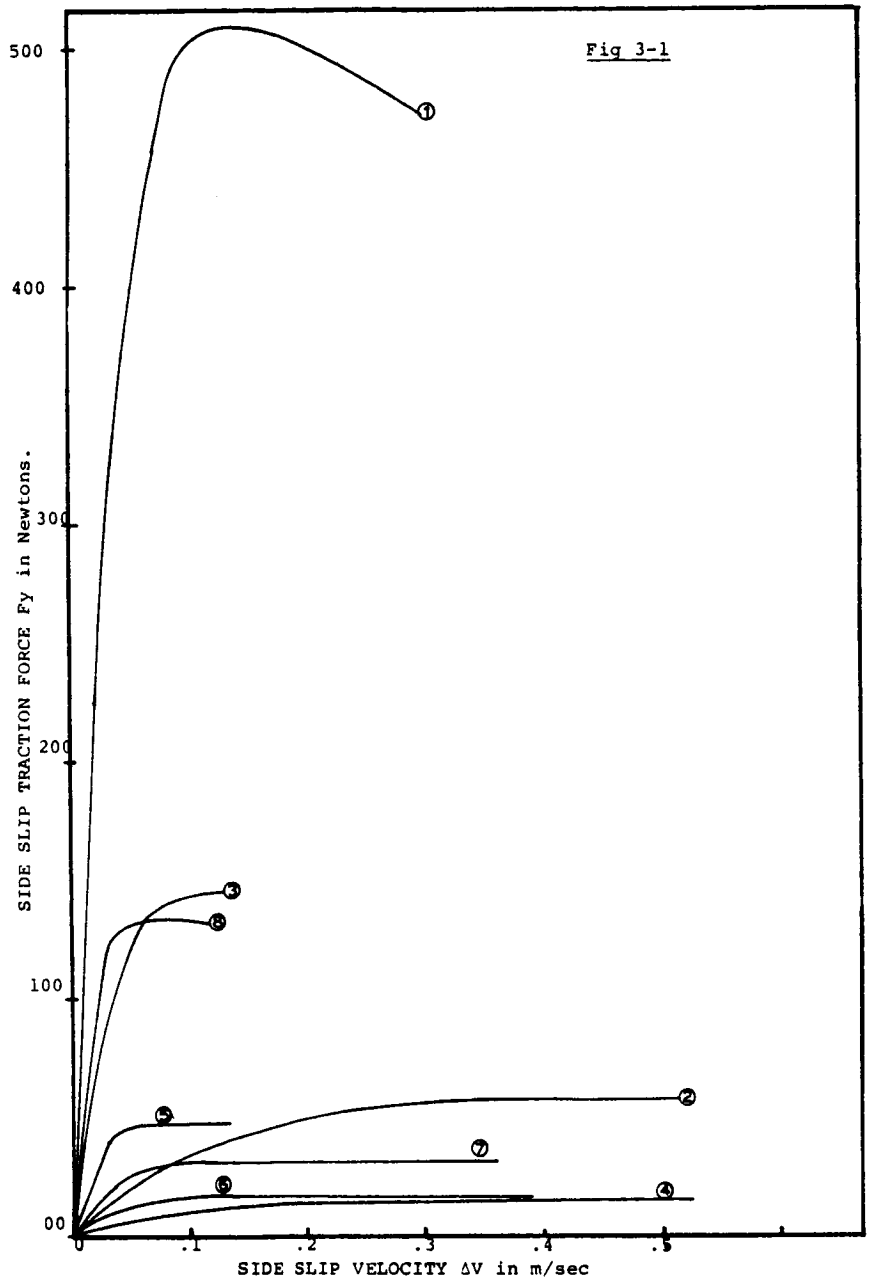

Figure 3-1: Example of the typical side slip traction curves measured in this investigation. The following conditions apply;

Fluid type (-)	curve number (-)	inlet temp (C)	Hertz press. (GPa)	speed U (m/sec)	aspect ratio (-)	normal load (N)
SANTO 50	1	32	1.45	20	5	5000
"	2	69	1.0	80	5	1500
"	3	29	1.9	20	1	1400
"	4	69	1.0	80	1	200
TDF-88	5	30	1.9	10	1	416
" "	6	70	1.45	30	1	185
"	7	70	1.0	30	5	460
"	8	33	1.45	10	5	1400

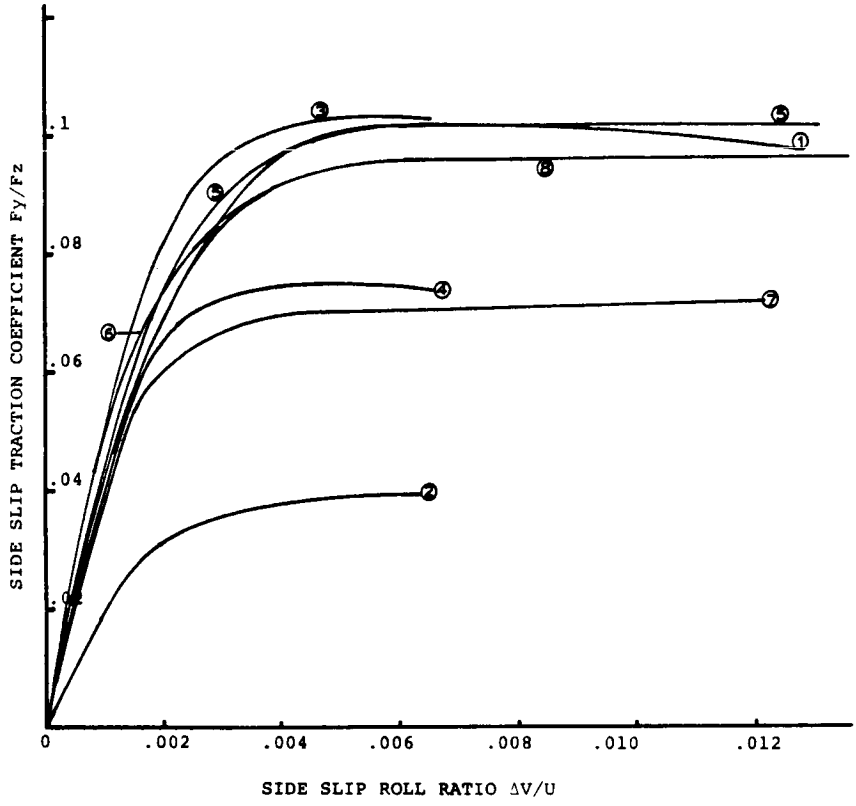

Figure 3-2: The typical traction curves of figure 3-1 plotted in the form of traction coefficient versus slide roll ratio. The curve numbering is the same as in the previous figure.

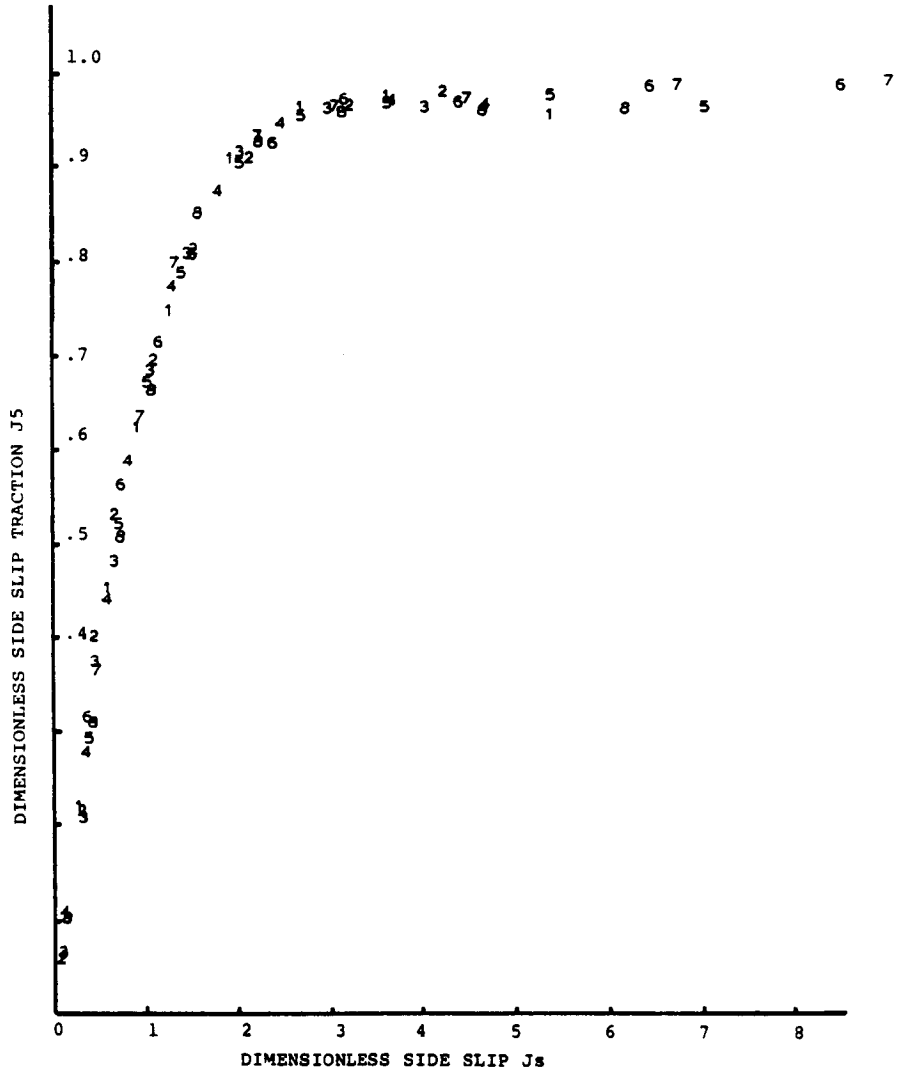

Figure 3-3: Traction curves reduced to the standard form for the Elastic/Plastic traction model. The numbers represent experimental data points from the 8 typical traction curves as shown in figure 3-1.

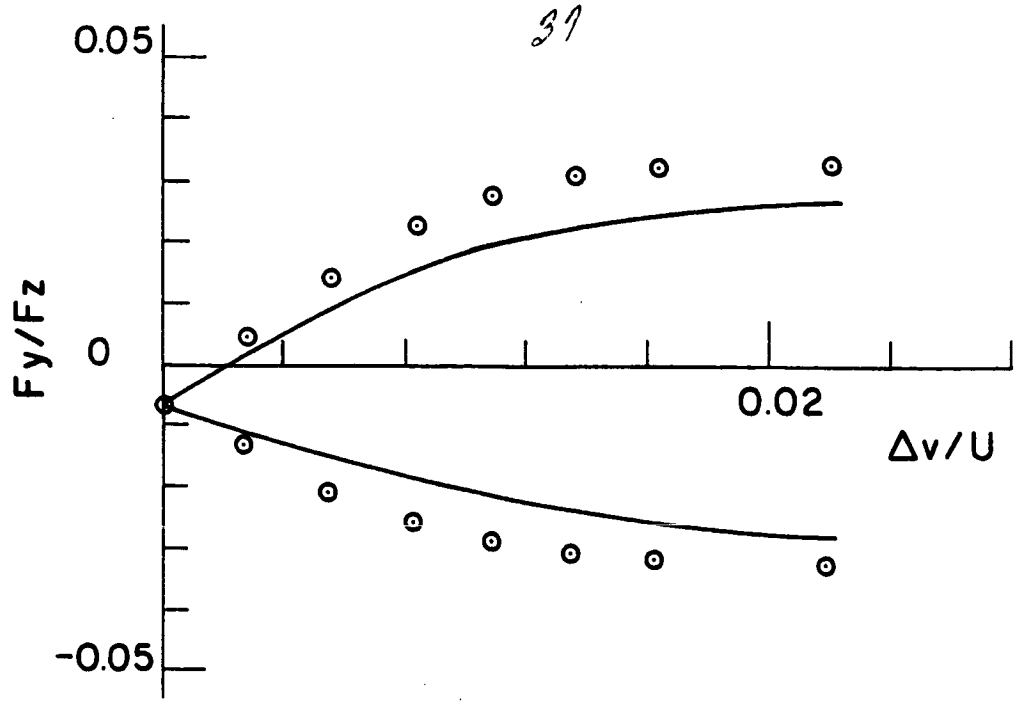

Figure 4-1: Comparison between theoretical and experimental side slip with spin traction for SANTO-TRAC 50 under the following conditions; speed =80 m/sec; Hertz pressure =1.45 GPa; inlet temperature =73 'C; aspect ratio k=5.0 and spin angle =30 degrees. Circles represent experimental values .

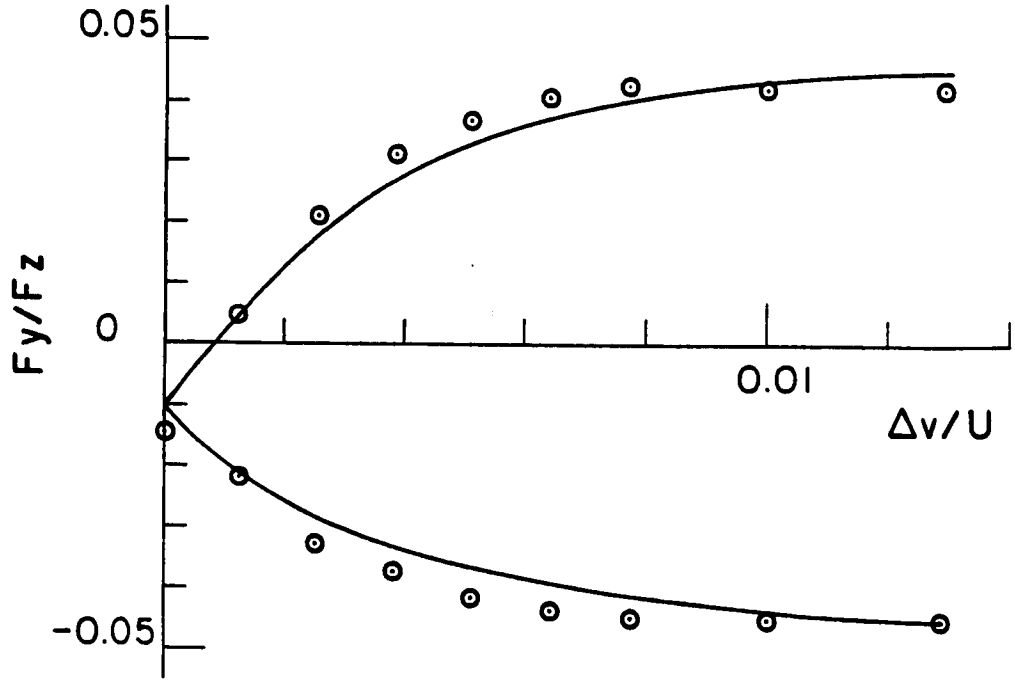

Figure 4-2: Comparison between theoretical and experimental side slip with spin traction for TDF-88 under the following conditions; speed =20 m/sec; Hertz pressure =1.0 GPa; inlet temperature =50 'C; aspect ratio k=5.0 and spin angle =15 degrees. Circles represent experimental values .

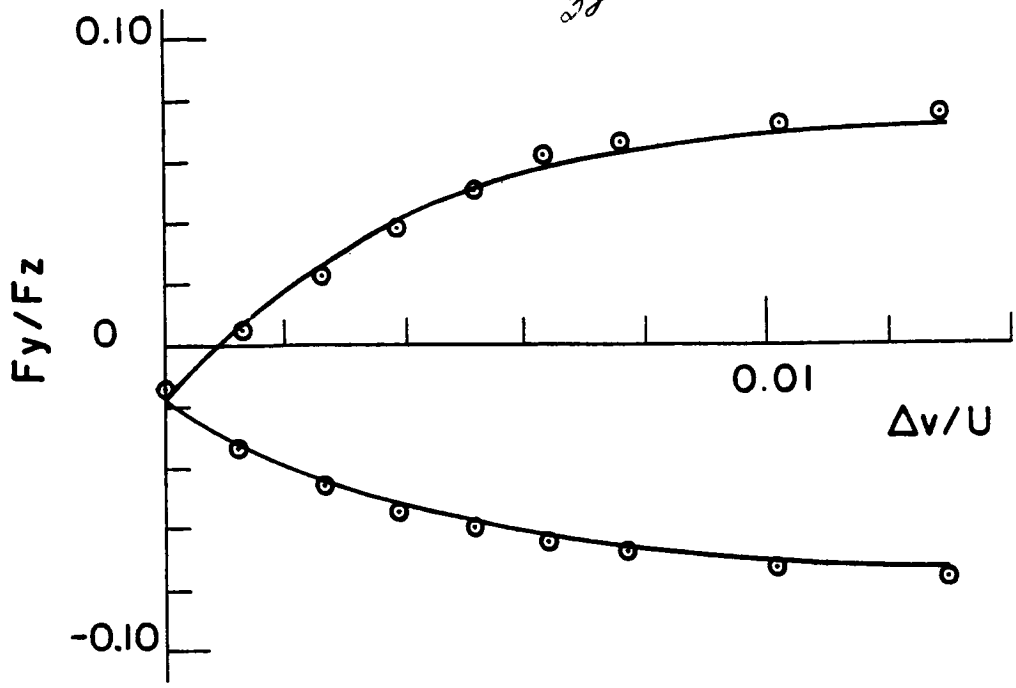

Figure 4-3: Comparison between theoretical and experimental side slip with spin traction for SANTO-TRAC 50 under the following conditions; speed =20 m/sec; Hertz pressure =1.9 GPa; inlet temperature =70 'C; aspect ratio k=1.0 and spin angle =6 degrees. Circles represent experimental values .

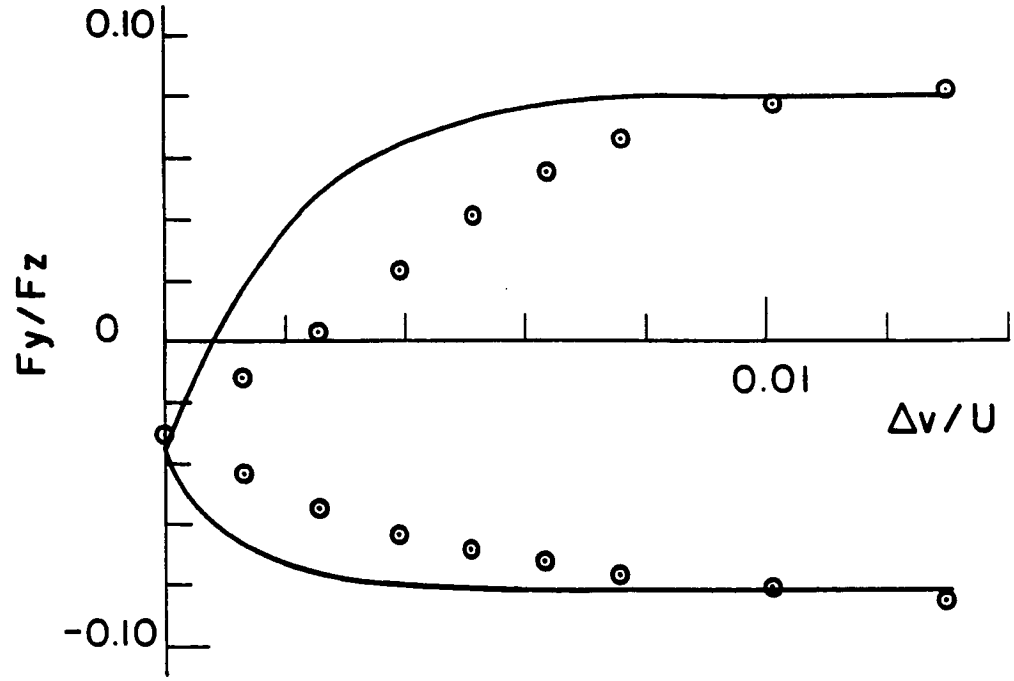

Figure 4-4: Comparison between theoretical and experimental side slip with spin traction for SANTO-TRAC 50 under the following conditions; speed =20 m/sec; Hertz pressure =1.22 GPa; inlet temperature =32.5 'C; aspect ratio k=1.0 and spin angle =16 degrees. Circles represent experimental values .

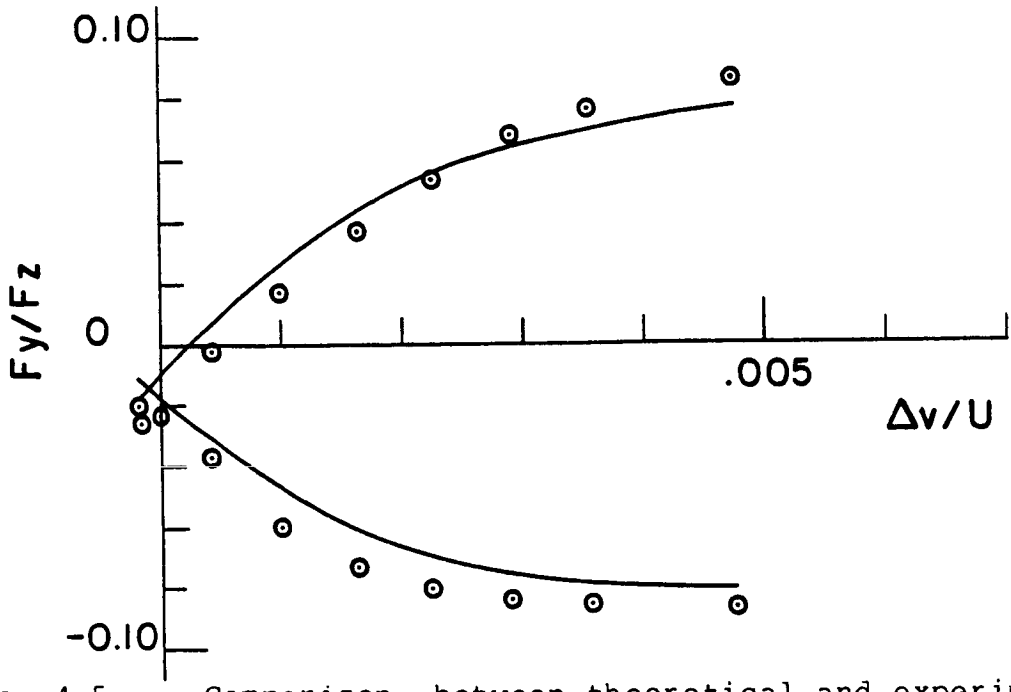

Figure 4-5: Comparison between theoretical and experimental side slip with spin traction for TDF-88 under the following conditions; speed =20 m/sec; Hertz pressure =1.9 GPa; inlet temperature =70 'C; aspect ratio k=1.0 and spin angle =6 degrees. Circles represent experimental values .

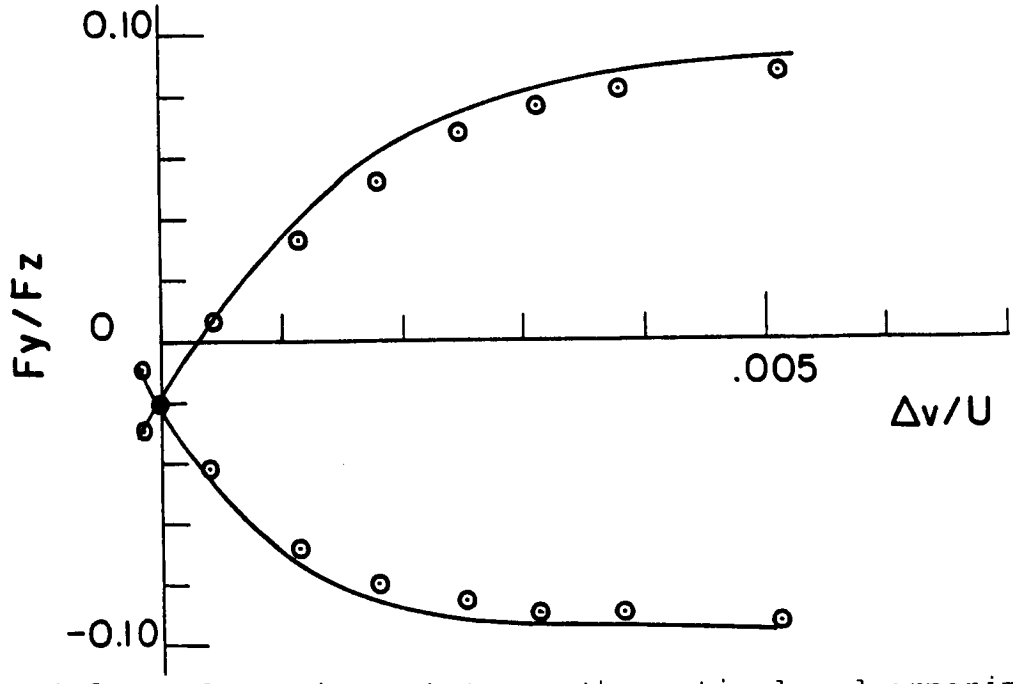

Figure 4-6: Comparison between theoretical and experimental side slip with spin traction for TDF-88 under the following conditions; speed =80 m/sec; Hertz pressure =1.0 GPa; inlet temperature =50 'C; aspect ratio k=5.0 and spin angle =15 degrees. Circles represent experimental values .

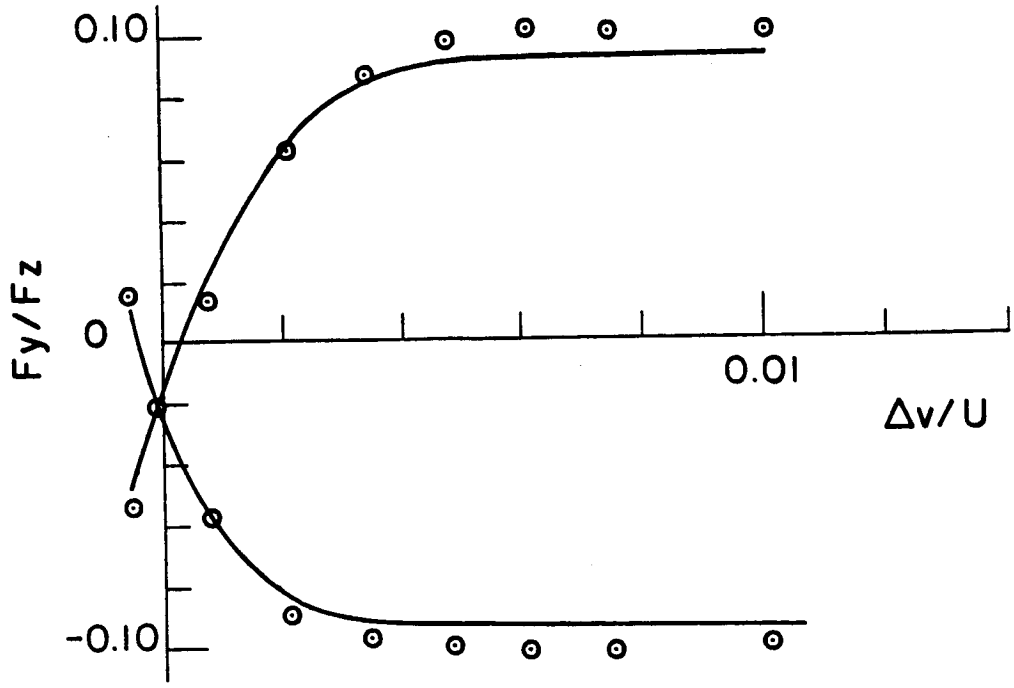

Figure 4-7: Comparison between theoretical and experimental side slip with spin traction for TDF-88 under the following conditions; speed =30 m/sec; Hertz pressure =1.45 GPa; inlet temperature =29 'C; aspect ratio k=1.0 and spin angle =6 degrees. Circles represent experimental values .

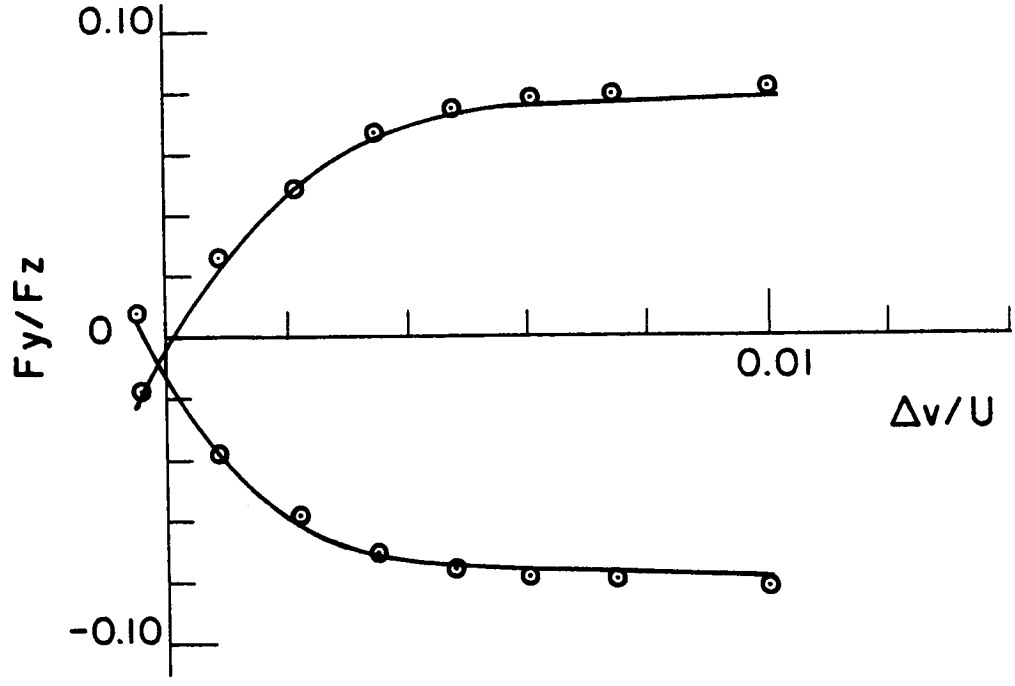

Figure 4-8: Comparison between theoretical and experimental side slip with spin traction for SANTO-TRAC 50 under the following conditions; speed =20 m/sec; Hertz pressure =1.0 GPa; inlet temperature =70 'C; aspect ratio k=5.0 and spin angle =6 degrees. Circles represent experimental values

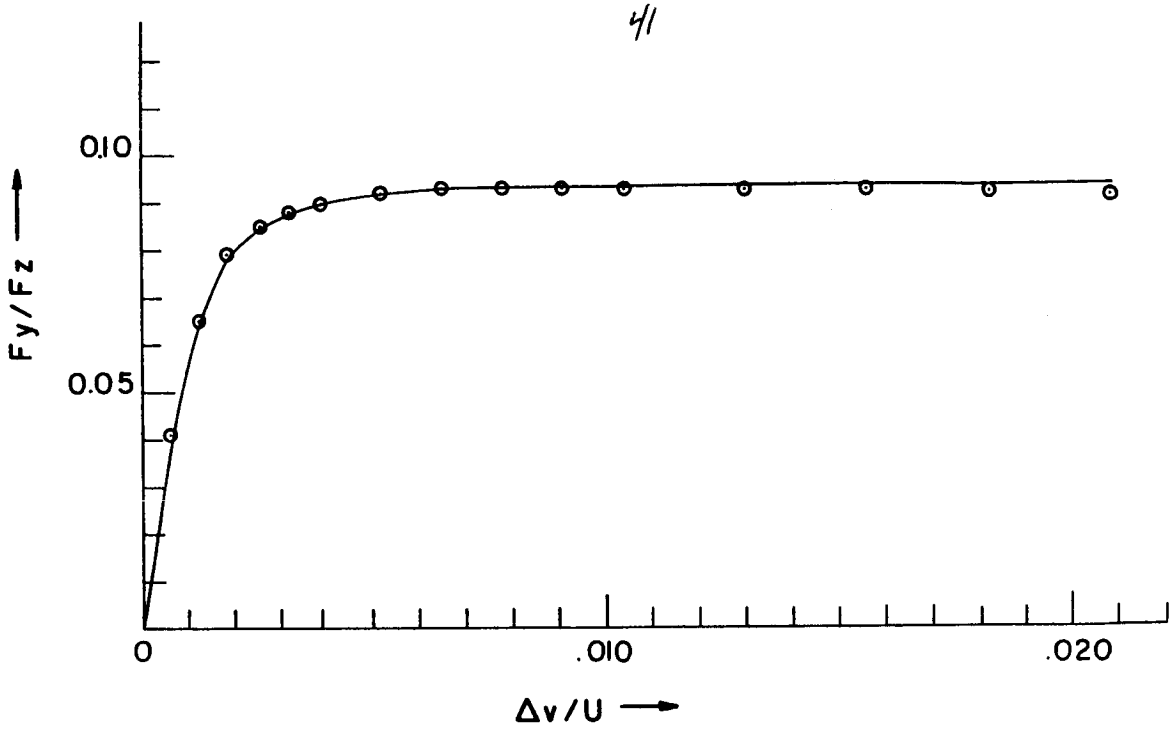

Figure 4-9: Comparison between theoretical and experimental side slip traction for SANTO-TRAC 50 under the following conditions; speed =20 m/sec; Hertz pressure =2.53 GPa; inlet temperature =70; aspect ratio k= .5 . Circles indicate experimental values.

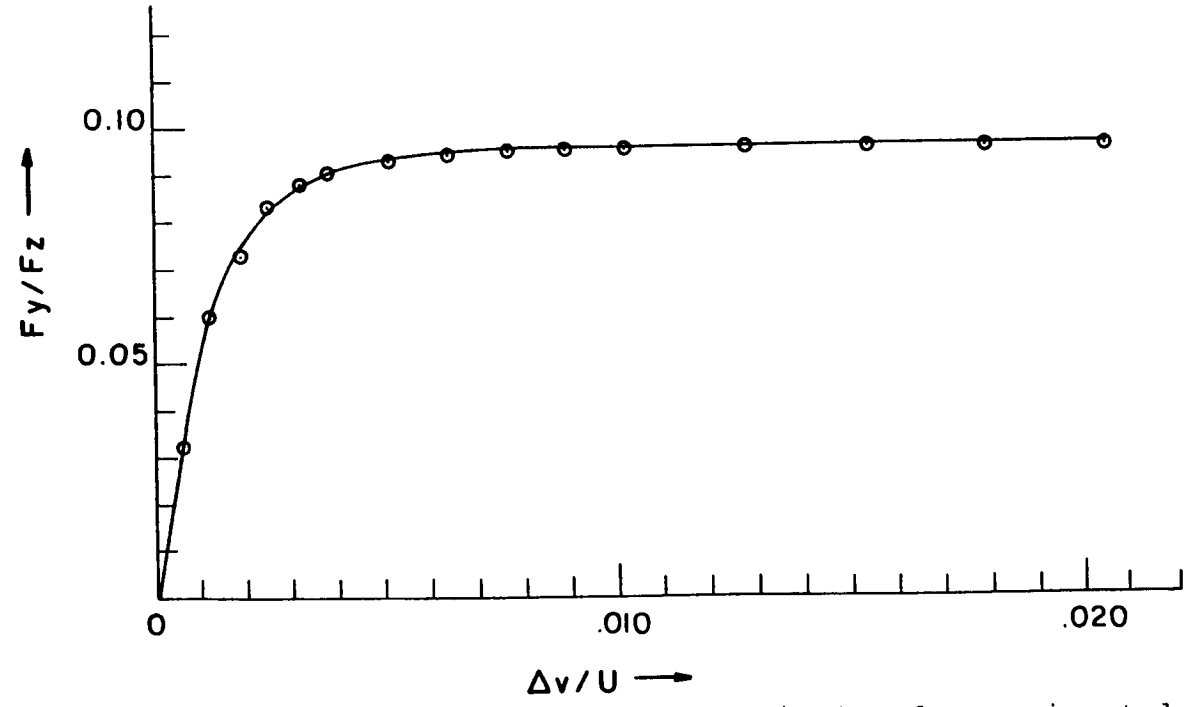

Figure 4-10: Comparison between theoretical and experimental side slip traction for SANTO-TRAC 50 under the following conditions; speed =20 m/sec; Hertz pressure =1.96GPa; inlet temperature =70; aspect ratio k=1.0 . Circles indicate experimental values.

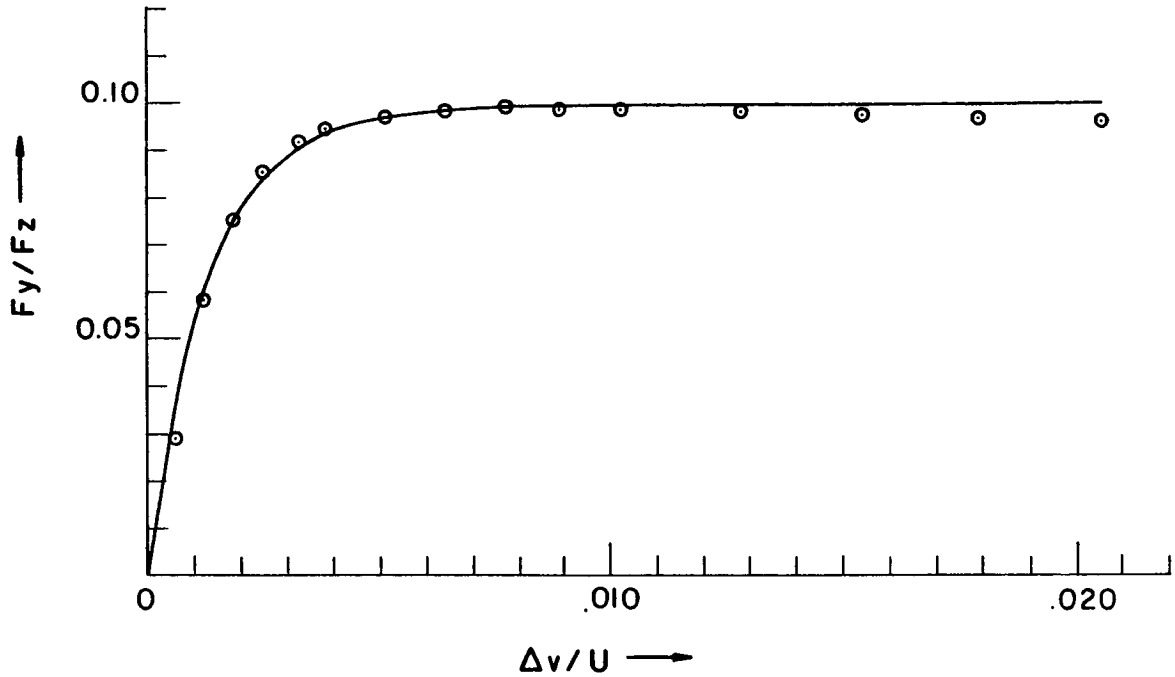

Figure 4-11: Comparison between theoretical and experimental side slip traction for SANTO-TRAC 50 under the following conditions; speed =20 m/sec; Hertz pressure =1.45 GPa; inlet temperature =70; aspect ratio k=2.0 . Circles indicate experimental values.

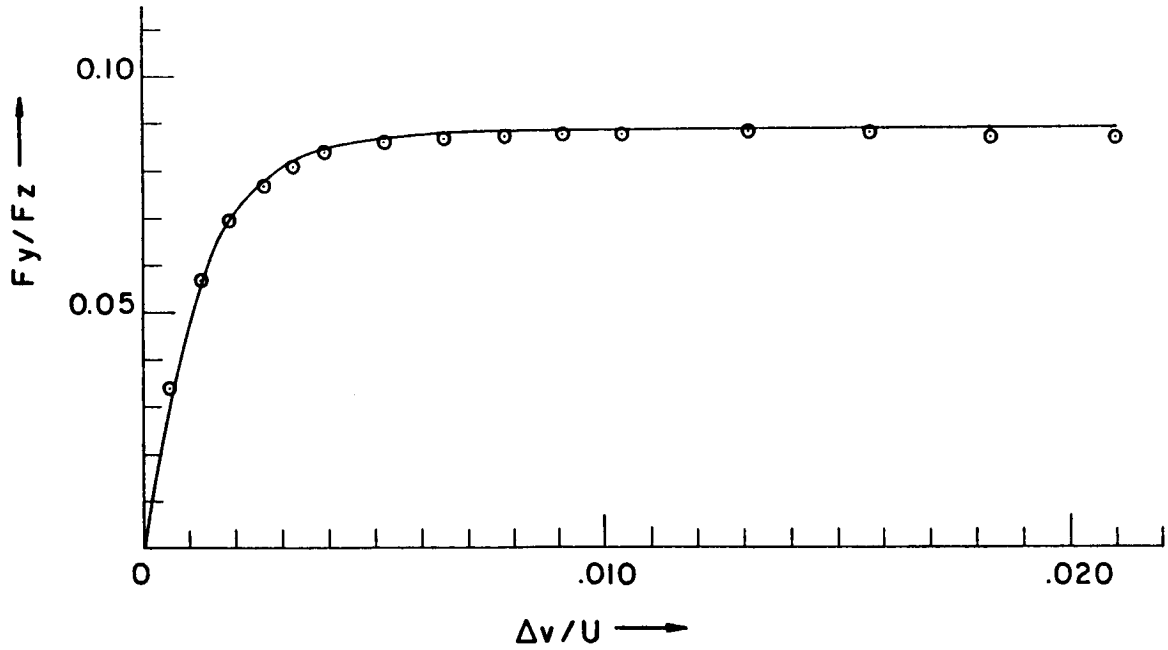

Figure 4-12: Comparison between theoretical and experimental side slip traction for SANTO-TRAC 50 under the following conditions; speed =20 m/sec; Hertz pressure =1.22 GPa; inlet temperature =70; aspect ratio k=5.0 . Circles indicate experimental values.

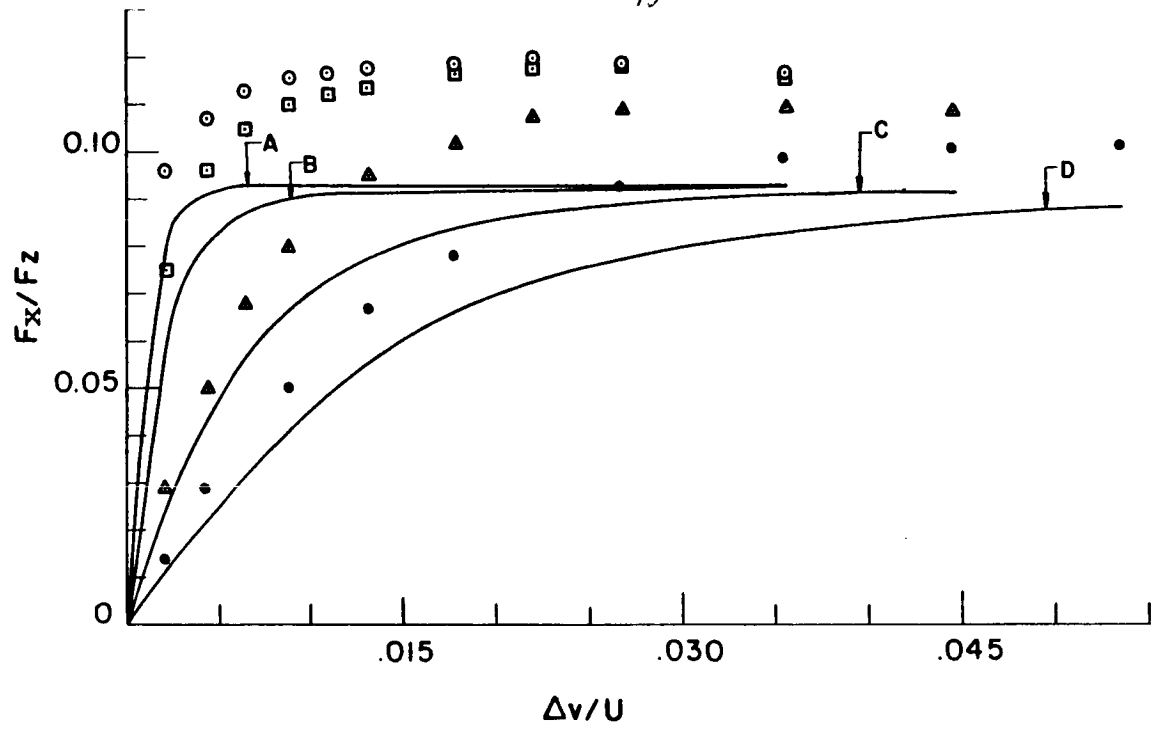

Figure 4-13: Comparison between theoretical and experimental side slip and longitudinal slip traction for SANTO-TRAC 50 under the following conditions; speed =20 m/sec; Hertz pressure =2.53 GPa; inlet temperature =70; aspect ratio k= .5 . The following side slip was applied; ⊙ =0.0% (curve A predicted), ⊡ =.285% (curve B predicted), Δ =.920% (curve C predicted), ● =1.86% (curve D predicted).

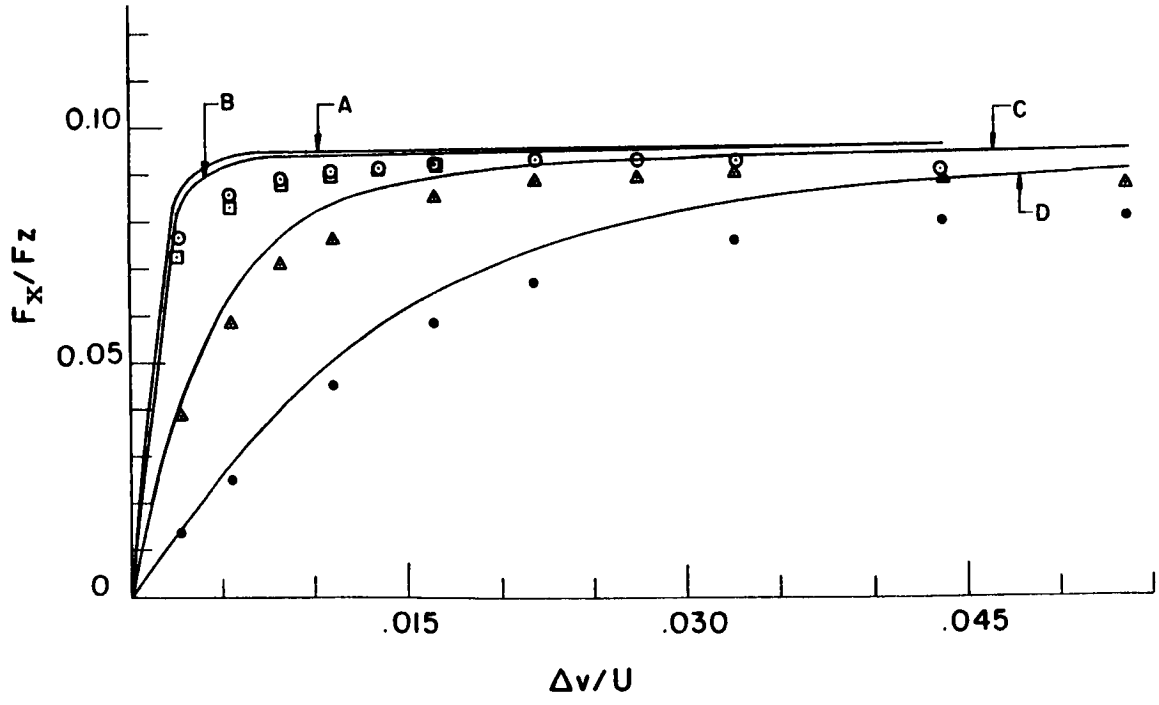

Figure 4-14: Comparison between theoretical and experimental side slip and longitudinal slip traction for SANTO-TRAC 50 under the following conditions; speed =20 m/sec; Hertz pressure =1.90 GPa; inlet temperature =70; aspect ratio k=1.0 . The following side slip was applied; ⊙ =0.0% (curve A predicted), ⊡ =.142% (curve B predicted), Δ =.668% (curve C predicted), ● =1.75% (curve D predicted).

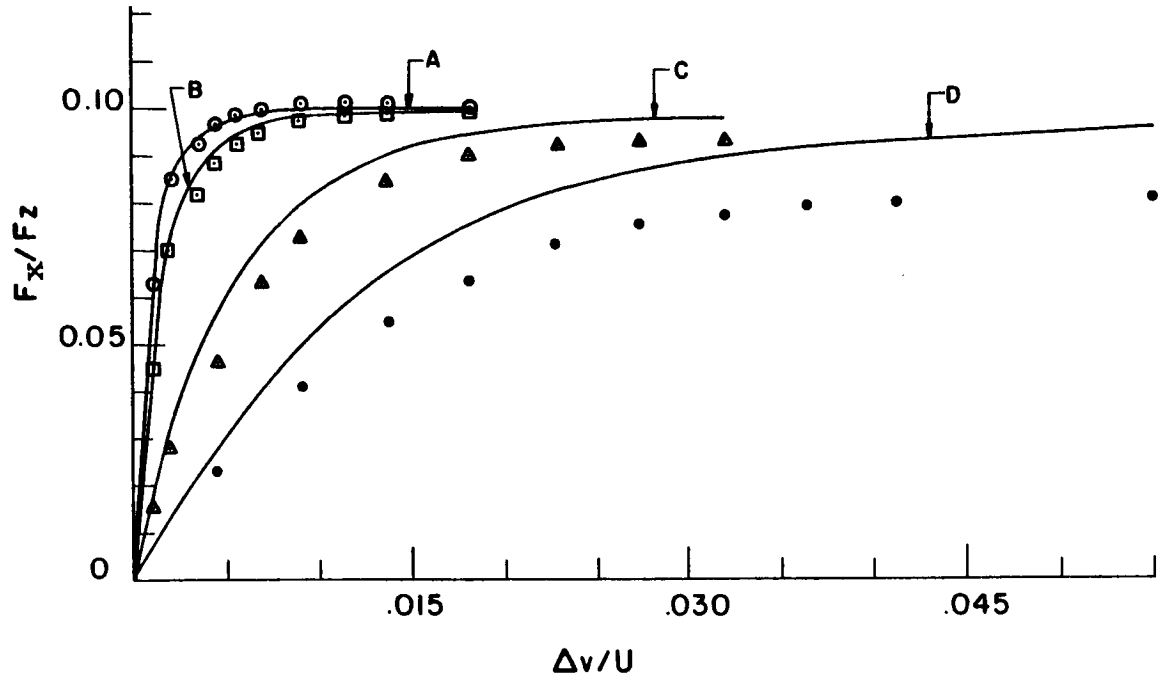

Figure 4-15: Comparison between theoretical and experimental side slip and longitudinal slip traction for SANTO-TRAC 50 under the following conditions; speed =20 m/sec; Hertz pressure =1.45 GPa; inlet temperature =70; aspect ratio k=2.0 . The following side slip was applied; ⊙=0.0% (curve A predicted), ⊡=.207% (curve B predicted), Δ=.827% (curve C predicted), ●=1.94% (curve D predicted).

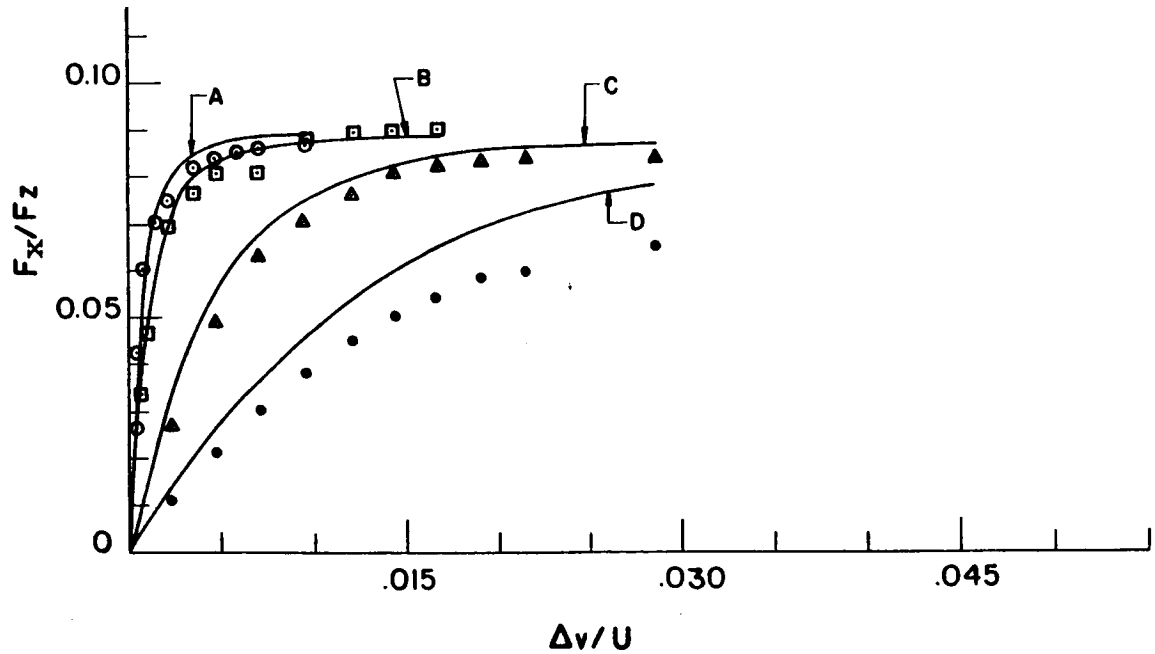

Figure 4-16: Comparison between theoretical and experimental side slip and longitudinal slip traction for SANTO-TRAC 50 under the following conditions; speed =20 m/sec; Hertz pressure =1.22 GPa; inlet temperature =70; aspect ratio k=5.0 . The following side slip was applied; ⊙=0.0% (curve A predicted), ⊡=.180% (curve B predicted), Δ=.741% (curve C predicted), ●=1.89% (curve D predicted).

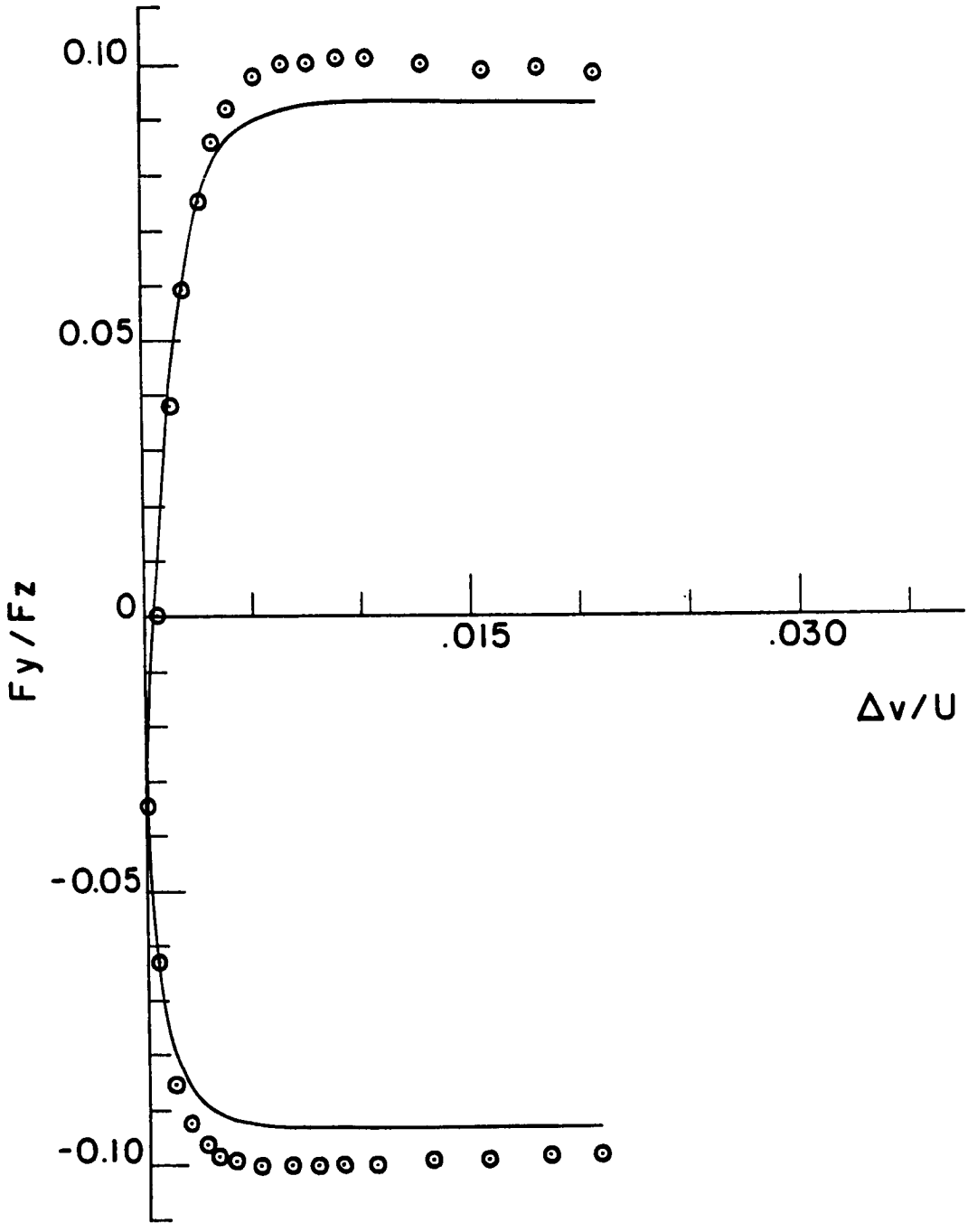

Figure 4-17: Comparison between theoretical and experimental side slip with spin traction for SANTO-TRAC 50 under the following conditions; speed =20 m/sec; Hertz pressure =2.53 GPa; inlet temperature =70; aspect ratio k= .5 and 6 degrees spin. The circles represent experimental values.

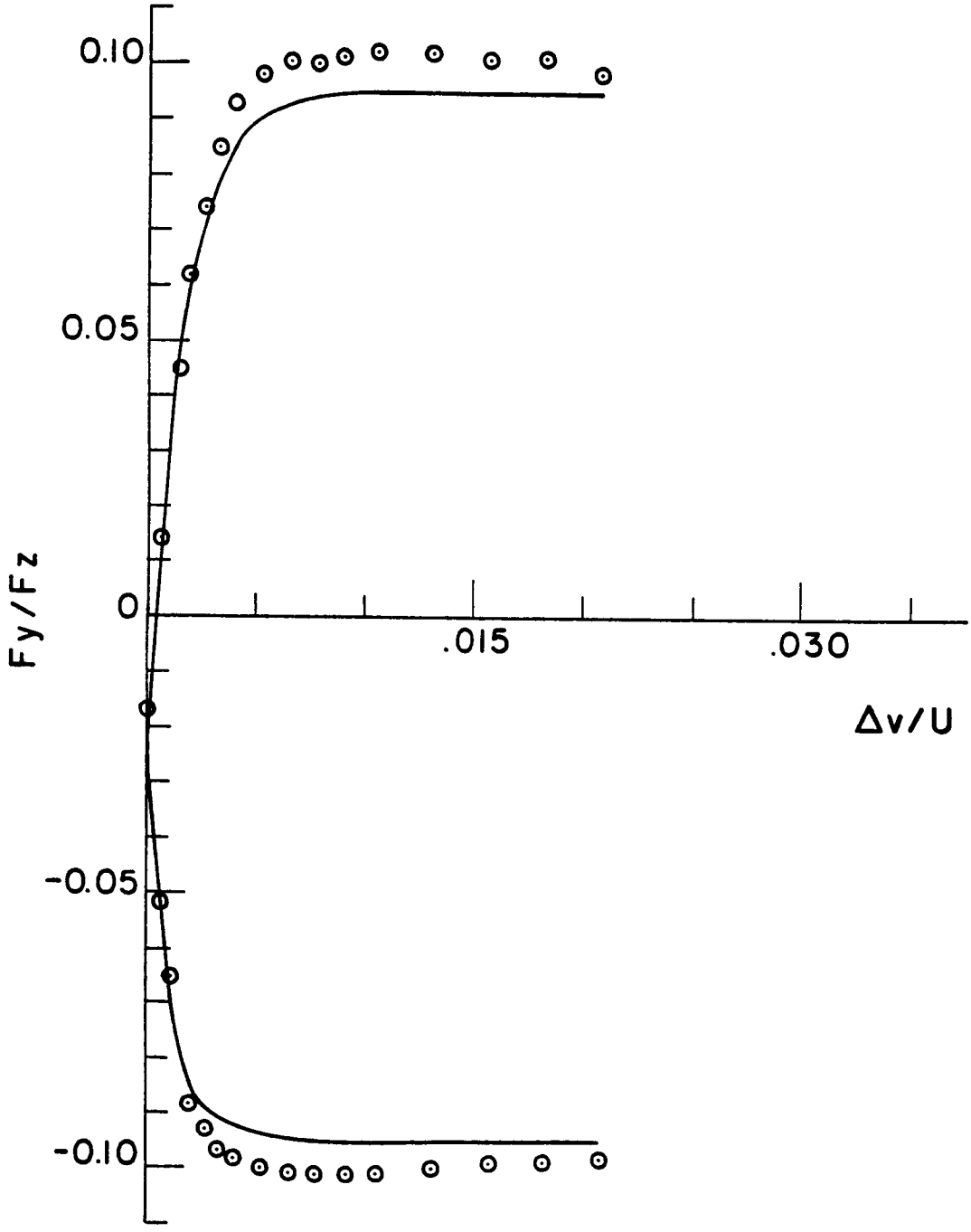

Figure 4-18: Comparison between theoretical and experimental side slip with spin traction for SANTO-TRAC 50 under the following conditions; speed =20 m/sec; Hertz pressure =1.90 GPa; inlet temperature =70; aspect ratio k=1.0 and 6 degrees spin. The circles represent experimental values.

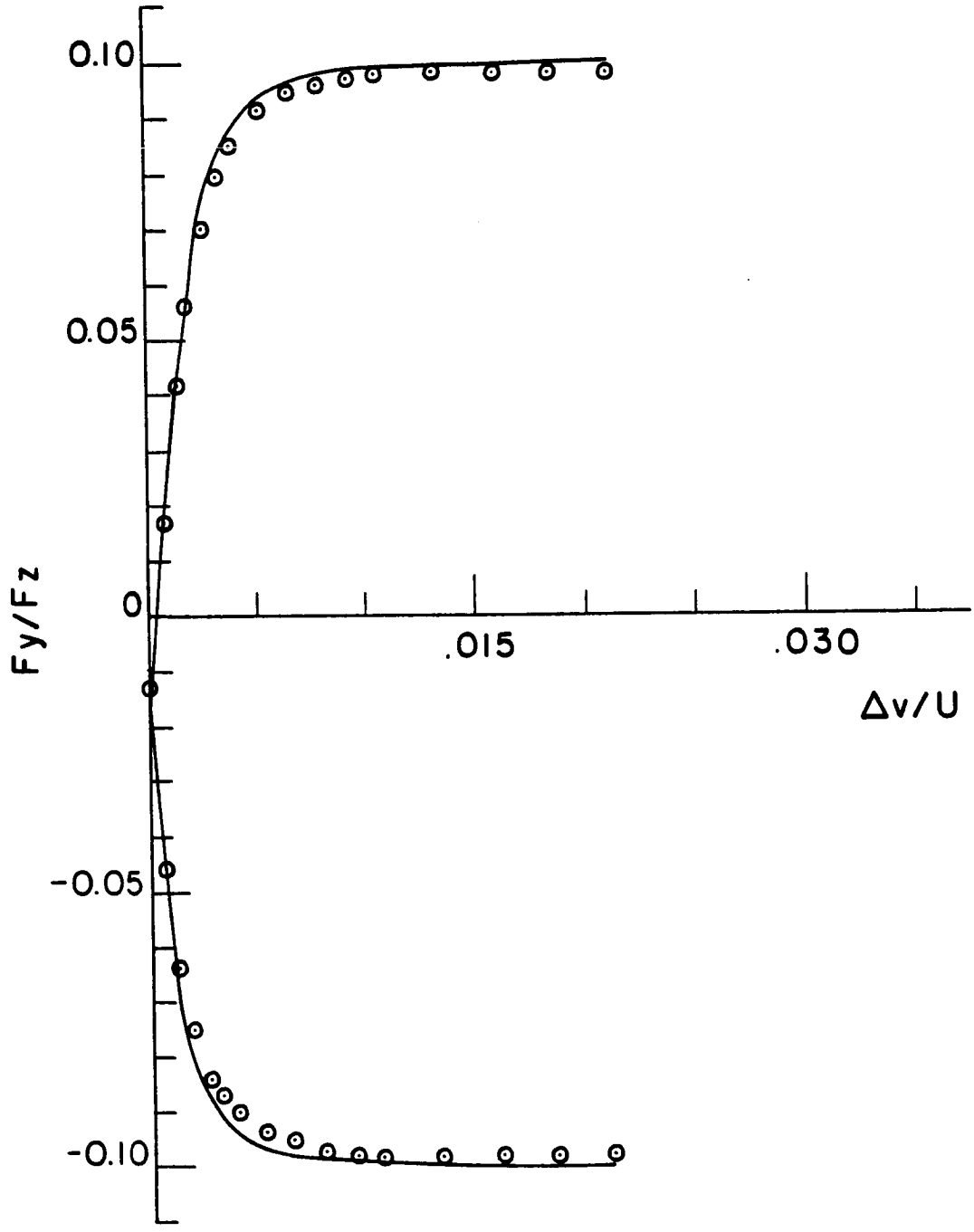

Figure 4-19: Comparison between theoretical and experimental side slip with spin traction for SANTO-TRAC 50 under the following conditions; speed =20 m/sec; Hertz pressure =1.45 GPa; inlet temperature =70; aspect ratio k=2.0 and 6 degrees spin. The circles represent experimental values.

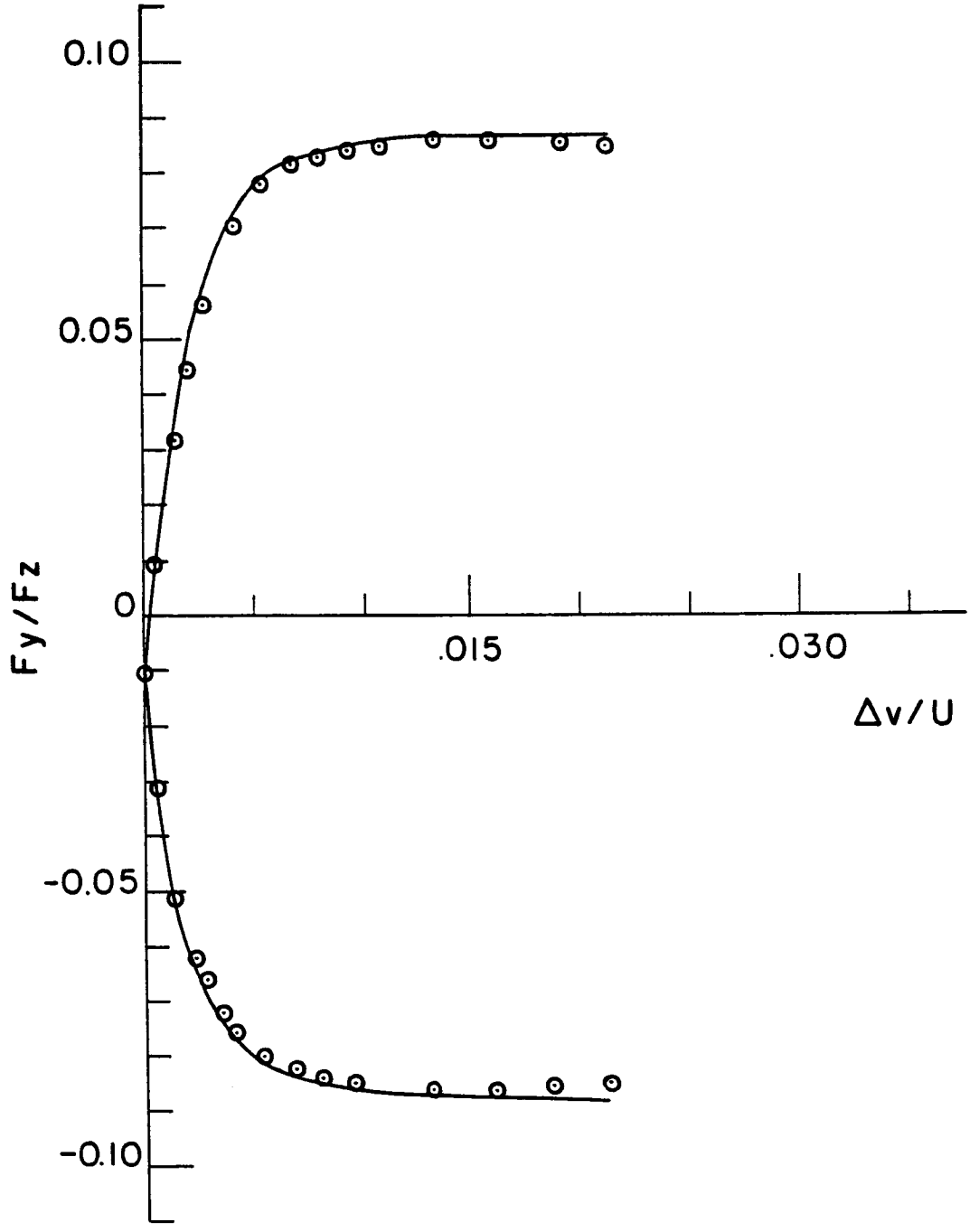

Figure 4-20: Comparison between theoretical and experimental side slip with spin traction for SANTO-TRAC 50 under the following conditions; speed =20 m/sec; Hertz pressure =1.22 GPa; inlet temperature =70; aspect ratio k=5.0 and 6 degrees spin. The circles represent experimental values.

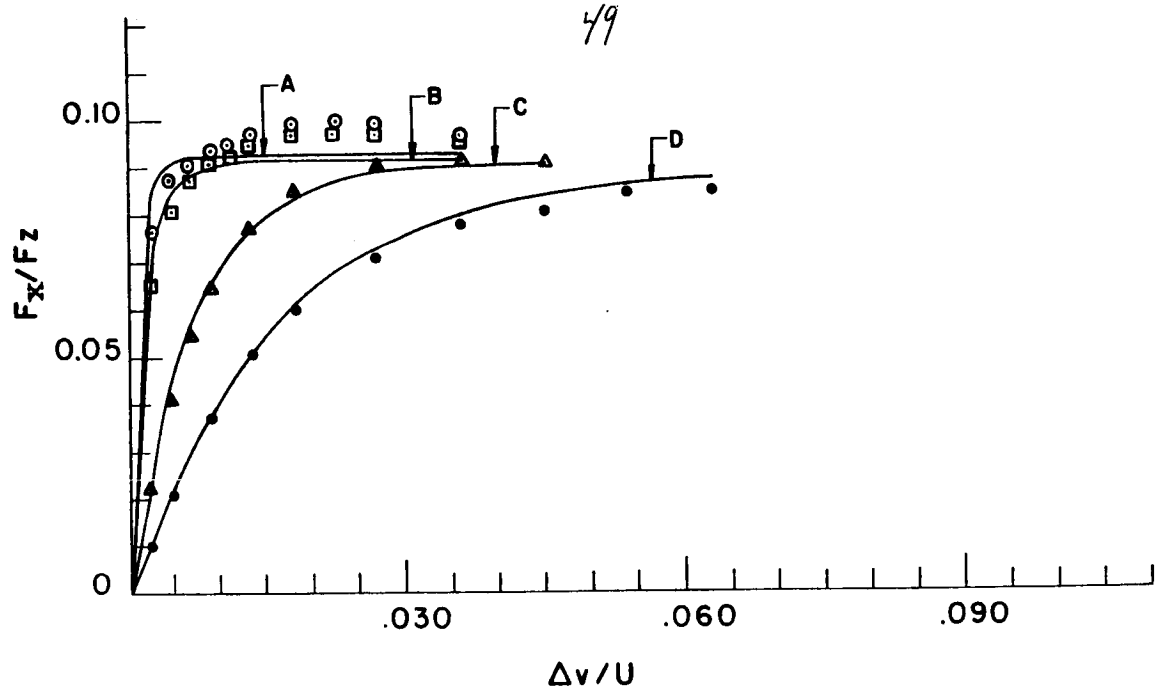

Figure 4-21: Comparison between theoretical and experimental side slip, spin and longitudinal slip traction for SANTO-TRAC 50 under the following conditions; speed =20 m/sec; Hertz pressure =2.53 GPa; inlet temperature =70; aspect ratio k= .5 and 6 degrees spin. The following side slip was applied; ⊙=0.0% (curve A predicted), ⊡=.241%(curve B predicted), ▲=.933% (curve C predicted), ●=2.17% (curve D predicted).

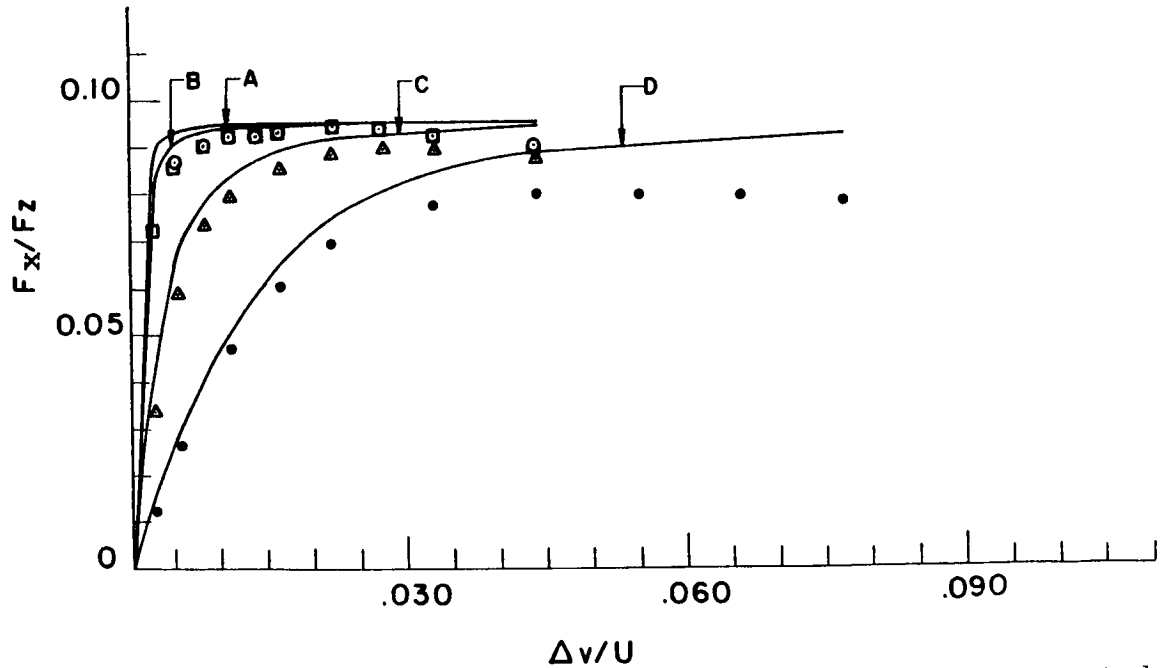

Figure 4-22: Comparison between theoretical and experimental side slip, spin and longitudinal slip traction for SANTO-TRAC 50 under the following conditions; speed =20 m/sec; Hertz pressure =1.90 GPa; inlet temperature =70; aspect ratio k=1.0 and 6 degrees spin. The following side slip was applied; ⊙=0.0% (curve A predicted), ⊡=.095%(curve B predicted), ▲=.655% (curve C predicted), ●=1.75% (curve D predicted).

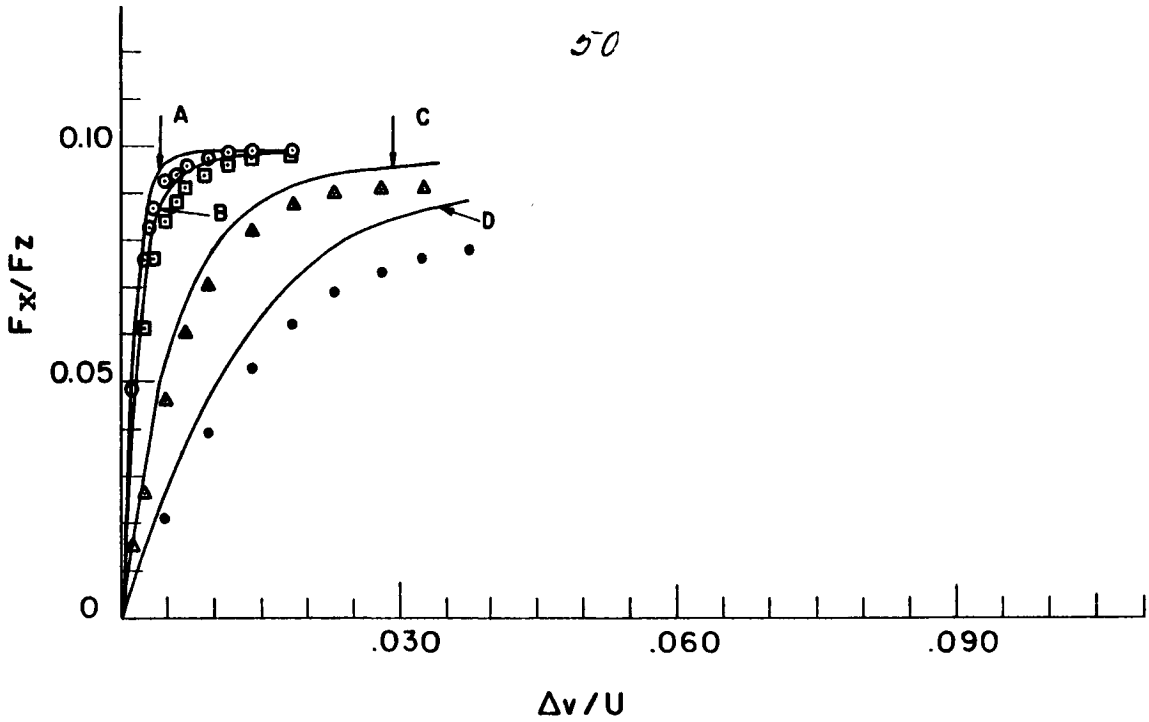

Figure 4-23: Comparison between theoretical and experimental side slip, spin and longitudinal slip traction for SANTO-TRAC 50 under the following conditions; speed =20 m/sec; Hertz pressure =1.45 GPa; inlet temperature =70; aspect ratio k=2.0 and 6 degrees spin. The following side slip was applied; ⊙=0.0% (curve A predicted), ⊡=.224%(curve B predicted), ▲ =.899% (curve C predicted), ●=2.06% (curve D predicted).

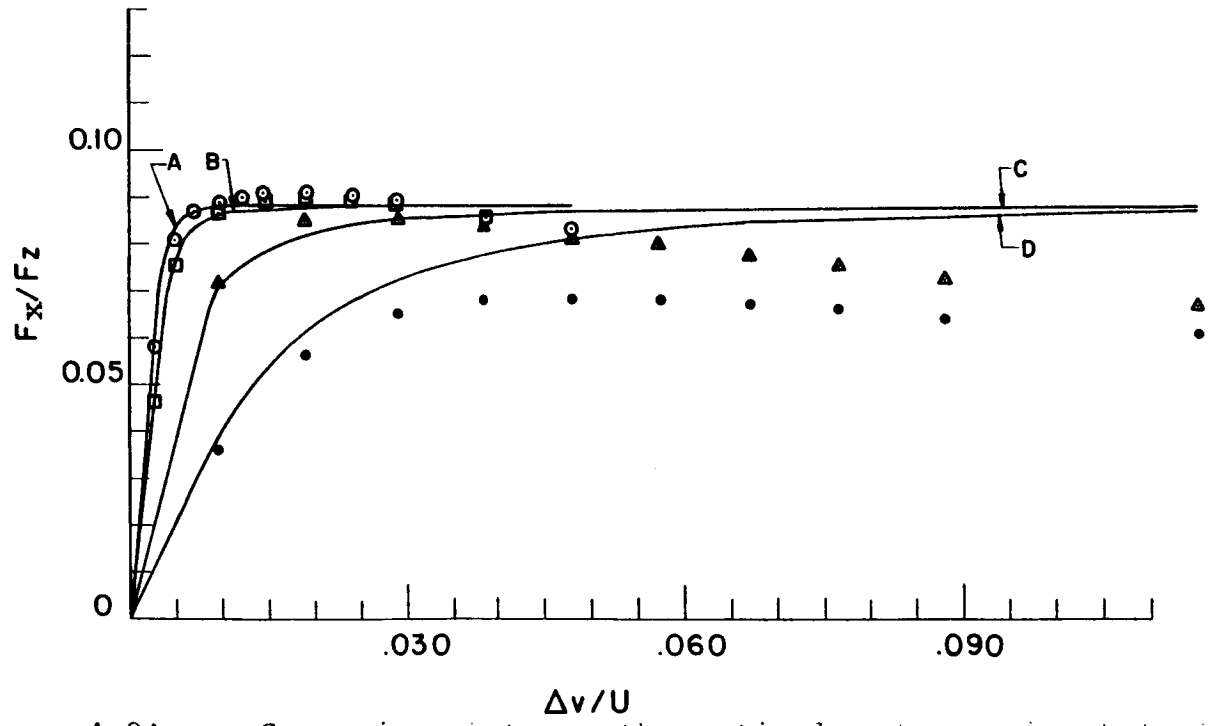

Figure 4-24: Comparison between theoretical and experimental side slip, spin and longitudinal slip traction for SANTO-TRAC 50 under the following conditions; speed =20 m/sec; Hertz pressure =1.22 GPa; inlet temperature =70; aspect ratio k=5.0 and 6 degrees spin. The following side slip was applied; ⊙=0.0% (curve A predicted), ⊡=.192%(curve B predicted), ▲ =.720% (curve C predicted), ●=2.0% (curve D predicted).

APPENDIX I

This appendix contains the data for the traction curves shown in figures 2-4-2-12 on both the standard parameters and the reduced parameters based on the elastic/plastic model.

TRACE NUMBER 79053101

SANTOTRAC 50

ASPECT RATIO = 5
TRACTION SLOPE (-) = 45
PEAK TRACTION COEF. (-) = .105
NORMAL LOAD (N) = 5000
HERTZ PRESSURE (GPA) = 1.45
INLET TEMPERATURE (C) = 32
SURFACE SPEED (M/S) = 20

JS	J5	DV/U	FY/FZ	DV	FY
.241745351	.21	4.788E-04	.02205	9.57599999E-03	110.25
.587095851	.448	1.1628E-03	.04704	.023256	235.2
.932446352	.63	1.8468E-03	.06615	.036936	330.75
1.27779685	.749	2.5308E-03	.078645	.050616	393.225
1.96849785	.91	3.8988E-03	.09555	.0779759999	477.75
2.65919886	.966	5.2668E-03	.10143	.105336	507.15
3.69525036	.973	7.3188E-03	.102165	.146376	510.825
5.42200286	.952	.0107388	.09996	.214776	499.8
7.14875537	.917	.0141588	.096285	.283176	481.425

TRACE NUMBER 79012603
ASPECT RATIO = 5
TRACTION SLOPE (-) = 23
PEAK TRACTION COEF. (-) = .04
NORMAL LOAD (N) = 1500
HERTZ PRESSURE (GPA) = 1
INLET TEMPERATURE (C) = 69
SURFACE SPEED (M/S) = 80

JS	J5	DV/U	FY/FZ	DV	FY
.062998697	.0536666667	9.3E-05	2.14666667E-03	7.44E-03	3.22
.272994354	.214666667	4.03E-04	8.58666667E-03	.03224	12.90
.48299001	.4025	7.13E-04	.0161	.05704	24.15
.692985666	.52325	1.023E-03	.02093	.08184	31.395
1.11297698	.697666667	1.643E-03	.0279066667	.13144	41.86
1.53296829	.818416667	2.263E-03	.0327366667	.18104	49.105
2.16295526	.912333333	3.193E-03	.0364933333	.25544	54.74
3.21293355	.966	4.743E-03	.03864	.37944	57.96
4.26291183	.979416667	6.293E-03	.0391766667	.50344	58.765

SANTOTRAC 50

TRACE NUMBER 79032904
ASPECT RATIO = 1
TRACTION SLOPE (-) = 58
PEAK TRACTION COEF. (-) = .107
NORMAL LOAD (N) = 1400
HERTZ PRESSURE (GPA) = 1.9
INLET TEMPERATURE (C) = 29
SURFACE SPEED (M/S) = 20

JS	J5	DV/U	FY/FZ	DV	FY
.0791856844	.0630841121	1.24E-04	6.75E-03	2.48E-03	9.45
.277149895	.214485981	4.34E-04	.02295	8.68E-03	32.13
.475114107	.346962617	7.44E-04	.037125	.01488	51.975
.673078318	.485747664	1.054E-03	.051975	.02108	72.765
1.06900674	.681308411	1.674E-03	.0729	.03348	102.06
1.46493516	.813785047	2.294E-03	.087075	.04588	121.905
2.0588278	.921028037	3.224E-03	.09855	.06448	137.97
3.04864885	.965186916	4.774E-03	.103275	.0954799999	144.595
4.0384699	.965186916	6.324E-03	.103275	.12648	144.595

TRACE NUMBER 79031106
ASPECT RATIO = 1
TRACTION SLOPE (-) = 50
PEAK TRACTION COEF. (-) = .077
NORMAL LOAD (N) = 200
HERTZ PRESSURE (GPA) = 1
INLET TEMPERATURE (C) = 69
SURFACE SPEED (M/S) = 80

JS	J5	DV/U	FY/FZ	DV	FY
.118574623	.104707792	1.55E-04	8.0625E-03	.0124	1.6125
.355723868	.279220779	4.65E-04	.0215	.0372	4.3
.592873113	.439772727	7.75E-04	.0338625	.062	6.7725
.830022358	.593344156	1.085E-03	.0456875	.0868	9.1375
1.30432085	.781818182	1.705E-03	.0602	.1364	12.04
1.77861934	.879545455	2.325E-03	.067725	.186	13.545
2.49006708	.949350649	3.255E-03	.0731	.2604	14.62
3.6758133	.970292208	4.805E-03	.0747125	.3844	14.9425
4.86155953	.963311689	6.355E-03	.074175	.5084	14.835

ORIGINAL PAGE IS
OF POOR QUALITY

TRACE NUMBER 79111904 TDF 88
ASPECT RATIO = 1
TRACTION SLOPE (-) = 50
PEAK TRACTION COEF. (-) = .105
NORMAL LOAD (N) = 416
HERTZ PRESSURE (GPA) = 1.9
INLET TEMPERATURE (C) = 30
SURFACE SPEED (M/S) = 10

JS	JS	DV/U	FY/FZ	DV	FY
.398533131	.292239011	7.104E-04	.0306850962	7.104E-03	12.765
.730644075	.520947803	1.3024E-03	.0546995193	.013024	22.755
1.06275502	.67342033	1.8944E-03	.0707091346	.018944	29.415
1.39486596	.787774726	2.4864E-03	.0827163462	.024864	34.41
2.05908785	.914835165	3.6704E-03	.0960576923	.036704	39.96
2.72330973	.952953297	4.8544E-03	.100060096	.048544	41.625
3.71964256	.965659341	6.6304E-03	.101394231	.066304	42.18
5.38019728	.978365385	9.5904E-03	.102728365	.095904	42.735
7.04075199	.965659341	.0125504	.101394231	.125504	42.18

TRACE NUMBER 79113006
ASPECT RATIO = 1
TRACTION SLOPE (-) = 55
PEAK TRACTION COEF. (-) = .097
NORMAL LOAD (N) = 185
HERTZ PRESSURE (GPA) = 1.45
INLET TEMPERATURE (C) = 70
SURFACE SPEED (M/S) = 30

JS	JS	DV/U	FY/FZ	DV	FY
.327049236	.310950125	4.89600001E-04	.0301621622	.014688	5.59
.73586078	.559710226	1.1016E-03	.0542918919	.033048	10.044
1.14467232	.715185289	1.7136E-03	.069372973	.051408	12.934
1.55348387	.808470326	2.3256E-03	.0784216217	.069768	14.508
2.37110696	.922485372	3.5496E-03	.0894810811	.106488	16.554
3.18873005	.974310393	4.7736E-03	.0945081081	.143208	17.484
4.41516468	.974310393	6.6096E-03	.0945081081	.198288	17.484
6.4592224	.984675397	9.6696E-03	.0955135135	.290088	17.67
8.50328012	.984675397	.0127296	.0955135135	.381888	17.67

TDF 88

TRACE NUMBER 79113004
ASPECT RATIO = 5
TRACTION SLOPE (-) = 45
PEAK TRACTION COEF. (-) = .072
NORMAL LOAD (N) = 460
HERTZ PRESSURE (GPA) = 1
INLET TEMPERATURE (C) = 70
SURFACE SPEED (M/S) = 30

JS	J5	DV/U	FY/FZ	DV	FY
0	0	0	0	0	0
.450621816	.368357488	6.12E-04	.0265217391	.01836	12.2
.901243632	.635416667	1.224E-03	.04575	.03672	21.045
1.35186545	.801177536	1.836E-03	.0576847826	.05508	26.535
2.25310908	.930102657	3.06E-03	.0669673913	.0918000001	30.805
3.15435271	.966938406	4.284E-03	.0696195652	.12852	32.025
4.50621816	.976147343	6.12E-03	.0702826087	.1836	32.33
6.75932724	.994565217	9.18E-03	.0716086956	.2754	32.94
9.01243633	.994565217	.01224	.0716086956	.3672	32.94

TRACE NUMBER 79110311
ASPECT RATIO = 5
TRACTION SLOPE (-) = 45
PEAK TRACTION COEF. (-) = .1
NORMAL LOAD (N) = 1400
HERTZ PRESSURE (GPA) = 1.45
INLET TEMPERATURE (C) = 33
SURFACE SPEED (M/S) = 10

JS	J5	DV/U	FY/FZ	DV	FY
.12129679	.109714286	2.288E-04	.0109714286	2.288E-03	15.36
.424538765	.322285714	8.008E-04	.0322285714	8.008E-03	45.12
.72778074	.514285714	1.3728E-03	.0514285714	.013728	72
1.03102271	.672	1.9448E-03	.0672	.019448	94.08
1.63750666	.850285714	3.0888E-03	.0850285715	.030888	119.04
2.24399062	.932571429	4.2328E-03	.0932571429	.042328	130.56
3.15371654	.96	5.9488E-03	.096	.059488	134.4
4.66992641	.96	8.8088E-03	.096	.088088	134.4
6.18613629	.96	.0116688	.096	.116688	134.4

APPENDIX II

This appendix contains all the traction data generated on the two fluids under conditions of side slip and spin. Both high speed and low speed machine were used. Test numbers lower than 791103-00 are performed on the high speed machine while test numbers higher than that are all results from the low speed machine. The following data sets are contained in this Appendix;

FLUID	ASPECTRATIO	SPIN ANGLE	#of TESTS	PAGE #
SANTO 50	5	0	31	II-1
" "	5	6	2	II-2
" "	5	15	49	II-3
" "	5	30	26	II-5
" "	2	0	4	II-6
" "	2	6	4	II-7
" "	1	0	38	II-8
" "	1	6	5	II-9
" "	1	15	13	II-10
" "	1	30	19	II-11
TDF-88	5	0	30	II-12
" "	5	6	17	II-13
" "	5	15	3	II-14
" "	2	0	20	II-15
" "	2	6	9	II-16
" "	1	0	40	II-17
" "	1	6	13	II-18
" "	.5	0	15	II-19
" "	.5	6	5	II-20

FILE: DATA FCRIBAN * 11/12/80 19:09:00 UNIVERSITY OF WATERLOO PAGE 001

:READ DATA FCRIBAN A1 DSE191 08/01/80 09:28:00

C
C RESULTS OF SIDE SLIP TRACTION TESTS WITH SANTO 50 FLUID
C USING AN ASPECT RATIO OF 5.0 AND WITH 0 DEGREES SKIN.
C
C
C
C
C
C

	TEST NOS.	SPEED (M/S)	TEMP (C)	SKIN DEG	ASPECT (-)	SIDE SLIP	PRESS. (GPA)	SLOPE (-)	TRACT. COEFF.
1	790726-02	20.0	32.5	00.0	5.0	+/-1.0	1.22	37.0	0.094
2	790726-02	50.0	32.5	00.0	5.0	+/-1.0	1.22	32.0	0.079
3	790726-02	80.0	32.5	00.0	5.0	+/-1.0	1.22	28.0	0.065
4	790726-03	20.0	50.0	00.0	5.0	+/-1.0	1.22	38.0	0.092
5	790726-03	50.0	50.0	00.0	5.0	+/-1.0	1.22	36.5	0.078
6	790726-03	80.0	50.0	00.0	5.0	+/-1.0	1.22	29.2	0.065
7	790601-01	80.0	33.0	00.0	5.0	+/-1.0	1.45	34.9	0.076
8	790531-01	20.0	32.0	00.0	5.0	+/-1.0	1.45	47.4	0.103
9	790531-02	50.0	33.0	00.0	5.0	+/-1.0	1.45	39.8	0.090
10	790531-03	20.0	50.0	00.0	5.0	+/-1.0	1.45	48.5	0.100
11	790531-04	50.0	50.0	00.0	5.0	+/-1.0	1.45	40.0	0.087
12	790531-05	80.0	50.0	00.0	5.0	+/-1.0	1.45	38.0	0.076
13	790531-06	80.0	72.0	00.0	5.0	+/-1.0	1.45	37.2	0.070
14	790531-07	20.0	69.0	00.0	5.0	+/-1.0	1.45	44.0	0.087
15	790531-08	50.0	73.5	00.0	5.0	+/-1.0	1.45	40.0	0.079
16	790123-01	20.0	30.0	00.0	5.0	+/-1.0	1.00	49.1	0.085
17	790123-02	50.0	30.0	00.0	5.0	+/-1.0	1.00	34.7	0.062
18	790123-03	80.0	30.0	00.0	5.0	+/-1.0	1.00	29.2	0.047
19	790123-04	20.0	50.0	00.0	5.0	+/-1.0	1.00	47.9	0.077
20	790123-05	50.0	50.0	00.0	5.0	+/-1.0	1.00	39.4	0.058
21	790123-06	80.0	50.0	00.0	5.0	+/-1.0	1.00	29.6	0.040
22	790126-02	50.0	73.0	00.0	5.0	+/-1.0	1.00	29.0	0.054
23	790126-03	80.0	73.0	00.0	5.0	+/-1.0	1.00	22.2	0.040
24	790628-01	20.0	45.0	00.0	5.0	+/-1.0	1.45	45.0	0.097
25	790628-02	50.0	40.0	00.0	5.0	+/-1.0	1.45	42.5	0.086
26	790628-03	80.0	50.0	00.0	5.0	+/-1.0	1.45	38.5	0.075
27	790727-03	20.0	73.0	00.0	5.0	+/-1.0	1.22	37.8	0.077
28	790727-03	50.0	73.0	00.0	5.0	+/-1.0	1.22	29.5	0.063
29	790727-03	80.0	73.0	00.0	5.0	+/-1.0	1.22	28.2	0.055
30	800627-01	20.0	70.0	00.0	5.0	+/-1.0	1.22	48.7	0.087
31	790126-01	20.0	69.0	00.0	5.0	+/-1.0	1.00	40.3	0.063
32	(								
33									
34									
35									
36									
37									
38									
39									
40									
41									
42									
43									
44									
45									

DAT00010
DAT00020
DAT00030
DAT00040
DAT00050
DAT00060
DAT00070
DAT00080
DAT00090
DAT00100
DAT00110
DAT00120
DAT00130
DAT00140
DAT00150
DAT00160
DAT00170
DAT00180
DAT00190
DAT00200
DAT00210
DAT00220
DAT00230
DAT00240
DAT00250
DAT00260
DAT00270
DAT00280
DAT00290
DAT00300
DAT00310
DAT00320
DAT00330
DAT00340
DAT00350
DAT00360
DAT00370
DAT00380
DAT00390
DAT00400
DAT00410
DAT00420
DAT00430
DAT00440
DAT00450
DAT00460
DAT00470
DAT00480
DAT00490
DAT00500
DAT00510
DAT00520
DAT00530
DAT00540
DAT00550

ORIGINAL PAGE IS
OF POOR QUALITY

C

FILE: DATA FORTRAN * 11/12/80 19:09:00 UNIVERSITY OF WATERLOO PAGE

```
C
C
C     RESULTS OF SIDE SLIP TRACTION TESTS WITH SANIC 50 FLUID
C     USING AN ASPECT RATIO OF 5.0 AND WITH 6.0 DEGREES SPIN.
C
C
C
C
C
```

	TEST NOS.	SPEED (M/S)	TEMP (C)	SPIN DEG	ASPECT (-)	SIDE SLIP	PRESS. (GPA.)	SLOPE (-)	TRACT. COEFF.
1	800628-01	20.0	70.0	06.0	5.0	+/-1.0	1.00	-	0.082
2	800628-03	20.0	70.0	06.0	5.0	+/-1.0	1.22	-	0.086

ORIGINAL PAGE IS
OF POOR QUALITY

```
C
```

FILE: DATA FORTRAN * 11/12/80 19:09:00 UNIVERSITY OF WATERLOO PAGE

RESULTS OF SIDE SLIP TRACTION TESTS WITH SANTO 50 FLUID
USING AN ASPECT RATIO OF 5.0 AND WITH 15 DEGREES SKIN.

	TEST NOS.	SPEED (M/S)	TEMP (C)	SKIN DEG	ASPECT (-)	SIDE SLIP	PRESS. (GPA)	SLOPE (-)	TRACT. COEFF.
1	790726-01	20.0	32.5	15.0	5.0	+/-1.0	1.22	-	0.094
2	790726-01	50.0	32.5	15.0	5.0	+/-1.0	1.22	-	0.064
3	790726-01	80.0	32.5	15.0	5.0	+/-1.0	1.22	-	0.051
4	790629-01	80.0	33.0	15.0	5.0	+/-1.0	1.45	-	0.052
5	790629-02	50.0	35.0	15.0	5.0	+/-1.0	1.45	-	0.067
6	790629-03	20.0	33.0	15.0	5.0	+/-1.0	1.45	-	0.083
7	790629-04	50.0	47.0	15.0	5.0	+/-1.0	1.45	-	0.067
8	790629-05	20.0	33.0	15.0	5.0	+/-1.0	1.45	-	0.084
9	790629-06	50.0	37.0	15.0	5.0	+/-1.0	1.45	-	0.069
10	790629-07	80.0	57.0	15.0	5.0	+/-1.0	1.45	-	0.055
11	790629-08	80.0	50.0	15.0	5.0	+/-1.0	1.45	-	0.056
12	790629-09	20.0	30.0	15.0	5.0	+/-1.0	1.45	-	0.083
13	790629-10	50.0	33.0	15.0	5.0	+/-1.0	1.45	-	0.069
14	790629-11	80.0	50.0	15.0	5.0	+/-1.0	1.45	-	0.055
15	790629-12	50.0	70.0	15.0	5.0	+/-1.0	1.45	-	0.063
16	790629-13	80.0	70.0	15.0	5.0	+/-1.0	1.45	-	0.057
17	790629-14	20.0	70.0	15.0	5.0	+/-1.0	1.45	-	0.079
18	790629-15	80.0	47.0	15.0	5.0	+/-1.0	1.45	-	0.056
19	790629-16	80.0	55.0	15.0	5.0	+/-1.0	1.45	-	0.055
20	790726-04	20.0	50.0	15.0	5.0	+/-1.0	1.22	-	0.085
21	790726-04	80.0	50.0	15.0	5.0	+/-1.0	1.22	-	0.051
22	790727-02	20.0	73.0	15.0	5.0	+/-1.0	1.22	-	0.079
23	790727-02	50.0	73.0	15.0	5.0	+/-1.0	1.22	-	0.065
24	790727-02	80.0	73.0	15.0	5.0	+/-1.0	1.22	-	0.056
25	790628-06	20.0	50.0	15.0	5.0	+/-1.0	1.45	-	0.082
26	790628-04	80.0	63.0	15.0	5.0	+/-1.0	1.45	-	0.055
27	790628-05	50.0	60.0	15.0	5.0	+/-1.0	1.45	-	0.065
28	790718-01	20.0	35.0	15.0	5.0	+/-1.0	1.00	-	0.103
29	790718-02	50.0	35.0	15.0	5.0	+/-1.0	1.00	-	0.077
30	790718-03	80.0	37.0	15.0	5.0	+/-1.0	1.00	-	0.065
31	790718-04	20.0	37.0	15.0	5.0	+/-1.0	1.00	-	0.082
32	790718-05	50.0	35.0	15.0	5.0	+/-1.0	1.00	-	0.064
33	790718-06	35.0	35.0	15.0	5.0	+/-1.0	1.00	-	0.075
34	790726-05	20.0	50.0	15.0	5.0	+/-1.0	1.00	-	0.084
35	790726-05	50.0	50.0	15.0	5.0	+/-1.0	1.00	-	0.063
36	790726-05	80.0	50.0	15.0	5.0	+/-1.0	1.00	-	0.048
37	790726-04	50.0	50.0	15.0	5.0	+/-1.0	1.22	-	0.062
38	790727-01	20.0	67.0	15.0	5.0	+/-1.0	1.00	-	0.085
39	790727-01	50.0	67.0	15.0	5.0	+/-1.0	1.00	-	0.069
40	790727-01	80.0	67.0	15.0	5.0	+/-1.0	1.00	-	0.059
41	790901-01	20.0	50.0	15.0	5.0	+/-1.0	1.00	-	0.077
42	790901-01	50.0	50.0	15.0	5.0	+/-1.0	1.00	-	0.059
43	790901-01	80.0	50.0	15.0	5.0	+/-1.0	1.00	-	0.045
44	790901-02	20.0	30.0	15.0	5.0	+/-1.0	1.00	-	0.101
45	C								

FILE: DATA FORTRAN * 11/12/80 19:09:00 UNIVERSITY OF WATERLOO PAGE

C DATA
C DATA
C RESULTS OF SIDE SLIP TRACTION TESTS WITH SANTO 50 FLUID DATA
C USING AN ASPECT RATIO OF 5.0 AND WITH 15 DEGREES SKIN. DATA
C DATA
C DATA
C TEST NOS. SPEED TEMP SKIN ASPECT SIDE PRESS. SLOPE TRACT. DATA
C (M/S) (C) DEG (-) SLIP (GPA) (-) COEFF. DATA
C DATA

1	790901-02	80.0	30.0	15.0	5.0	+/-1.0	1.00	-	0.057
2	790901-03	20.0	65.0	15.0	5.0	+/-1.0	1.00	-	0.092
3	790901-03	50.0	65.0	15.0	5.0	+/-1.0	1.00	-	0.070
4	790901-03	80.0	65.0	15.0	5.0	+/-1.0	1.00	-	0.056
5	790901-02	50.0	30.0	15.0	5.0	+/-1.0	1.00	-	0.073
6	C								
7									
8									
9									
10									
11									
12									
13									
14									
15									
16									
17									
18									
19									
20									
21									
22									
23									
24									
25									
26									
27									
28									
29									
30									
31									
32									
33									
34									
35									
36									
37									
38									
39									
40									
41									
42									
43									
44									
45									

C DATA

C
C
C RESULTS OF SIDE SLIP TRACTION TESTS WITH SANTO 50 FLUID
C USING AN ASPECT RATIO OF 5.0 AND WITH 30.0 DEGREES SPIN.
C
C
C
C
C

	TEST NOS.	SPEED (M/S)	TEMP (C)	SPIN DEG	ASPECT (-)	SLIP SLIP	PRESS. (GPA)	SLOPE (-)	TRACT. COEFF.
1	790728-01	20.0	35.0	30.0	5.0	+/-1.0	1.45	-	0.059
2	790728-01	50.0	35.0	30.0	5.0	+/-1.0	1.45	-	0.040
3	790728-01	80.0	35.0	30.0	5.0	+/-1.0	1.45	-	0.031
4	790202-01	20.0	32.0	30.0	5.0	+/-1.0	1.00	-	0.071
5	790202-02	50.0	36.0	30.0	5.0	+/-1.0	1.00	-	0.046
6	790202-03	80.0	37.0	30.0	5.0	+/-1.0	1.00	-	0.035
7	790206-01	80.0	27.0	30.0	5.0	+/-1.0	1.00	-	0.035
8	790727-04	20.0	73.0	30.0	5.0	+/-1.0	1.45	-	0.064
9	790727-04	80.0	73.0	30.0	5.0	+/-1.0	1.45	-	0.033
10	790126-04	20.0	69.0	30.0	5.0	+/-1.0	1.00	-	0.065
11	790126-05	50.0	68.0	30.0	5.0	+/-1.0	1.00	-	0.046
12	790126-06	80.0	71.0	30.0	5.0	+/-1.0	1.00	-	0.034
13	790728-02	20.0	53.0	30.0	5.0	+/-1.0	1.45	-	0.061
14	790728-02	50.0	53.0	30.0	5.0	+/-1.0	1.45	-	0.043
15	790728-02	80.0	53.0	30.0	5.0	+/-1.0	1.45	-	0.034
16	790601-02	20.0	47.0	30.0	5.0	+/-1.0	1.45	-	0.071
17	790831-02	20.0	50.0	30.0	5.0	+/-1.0	1.22	-	0.089
18	790831-02	50.0	50.0	30.0	5.0	+/-1.0	1.22	-	0.059
19	790831-02	80.0	50.0	30.0	5.0	+/-1.0	1.22	-	0.045
20	790831-01	20.0	30.0	30.0	5.0	+/-1.0	1.22	-	0.097
21	790831-01	50.0	30.0	30.0	5.0	+/-1.0	1.22	-	0.062
22	790831-01	80.0	30.0	30.0	5.0	+/-1.0	1.22	-	0.049
23	790831-03	20.0	70.0	30.0	5.0	+/-1.0	1.22	-	0.085
24	790831-03	50.0	70.0	30.0	5.0	+/-1.0	1.22	-	0.054
25	790831-01	80.0	70.0	30.0	5.0	+/-1.0	1.22	-	0.046
26	790727-04	50.0	73.0	30.0	5.0	+/-1.0	1.45	-	0.041
27	C								
28									
29									
30									
31									
32									
33									
34									
35									
36									
37									
38									
39									
40									
41									
42									
43									
44									
45									

C

DAT0221
DAT0222
DAT0223
DAT0224
DAT0225
DAT0226
DAT0227
DAT0228
DAT0229
DAT0230
DAT0231
DAT0232
DAT0233
DAT0234
DAT0235
DAT0236
DAT0237
DAT0238
DAT0239
DAT0240
DAT0241
DAT0242
DAT0243
DAT0244
DAT0245
DAT0246
DAT0247
DAT0248
DAT0249
DAT0250
DAT0251
DAT0252
DAT0253
DAT0254
DAT0255
DAT0256
DAT0257
DAT0258
DAT0259
DAT0260
DAT0261
DAT0262
DAT0263
DAT0264
DAT0265
DAT0266
DAT0267
DAT0268
DAT0269
DAT0270
DAT0271

ORIGINAL PAGE IS OF POOR QUALITY

FILE: DATA FORTRAN * 11/12/80 19:09:00 UNIVERSITY OF WATERLOO PAGE

C
C RESULTS OF SIDE SLIP TRACTION TESTS WITH SANTO 50 FLUID
C USING AN ASPECT RATIO OF 2.0 AND WITH 0 DEGREES SPIN.
C
C
C

	TEST NOS.	SPEED (M/S)	TEMP (C)	SPIN DEG	ASPECT (-)	SIDE SLIP	PRESS. (GPA.)	SLOPE (-)	TRACT. COEFF.
1	800626-15	20.0	70.0	00.0	2.0	+/-1.0	1.45	47.7	0.095
2	800626-07	20.0	70.0	00.0	2.0	+/-1.0	1.00	51.1	0.090
3	800626-10	20.0	70.0	00.0	2.0	+/-1.0	1.00	44.7	0.082
4	800626-12	20.0	70.0	00.0	2.0	+/-1.0	1.45	53.2	0.094
5	C								
6									
7									
8									
9									
10									
11									
12									
13									
14									
15									
16									
17									
18									
19									
20									
21									
22									
23									
24									
25									
26									
27									
28									
29									
30									
31									
32									
33									
34									
35									
36									
37									
38									
39									
40									
41									
42									
43									
44									
45									

C

RESULTS OF SIDE SLIP TRACTION TESTS WITH SANIC 50 FLUID
USING AN ASPECT RATIO OF 2.0 AND WITH 6.0 DEGREES SKIN.

	TEST NOS.	SPEED (M/S)	TEMP (C)	SKIN DEG	ASPECT (-)	SIDE SLIP	PRESS. (GPA.)	SLOPE (-)	TRACT. COEFF.
1	800626-13	20.0	70.0	06.0	2.0	+/-1.0	1.45	-	0.095
2	800626-07	20.0	70.0	06.0	2.0	+/-1.0	1.00	-	0.077
3	800626-08	20.0	68.0	06.0	2.0	+/-1.0	1.00	-	0.078
4	800626-12	20.0	70.0	06.0	2.0	+/-1.0	1.45	-	0.087
5	C								
6									
7									
8									
9									
10									
11									
12									
13									
14									
15									
16									
17									
18									
19									
20									
21									
22									
23									
24									
25									
26									
27									
28									
29									
30									
31									
32									
33									
34									
35									
36									
37									
38									
39									
40									
41									
42									
43									
44									
45									

FILE: DATA FORTRAN * 11/12/80 19:09:00 UNIVERSITY OF WATERLOO PAGE

C
C
C RESULTS OF SIDE SLIP TRACTION TESTS WITH SANTO 50 FLUID
C USING AN ASPECT RATIO OF 1.0 AND WITH 0 DEGREES SKIN.
C
C
C
C
C

	TEST NOS.	SPEED (M/S)	TEMP (C)	SKIN DEG	ASPECT (-)	SIDE SLIP	PRESS. (GPA)	SLOPE (-)	TRACT. COEFF.
1	790329-01	50.0	28.0	00.0	1.0	+/-1.0	1.00	39.6	0.085
2	790329-02	50.0	28.0	00.0	1.0	+/-1.0	1.45	48.4	0.087
3	790329-03	50.0	31.0	00.0	1.0	+/-1.0	1.90	40.1	0.096
4	790329-04	20.0	29.0	00.0	1.0	+/-1.0	1.90	41.1	0.104
5	790329-05	30.0	29.0	00.0	1.0	+/-1.0	1.90	38.8	0.091
6	790311-02	50.0	32.0	00.0	1.0	+/-1.0	1.45	53.3	0.093
7	790311-03	50.0	33.0	00.0	1.0	+/-1.0	1.90	41.1	0.089
8	790311-04	20.0	67.0	00.0	1.0	+/-1.0	1.00	57.4	0.082
9	790311-05	50.0	67.0	00.0	1.0	+/-1.0	1.00	50.9	0.075
10	790311-06	30.0	69.0	00.0	1.0	+/-1.0	1.00	43.5	0.076
11	790311-07	20.0	67.5	00.0	1.0	+/-1.0	1.45	56.8	0.084
12	790311-08	50.0	67.5	00.0	1.0	+/-1.0	1.45	53.6	0.081
13	790311-09	30.0	68.0	00.0	1.0	+/-1.0	1.45	49.1	0.076
14	790311-10	50.0	69.0	00.0	1.0	+/-1.0	1.90	54.9	0.091
15	800623-01	20.0	70.0	00.0	1.0	+/-1.0	1.45	48.5	0.084
16	800623-02	20.0	70.0	00.0	1.0	+/-1.0	1.45	49.9	0.084
17	800623-06	20.0	70.0	00.0	1.0	+/-1.0	1.90	59.0	0.097
18	800623-07	20.0	70.0	00.0	1.0	+/-1.0	1.90	56.2	0.094
19	800626-03	20.0	70.0	00.0	1.0	+/-1.0	1.90	62.4	0.096
20	781021-01	20.0	55.0	00.0	1.0	+/-1.0	1.00	55.0	0.083
21	781021-02	50.0	55.0	00.0	1.0	+/-1.0	1.00	45.6	0.068
22	781021-04	30.0	55.0	00.0	1.0	+/-1.0	1.00	42.0	0.060
23	781021-05	20.0	51.0	00.0	1.0	+/-1.0	1.45	59.2	0.095
24	781021-06	50.0	54.0	00.0	1.0	+/-1.0	1.45	58.0	0.088
25	781028-07	30.0	55.0	00.0	1.0	+/-1.0	1.45	52.0	0.078
26	781021-09	20.0	48.0	00.0	1.0	+/-1.0	1.90	54.0	0.099
27	781021-10	50.0	52.0	00.0	1.0	+/-1.0	1.90	50.4	0.092
28	781021-08	30.0	52.0	00.0	1.0	+/-1.0	1.90	51.0	0.093
29	781016-01	20.0	66.0	00.0	1.0	+/-1.0	1.00	54.0	0.070
30	781016-02	50.0	66.0	00.0	1.0	+/-1.0	1.00	45.4	0.063
31	781016-03	30.0	66.0	00.0	1.0	+/-1.0	1.00	39.6	0.056
32	781019-01	20.0	66.0	00.0	1.0	+/-1.0	1.45	60.4	0.097
33	781019-02	50.0	66.0	00.0	1.0	+/-1.0	1.45	55.5	0.081
34	781019-03	30.0	66.0	00.0	1.0	+/-1.0	1.45	51.4	0.074
35	781020-01	20.0	66.0	00.0	1.0	+/-1.0	1.90	53.2	0.088
36	781020-02	50.0	66.0	00.0	1.0	+/-1.0	1.90	49.4	0.083
37	781019-03	30.0	66.0	00.0	1.0	+/-1.0	1.90	50.0	0.079
38	790311-01	50.0	32.0	00.0	1.0	+/-1.0	1.00	34.3	0.065
39	C								
40									
41									
42									
43									
44									
45									

C

RESULTS OF SIDE SLIP TRACTION TESTS WITH SANIO 5C FLUID
USING AN ASPECT RATIO OF 1.0 AND WITH 6.0 DEGREES SPIN.

	TEST NOS.	SPEED (M/S)	TEMP (C)	SPIN DEG	ASPECT (-)	SIDE SLIP	PRESS. (GPA.)	SLOPE (-)	TRACT. COEFF.
1	800623-01	20.0	70.0	06.0	1.0	+/-1.0	1.45	-	0.085
2	800623-04	20.0	70.0	06.0	1.0	+/-1.0	1.45	-	0.087
3	800623-06	20.0	70.0	06.0	1.0	+/-1.0	1.90	-	0.100
4	800623-09	20.0	70.0	06.0	1.0	+/-1.0	1.90	-	0.083
5	800626-01	20.0	70.0	06.0	1.0	+/-1.0	1.90	-	0.100
6	C								
7									
8									
9									
10									
11									
12									
13									
14									
15									
16									
17									
18									
19									
20									
21									
22									
23									
24									
25									
26									
27									
28									
29									
30									
31									
32									
33									
34									
35									
36									
37									
38									
39									
40									
41									
42									
43									
44									
45									

FILE: DATA FORTRAN * 11/12/80 19:09:00 UNIVERSITY OF WATERLOO PAGE

ORIGINAL PAGE IS
OF POOR QUALITY

C
C
C RESULTS OF SIDE SLIP TRACTION TESTS WITH SANTO 50 FLUID
C USING AN ASPECT RATIO OF 1.0 AND WITH 15.0 DEGREES SPIN.
C
C
C
C

	TEST NOS.	SPEED (M/S)	TEMP (C)	SPIN DEG	ASPECT (-)	SIDE SLIP	PRESS. (GPA)	SLOPE (-)	TRACT. COEFF.
1	790413-05	20.0	65.0	15.0	1.0	+/-1.0	1.00	-	0.068
2	790413-02	20.0	65.0	15.0	1.0	+/-1.0	1.45	-	0.082
3	790410-01	50.0	31.5	15.0	1.0	+/-1.0	1.90	-	0.080
4	790410-02	50.0	29.0	15.0	1.0	+/-1.0	1.90	-	0.090
5	790410-03	50.0	34.0	15.0	1.0	+/-1.0	1.45	-	0.082
6	790410-04	50.0	34.0	15.0	1.0	+/-1.0	1.45	-	0.082
7	790410-05	50.0	31.0	15.0	1.0	+/-1.0	1.00	-	0.060
8	790410-06	50.0	31.0	15.0	1.0	+/-1.0	1.00	-	0.060
9	790413-01	50.0	65.0	15.0	1.0	+/-1.0	1.90	-	0.088
10	790413-03	50.0	65.0	15.0	1.0	+/-1.0	1.45	-	0.077
11	790413-06	50.0	64.0	15.0	1.0	+/-1.0	1.00	-	0.057
12	790413-07	50.0	65.0	15.0	1.0	+/-1.0	1.00	-	0.060
13	790413-04	80.0	65.0	15.0	1.0	+/-1.0	1.45	-	0.070
14	C								
15									
16									
17									
18									
19									
20									
21									
22									
23									
24									
25									
26									
27									
28									
29									
30									
31									
32									
33									
34									
35									
36									
37									
38									
39									
40									
41									
42									
43									
44									
45									

C

RESULTS OF SIDE SLIP TRACTION TESTS WITH SAMIC 5C FLUID
USING AN ASPECT RATIO OF 1.0 AND WITH 30.0 DEGREES SKIN.

	TEST NOS.	SPEED (M/S)	TEMP (C)	SKIN DEG	ASPECT (-)	SIDE SLIP	PRESS. (GPA)	SLOPE (-)	TRACT. COEFF.
1	790317-01	50.0	31.0	30.0	1.0	+/-1.0	1.00	-	0.077
2	790317-02	50.0	31.5	30.0	1.0	+/-1.0	1.45	-	0.081
3	790317-03	50.0	32.0	30.0	1.0	+/-1.0	1.45	-	0.081
4	790317-04	50.0	33.0	30.0	1.0	+/-1.0	1.90	-	0.074
5	790317-05	50.0	35.0	30.0	1.0	+/-1.0	1.90	-	0.074
6	790317-06	20.0	67.0	30.0	1.0	+/-1.0	1.45	-	0.089
7	790317-07	20.0	70.0	30.0	1.0	+/-1.0	1.45	-	0.077
8	790317-08	30.0	73.0	30.0	1.0	+/-1.0	1.45	-	0.067
9	790317-09	50.0	67.0	30.0	1.0	+/-1.0	1.90	-	0.078
10	790311-11	20.0	66.0	30.0	1.0	+/-1.0	1.00	-	0.066
11	790311-12	50.0	66.0	30.0	1.0	+/-1.0	1.00	-	0.059
12	790311-13	30.0	69.0	30.0	1.0	+/-1.0	1.00	-	0.057
13	790311-14	20.0	67.0	30.0	1.0	+/-1.0	1.45	-	0.083
14	790311-15	50.0	67.0	30.0	1.0	+/-1.0	1.45	-	0.076
15	790311-16	30.0	67.5	30.0	1.0	+/-1.0	1.45	-	0.066
16	790311-17	50.0	70.0	30.0	1.0	+/-1.0	1.90	-	0.078
17	790311-18	50.0	70.0	30.0	1.0	+/-1.0	1.90	-	0.078
18	790317-01	20.0	31.0	30.0	1.0	+/-1.0	1.00	-	0.102
19	790317-01	20.0	31.0	30.0	1.0	+/-1.0	1.00	-	0.102
20	C								
21									
22									
23									
24									
25									
26									
27									
28									
29									
30									
31									
32									
33									
34									
35									
36									
37									
38									
39									
40									
41									
42									
43									
44									
45									

C

C
C
C RESULTS OF SIDE SLIP TRACTION TESTS WITH TDF-88 FLUID
C USING AN ASPECT RATIO OF 5.0 AND WITH 0 DEGREES SPIN.
C
C
C
C
C

	TEST NOS.	SPEED (M/S)	TEMP (C)	SPIN DEG	ASPECT (-)	SIDE SLIP	PRESS. (GPA.)	SLOPE (-)	TRACT. COEFF.
1	791103-10	10.0	33.0	00.0	5.0	+/-1.0	1.00	38.6	0.095
2	791103-10	20.0	33.0	00.0	5.0	+/-1.0	1.00	34.8	0.080
4	791103-11	10.0	33.0	00.0	5.0	+/-1.0	1.45	40.6	0.096
4	791103-11	20.0	33.0	00.0	5.0	+/-1.0	1.45	39.3	0.090
5	791103-11	30.0	33.0	00.0	5.0	+/-1.0	1.45	38.1	0.084
6	791128-01	10.0	30.0	00.0	5.0	+/-1.0	1.45	39.4	0.090
7	791128-01	20.0	30.0	00.0	5.0	+/-1.0	1.45	37.2	0.083
8	791128-01	30.0	30.0	00.0	5.0	+/-1.0	1.45	35.9	0.078
9	791123-01	10.0	30.0	00.0	5.0	+/-1.0	1.00	34.6	0.095
10	791123-01	20.0	30.0	00.0	5.0	+/-1.0	1.00	33.3	0.085
11	791123-01	30.0	30.0	00.0	5.0	+/-1.0	1.00	32.8	0.079
12	791130-04	10.0	70.0	00.0	5.0	+/-1.0	1.00	56.5	0.083
13	791130-04	20.0	70.0	00.0	5.0	+/-1.0	1.00	51.4	0.077
14	791130-04	30.0	70.0	00.0	5.0	+/-1.0	1.00	42.6	0.071
15	791120-07	10.0	70.0	00.0	5.0	+/-1.0	1.00	51.1	0.079
16	791120-07	20.0	70.0	00.0	5.0	+/-1.0	1.00	43.9	0.074
17	791120-07	30.0	70.0	00.0	5.0	+/-1.0	1.00	39.5	0.069
18	791120-08	10.0	70.0	00.0	5.0	+/-1.0	1.45	47.0	0.084
19	791120-08	20.0	70.0	00.0	5.0	+/-1.0	1.45	42.2	0.081
20	791120-08	30.0	70.0	00.0	5.0	+/-1.0	1.45	40.8	0.076
21	791004-02	30.0	47.0	00.0	5.0	+/-1.0	1.00	34.7	0.069
22	791004-04	20.0	50.0	00.0	5.0	+/-1.0	1.00	44.1	0.079
23	791004-04	30.0	50.0	00.0	5.0	+/-1.0	1.00	38.9	0.064
24	791004-04	30.0	50.0	00.0	5.0	+/-1.0	1.00	34.0	0.050
25	800529-01	20.0	70.0	00.0	5.0	+/-1.0	1.00	38.0	0.071
26	800529-03	20.0	70.0	00.0	5.0	+/-1.0	1.22	49.0	0.082
27	791004-01	30.0	70.0	00.0	5.0	+/-1.0	1.00	27.6	0.044
28	791103-10	10.0	33.0	00.0	5.0	+/-1.0	1.00	48.0	0.095
29	791103-10	20.0	33.0	00.0	5.0	+/-1.0	1.00	35.5	0.080
30	791103-10	30.0	33.0	00.0	5.0	+/-1.0	1.00	39.0	0.070
31	(								
32									
33									
34									
35									
36									
37									
38									
39									
40									
41									
42									
43									
44									
45									

C

RESULTS OF SIDE SLIP TRACTION TESTS WITH IDF-68 FLUID
USING AN ASPECT RATIO OF 5.0 AND WITH 6.0 DEGREES SPIN.

	TEST NO.	SPEED (M/S)	TEMP (C)	SPIN DEG	ASPECT (-)	SIDE SLIP	PRESS. (GPA.)	SLOPE (-)	TRACT. COEFF.
1	791127-01	10.0	30.0	06.0	5.0	+/-1.0	1.00	-	0.086
2	791127-01	20.0	30.0	06.0	5.0	+/-1.0	1.00	-	0.079
3	791127-01	30.0	30.0	06.0	5.0	+/-1.0	1.00	-	0.076
4	791127-02	10.0	30.0	06.0	5.0	+/-1.0	1.45	-	0.087
5	791127-02	20.0	30.0	06.0	5.0	+/-1.0	1.45	-	0.082
6	791127-02	30.0	30.0	06.0	5.0	+/-1.0	1.45	-	0.080
7	791127-03	10.0	70.0	06.0	5.0	+/-1.0	1.45	-	0.084
8	791127-03	20.0	70.0	06.0	5.0	+/-1.0	1.45	-	0.080
9	791127-04	10.0	70.0	06.0	5.0	+/-1.0	1.00	-	0.089
10	791127-04	20.0	70.0	06.0	5.0	+/-1.0	1.00	-	0.084
11	791127-04	30.0	70.0	06.0	5.0	+/-1.0	1.00	-	0.080
12	800529-07	20.0	70.0	06.0	5.0	+/-1.0	1.22	-	0.083
13	791003-01	20.0	40.0	06.0	5.0	+/-1.0	1.00	-	0.074
14	791003-01	45.0	40.0	06.0	5.0	+/-1.0	1.00	-	0.061
15	791127-03	10.0	70.0	06.0	5.0	+/-1.0	1.45	-	0.084
16	791127-03	20.0	70.0	06.0	5.0	+/-1.0	1.45	-	0.080
17	791127-03	30.0	70.0	06.0	5.0	+/-1.0	1.45	-	0.078

C

FILE: DATA FORTRAN * 11/12/80 19:09:00 UNIVERSITY OF WATERLOO PAG

```
C                                                                       DAT
C                                                                       DAT
C     RESULTS OF SIDE SLIP TRACTION TESTS WITH IRF-88 FLUID             DAT
C     USING AN ASPECT RATIO OF 5.0 AND WITH 15.0 DEGREES SPIN           DAT
C                                                                       DAT
C                                                                       DAT
C        TEST NOS.  SPEED  TEMP  SPIN ASPECT SLIP  PRESS. SLOPE TRACT. DAT
C                   (M/S)  ( C)   DEG  ( - ) SLIP (GPA.) ( - ) COEFF.  DAT
C                                                                       DAT
  1  791004-03  20.0  50.0  15.0  5.0  +/-1.0  1.00   -   0.060       DAT
  2  791004-03  50.0  50.0  15.0  5.0  +/-1.0  1.00   -   0.061       DAT
  3  791004-03  80.0  50.0  15.0  5.0  +/-1.0  1.00   -   0.045       DAT
  4        0                                                            DAT
  5                                                                     DAT
  6                                                                     DAT
  7                                                                     DAT
  8                                                                     DAT
  9                                                                     DAT
 10                                                                     DAT
 11                                                                     DAT
 12                                                                     DAT
 13                                                                     DAT
 14                                                                     DAT
 15                                                                     DAT
 16                                                                     DAT
 17                                                                     DAT
 18                                                                     DAT
 19                                                                     DAT
 20                                                                     DAT
 21                                                                     DAT
 22                                                                     DAT
 23                                                                     DAT
 24                                                                     DAT
 25                                                                     DAT
 26                                                                     DAT
 27                                                                     DAT
 28                                                                     DAT
 29                                                                     DAT
 30                                                                     DAT
 31                                                                     DAT
 32                                                                     DAT
 33                                                                     DAT
 34                                                                     DAT
 35                                                                     DAT
 36                                                                     DAT
 37                                                                     DAT
 38                                                                     DAT
 39                                                                     DAT
 40                                                                     DAT
 41                                                                     DAT
 42                                                                     DAT
 43                                                                     DAT
 44                                                                     DAT
 45                                                                     DAT
C                                                                       DAT
```

RESULTS OF SIDE SLIP TRACTION TESTS WITH IRF-88 FLUID
USING AN ASPECT RATIO OF 2.0 AND WITH 0 DEGREES SKIN.

	TEST NOS.	SPEED (M/S)	TEMP (C)	SKIN DEG	ASPECT (-)	SLIP	PRESS. (GPA.)	SLOPE (-)	TRACT. COEFF.
1	791103-06	10.0	32.0	00.0	2.0	+/-1.0	1.00	55.6	0.100
2	791103-06	20.0	32.0	00.0	2.0	+/-1.0	1.00	41.1	0.088
3	791103-06	30.0	32.0	00.0	2.0	+/-1.0	1.00	36.6	0.080
4	791103-08	10.0	33.0	00.0	2.0	+/-1.0	1.45	47.0	0.101
5	791103-08	20.0	33.0	00.0	2.0	+/-1.0	1.45	43.2	0.093
6	791103-08	30.0	33.0	00.0	2.0	+/-1.0	1.45	40.9	0.087
7	791103-07	30.0	32.0	00.0	2.0	+/-1.0	1.00	35.6	0.081
8	791103-09	30.0	33.0	00.0	2.0	+/-1.0	1.45	39.4	0.084
9	791115-05	10.0	70.0	00.0	2.0	+/-1.0	1.00	54.3	0.084
10	791115-05	20.0	70.0	00.0	2.0	+/-1.0	1.00	47.1	0.080
11	791115-05	30.0	70.0	00.0	2.0	+/-1.0	1.00	43.4	0.075
12	791115-06	30.0	70.0	00.0	2.0	+/-1.0	1.00	43.7	0.076
13	791115-07	30.0	70.0	00.0	2.0	+/-1.0	1.45	49.0	0.084
14	791115-08	10.0	70.0	00.0	2.0	+/-1.0	1.45	55.8	0.090
15	791115-08	20.0	70.0	00.0	2.0	+/-1.0	1.45	51.9	0.086
16	791115-08	30.0	70.0	00.0	2.0	+/-1.0	1.45	51.9	0.083
17	800523-01	20.0	70.0	00.0	2.0	+/-1.0	1.45	55.7	0.094
18	800526-02	20.0	70.0	00.0	2.0	+/-1.0	1.00	34.4	0.073
19	800526-06	20.0	70.0	00.0	2.0	+/-1.0	1.45	47.6	0.087
20	800526-07	20.0	70.0	00.0	2.0	+/-1.0	1.45	45.6	0.086
21	(								

```
C                                                                               DAT0
C                                                                               DAT0
C     RESULTS OF SIDE SLIP TRACTION TESTS WITH TDF-88 FLUID                     DAT0
C     USING AN ASPECT RATIO OF 2.0 AND WITH 6.0 DEGREES SPIN.                   DAT0
C                                                                               DAT0
C                                                                               DAT0
C                                                                               DAT0
C          TEST NOS.  SPEED  TEMP  SPIN ASPECT SIDE  PRESS. SLOPE TRACT.  DAT0
C                     (M/S)  ( C)   DEG  ( - ) SLIP  (GPA.) ( - ) COEFF.  DAT0
C                                                                               DAT0
      1  791103-07   30.0   32.0  06.0  2.0  +/-1.0  1.00    -   0.078   DAT0
      2  791103-09   30.0   33.0  06.0  2.0  +/-1.0  1.45    -   0.082   DAT0
      3  791115-06   30.0   70.0  06.0  2.0  +/-1.0  1.00    -   0.075   DAT0
      4  791115-07   30.0   70.0  06.0  2.0  +/-1.0  1.00    -   0.082   DAT0
      5  800523-01   20.0   70.0  06.0  2.0  +/-1.0  1.45    -   0.093   DAT0
      6  800526-01   20.0   70.0  06.0  2.0  +/-1.0  1.00    -   0.065   DAT0
      7  800526-04   20.0   70.0  06.0  2.0  +/-1.0  1.00    -   0.067   DAT0
      8  800526-05   20.0   70.0  06.0  2.0  +/-1.0  1.45    -   0.086   DAT0
      9  800526-09   20.0   70.0  06.0  2.0  +/-1.0  1.45    -   0.092   DAT0
     10        C                                                            DAT0
     11                                                                     DAT0
     12                                                                     DAT0
     13                                                                     DAT0
     14                                                                     DAT0
     15                                                                     DAT0
     16                                                                     DAT0
     17                                                                     DAT0
     18                                                                     DAT0
     19                                                                     DAT0
     20                                                                     DAT0
     21                                                                     DAT0
     22                                                                     DAT0
     23                                                                     DAT0
     24                                                                     DAT0
     25                                                                     DAT0
     26                                                                     DAT0
     27                                                                     DAT0
     28                                                                     DAT0
     29                                                                     DAT0
     30                                                                     DAT0
     31                                                                     DAT0
     32                                                                     DAT0
     33                                                                     DAT0
     34                                                                     DAT0
     35                                                                     DAT0
     36                                                                     DAT0
     37                                                                     DAT0
     38                                                                     DAT0
     39                                                                     DAT0
     40                                                                     DAT0
     41                                                                     DAT0
     42                                                                     DAT0
     43                                                                     DAT0
     44                                                                     DAT0
     45                                                                     DAT0
C                                                                               DAT0
```

RESULTS OF SIDE SLIP TRACTION TESTS WITH TDF-88 FLUID
USING AN ASPECT RATIO OF 1.0 AND WITH 0 DEGREES SLIP.

	TEST NOS.	SPEED (M/S)	TEMP (C)	SLIP DEG	ASPECT (-)	SLIP SLIP	PRESS. (GPA.)	SLOPE (-)	TRACT. COEFF.
1	791119-01	10.0	28.0	00.0	1.0	+/-1.0	1.45	47.9	0.101
2	791119-01	20.0	28.0	00.0	1.0	+/-1.0	1.45	39.1	0.090
3	791119-01	30.0	29.0	00.0	1.0	+/-1.0	1.45	38.5	0.083
4	791119-02	30.0	29.0	00.0	1.0	+/-1.0	1.45	37.4	0.085
5	791119-03	30.0	30.0	00.0	1.0	+/-1.0	1.90	45.0	0.089
6	791119-04	10.0	30.0	00.0	1.0	+/-1.0	1.90	49.3	0.099
7	791119-04	20.0	30.0	00.0	1.0	+/-1.0	1.90	45.9	0.095
8	791119-04	30.0	30.0	00.0	1.0	+/-1.0	1.90	43.1	0.089
9	791120-01	10.0	30.0	00.0	1.0	+/-1.0	1.45	47.9	0.100
10	791120-01	20.0	30.0	00.0	1.0	+/-1.0	1.45	43.2	0.092
11	791120-01	30.0	30.0	00.0	1.0	+/-1.0	1.45	37.1	0.084
12	791120-02	30.0	30.0	00.0	1.0	+/-1.0	1.45	36.9	0.080
13	791120-03	30.0	30.0	00.0	1.0	+/-1.0	1.90	42.6	0.091
14	791120-04	10.0	30.0	00.0	1.0	+/-1.0	1.90	48.0	0.100
15	791120-04	20.0	30.0	00.0	1.0	+/-1.0	1.90	43.7	0.093
16	791120-04	30.0	30.0	00.0	1.0	+/-1.0	1.90	40.6	0.090
17	791120-05	10.0	68.0	00.0	1.0	+/-1.0	1.90	52.9	0.096
18	791120-05	20.0	68.0	00.0	1.0	+/-1.0	1.90	51.6	0.093
19	791120-05	30.0	68.0	00.0	1.0	+/-1.0	1.90	49.9	0.090
20	791120-06	30.0	68.0	00.0	1.0	+/-1.0	1.90	51.2	0.091
21	791130-01	10.0	30.0	00.0	1.0	+/-1.0	1.45	44.5	0.096
22	791130-01	20.0	30.0	00.0	1.0	+/-1.0	1.45	36.1	0.086
23	791130-01	30.0	30.0	00.0	1.0	+/-1.0	1.45	28.4	0.091
24	791130-02	30.0	30.0	00.0	1.0	+/-1.0	1.45	31.6	0.082
25	791130-03	30.0	70.0	00.0	1.0	+/-1.0	1.45	55.4	0.092
26	791130-05	10.0	70.0	00.0	1.0	+/-1.0	1.45	66.0	0.098
27	791130-05	20.0	70.0	00.0	1.0	+/-1.0	1.45	58.3	0.095
28	791130-05	30.0	70.0	00.0	1.0	+/-1.0	1.45	51.1	0.092
29	800514-01	20.0	70.0	00.0	1.0	+/-1.0	1.45	45.1	0.093
30	800514-02	20.0	70.0	00.0	1.0	+/-1.0	1.90	53.7	0.094
31	800514-03	20.0	70.0	00.0	1.0	+/-1.0	1.90	56.1	0.097
32	800514-04	20.0	70.0	00.0	1.0	+/-1.0	1.45	46.9	0.083
33	800514-09	20.0	70.0	00.0	1.0	+/-1.0	1.90	46.5	0.088
34	791103-03	10.0	31.0	00.0	1.0	+/-1.0	1.45	52.0	0.114
35	791103-03	20.0	31.0	00.0	1.0	+/-1.0	1.45	43.9	0.105
36	791103-01	10.0	30.0	00.0	1.0	+/-1.0	1.00	39.4	0.083
37	791103-02	20.0	30.0	00.0	1.0	+/-1.0	1.00	37.0	0.080
38	791130-06	10.0	70.0	00.0	1.0	+/-1.0	1.45	66.5	0.093
39	791130-06	20.0	70.0	00.0	1.0	+/-1.0	1.45	57.0	0.096
40	791130-06	30.0	70.0	00.0	1.0	+/-1.0	1.45	49.9	0.092
41	C								
42									
43									
44									
45									

FILE: DATA FORTRAN * 11/12/80 19:09:00 UNIVERSITY OF WATERLOO PAGE

RESULTS OF SIDE SLIP INTERACTION TESTS WITH TDF-88 FLUID
USING AN ASPECT RATIO OF 1.0 AND WITH 6.0 DEGREES SPIN.

	TEST NOS.	SPEED (M/S)	TEMP (C)	SPIN DEG	ASPECT (-)	SLIP SLIP	PRESS. (GPA.)	SLOPE (-)	INTERF. COEFF.
1	791119-02	30.0	29.0	06.0	1.0	+/-1.0	1.45	-	0.085
2	791119-03	30.0	30.0	06.0	1.0	+/-1.0	1.90	-	0.089
3	791120-02	30.0	30.0	06.0	1.0	+/-1.0	1.45	-	0.085
4	791120-03	30.0	30.0	06.0	1.0	+/-1.0	1.90	-	0.089
5	791120-06	30.0	68.0	06.0	1.0	+/-1.0	1.90	-	0.083
6	791130-02	30.0	30.0	06.0	1.0	+/-1.0	1.45	-	0.083
7	791130-03	30.0	70.0	06.0	1.0	+/-1.0	1.45	-	0.090
8	800514-01	20.0	70.0	06.0	1.0	+/-1.0	1.45	-	0.081
9	800514-02	20.0	70.0	06.0	1.0	+/-1.0	1.90	-	0.092
10	800514-10	20.0	70.0	06.0	1.0	+/-1.0	1.90	-	0.089
11	800514-12	20.0	70.0	06.0	1.0	+/-1.0	1.45	-	0.079
12	791103-04	10.0	32.0	06.0	1.0	+/-1.0	1.45	-	0.115
13	791103-04	20.0	32.0	06.0	1.0	+/-1.0	1.45	-	0.105
14	C								

```
C
C
C     RESULTS OF SIDE SLIP INTERACTION TESTS WITH TIF-88 FLUID
C     USING AN ASPECT RATIO OF 0.5 AND WITH 0 DEGREES SKIN.
C
C
C
C
C
C
```

	TEST NOS.	SPEED (M/S)	TEMP (C)	SKIN DEG	ASPECT (-)	SIDE SLIP	PRESS. (GPA.)	SLOPE (-)	TRACT. COEFF.
1	791113-01	10.0	33.0	00.0	0.5	+/-1.0	1.90	59.5	0.105
2	791113-01	20.0	33.0	00.0	0.5	+/-1.0	1.90	44.0	0.098
3	791113-01	30.0	33.0	00.0	0.5	+/-1.0	1.90	37.0	0.092
4	791113-02	10.0	32.0	00.0	0.5	+/-1.0	1.80	64.8	0.111
5	791113-02	20.0	32.0	00.0	0.5	+/-1.0	1.80	46.4	0.102
6	791113-02	30.0	32.0	00.0	0.5	+/-1.0	1.80	31.5	0.092
7	791113-03	20.0	33.0	00.0	0.5	+/-1.0	1.80	40.7	0.101
8	791113-04	30.0	33.0	00.0	0.5	+/-1.0	1.90	43.2	0.094
9	791115-01	10.0	70.0	00.0	0.5	+/-1.0	1.80	89.3	0.111
10	791115-01	20.0	70.0	00.0	0.5	+/-1.0	1.80	73.9	0.108
11	791115-02	15.0	68.0	00.0	0.5	+/-1.0	1.80	81.3	0.110
12	791115-03	27.5	66.0	00.0	0.5	+/-1.0	1.90	63.2	0.099
13	791115-04	10.0	70.0	00.0	0.5	+/-1.0	1.90	78.7	0.104
14	791115-04	20.0	70.0	00.0	0.5	+/-1.0	1.90	67.5	0.101
15	791115-04	27.5	70.0	00.0	0.5	+/-1.0	1.90	65.3	0.099
16	(								
17									
18									
19									
20									
21									
22									
23									
24									
25									
26									
27									
28									
29									
30									
31									
32									
33									
34									
35									
36									
37									
38									
39									
40									
41									
42									
43									
44									
45									


```
C
```

FILE: DATA FORTRAN * 11/12/80 19:09:00 UNIVERSITY OF WATERLOO PAGE

C
C
C RESULTS OF SIDE SLIP TRACTION TESTS WITH TDF-88 FLUID
C USING AN ASPECT RATIO OF 0.5 AND WITH 6.0 DEGREES SPIN.
C
C
C
C
C

	TEST NOS.	SPEED (M/S)	TEMP (C)	SPIN DEG	ASPECT (-)	SLIP	PRESS. (GPA.)	SLOPE (-)	TRACT. COEFF.
1	791113-03	20.0	33.0	06.0	0.5	+/-1.0	1.60	-	0.098
2	791113-04	30.0	33.0	06.0	0.5	+/-1.0	1.90	-	0.092
3	791115-02	15.0	66.0	06.0	0.5	+/-1.0	1.60	-	0.106
4	791115-03	10.0	66.0	06.0	0.5	+/-1.0	1.90	-	0.099
5	791115-05	27.5	66.0	06.0	0.5	+/-1.0	1.90	-	0.095
6	(								
7									
8									
9									
10									
11									
12									
13									
14									
15									
16									
17									
18									
19									
20									
21									
22									
23									
24									
25									
26									
27									
28									
29									
30									
31									
32									
33									
34									
35									
36									
37									
38									
39									
40									
41									
42									
43									
44									
45									

C

DAT1

APPENDIX III

The data shown in appendix II was used in the data correlation for purposes of interpolation by computer means. The sub appendices consist of;

FLUID	CORRELATION ON	SPIN	#DATA POINTS	APPENDIX
SANTO 50	SLOPE	NO	73	III-A
TDF 88	SLOPE	NO	105	III-B
SANTO 50	TRACTION COEFF	NO	53	III-C
TDF 88	TRACTION COEFF	NO	94	III-D
SANTO 50	TRACTION COEFF	YES	193	III-E
TDF 88	TRACTION COEFF	YES	152	III-F

APPENDIX III-A

Correlation for
SANTO-50 on slope of side slip traces
zero degrees spin.

THIS CORRELATION, FOR OF TO 16 DEGREES OF FREEDOM, IS PERFORMED WITH RESPECT TO THE SLOPES OF THE SIDE SLIP TRACTION TRACES.

THE NUMBER OF DEGREES OF FREEDOM FOR THIS CORRELATION IS; 16

THE COEFFICIENTS ARE

0.450E 02	-0.719E 01	0.114E 02	0.109E 02
-0.701E-01	-0.817E-01	0.444E 00	0.805E 00
-0.755E 01	-0.577E 00	0.124E 02	0.115E 02
-0.921E-02	-0.759E-01	0.173E 00	0.250E-01

	TEST NOS.	SPEED* (M/S)	TEMP* (C)	SKIN* DEG	ASPECT* (-)	PRESS.* (GPA)	SLOPE (-)	TRACT. COEFF.	EST.	PERCENT ERROR
1	790726- 2	-0.6	-0.4	0.0	0.8	-0.11	37.0	0.094	43.288	-15.9
2	790726- 2	0.1	-0.4	0.0	0.8	-0.11	32.0	0.079	36.641	-13.6
3	790726- 2	0.7	-0.4	0.0	0.8	-0.11	28.0	0.065	29.994	-6.5
4	790726- 3	-0.6	-0.1	0.0	0.8	-0.11	38.0	0.092	45.084	-17.1
5	790726- 3	0.1	-0.1	0.0	0.8	-0.11	36.5	0.078	38.366	-5.0
6	790726- 3	0.7	-0.1	0.0	0.8	-0.11	29.2	0.065	32.347	-11.1
7	790601- 1	0.7	-0.4	0.0	0.8	0.06	34.9	0.076	35.619	-2.0
8	790531- 1	-0.6	-0.4	0.0	0.8	0.06	47.4	0.103	44.227	6.7
9	790531- 2	0.1	-0.4	0.0	0.8	0.06	39.8	0.090	39.925	-0.3
10	790531- 3	-0.6	-0.1	0.0	0.8	0.06	48.5	0.100	44.364	8.5
11	790531- 4	0.1	-0.1	0.0	0.8	0.06	40.0	0.087	40.597	-1.5
12	790531- 5	0.7	-0.1	0.0	0.8	0.06	36.0	0.076	36.631	3.7
13	790531- 6	0.7	0.3	0.0	0.8	0.06	37.2	0.070	34.955	6.1
14	790531- 7	-0.6	0.3	0.0	0.8	0.06	44.0	0.087	43.987	0.0
15	790531- 8	0.1	0.3	0.0	0.8	0.06	40.0	0.079	39.504	1.2
16	790123- 1	-0.6	-0.5	0.0	0.8	-0.27	49.1	0.085	42.298	15.0
17	790123- 2	0.1	-0.5	0.0	0.8	-0.27	34.7	0.062	33.394	3.8
18	790123- 3	0.7	-0.5	0.0	0.8	-0.27	29.2	0.047	24.490	17.7
19	790123- 4	-0.6	-0.1	0.0	0.8	-0.27	47.9	0.077	45.582	5.0
20	790123- 5	0.1	-0.1	0.0	0.8	-0.27	39.4	0.058	37.405	5.2
21	790123- 6	0.7	-0.1	0.0	0.8	-0.27	29.6	0.046	29.228	1.3
22	790126- 2	0.1	0.3	0.0	0.8	-0.27	26.0	0.054	31.066	-6.9
23	790126- 3	0.7	0.3	0.0	0.8	-0.27	22.2	0.040	21.740	2.1
24	790628- 1	-0.6	-0.2	0.0	0.8	0.06	45.0	0.087	44.347	1.5
25	790628- 2	0.1	-0.3	0.0	0.8	0.06	42.5	0.086	40.016	6.1
26	790628- 3	0.7	-0.1	0.0	0.8	0.06	38.5	0.075	36.631	5.0
27	790727- 3	-0.6	0.3	0.0	0.8	-0.11	37.8	0.077	42.105	-11.5
28	790727- 3	0.1	0.3	0.0	0.8	-0.11	29.5	0.063	35.188	-17.7
29	790727- 3	0.7	0.3	0.0	0.8	-0.11	28.2	0.055	28.210	-0.0
30	800627- 1	-0.6	0.3	0.0	0.8	-0.11	48.7	0.087	42.042	14.8
31	790126- 1	-0.6	0.3	0.0	0.8	-0.27	40.3	0.063	40.079	0.6
32	800626-15	-0.6	0.3	0.0	-0.3	0.06	47.7	0.095	51.163	-7.0
33	800626- 7	-0.6	0.3	0.0	-0.3	-0.27	51.1	0.090	49.949	2.3
34	800626-16	-0.6	0.3	0.0	-0.3	-0.27	44.7	0.082	49.949	-11.1
35	800626-12	-0.6	0.3	0.0	-0.3	0.06	53.2	0.094	51.163	3.9
36	790329- 1	0.1	-0.5	0.0	-0.8	-0.27	39.8	0.085	47.593	-18.5
37	790329- 2	0.1	-0.5	0.0	-0.8	0.06	48.4	0.087	49.270	-1.8
38	790329- 3	0.1	-0.4	0.0	-0.8	0.39	40.1	0.096	50.951	-24.2
39	790329- 4	-0.6	-0.5	0.0	-0.8	0.39	41.1	0.104	54.480	-28.9
40	790329- 5	0.7	-0.5	0.0	-0.8	0.39	38.8	0.091	47.439	-20.2
41	790311- 2	0.1	-0.4	0.0	-0.8	0.06	53.3	0.093	49.276	7.6
42	790311- 3	0.1	-0.4	0.0	-0.8	0.39	41.1	0.093	50.953	-21.7
43	790311- 4	-0.6	0.2	0.0	-0.8	-0.27	57.4	0.082	53.209	7.8

44	790311- 5	0.1	0.2	0.0	-0.6	-0.27	50.9	0.075	47.599	6.7
45	790311- 6	0.7	0.3	0.0	-0.6	-0.27	43.5	0.076	41.991	3.5
46	790311- 7	-0.6	0.2	0.0	-0.6	0.06	56.8	0.084	53.517	6.0
47	790311- 8	0.1	0.2	0.0	-0.6	0.06	53.6	0.081	49.156	8.7
48	790311- 9	0.7	0.2	0.0	-0.6	0.06	49.1	0.076	44.793	9.2
49	790311-10	0.1	0.3	0.0	-0.6	0.39	54.9	0.091	50.729	7.9
50	800623- 1	-0.6	0.3	0.0	-0.6	0.06	48.5	0.084	53.552	-9.9
51	800623- 2	-0.6	0.3	0.0	-0.6	0.06	49.9	0.084	53.552	-7.1
52	800623- 6	-0.6	0.3	0.0	-0.6	0.39	59.6	0.097	53.897	10.1
53	800623- 7	-0.6	0.3	0.0	-0.6	0.39	56.2	0.094	53.897	4.2
54	800626- 3	-0.6	0.3	0.0	-0.6	0.39	62.4	0.096	53.897	14.7
55	781021- 1	-0.6	0.0	0.0	-0.6	-0.27	55.6	0.083	54.364	2.2
56	781021- 2	0.1	0.0	0.0	-0.6	-0.27	45.6	0.068	47.685	-4.5
57	781021- 4	0.7	0.0	0.0	-0.6	-0.27	42.0	0.060	41.006	2.4
58	781021- 5	-0.6	-0.1	0.0	-0.6	0.06	59.2	0.095	54.429	8.4
59	781021- 6	0.1	-0.0	0.0	-0.6	0.06	58.0	0.086	50.331	14.2
60	781021- 7	0.7	0.0	0.0	-0.6	0.06	52.0	0.078	51.656	0.7
61	781021- 9	-0.6	-0.1	0.0	-0.6	0.39	54.0	0.099	55.071	-2.0
62	781021-10	0.1	-0.1	0.0	-0.6	0.39	50.4	0.092	51.548	-2.3
63	781021- 8	0.7	-0.1	0.0	-0.6	0.39	51.0	0.086	46.910	8.4
64	781016- 1	-0.6	0.2	0.0	-0.6	-0.27	54.0	0.070	53.210	1.5
65	781016- 2	0.1	0.2	0.0	-0.6	-0.27	45.4	0.063	47.599	-4.7
66	781016- 3	0.7	0.2	0.0	-0.6	-0.27	39.6	0.056	41.989	-5.9
67	781019- 1	-0.6	0.2	0.0	-0.6	0.06	60.4	0.087	53.488	12.2
68	781019- 2	0.1	0.2	0.0	-0.6	0.06	55.5	0.081	49.146	12.4
69	781019- 3	0.7	0.2	0.0	-0.6	0.06	51.4	0.074	44.803	15.3
70	781020- 1	-0.6	0.2	0.0	-0.6	0.39	53.2	0.088	53.765	-1.1
71	781020- 2	0.1	0.2	0.0	-0.6	0.39	49.4	0.083	50.693	-2.6
72	781019- 3	0.7	0.2	0.0	-0.6	0.39	50.6	0.079	47.616	6.1
73	790311- 1	0.1	-0.4	0.0	-0.6	-0.27	34.3	0.065	47.599	-38.4

THE MEAN OF THE ERROR IS -0.5288
THE STANDARD DEVIATION OF THE SPEED IS 10.742

THE MEAN VELOCITY IS; 45.890 M/SEC
THE MEAN PRESSURE IS; 1.369 GPA
THE MEAN TEMPERATURE IS; 54.890 DEGREES C
THE MEAN SLIP PARAMETER IS; 0.000
THE MEAN ASPECT PARAMETER IS; 2.783

ORIGINAL PAGE IS OF POOR QUALITY

STATEMENTS EXECUTED= 59948

CORE USAGE OBJECT CODE= 9016 BYTES,ARRAY AREA= 5950 BYTES,[illegible]

DIAGNOSTICS NUMBER OF ERRORS= 0, NUMBER OF WARNINGS= 0, [illegible]

COMPILE TIME= 1.09 SEC,EXECUTION TIME= 6.27 SEC, 16.40.45 [illegible]

CASTOR

APPENDIX III-B

Correlation for
TDF-88 on slope of side slip traces
zero degrees spin.

THIS CORRELATION, FOR OF TC 16 DEGREES OF FREEDOM, IS PERFORMED WITH RESPECT TO THE SLOPES OF THE SIDE SLIP TRACTION TRACES.

THE NUMBER OF DEGREES OF FREEDOM FOR THIS CORRELATION IS; 16

THE COEFFICIENTS ARE

0.452E 02	-0.492E 01	0.694E 01	-0.102E 02
0.202E 01	-0.154E 01	-0.559E 00	0.609E 00
-0.124E 02	0.101E 02	0.157E 02	0.270E 01
-0.639E 00	0.558E 00	0.245E 01	-0.196E 01

	TEST NOS.	SPEED* (M/S)	TEMP* (C)	SKIN* DEG	ASPECT* (-)	PRESS.* (GPA)	SLOPE (-)	TRACT. COEFF.	EST.	PERCENT ERROR
1	791103-10	-0.6	-0.3	0.0	1.2	-0.30	38.6	0.095	43.822	-12.7
2	791103-10	-0.1	-0.3	0.0	1.2	-0.30	34.8	0.080	41.240	-17.1
3	791103-11	-0.6	-0.3	0.0	1.2	0.02	40.6	0.096	38.648	4.9
4	791103-11	-0.1	-0.3	0.0	1.2	0.02	39.3	0.090	38.703	1.5
5	791103-11	0.3	-0.3	0.0	1.2	0.02	38.1	0.084	38.753	-1.7
6	791128- 1	-0.6	-0.4	0.0	1.2	0.02	39.4	0.090	38.712	1.8
7	791128- 1	-0.1	-0.4	0.0	1.2	0.02	37.2	0.083	38.774	-4.1
8	791128- 1	0.3	-0.4	0.0	1.2	0.02	35.9	0.078	38.837	-7.9
9	791123- 1	-0.6	-0.4	0.0	1.2	-0.30	34.6	0.095	43.865	-23.9
10	791123- 1	-0.1	-0.4	0.0	1.2	-0.30	33.3	0.085	41.286	-21.7
11	791123- 1	0.3	-0.4	0.0	1.2	-0.30	32.8	0.079	38.706	-16.8
12	791130- 4	-0.6	0.4	0.0	1.2	-0.30	56.5	0.083	44.311	24.5
13	791130- 4	-0.1	0.4	0.0	1.2	-0.30	51.4	0.077	41.756	20.9
14	791130- 4	0.3	0.4	0.0	1.2	-0.30	42.6	0.071	39.202	8.3
15	791120- 7	-0.6	0.4	0.0	1.2	-0.30	51.1	0.079	44.311	14.3
16	791120- 7	-0.1	0.4	0.0	1.2	-0.30	43.9	0.074	41.756	5.0
17	791120- 7	0.3	0.4	0.0	1.2	-0.30	39.5	0.069	39.202	0.8
18	791120- 8	-0.6	0.4	0.0	1.2	0.02	47.0	0.084	39.364	17.8
19	791120- 8	-0.1	0.4	0.0	1.2	0.02	42.2	0.081	39.508	6.8
20	791120- 8	0.3	0.4	0.0	1.2	0.02	40.8	0.078	39.652	2.9
21	791004- 2	1.2	-0.0	0.0	1.2	-0.30	34.7	0.059	31.215	10.6
22	791004- 4	-0.1	0.0	0.0	1.2	-0.30	44.1	0.079	46.614	-5.5
23	791004- 4	1.2	0.0	0.0	1.2	-0.30	38.9	0.064	39.715	-2.1
24	791004- 4	2.6	0.0	0.0	1.2	-0.30	34.0	0.050	32.815	3.5
25	800529- 1	-0.1	0.4	0.0	1.2	-0.30	38.0	0.071	41.756	-9.4
26	800529- 3	-0.1	0.4	0.0	1.2	-0.14	49.0	0.082	40.657	19.8
27	791004- 1	2.6	0.4	0.0	1.2	-0.30	27.6	0.044	26.428	4.3
28	791103-10	-0.6	-0.3	0.0	1.2	-0.30	48.0	0.095	43.822	9.1
29	791103-10	-0.1	-0.3	0.0	1.2	-0.30	35.5	0.080	41.240	-15.0
30	791103-10	0.3	-0.3	0.0	1.2	-0.30	30.0	0.070	38.658	-25.6
31	791103- 6	-0.6	-0.3	0.0	-0.1	-0.30	55.6	0.100	44.213	23.1
32	791103- 6	-0.1	-0.3	0.0	-0.1	-0.30	41.1	0.088	38.065	7.7
33	791103- 6	0.3	-0.3	0.0	-0.1	-0.30	36.6	0.080	31.917	13.7
34	791103- 8	-0.6	-0.3	0.0	-0.1	0.02	47.0	0.101	45.544	3.1
35	791103- 8	-0.1	-0.3	0.0	-0.1	0.02	43.2	0.093	40.533	6.4
36	791103- 8	0.3	-0.3	0.0	-0.1	0.02	40.9	0.087	35.522	14.1
37	791103- 7	0.3	-0.3	0.0	-0.1	-0.30	35.6	0.081	31.917	10.9
38	791103- 9	0.3	-0.3	0.0	-0.1	0.02	39.4	0.084	35.522	10.4
39	791115- 5	-0.6	0.4	0.0	-0.1	-0.30	64.3	0.084	60.999	5.3
40	791115- 5	-0.1	0.4	0.0	-0.1	-0.30	47.1	0.080	51.367	-8.7
41	791115- 5	0.3	0.4	0.0	-0.1	-0.30	43.4	0.075	41.735	3.9
42	791115- 6	0.3	0.4	0.0	-0.1	-0.30	43.7	0.076	41.735	4.6
43	791115- 7	0.3	0.4	0.0	-0.1	0.02	49.0	0.084	46.131	6.2

44	791115- 8	-0.6	0.4	0.0	-0.1	0.02	55.8	0.090	59.293	-6.1
45	791115- 8	-0.1	0.4	0.0	-0.1	0.02	51.9	0.086	52.712	-1.6
46	791115- 8	0.3	0.4	0.0	-0.1	0.02	51.9	0.083	46.131	11.8
47	800523- 1	-0.1	0.4	0.0	-0.1	0.02	55.7	0.094	52.712	5.5
48	800526- 2	-0.1	0.4	0.0	-0.1	-0.30	34.4	0.073	51.367	-41.2
49	800526- 6	-0.1	0.4	0.0	-0.1	0.02	47.6	0.087	52.712	-10.2
50	800526- 7	-0.1	0.4	0.0	-0.1	0.02	45.6	0.086	52.712	-14.5
51	791119- 1	-0.6	-0.4	0.0	-0.6	0.02	47.9	0.101	50.270	-4.8
52	791119- 1	-0.1	-0.4	0.0	-0.6	0.02	39.1	0.090	43.285	-10.2
53	791119- 1	0.3	-0.4	0.0	-0.6	0.02	38.5	0.083	36.301	5.9
54	791119- 2	0.3	-0.4	0.0	-0.6	0.02	37.4	0.085	36.004	3.8
55	791119- 3	0.3	-0.4	0.0	-0.6	0.33	45.0	0.089	40.941	9.5
56	791119- 4	-0.6	-0.4	0.0	-0.6	0.33	49.3	0.099	53.281	-7.8
57	791119- 4	-0.1	-0.4	0.0	-0.6	0.33	45.9	0.095	47.111	-2.6
58	791119- 4	0.3	-0.4	0.0	-0.6	0.33	43.1	0.089	40.941	5.1
59	791120- 1	-0.6	-0.4	0.0	-0.6	0.02	47.9	0.100	49.451	-3.2
60	791120- 1	-0.1	-0.4	0.0	-0.6	0.02	43.2	0.092	42.563	1.5
61	791120- 1	0.3	-0.4	0.0	-0.6	0.02	37.1	0.084	35.675	3.9
62	791120- 2	0.3	-0.4	0.0	-0.6	0.02	36.9	0.086	35.675	3.4
63	791120- 3	0.3	-0.4	0.0	-0.6	0.33	42.6	0.091	40.941	4.0
64	791120- 4	-0.6	-0.4	0.0	-0.6	0.33	48.0	0.100	53.281	-10.5
65	791120- 4	-0.1	-0.4	0.0	-0.6	0.33	43.7	0.095	47.111	-7.5
66	791120- 4	0.3	-0.4	0.0	-0.6	0.33	40.6	0.090	40.941	-0.8
67	791120- 5	-0.6	0.4	0.0	-0.6	0.33	52.9	0.096	65.919	-22.2
68	791120- 5	-0.1	0.4	0.0	-0.6	0.33	50.6	0.093	60.289	-17.6
69	791120- 5	0.3	0.4	0.0	-0.6	0.33	49.5	0.090	54.660	-9.1
70	791120- 6	0.3	0.4	0.0	-0.6	0.33	51.2	0.091	54.660	-6.5
71	791130- 1	-0.6	-0.4	0.0	-0.6	0.02	44.5	0.096	49.451	-10.6
72	791130- 1	-0.1	-0.4	0.0	-0.6	0.02	36.1	0.086	42.563	-15.5
73	791130- 1	0.3	-0.4	0.0	-0.6	0.02	28.4	0.081	35.675	-23.0
74	791130- 2	0.3	-0.4	0.0	-0.6	0.02	31.6	0.082	35.675	-12.2
75	791130- 3	0.3	0.4	0.0	-0.6	0.02	55.4	0.092	48.290	13.9
76	791130- 5	-0.6	0.4	0.0	-0.6	0.02	66.0	0.098	65.937	0.1
77	791130- 5	-0.1	0.4	0.0	-0.6	0.02	58.3	0.095	57.114	2.1
78	791130- 5	0.3	0.4	0.0	-0.6	0.02	51.1	0.092	48.290	5.7
79	800514- 1	-0.1	0.4	0.0	-0.6	0.02	45.1	0.083	57.114	-23.8
80	800514- 2	-0.1	0.4	0.0	-0.6	0.33	53.7	0.094	59.657	-10.5
81	800514- 3	-0.1	0.4	0.0	-0.6	0.33	56.1	0.097	59.657	-6.2
82	800514- 4	-0.1	0.4	0.0	-0.6	0.02	46.9	0.083	57.114	-19.8
83	800514- 8	-0.1	0.4	0.0	-0.6	0.33	46.5	0.088	59.657	-25.2
84	791103- 3	-0.6	-0.4	0.0	-0.6	0.02	52.0	0.114	48.974	6.0
85	791103- 3	-0.1	-0.4	0.0	-0.6	0.02	43.9	0.105	42.142	4.1
86	791103- 1	-0.6	-0.4	0.0	-0.6	-0.30	39.4	0.089	45.621	-14.7
87	791103- 2	-0.1	-0.4	0.0	-0.6	-0.30	27.0	0.080	38.015	-34.9
88	791130- 6	-0.6	0.4	0.0	-0.6	0.02	66.5	0.098	65.937	0.9
89	791130- 6	-0.1	0.4	0.0	-0.6	0.02	57.0	0.096	57.114	-0.2
90	791130- 6	0.3	0.4	0.0	-0.6	0.02	49.9	0.092	48.290	3.3
91	791113- 1	-0.6	-0.3	0.0	-0.8	0.33	59.5	0.105	54.436	8.9
92	791113- 1	-0.1	-0.3	0.0	-0.8	0.33	44.0	0.098	47.101	-6.8
93	791113- 1	0.3	-0.3	0.0	-0.8	0.33	37.0	0.092	39.767	-7.2
94	791113- 2	-0.6	-0.3	0.0	-0.8	0.12	64.8	0.111	51.416	23.3
95	791113- 2	-0.1	-0.3	0.0	-0.8	0.12	46.4	0.102	43.896	5.5
96	791113- 2	0.3	-0.3	0.0	-0.8	0.12	31.5	0.092	36.876	-14.4
97	791113- 3	-0.1	-0.3	0.0	-0.8	0.12	46.7	0.101	43.332	-6.3
98	791113- 4	0.3	-0.3	0.0	-0.8	0.33	43.2	0.094	39.767	8.3
99	791115- 1	-0.6	0.4	0.0	-0.8	0.12	89.8	0.111	69.230	29.3
100	791115- 1	-0.1	0.4	0.0	-0.8	0.12	73.9	0.109	60.362	20.4
101	791115- 2	-0.3	0.4	0.0	-0.8	0.12	81.3	0.110	65.616	21.6
102	791115- 3	0.2	0.3	0.0	-0.8	0.33	63.2	0.099	59.043	6.6
103	791115- 4	-0.6	0.4	0.0	-0.8	0.33	73.7	0.104	69.174	6.3

```
104        791115- 4  -0.1    0.4    0.0 -0.8   0.33   67.5   0.101   62.457     7.8
105        791115- 4   0.2    0.4    0.0 -0.8   0.33   65.3   0.099   57.418    12.9

THE MEAN OF THE ERROR IS -0.738%
THE STANDARD DEVIATION OF THE ERROR IS   13.074

THE MEAN VELOCITY IS;  22.476 M/SEC
THE MEAN PRESSURE IS;   1.424 GPA
THE MEAN TEMPERATURE IS;  49.076 DEGREES C
THE MEAN SKID PARAMETER IS;   0.000
THE MEAN ASPECT PARAMETER IS;   2.262

STATEMENTS EXECUTED=   81000

CORE USAGE       OBJECT CODE=    9016 BYTES,ARRAY AREA=   10756 BYTES,TOTAL AR

DIAGNOSTICS       NUMBER OF ERRORS=       0, NUMBER OF WARNINGS=       0, NUM

COMPILE TIME=     0.99 SEC,EXECUTION TIME=     7.38 SEC,      19.34.12     WEDNE

          C$SIOE
```

APPENDIX III-C

Correlation for
SANTO-50 on traction coeffcient
zero degrees spin.

THIS CORRELATION, FOR UP TO 16 DEGREES OF FREEDOM, IS PERFORMED WITH RESPECT TO THE TRACTION COEFFICIENT.

THE NUMBER OF DEGREES OF FREEDOM FOR THIS CORRELATION IS; 16

THE COEFFICIENTS ARE

0.843E-01	-0.685E-02	0.434E-01	0.421E-01
-0.960E-03	0.114E-02	-0.449E-03	-0.120E-02
-0.197E-01	0.299E-02	0.350E-01	0.664E-02
0.172E-02	-0.317E-02	-0.285E-02	0.956E-02

	TEST NOS.	SPEED *	TEMP *	SPIN *	ASPECT *	PRESS. *	SLOPE (-)	TRACT. COEFF.	EST.	PERCENT ERROR
1	790726- 2	-0.6	-0.4	0.0	0.5	-0.10	37.0	0.094	0.087	7.4
2	790726- 2	0.1	-0.4	0.0	0.5	-0.10	32.0	0.079	0.073	8.3
3	790726- 2	0.8	-0.4	0.0	0.5	-0.10	28.0	0.065	0.058	11.3
4	790726- 3	-0.6	-0.1	0.0	0.5	-0.10	38.0	0.092	0.091	1.4
5	790726- 3	0.1	-0.1	0.0	0.5	-0.10	36.5	0.078	0.076	2.0
6	790726- 3	0.8	-0.1	0.0	0.5	-0.10	29.2	0.065	0.062	4.8
7	790601- 1	0.8	-0.4	0.0	0.5	0.07	34.9	0.076	0.074	2.8
8	790531- 1	-0.6	-0.4	0.0	0.5	0.07	47.4	0.103	0.096	7.5
9	790531- 2	0.1	-0.4	0.0	0.5	0.07	39.8	0.090	0.085	6.0
10	790531- 3	-0.6	-0.1	0.0	0.5	0.07	48.5	0.100	0.103	-3.4
11	790531- 4	0.1	-0.1	0.0	0.5	0.07	40.0	0.087	0.090	-3.7
12	790531- 5	0.8	-0.1	0.0	0.5	0.07	38.0	0.076	0.077	-1.4
13	790531- 6	0.8	0.3	0.0	0.5	0.07	37.2	0.070	0.073	-3.6
14	790531- 7	-0.6	0.3	0.0	0.5	0.07	44.0	0.087	0.092	-5.4
15	790531- 8	0.1	0.4	0.0	0.5	0.07	40.0	0.079	0.082	-4.3
16	790123- 1	-0.6	-0.4	0.0	0.5	-0.26	49.1	0.085	0.079	6.7
17	790123- 2	0.1	-0.4	0.0	0.5	-0.26	34.7	0.062	0.061	1.3
18	790123- 3	0.8	-0.4	0.0	0.5	-0.26	29.2	0.047	0.043	9.2
19	790123- 4	-0.6	-0.1	0.0	0.5	-0.26	47.9	0.077	0.078	-1.4
20	790123- 5	0.1	-0.1	0.0	0.5	-0.26	39.4	0.058	0.063	-8.6
21	790123- 6	0.8	-0.1	0.0	0.5	-0.26	29.6	0.046	0.048	-4.2
22	790126- 2	0.1	0.4	0.0	0.5	-0.26	29.0	0.054	0.060	-11.2
23	790126- 3	0.8	0.4	0.0	0.5	-0.26	22.2	0.040	0.041	-2.2
24	790628- 1	-0.6	-0.2	0.0	0.5	0.07	45.0	0.097	0.098	-0.9
25	790628- 2	0.1	-0.3	0.0	0.5	0.07	42.5	0.086	0.085	0.8
26	790628- 3	0.8	-0.1	0.0	0.5	0.07	38.5	0.075	0.077	-2.7
27	790727- 3	-0.6	0.4	0.0	0.5	-0.10	37.8	0.077	0.086	-11.0
28	790727- 3	0.1	0.4	0.0	0.5	-0.10	29.5	0.063	0.071	-12.2
29	790727- 3	0.8	0.4	0.0	0.5	-0.10	28.2	0.055	0.056	-2.5
30	800627- 1	-0.6	0.3	0.0	0.5	-0.10	46.7	0.087	0.086	1.4
31	800626-15	-0.6	0.3	0.0	-0.4	0.07	47.7	0.095	0.090	5.3
32	800626- 7	-0.6	0.3	0.0	-0.4	-0.26	51.1	0.090	0.083	7.9
33	800626-16	-0.6	0.3	0.0	-0.4	-0.26	44.7	0.082	0.083	-1.5
34	800626-12	-0.6	0.3	0.0	-0.4	0.07	53.2	0.094	0.090	4.2
35	790329- 1	0.1	-0.5	0.0	-0.7	-0.26	39.6	0.085	0.084	0.6
36	790329- 2	0.1	-0.5	0.0	-0.7	0.07	48.4	0.087	0.091	-4.2
37	790329- 3	0.1	-0.4	0.0	-0.7	0.40	40.1	0.096	0.097	-1.5
38	790329- 4	-0.6	-0.5	0.0	-0.7	0.40	41.1	0.104	0.104	0.3
39	790329- 5	0.8	-0.5	0.0	-0.7	0.40	38.9	0.091	0.091	0.5
40	790311- 2	0.1	-0.4	0.0	-0.7	0.07	53.3	0.093	0.091	1.9
41	790311- 3	0.1	-0.4	0.0	-0.7	0.40	41.1	0.099	0.098	1.2
42	790311- 4	-0.6	0.3	0.0	-0.7	-0.26	57.4	0.082	0.080	2.0
43	790311- 5	0.1	0.3	0.0	-0.7	-0.26	50.9	0.075	0.078	-3.4

44	790311- 6	0.8	0.3	0.0	-0.7	-0.26	43.5	0.076	0.073	3.8
45	790311- 7	-0.6	0.3	0.0	-0.7	0.07	56.8	0.084	0.087	-4.0
46	790311- 8	0.1	0.3	0.0	-0.7	0.07	53.6	0.081	0.083	-2.0
47	790311- 9	0.8	0.3	0.0	-0.7	0.07	49.1	0.076	0.078	-2.3
48	790311-10	0.1	0.3	0.0	-0.7	0.40	54.9	0.091	0.088	3.2
49	800623- 1	-0.6	0.3	0.0	-0.7	0.07	48.5	0.084	0.089	-6.3
50	800623- 2	-0.6	0.3	0.0	-0.7	0.07	49.9	0.084	0.089	-6.3
51	800623- 6	-0.6	0.3	0.0	-0.7	0.40	59.6	0.097	0.095	2.5
52	800623- 7	-0.6	0.3	0.0	-0.7	0.40	56.2	0.094	0.095	-0.7
53	800626- 3	-0.6	0.3	0.0	-0.7	0.40	62.4	0.096	0.095	1.4

THE MEAN OF THE ERROR IS -0.116%
THE STANDARD DEVIATION OF THE ERROR IS 5.186

THE MEAN VELOCITY IS; 44.906 M/SEC
THE MEAN PRESSURE IS; 1.356 GPA
THE MEAN TEMPERATURE IS; 53.491 DEGREES C
THE MEAN SPIN PARAMETER IS; 0.000
THE MEAN ASPECT PARAMETER IS; 3.340

STATEMENTS EXECUTED= 4627

CORE USAGE OBJECT CODE= 8952 BYTES, ARRAY AREA= 5950 BYTES, TOTAL

DIAGNOSTICS NUMBER OF ERRORS= 0, NUMBER OF WARNINGS= 0,

COMPILE TIME= 0.58 SEC, EXECUTION TIME= 3.30 SEC, 9.23.27

C$STOP

ORIGINAL PAGE IS OF POOR QUALITY

APPENDIX III-D

Correlation for
TDF-88 on traction coefficient
zero degrees spin.

THIS CORRELATION, FOR UP TO 16 DEGREES OF FREEDOM, IS PERFORMED WITH RESPECT TO THE TRACTION COEFFICIENT.

THE NUMBER OF DEGREES OF FREEDOM FOR THIS CORRELATION IS; 16

THE COEFFICIENTS ARE

0.877E-01	-0.515E-02	0.154E-01	-0.379E-02
-0.676E-03	-0.428E-03	0.444E-03	-0.346E-02
-0.126E-01	0.356E-02	0.141E-01	0.764E-02
0.167E-02	0.317E-03	-0.851E-04	0.532E-02

	TEST NOS.	SPEED *	TEMP *	SPIN *	ASPECT *	PRESS. *	SLOPE (-)	TRACT. COEFF.	EST.	PERCENT ERROR
1	791103-10	-0.6	-0.3	0.0	1.2	-0.31	38.6	0.095	0.087	9.1
2	791103-10	-0.1	-0.3	0.0	1.2	-0.31	34.8	0.080	0.080	0.3
3	791103-11	-0.6	-0.3	0.0	1.2	0.00	40.6	0.096	0.093	3.2
4	791103-11	-0.1	-0.3	0.0	1.2	0.00	39.3	0.090	0.087	3.9
5	791103-11	0.3	-0.3	0.0	1.2	0.00	38.1	0.084	0.080	4.9
6	791128- 1	-0.6	-0.4	0.0	1.2	0.00	39.4	0.090	0.092	-2.1
7	791128- 1	-0.1	-0.4	0.0	1.2	0.00	37.2	0.083	0.086	-3.4
8	791128- 1	0.3	-0.4	0.0	1.2	0.00	35.9	0.078	0.080	-2.5
9	791123- 1	-0.6	-0.4	0.0	1.2	-0.31	34.6	0.095	0.087	9.1
10	791123- 1	-0.1	-0.4	0.0	1.2	-0.31	33.3	0.085	0.080	6.4
11	791123- 1	0.3	-0.4	0.0	1.2	-0.31	32.8	0.079	0.073	8.3
12	791130- 4	-0.6	0.4	0.0	1.2	-0.31	56.5	0.083	0.086	-4.1
13	791130- 4	-0.1	0.4	0.0	1.2	-0.31	51.4	0.077	0.080	-3.3
14	791130- 4	0.3	0.4	0.0	1.2	-0.31	42.6	0.071	0.073	-2.4
15	791120- 7	-0.6	0.4	0.0	1.2	-0.31	51.1	0.079	0.086	-9.1
16	791120- 7	-0.1	0.4	0.0	1.2	-0.31	43.9	0.074	0.080	-7.3
17	791120- 7	0.3	0.4	0.0	1.2	-0.31	39.5	0.069	0.073	-5.3
18	791120- 8	-0.6	0.4	0.0	1.2	0.00	47.0	0.084	0.080	4.5
19	791120- 8	-0.1	0.4	0.0	1.2	0.00	42.2	0.081	0.079	2.7
20	791120- 8	0.3	0.4	0.0	1.2	0.00	40.8	0.078	0.077	0.8
21	791004- 2	1.2	-0.1	0.0	1.2	-0.31	34.7	0.059	0.058	1.9
22	791004- 4	-0.1	0.0	0.0	1.2	-0.31	44.1	0.079	0.077	2.3
23	791004- 4	1.2	0.0	0.0	1.2	-0.31	38.9	0.064	0.064	0.5
24	791004- 4	2.6	0.0	0.0	1.2	-0.31	34.0	0.050	0.050	-0.2
25	800529- 1	-0.1	0.4	0.0	1.2	-0.31	38.0	0.071	0.080	-11.5
26	800529- 3	-0.1	0.4	0.0	1.2	-0.16	49.0	0.082	0.079	3.4
27	791103- 6	-0.6	-0.4	0.0	-0.1	-0.31	55.6	0.100	0.098	1.8
28	791103- 6	-0.1	-0.4	0.0	-0.1	-0.31	41.1	0.088	0.088	-0.2
29	791103- 6	0.3	-0.4	0.0	-0.1	-0.31	36.6	0.080	0.078	2.2
30	791103- 8	-0.6	-0.3	0.0	-0.1	0.00	47.0	0.101	0.100	0.9
31	791103- 8	-0.1	-0.3	0.0	-0.1	0.00	43.2	0.093	0.092	1.0
32	791103- 8	0.3	-0.3	0.0	-0.1	0.00	40.9	0.087	0.084	3.4
33	791103- 7	0.3	-0.4	0.0	-0.1	-0.31	35.6	0.081	0.079	3.5
34	791103- 9	0.3	-0.3	0.0	-0.1	0.00	39.4	0.084	0.084	-0.1
35	791115- 5	-0.6	0.4	0.0	-0.1	-0.31	64.3	0.084	0.088	-4.2
36	791115- 5	-0.1	0.4	0.0	-0.1	-0.31	47.1	0.080	0.083	-3.1
37	791115- 5	0.3	0.4	0.0	-0.1	-0.31	43.4	0.075	0.077	-2.5
38	791115- 6	0.3	0.4	0.0	-0.1	-0.31	43.7	0.076	0.077	-1.2
39	791115- 7	0.3	0.4	0.0	-0.1	0.00	49.0	0.084	0.084	0.4
40	791115- 8	-0.6	0.4	0.0	-0.1	0.00	55.8	0.090	0.092	-1.9
41	791115- 8	-0.1	0.4	0.0	-0.1	0.00	51.9	0.086	0.088	-2.0
42	791115- 8	0.3	0.4	0.0	-0.1	0.00	51.9	0.083	0.084	-0.8
43	800523- 1	-0.1	0.4	0.0	-0.1	0.00	55.7	0.094	0.088	6.5

44	800526- 2	-0.1	0.4	0.0	-0.1	-0.31	34.4	0.073	0.083	-12.4
45	800526- 6	-0.1	0.4	0.0	-0.1	0.00	47.6	0.087	0.088	-0.8
46	800526- 7	-0.1	0.4	0.0	-0.1	0.00	45.6	0.086	0.083	-2.0
47	791119- 1	-0.6	-0.4	0.0	-0.6	0.00	47.9	0.101	0.102	-0.5
48	791119- 1	-0.1	-0.4	0.0	-0.6	0.00	39.1	0.090	0.093	-3.8
49	791119- 1	0.3	-0.4	0.0	-0.6	0.00	38.5	0.083	0.085	-2.9
50	791119- 2	0.3	-0.4	0.0	-0.6	0.00	37.4	0.085	0.085	-0.5
51	791119- 3	0.3	-0.4	0.0	-0.6	0.31	45.0	0.089	0.091	-2.1
52	791119- 4	-0.6	-0.4	0.0	-0.6	0.31	49.3	0.099	0.102	-3.4
53	791119- 4	-0.1	-0.4	0.0	-0.6	0.31	45.9	0.095	0.097	-1.7
54	791119- 4	0.3	-0.4	0.0	-0.6	0.31	43.1	0.089	0.091	-2.1
55	791120- 1	-0.6	-0.4	0.0	-0.6	0.00	47.9	0.100	0.102	-1.8
56	791120- 1	-0.1	-0.4	0.0	-0.6	0.00	43.2	0.092	0.094	-1.8
57	791120- 1	0.3	-0.4	0.0	-0.6	0.00	37.1	0.084	0.085	-1.7
58	791120- 2	0.3	-0.4	0.0	-0.6	0.00	36.9	0.086	0.085	0.7
59	791120- 3	0.3	-0.4	0.0	-0.6	0.31	42.6	0.091	0.091	0.1
60	791120- 4	-0.6	-0.4	0.0	-0.6	0.31	48.0	0.100	0.102	-2.4
61	791120- 4	-0.1	-0.4	0.0	-0.6	0.31	43.7	0.095	0.097	-1.7
62	791120- 4	0.3	-0.4	0.0	-0.6	0.31	40.6	0.090	0.091	-1.0
63	791120- 5	-0.6	0.4	0.0	-0.6	0.31	52.9	0.096	0.102	-6.5
64	791120- 5	-0.1	0.4	0.0	-0.6	0.31	50.6	0.093	0.098	-5.1
65	791120- 5	0.3	0.4	0.0	-0.6	0.31	49.9	0.090	0.093	-3.7
66	791120- 6	0.3	0.4	0.0	-0.6	0.31	51.2	0.091	0.093	-2.6
67	791130- 1	-0.6	-0.4	0.0	-0.6	0.00	44.5	0.096	0.102	-5.9
68	791130- 1	-0.1	-0.4	0.0	-0.6	0.00	36.1	0.086	0.094	-8.5
69	791130- 1	0.3	-0.4	0.0	-0.6	0.00	28.4	0.031	0.035	-5.3
70	791130- 2	0.3	-0.4	0.0	-0.6	0.00	31.6	0.082	0.085	-4.1
71	791130- 3	0.3	0.4	0.0	-0.6	0.00	55.4	0.092	0.086	7.0
72	791130- 5	-0.6	0.4	0.0	-0.6	0.00	66.0	0.098	0.096	2.5
73	791130- 5	-0.1	0.4	0.0	-0.6	0.00	56.3	0.095	0.091	4.6
74	791130- 5	0.3	0.4	0.0	-0.6	0.00	51.1	0.092	0.086	7.0
75	800514- 1	-0.1	0.4	0.0	-0.6	0.00	45.1	0.083	0.091	-8.4
76	800514- 2	-0.1	0.4	0.0	-0.6	0.31	53.7	0.094	0.098	-4.0
77	800514- 3	-0.1	0.4	0.0	-0.6	0.31	56.1	0.097	0.098	-0.8
78	800514- 4	-0.1	0.4	0.0	-0.6	0.00	46.9	0.083	0.091	-8.4
79	800514- 9	-0.1	0.4	0.0	-0.6	0.31	46.5	0.088	0.098	-10.8
80	791113- 1	-0.6	-0.3	0.0	-0.8	0.31	59.5	0.105	0.103	2.1
81	791113- 1	-0.1	-0.3	0.0	-0.8	0.31	44.0	0.093	0.097	4.7
82	791113- 1	0.3	-0.3	0.0	-0.8	0.31	37.0	0.092	0.091	1.0
83	791113- 2	-0.6	-0.4	0.0	-0.8	0.10	64.8	0.111	0.103	7.2
84	791113- 2	-0.1	-0.4	0.0	-0.8	0.10	46.4	0.102	0.096	6.4
85	791113- 2	0.3	-0.4	0.0	-0.8	0.10	31.5	0.092	0.088	4.7
86	791113- 3	-0.1	-0.3	0.0	-0.8	0.10	40.7	0.101	0.096	5.6
87	791113- 4	0.3	-0.3	0.0	-0.8	0.31	43.2	0.094	0.091	3.2
88	791115- 1	-0.6	0.4	0.0	-0.8	0.10	89.8	0.111	0.100	10.1
89	791115- 1	-0.1	0.4	0.0	-0.8	0.10	73.9	0.103	0.095	15.0
90	791115- 2	-0.3	0.4	0.0	-0.8	0.10	31.3	0.110	0.098	14.1
91	791115- 3	0.2	0.3	0.0	-0.8	0.31	65.2	0.099	0.096	2.9
92	791115- 4	-0.6	0.4	0.0	-0.8	0.31	73.7	0.104	0.106	-1.5
93	791115- 4	-0.1	0.4	0.0	-0.8	0.31	67.6	0.101	0.100	0.7
94	791115- 4	0.2	0.4	0.0	-0.8	0.31	65.3	0.099	0.096	3.0

THE MEAN OF THE ERROR IS -0.119%
THE STANDARD DEVIATION OF THE ERROR IS 5.009%

THE MEAN VELOCITY IS: 22.340 M/SEC
THE MEAN PRESSURE IS: 1.449 GPA
THE MEAN TEMPERATURE IS: 49.489 DEGREES C
THE MEAN SPIN PARAMETER IS: 0.000
THE MEAN ASPECT PARAMETER IS: 2.233

APPENDIX III-E

Correlation for
SANTO-50 on traction coefficient
including spin.

THE INPUT DATA FOR CORRELATION IS;

	TEST NOS.	SPEED (M/S)	TEMP (C)	SPIN DEG	ASPECT (-)	SIDE SLIP	PRESS. (GPA)	SLOPE (-)	TRACT. COEFF.
1	790726- 2	20.0	32.5	0.0	5.0		1.22	37.0	0.094
2	790726- 2	50.0	32.5	0.0	5.0		1.22	32.0	0.079
3	790726- 2	80.0	32.5	0.0	5.0		1.22	28.0	0.065
4	790726- 3	20.0	50.0	0.0	5.0		1.22	38.0	0.092
5	790726- 3	50.0	50.0	0.0	5.0		1.22	36.5	0.078
6	790726- 3	80.0	50.0	0.0	5.0		1.22	29.2	0.065
7	790601- 1	80.0	33.0	0.0	5.0		1.45	34.9	0.076
8	790531- 1	20.0	32.0	0.0	5.0		1.45	47.4	0.103
9	790531- 2	50.0	33.0	0.0	5.0		1.45	39.8	0.090
10	790531- 3	20.0	50.0	0.0	5.0		1.45	48.5	0.100
11	790531- 4	50.0	50.0	0.0	5.0		1.45	40.0	0.087
12	790531- 5	80.0	50.0	0.0	5.0		1.45	38.0	0.076
13	790531- 6	80.0	72.0	0.0	5.0		1.45	37.2	0.070
14	790531- 7	20.0	69.0	0.0	5.0		1.45	44.0	0.087
15	790531- 8	50.0	73.5	0.0	5.0		1.45	40.0	0.079
16	790123- 1	20.0	30.0	0.0	5.0		1.00	49.1	0.085
17	790123- 2	50.0	30.0	0.0	5.0		1.00	34.7	0.062
18	790123- 3	80.0	30.0	0.0	5.0		1.00	29.2	0.047
19	790123- 4	20.0	50.0	0.0	5.0		1.00	47.9	0.077
20	790123- 5	50.0	50.0	0.0	5.0		1.00	39.4	0.058
21	790123- 6	80.0	50.0	0.0	5.0		1.00	29.6	0.046
22	790126- 2	80.0	73.0	0.0	5.0		1.00	29.0	0.054
23	790126- 3	80.0	73.0	0.0	5.0		1.00	22.2	0.040
24	790628- 1	20.0	45.0	0.0	5.0		1.45	45.0	0.097
25	790628- 2	50.0	40.0	0.0	5.0		1.45	42.5	0.086
26	790628- 3	80.0	50.0	0.0	5.0		1.45	38.5	0.075
27	790727- 3	20.0	73.0	0.0	5.0		1.22	37.8	0.077
28	790727- 3	50.0	73.0	0.0	5.0		1.22	29.5	0.063
29	790727- 3	80.0	73.0	0.0	5.0		1.22	28.2	0.055
30	800627- 1	20.0	70.0	0.0	5.0		1.22	48.7	0.087
31	790126- 1	20.0	69.0	0.0	5.0		1.00	40.3	0.063
32	800628- 1	20.0	70.0	6.0	5.0		1.00	0.0	0.082
33	800628- 3	20.0	70.0	6.0	5.0		1.22	0.0	0.086
34	791127- 3	10.0	70.0	6.0	5.0		1.45	0.0	0.084
35	791127- 3	20.0	70.0	6.0	5.0		1.45	0.0	0.080
36	791127- 3	30.0	70.0	6.0	5.0		1.45	0.0	0.078
37	790726- 1	20.0	32.5	15.0	5.0		1.22	0.0	0.084
38	790726- 1	50.0	32.5	15.0	5.0		1.22	0.0	0.064
39	790726- 1	80.0	32.5	15.0	5.0		1.22	0.0	0.051
40	790629- 1	80.0	33.0	15.0	5.0		1.45	0.0	0.052
41	790629- 2	50.0	35.0	15.0	5.0		1.45	0.0	0.067
42	790629- 3	20.0	33.0	15.0	5.0		1.45	0.0	0.083
43	790629- 4	50.0	47.0	15.0	5.0		1.45	0.0	0.067
44	790629- 5	20.0	33.0	15.0	5.0		1.45	0.0	0.084
45	790629- 6	50.0	37.0	15.0	5.0		1.45	0.0	0.069
46	790629- 7	80.0	57.0	15.0	5.0		1.45	0.0	0.055
47	790629- 8	80.0	50.0	15.0	5.0		1.45	0.0	0.056
48	790629- 9	20.0	30.0	15.0	5.0		1.45	0.0	0.085
49	790629-10	50.0	33.0	15.0	5.0		1.45	0.0	0.069
50	790629-11	80.0	50.0	15.0	5.0		1.45	0.0	0.055
51	790629-12	50.0	70.0	15.0	5.0		1.45	0.0	0.068
52	790629-13	80.0	70.0	15.0	5.0		1.45	0.0	0.057
53	790629-14	20.0	70.0	15.0	5.0		1.45	0.0	0.079
54	790629-15	30.0	47.0	15.0	5.0		1.45	0.0	0.056
55	790629-16	80.0	55.0	15.0	5.0		1.45	0.0	0.055

56	790726- 4	20.0	50.0	15.0	5.0	1.22	0.0	0.083
57	790726- 4	80.0	50.0	15.0	5.0	1.22	0.0	0.051
58	790727- 2	20.0	73.0	15.0	5.0	1.22	0.0	0.079
59	790727- 2	50.0	73.0	15.0	5.0	1.22	0.0	0.065
60	790727- 2	80.0	73.0	15.0	5.0	1.22	0.0	0.056
61	790628- 6	20.0	50.0	15.0	5.0	1.45	0.0	0.082
62	790628- 4	80.0	63.0	15.0	5.0	1.45	0.0	0.055
63	790628- 5	50.0	60.0	15.0	5.0	1.45	0.0	0.065
64	790718- 1	20.0	35.0	15.0	5.0	1.00	0.0	0.103
65	790718- 2	50.0	35.0	15.0	5.0	1.00	0.0	0.077
66	790718- 3	80.0	37.0	15.0	5.0	1.00	0.0	0.065
67	790718- 4	20.0	37.0	15.0	5.0	1.00	0.0	0.082
68	790718- 5	50.0	35.0	15.0	5.0	1.60	0.0	0.064
69	790718- 6	35.0	35.0	15.0	5.0	1.60	0.0	0.075
70	790726- 5	20.0	50.0	15.0	5.0	1.00	0.0	0.084
71	790726- 5	50.0	50.0	15.0	5.0	1.00	0.0	0.063
72	790726- 5	80.0	50.0	15.0	5.0	1.00	0.0	0.043
73	790726- 4	50.0	50.0	15.0	5.0	1.22	0.0	0.062
74	790727- 1	20.0	67.0	15.0	5.0	1.00	0.0	0.085
75	790727- 1	50.0	67.0	15.0	5.0	1.00	0.0	0.069
76	790727- 1	80.0	67.0	15.0	5.0	1.00	0.0	0.059
77	790901- 1	20.0	50.0	15.0	5.0	1.00	0.0	0.077
78	790901- 1	50.0	50.0	15.0	5.0	1.00	0.0	0.055
79	790901- 1	80.0	50.0	15.0	5.0	1.00	0.0	0.045
80	790901- 2	20.0	30.0	15.0	5.0	1.00	0.0	0.101
81	790901- 2	80.0	30.0	15.0	5.0	1.00	0.0	0.057
82	790901- 3	20.0	65.0	15.0	5.0	1.00	0.0	0.092
83	790901- 3	50.0	65.0	15.0	5.0	1.00	0.0	0.070
84	790901- 3	80.0	65.0	15.0	5.0	1.00	0.0	0.058
85	790901- 2	50.0	30.0	15.0	5.0	1.00	0.0	0.073
86	790728- 1	20.0	35.0	30.0	5.0	1.45	0.0	0.059
87	790728- 1	50.0	35.0	30.0	5.0	1.45	0.0	0.040
88	790728- 1	80.0	35.0	30.0	5.0	1.45	0.0	0.031
89	790202- 1	20.0	32.0	30.0	5.0	1.00	0.0	0.071
90	790202- 2	50.0	36.0	30.0	5.0	1.00	0.0	0.046
91	790202- 3	80.0	37.0	30.0	5.0	1.00	0.0	0.035
92	790206- 1	80.0	27.0	30.0	5.0	1.00	0.0	0.035
93	790727- 4	20.0	73.0	30.0	5.0	1.45	0.0	0.064
94	790727- 4	80.0	73.0	30.0	5.0	1.45	0.0	0.033
95	790126- 4	20.0	69.0	30.0	5.0	1.00	0.0	0.065
96	790126- 5	50.0	68.0	30.0	5.0	1.00	0.0	0.046
97	790126- 5	80.0	71.0	30.0	5.0	1.00	0.0	0.034
98	790728- 2	20.0	53.0	30.0	5.0	1.45	0.0	0.061
99	790728- 2	50.0	53.0	30.0	5.0	1.45	0.0	0.043
100	790728- 2	80.0	53.0	30.0	5.0	1.45	0.0	0.034
101	790801- 2	20.0	47.0	30.0	5.0	1.45	0.0	0.071
102	790831- 2	20.0	50.0	30.0	5.0	1.22	0.0	0.088
103	790831- 2	50.0	50.0	30.0	5.0	1.22	0.0	0.059
104	790831- 2	80.0	50.0	30.0	5.0	1.22	0.0	0.045
105	790831- 1	20.0	30.0	30.0	5.0	1.22	0.0	0.097
106	790831- 1	50.0	30.0	30.0	5.0	1.22	0.0	0.062
107	790831- 1	80.0	30.0	30.0	5.0	1.22	0.0	0.049
108	790831- 3	20.0	70.0	30.0	5.0	1.22	0.0	0.085
109	790831- 3	50.0	70.0	30.0	5.0	1.22	0.0	0.054
110	790831- 1	80.0	70.0	30.0	5.0	1.22	0.0	0.046
111	800626-15	20.0	70.0	0.0	2.0	1.45	47.7	0.095
112	800626- 7	20.0	70.0	0.0	2.0	1.00	51.1	0.090
113	800626-10	20.0	70.0	0.0	2.0	1.00	44.7	0.082
114	800626-12	20.0	70.0	0.0	2.0	1.45	53.2	0.094
115	800626-13	20.0	70.0	0.0	2.0	1.45	0.0	0.095

116	800626- 7	20.0	70.0	6.0	2.0	1.00	0.0	0.077
117	800626- 8	20.0	68.0	6.0	2.0	1.00	0.0	0.078
118	800626-12	20.0	70.0	6.0	2.0	1.45	0.0	0.087
119	790329- 1	50.0	28.0	0.0	1.0	1.00	39.6	0.085
120	790329- 2	50.0	28.0	0.0	1.0	1.45	48.4	0.087
121	790329- 3	50.0	31.0	0.0	1.0	1.90	40.1	0.096
122	790329- 4	20.0	29.0	0.0	1.0	1.90	41.1	0.104
123	790329- 5	80.0	29.0	0.0	1.0	1.90	38.8	0.091
124	790311- 2	50.0	32.0	0.0	1.0	1.45	53.3	0.093
125	790311- 3	50.0	33.0	0.0	1.0	1.90	41.1	0.099
126	790311- 4	20.0	67.0	0.0	1.0	1.00	57.4	0.082
127	790311- 5	50.0	67.0	0.0	1.0	1.00	50.9	0.075
128	790311- 6	80.0	69.0	0.0	1.0	1.00	43.5	0.076
129	790311- 7	20.0	67.5	0.0	1.0	1.45	56.8	0.084
130	790311- 8	50.0	67.5	0.0	1.0	1.45	53.6	0.081
131	790311- 9	80.0	68.0	0.0	1.0	1.45	49.1	0.076
132	790311-10	50.0	69.0	0.0	1.0	1.90	54.9	0.091
133	800623- 1	20.0	70.0	0.0	1.0	1.45	48.5	0.084
134	800623- 2	20.0	70.0	0.0	1.0	1.45	49.9	0.084
135	800623- 6	20.0	70.0	0.0	1.0	1.90	59.6	0.097
136	800623- 7	20.0	70.0	0.0	1.0	1.90	56.2	0.094
137	800626- 3	20.0	70.0	0.0	1.0	1.90	62.4	0.096
138	781021- 1	20.0	55.0	0.0	1.0	1.00	55.6	0.083
139	781021- 2	50.0	55.0	0.0	1.0	1.00	45.6	0.068
140	781021- 4	80.0	55.0	0.0	1.0	1.00	42.0	0.060
141	781021- 5	20.0	51.0	0.0	1.0	1.45	59.2	0.085
142	781021- 6	50.0	54.0	0.0	1.0	1.45	58.0	0.086
143	781023- 7	80.0	55.0	0.0	1.0	1.45	52.0	0.079
144	781021- 9	20.0	48.0	0.0	1.0	1.90	54.0	0.099
145	781021-10	50.0	52.0	0.0	1.0	1.90	50.4	0.092
146	781021- 8	80.0	52.0	0.0	1.0	1.90	51.0	0.086
147	781016- 1	20.0	66.0	0.0	1.0	1.00	54.0	0.070
148	781016- 2	50.0	66.0	0.0	1.0	1.00	45.4	0.063
149	781016- 3	80.0	66.0	0.0	1.0	1.00	39.6	0.056
150	781019- 1	20.0	66.0	0.0	1.0	1.45	60.4	0.087
151	781019- 2	50.0	66.0	0.0	1.0	1.45	55.5	0.081
152	781019- 3	80.0	66.0	0.0	1.0	1.45	51.4	0.074
153	781020- 1	20.0	66.0	0.0	1.0	1.90	53.2	0.088
154	781020- 2	50.0	66.0	0.0	1.0	1.90	49.4	0.083
155	781019- 3	80.0	66.0	0.0	1.0	1.90	50.6	0.079
156	790311- 1	50.0	32.0	0.0	1.0	1.00	34.3	0.065
157	800623- 1	20.0	70.0	6.0	1.0	1.45	0.0	0.085
158	800623- 4	20.0	70.0	6.0	1.0	1.45	0.0	0.087
159	800623- 6	20.0	70.0	6.0	1.0	1.90	0.0	0.100
160	800623- 9	20.0	70.0	6.0	1.0	1.90	0.0	0.083
161	800626- 1	20.0	70.0	6.0	1.0	1.90	0.0	0.100
162	790413- 5	20.0	65.0	15.0	1.0	1.00	0.0	0.068
163	790413- 2	20.0	65.0	15.0	1.0	1.45	0.0	0.082
164	790410- 1	50.0	31.5	15.0	1.0	1.90	0.0	0.080
165	790410- 2	50.0	29.0	15.0	1.0	1.90	0.0	0.080
166	790410- 3	50.0	34.0	15.0	1.0	1.45	0.0	0.082
167	790410- 4	50.0	34.0	15.0	1.0	1.45	0.0	0.082
168	790410- 5	50.0	31.0	15.0	1.0	1.00	0.0	0.060
169	790410- 6	50.0	31.0	15.0	1.0	1.00	0.0	0.060
170	790413- 1	50.0	65.0	15.0	1.0	1.90	0.0	0.083
171	790413- 3	50.0	65.0	15.0	1.0	1.45	0.0	0.077
172	790413- 6	50.0	64.0	15.0	1.0	1.00	0.0	0.057
173	790413- 7	80.0	65.0	15.0	1.0	1.00	0.0	0.060
174	790413- 4	80.0	65.0	15.0	1.0	1.45	0.0	0.070
175	790317- 1	50.0	31.0	30.0	1.0	1.00	0.0	0.077

176	790317- 2	50.0	31.5	30.0	1.0	1.45	0.0	0.081
177	790317- 3	50.0	32.0	30.0	1.0	1.45	0.0	0.081
178	790317- 4	50.0	33.0	30.0	1.0	1.90	0.0	0.074
179	790317- 5	50.0	35.0	30.0	1.0	1.90	0.0	0.074
180	790317- 6	20.0	67.0	30.0	1.0	1.45	0.0	0.088
181	790317- 7	20.0	70.0	30.0	1.0	1.45	0.0	0.077
182	790317- 8	80.0	73.0	30.0	1.0	1.45	0.0	0.067
183	790317- 9	50.0	67.0	30.0	1.0	1.90	0.0	0.078
184	790311-11	20.0	66.0	30.0	1.0	1.00	0.0	0.066
185	790311-12	50.0	66.0	30.0	1.0	1.00	0.0	0.059
186	790311-13	80.0	69.0	30.0	1.0	1.00	0.0	0.057
187	790311-14	20.0	67.0	30.0	1.0	1.45	0.0	0.083
188	790311-15	50.0	67.0	30.0	1.0	1.45	0.0	0.076
189	790311-16	80.0	67.5	30.0	1.0	1.45	0.0	0.066
190	790311-17	50.0	70.0	30.0	1.0	1.90	0.0	0.078
191	790311-18	50.0	70.0	30.0	1.0	1.90	0.0	0.078
192	790317- 1	20.0	31.0	30.0	1.0	1.00	0.0	0.102
193	790317- 1	20.0	31.0	30.0	1.0	1.00	0.0	0.102

HIS CORRELATION, FOR UP TO 32 DEGREES OF FREEDOM, IS REFERENCED WITH RESPECT TO THE TRACTION COEFFICIENT.

THE NUMBER OF DEGREES OF FREEDOM FOR THIS CORRELATION IS; 32

THE COEFFICIENTS ARE

0.745E-01	-0.536E-02	-0.175E-02	-0.219E-02
0.204E-01	-0.208E-01	0.109E-01	-0.258E-02
-0.592E-03	-0.415E-03	0.705E-03	0.957E-03
0.176E-02	0.305E-02	-0.588E-02	-0.427E-02
-0.162E-01	-0.273E-02	-0.534E-02	-0.907E-03
0.490E-01	0.282E-01	-0.406E-01	-0.588E-01
0.324E-03	0.790E-04	-0.138E-04	-0.302E-03
-0.993E-02	-0.112E-01	0.212E-01	0.202E-01

	TEST NOS.	SPEED* (-)	TEMP* (-)	RAIN* (-)	EFFECT* (-)	PRESS* (-)	TRACT. COEFF.	EST.	PERCENT ERROR
1	790726- 2	-0.56	-0.39	-1.00	0.51	-0.08	0.094	0.087	7.703
2	790726- 2	0.09	-0.39	-1.00	0.51	-0.08	0.079	0.079	0.533
3	790726- 2	0.74	-0.39	-1.00	0.51	-0.08	0.065	0.062	4.104
4	790726- 3	-0.56	-0.06	-1.00	0.51	-0.08	0.092	0.091	1.615
5	790726- 3	0.09	-0.06	-1.00	0.51	-0.08	0.078	0.076	2.464
6	790726- 3	0.74	-0.06	-1.00	0.51	-0.08	0.065	0.062	5.249
7	790601- 1	0.74	-0.38	-1.00	0.51	0.09	0.076	0.075	1.474
8	790531- 1	-0.56	-0.40	-1.00	0.51	0.09	0.103	0.094	9.452
9	790531- 2	0.09	-0.38	-1.00	0.51	0.09	0.090	0.084	6.482
10	790531- 3	-0.56	-0.06	-1.00	0.51	0.09	0.100	0.104	-4.165
11	790531- 4	0.09	-0.06	-1.00	0.51	0.09	0.087	0.090	-3.544
12	790531- 5	0.74	-0.06	-1.00	0.51	0.09	0.076	0.076	-0.030
13	790531- 6	0.74	0.35	-1.00	0.51	0.09	0.070	0.074	-6.112
14	790531- 7	-0.56	0.29	-1.00	0.51	0.09	0.087	0.089	-2.244
15	790531- 8	0.09	0.38	-1.00	0.51	0.09	0.079	0.082	-3.739
16	790123- 1	-0.56	-0.44	-1.00	0.51	-0.25	0.085	0.081	5.239
17	790123- 2	0.09	-0.44	-1.00	0.51	-0.25	0.062	0.066	-5.600
18	790123- 3	0.74	-0.44	-1.00	0.51	-0.25	0.047	0.050	-7.162
19	790123- 4	-0.56	-0.06	-1.00	0.51	-0.25	0.077	0.077	-0.515
20	790123- 5	0.09	-0.06	-1.00	0.51	-0.25	0.058	0.063	-7.762
21	790123- 6	0.74	-0.06	-1.00	0.51	-0.25	0.046	0.048	-4.165
22	790126- 2	0.09	0.37	-1.00	0.51	-0.25	0.054	0.067	-21.223
23	790126- 3	0.74	0.37	-1.00	0.51	-0.25	0.040	0.051	-25.414
24	790628- 1	-0.56	-0.16	-1.00	0.51	0.09	0.097	0.097	0.194
25	790628- 2	0.09	-0.25	-1.00	0.51	0.09	0.086	0.085	1.215
26	790628- 3	0.74	-0.06	-1.00	0.51	0.09	0.075	0.076	-1.355
27	790727- 3	-0.56	0.37	-1.00	0.51	-0.08	0.077	0.086	-10.640
28	790727- 3	0.09	0.37	-1.00	0.51	-0.08	0.063	0.074	-16.309
29	790727- 3	0.74	0.37	-1.00	0.51	-0.08	0.055	0.063	-13.098
30	800627- 1	-0.56	0.31	-1.00	0.51	-0.08	0.087	0.085	1.744
31	790126- 1	-0.56	0.29	-1.00	0.51	-0.25	0.063	0.082	-26.742
32	800628- 1	-0.56	0.31	-0.66	0.51	-0.25	0.082	0.082	0.062
33	800628- 3	-0.56	0.31	-0.56	0.51	-0.08	0.086	0.084	2.028
34	791127- 3	-0.78	0.31	-0.50	0.51	0.09	0.084	0.089	-5.938
35	791127- 3	-0.56	0.31	-0.50	0.51	0.09	0.080	0.086	-7.543
36	791127- 3	-0.35	0.31	-0.50	0.51	0.09	0.078	0.083	-6.683
37	790726- 1	-0.56	-0.39	0.59	0.51	-0.08	0.084	0.082	1.853
38	790726- 1	0.09	-0.39	0.59	0.51	-0.08	0.064	0.067	-4.409
39	790726- 1	0.74	-0.39	0.59	0.51	-0.08	0.051	0.051	-0.764
40	790629- 1	0.74	-0.38	0.89	0.51	0.09	0.052	0.054	-3.911

41	790629- 2	0.09	-0.34	0.89	0.51	0.09	0.067	0.067	-0.284
42	790629- 3	-0.56	-0.38	0.89	0.51	0.09	0.083	0.080	3.434
43	790629- 4	0.09	-0.12	0.89	0.51	0.09	0.067	0.068	-1.807
44	790629- 5	-0.56	-0.38	0.89	0.51	0.09	0.084	0.080	4.632
45	790629- 6	0.09	-0.31	0.89	0.51	0.09	0.069	0.067	2.558
46	790629- 7	0.74	0.07	0.89	0.51	0.09	0.055	0.054	2.681
47	790629- 8	0.74	-0.06	0.89	0.51	0.09	0.056	0.054	2.779
48	790629- 9	-0.56	-0.44	0.89	0.51	0.09	0.083	0.080	3.580
49	790629-10	0.09	-0.38	0.89	0.51	0.09	0.069	0.067	2.739
50	790629-11	0.74	-0.06	0.89	0.51	0.09	0.055	0.054	0.977
51	790629-12	0.09	0.31	0.89	0.51	0.09	0.068	0.066	2.947
52	790629-13	0.74	0.31	0.89	0.51	0.09	0.057	0.054	5.600
53	790629-14	-0.56	0.31	0.89	0.51	0.09	0.079	0.078	1.077
54	790629-15	0.74	-0.12	0.89	0.51	0.09	0.056	0.054	3.184
55	790629-16	0.74	0.03	0.89	0.51	0.09	0.055	0.053	3.750
56	790726- 4	-0.56	-0.06	0.59	0.51	-0.08	0.083	0.086	-3.714
57	790726- 4	0.74	-0.06	0.59	0.51	-0.08	0.051	0.051	0.540
58	790727- 2	-0.56	0.37	0.59	0.51	-0.08	0.079	0.081	-2.463
59	790727- 2	0.09	0.37	0.59	0.51	-0.08	0.065	0.066	-2.003
60	790727- 2	0.74	0.37	0.59	0.51	-0.08	0.056	0.052	8.075
61	790628- 6	-0.56	-0.06	0.89	0.51	0.09	0.082	0.085	-3.306
62	790628- 4	0.74	0.18	0.89	0.51	0.09	0.055	0.054	2.156
63	790628- 5	0.09	0.12	0.89	0.51	0.09	0.065	0.065	-0.144
64	790718- 1	-0.56	-0.34	0.31	0.51	-0.25	0.103	0.082	22.692
65	790718- 2	0.09	-0.34	0.31	0.51	-0.25	0.077	0.064	18.025
66	790718- 3	0.74	-0.31	0.31	0.51	-0.25	0.065	0.048	34.291
67	790718- 4	-0.56	-0.31	0.31	0.51	-0.25	0.082	0.082	-0.333
68	790718- 5	0.09	-0.34	1.09	0.51	0.20	0.064	0.066	-3.023
69	790718- 6	-0.24	-0.34	1.09	0.51	0.20	0.075	0.072	4.523
70	790726- 5	-0.56	-0.06	0.31	0.51	-0.25	0.084	0.083	0.929
71	790726- 5	0.09	-0.06	0.31	0.51	-0.25	0.063	0.064	-1.446
72	790726- 5	0.74	-0.06	0.31	0.51	-0.25	0.048	0.045	7.326
73	790726- 4	0.09	-0.06	0.59	0.51	-0.08	0.062	0.068	-9.887
74	790727- 1	-0.56	0.25	0.31	0.51	-0.25	0.085	0.082	3.935
75	790727- 1	0.09	0.25	0.31	0.51	-0.25	0.069	0.065	6.593
76	790727- 1	0.74	0.25	0.31	0.51	-0.25	0.059	0.047	21.894
77	790901- 1	-0.56	-0.06	0.31	0.51	-0.25	0.077	0.083	-7.780
78	790901- 1	0.09	-0.06	0.31	0.51	-0.25	0.055	0.064	-15.083
79	790901- 1	0.74	-0.06	0.31	0.51	-0.25	0.045	0.045	0.865
80	790901- 2	-0.56	-0.44	0.31	0.51	-0.25	0.101	0.082	20.744
81	790901- 2	0.74	-0.44	0.31	0.51	-0.25	0.057	0.047	20.350
82	790901- 3	-0.56	0.22	0.31	0.51	-0.25	0.092	0.082	11.940
83	790901- 3	0.09	0.22	0.31	0.51	-0.25	0.070	0.065	7.999
84	790901- 3	0.74	0.22	0.31	0.51	-0.25	0.058	0.048	19.933
85	790901- 2	0.09	-0.44	0.31	0.51	-0.25	0.073	0.064	12.593
86	790728- 1	-0.56	-0.34	2.63	0.51	0.09	0.059	0.068	-13.757
87	790728- 1	0.09	-0.34	2.63	0.51	0.09	0.040	0.051	-25.166
88	790728- 1	0.74	-0.34	2.63	0.51	0.09	0.031	0.035	-12.035
89	790202- 1	-0.56	-0.40	1.51	0.51	-0.25	0.071	0.084	-16.515
90	790202- 2	0.09	-0.33	1.51	0.51	-0.25	0.046	0.069	-32.625
91	790202- 3	0.74	-0.31	1.51	0.51	-0.25	0.035	0.043	-20.415
92	790206- 1	0.74	-0.49	1.51	0.51	-0.25	0.035	0.043	-20.729
93	790727- 4	-0.56	0.37	2.63	0.51	0.09	0.064	0.068	-6.117
94	790727- 4	0.74	0.37	2.63	0.51	0.09	0.033	0.035	-6.117
95	790126- 4	-0.56	0.29	1.51	0.51	-0.25	0.065	0.081	-22.794
96	790126- 5	0.09	0.27	1.51	0.51	-0.25	0.046	0.068	-31.138
97	790126- 6	0.74	0.33	1.51	0.51	-0.25	0.034	0.044	-24.998
98	790728- 2	-0.56	-0.01	2.63	0.51	0.09	0.061	0.060	2.192
99	790728- 2	0.09	-0.01	2.63	0.51	0.09	0.043	0.046	-6.591
100	790728- 2	0.74	-0.01	2.63	0.51	0.09	0.034	0.032	5.514

101	790601- 2	-0.56	-0.12	2.63	0.51	0.09	0.071	0.067	5.319
102	790831- 2	-0.56	-0.06	2.06	0.51	-0.08	0.088	0.082	6.931
103	790831- 2	0.09	-0.06	2.06	0.51	-0.08	0.059	0.061	-3.972
104	790831- 2	0.74	-0.06	2.06	0.51	-0.08	0.045	0.041	10.139
105	790831- 1	-0.56	-0.44	2.06	0.51	-0.08	0.097	0.078	21.748
106	790831- 1	0.09	-0.44	2.06	0.51	-0.08	0.062	0.060	3.715
107	790831- 1	0.74	-0.44	2.06	0.51	-0.08	0.049	0.041	17.161
108	790831- 3	-0.56	0.31	2.06	0.51	-0.08	0.085	0.077	10.494
109	790831- 3	0.09	0.31	2.06	0.51	-0.08	0.054	0.059	-8.967
110	790831- 1	0.74	0.31	2.06	0.51	-0.08	0.046	0.042	10.142
111	800626-15	-0.56	0.31	-1.00	-0.40	0.09	0.095	0.088	7.661
112	800626- 7	-0.56	0.31	-1.00	-0.40	-0.25	0.090	0.080	12.197
113	800626-10	-0.56	0.31	-1.00	-0.40	-0.25	0.082	0.080	2.859
114	800626-12	-0.56	0.31	-1.00	-0.40	0.09	0.094	0.088	6.600
115	800626-13	-0.56	0.31	-0.71	-0.40	0.09	0.095	0.086	9.637
116	800626- 7	-0.56	0.31	-0.80	-0.40	-0.25	0.077	0.078	-1.820
117	800626- 8	-0.56	0.27	-0.80	-0.40	-0.25	0.078	0.078	-0.066
118	800626-12	-0.56	0.31	-0.71	-0.40	0.09	0.087	0.086	0.825
119	790329- 1	0.09	-0.48	-1.00	-0.70	-0.25	0.085	0.070	18.900
120	790329- 2	0.09	-0.48	-1.00	-0.70	0.09	0.087	0.082	6.500
121	790329- 3	0.09	-0.42	-1.00	-0.70	0.43	0.096	0.093	3.073
122	790329- 4	-0.56	-0.46	-1.00	-0.70	0.43	0.104	0.098	6.427
123	790329- 5	0.74	-0.46	-1.00	-0.70	0.43	0.091	0.088	3.081
124	790311- 2	0.09	-0.40	-1.00	-0.70	0.09	0.095	0.082	13.199
125	790311- 3	0.09	-0.38	-1.00	-0.70	0.43	0.099	0.093	6.641
126	790311- 4	-0.56	0.25	-1.00	-0.70	-0.25	0.082	0.079	3.754
127	790311- 5	0.09	0.25	-1.00	-0.70	-0.25	0.075	0.071	5.978
128	790311- 6	0.74	0.29	-1.00	-0.70	-0.25	0.076	0.062	19.952
129	790311- 7	-0.56	0.26	-1.00	-0.70	0.09	0.084	0.088	-4.178
130	790311- 8	0.09	0.26	-1.00	-0.70	0.09	0.081	0.081	-0.590
131	790311- 9	0.74	0.27	-1.00	-0.70	0.09	0.076	0.075	0.303
132	790311-10	0.09	0.29	-1.00	-0.70	0.43	0.091	0.092	-1.452
133	800623- 1	-0.56	0.31	-1.00	-0.70	0.09	0.084	0.088	-4.222
134	800623- 2	-0.56	0.31	-1.00	-0.70	0.09	0.084	0.088	-4.222
135	800623- 6	-0.56	0.31	-1.00	-0.70	0.43	0.097	0.096	0.697
136	800623- 7	-0.56	0.31	-1.00	-0.70	0.43	0.094	0.096	-2.445
137	800626- 3	-0.56	0.31	-1.00	-0.70	0.43	0.096	0.096	-0.339
138	781021- 1	-0.56	0.03	-1.00	-0.70	-0.25	0.083	0.082	1.631
139	781021- 2	0.09	0.03	-1.00	-0.70	-0.25	0.068	0.072	-5.301
140	781021- 4	0.74	0.03	-1.00	-0.70	-0.25	0.060	0.062	-2.856
141	781021- 5	-0.56	-0.05	-1.00	-0.70	0.09	0.095	0.089	6.188
142	781021- 6	0.09	0.01	-1.00	-0.70	0.09	0.086	0.081	6.307
143	781028- 7	0.74	0.03	-1.00	-0.70	0.09	0.078	0.077	1.455
144	781021- 9	-0.56	-0.10	-1.00	-0.70	0.43	0.099	0.099	-0.240
145	781021-10	0.09	-0.03	-1.00	-0.70	0.43	0.092	0.094	-2.632
146	781021- 8	0.74	-0.03	-1.00	-0.70	0.43	0.086	0.083	2.966
147	781016- 1	-0.56	0.24	-1.00	-0.70	-0.25	0.070	0.079	-12.135
148	781016- 2	0.09	0.24	-1.00	-0.70	-0.25	0.063	0.071	-11.504
149	781016- 3	0.74	0.24	-1.00	-0.70	-0.25	0.056	0.062	-10.711
150	781019- 1	-0.56	0.24	-1.00	-0.70	0.09	0.087	0.088	-0.634
151	781019- 2	0.09	0.24	-1.00	-0.70	0.09	0.081	0.081	-0.586
152	781019- 3	0.74	0.24	-1.00	-0.70	0.09	0.074	0.075	-1.872
153	781020- 1	-0.56	0.24	-1.00	-0.70	0.43	0.088	0.096	-8.315
154	781020- 2	0.09	0.24	-1.00	-0.70	0.43	0.083	0.092	-10.828
155	781019- 3	0.74	0.24	-1.00	-0.70	0.43	0.079	0.088	-11.356
156	790311- 1	0.09	-0.40	-1.00	-0.70	-0.25	0.065	0.070	-8.026
157	800623- 1	-0.56	0.31	-0.82	-0.70	0.09	0.085	0.087	-1.305
158	800623- 4	-0.56	0.31	-0.82	-0.70	0.09	0.087	0.087	0.521
159	800623- 6	-0.56	0.31	-0.77	-0.70	0.43	0.100	0.096	4.633
160	800623- 9	-0.56	0.31	-0.77	-0.70	0.43	0.083	0.096	-14.078

161	800626- 1	-0.56	0.31	-0.77	-0.70	0.43	0.100	0.096	4.603
162	790413- 5	-0.56	0.22	-0.57	-0.70	-0.25	0.068	0.072	-5.290
163	790413- 2	-0.56	0.22	-0.38	-0.70	0.09	0.082	0.084	-2.731
164	790410- 1	0.09	-0.41	-0.19	-0.70	0.43	0.080	0.084	-4.668
165	790410- 2	0.09	-0.46	-0.19	-0.70	0.43	0.080	0.084	-4.790
166	790410- 3	0.09	-0.36	-0.38	-0.70	0.09	0.082	0.080	3.016
167	790410- 4	0.09	-0.36	-0.38	-0.70	0.09	0.082	0.080	3.016
168	790410- 5	0.09	-0.42	-0.57	-0.70	-0.25	0.060	0.072	-18.493
169	790410- 6	0.09	-0.42	-0.57	-0.70	-0.25	0.060	0.072	-18.493
170	790413- 1	0.09	0.22	-0.19	-0.70	0.43	0.083	0.087	-4.366
171	790413- 3	0.09	0.22	-0.38	-0.70	0.09	0.077	0.076	0.993
172	790413- 6	0.09	0.20	-0.57	-0.70	-0.25	0.057	0.066	-14.759
173	790413- 7	0.31	0.22	-0.57	-0.70	-0.25	0.060	0.065	-7.424
174	790413- 4	0.74	0.22	-0.38	-0.70	0.09	0.070	0.068	2.654
175	790317- 1	0.09	-0.42	-0.12	-0.70	-0.25	0.077	0.074	4.075
176	790317- 2	0.09	-0.41	0.28	-0.70	0.09	0.081	0.077	4.870
177	790317- 3	0.09	-0.40	0.28	-0.70	0.09	0.081	0.077	4.802
178	790317- 4	0.09	-0.38	0.68	-0.70	0.43	0.074	0.074	-0.225
179	790317- 5	0.09	-0.34	0.68	-0.70	0.43	0.074	0.074	0.122
180	790317- 6	-0.56	0.25	0.28	-0.70	0.09	0.088	0.080	9.052
181	790317- 7	-0.56	0.31	0.28	-0.70	0.09	0.077	0.080	-3.721
182	790317- 8	0.74	0.37	0.28	-0.70	0.09	0.067	0.065	2.850
183	790317- 9	0.09	0.25	0.68	-0.70	0.43	0.078	0.080	-2.646
184	790311-11	-0.56	0.24	-0.12	-0.70	-0.25	0.066	0.066	0.322
185	790311-12	0.09	0.24	-0.12	-0.70	-0.25	0.059	0.062	-5.615
186	790311-13	0.74	0.29	-0.12	-0.70	-0.25	0.057	0.057	-0.672
187	790311-14	-0.56	0.25	0.28	-0.70	0.09	0.083	0.080	3.191
188	790311-15	0.09	0.25	0.28	-0.70	0.09	0.076	0.071	6.482
189	790311-16	0.74	0.26	0.28	-0.70	0.09	0.066	0.062	5.570
190	790311-17	0.09	0.31	0.68	-0.70	0.43	0.078	0.079	-1.839
191	790311-18	0.09	0.31	0.68	-0.70	0.43	0.078	0.079	-1.839
192	790317- 1	-0.56	-0.42	-0.12	-0.70	-0.25	0.102	0.102	-0.118
193	790317- 1	-0.56	-0.42	-0.12	-0.70	-0.25	0.102	0.102	-0.118

THE MEAN OF THE ERROR IS -0.458%
THE STANDARD DEVIATION OF THE ERROR IS 5.876%

THE MEAN VELOCITY IS; 45.933 M/SEC
THE MEAN PRESSURE IS; 1.331 ATM
THE MEAN TEMPERATURE IS; 53.420 DEGREES C
THE MEAN SEIN PARAMETER IS; 0.005766
THE MEAN ASPECT PARAMETER IS; 3.321

STATEMENTS EXECUTED= 523111

CORE USAGE OBJECT CODE= 9464 BYTES,ARRAY AREA= 16356 BYTES,TOTAL AR

DIAGNOSTICS NUMBER OF ERRORS= 0, NUMBER OF WARNINGS= 0,

COMPILE TIME= 1.12 SEC,EXECUTION TIME= 39.59 SEC, 23.25.11 MONDAY

CPSICE

APPENDIX III-F

Correlation for
TDF-88 on traction coefficient
including spin.

THE INPUT DATA FOR CORRELATION IS;

	TEST NOS.	SPEED (M/S)	TEMP (C)	SPIN DEG	ASPECT (-)	SIDE SLIP	PRESS. (GPA)	SLOPE (-)	TRACT. COEFF.
1	791103-10	10.0	33.0	0.0	5.0		1.00	38.6	0.095
2	791103-10	20.0	33.0	0.0	5.0		1.00	34.8	0.080
3	791103-11	10.0	33.0	0.0	5.0		1.45	40.6	0.096
4	791103-11	20.0	33.0	0.0	5.0		1.45	39.3	0.090
5	791103-11	30.0	33.0	0.0	5.0		1.45	38.1	0.084
6	791128- 1	10.0	30.0	0.0	5.0		1.45	39.4	0.090
7	791128- 1	20.0	30.0	0.0	5.0		1.45	37.2	0.083
8	791128- 1	30.0	30.0	0.0	5.0		1.45	35.9	0.078
9	791123- 1	10.0	30.0	0.0	5.0		1.00	34.6	0.095
10	791123- 1	20.0	30.0	0.0	5.0		1.00	33.3	0.085
11	791123- 1	30.0	30.0	0.0	5.0		1.00	32.0	0.079
12	791130- 4	10.0	70.0	0.0	5.0		1.00	56.5	0.083
13	791130- 4	20.0	70.0	0.0	5.0		1.00	51.4	0.077
14	791130- 4	30.0	70.0	0.0	5.0		1.00	42.6	0.071
15	791120- 7	10.0	70.0	0.0	5.0		1.00	51.1	0.079
16	791120- 7	20.0	70.0	0.0	5.0		1.00	43.9	0.074
17	791120- 7	30.0	70.0	0.0	5.0		1.00	39.5	0.069
18	791120- 8	10.0	70.0	0.0	5.0		1.45	47.0	0.084
19	791120- 8	20.0	70.0	0.0	5.0		1.45	42.2	0.081
20	791120- 8	30.0	70.0	0.0	5.0		1.45	40.8	0.078
21	791004- 2	50.0	47.0	0.0	5.0		1.00	34.7	0.059
22	791004- 4	20.0	50.0	0.0	5.0		1.00	44.1	0.079
23	791004- 4	50.0	50.0	0.0	5.0		1.00	38.9	0.064
24	791004- 4	80.0	50.0	0.0	5.0		1.00	34.0	0.050
25	800529- 1	20.0	70.0	0.0	5.0		1.00	38.0	0.071
26	800529- 3	20.0	70.0	0.0	5.0		1.22	49.0	0.082
27	791004- 1	80.0	70.0	0.0	5.0		1.00	27.6	0.044
28	791103-10	10.0	33.0	0.0	5.0		1.00	48.0	0.095
29	791103-10	20.0	33.0	0.0	5.0		1.00	35.5	0.080
30	791103-10	30.0	33.0	0.0	5.0		1.00	30.0	0.070
31	791127- 1	10.0	30.0	6.0	5.0		1.00	0.0	0.086
32	791127- 1	20.0	30.0	6.0	5.0		1.00	0.0	0.079
33	791127- 1	30.0	30.0	6.0	5.0		1.00	0.0	0.076
34	791127- 2	10.0	30.0	6.0	5.0		1.45	0.0	0.087
35	791127- 2	20.0	30.0	6.0	5.0		1.45	0.0	0.082
36	791127- 2	30.0	30.0	6.0	5.0		1.45	0.0	0.080
37	791127- 3	10.0	70.0	6.0	5.0		1.45	0.0	0.084
38	791127- 3	20.0	70.0	6.0	5.0		1.45	0.0	0.080
39	791127- 4	10.0	70.0	6.0	5.0		1.00	0.0	0.089
40	791127- 4	20.0	70.0	6.0	5.0		1.00	0.0	0.084
41	791127- 4	30.0	70.0	6.0	5.0		1.00	0.0	0.080
42	800529- 7	20.0	70.0	6.0	5.0		1.22	0.0	0.083
43	791003- 1	20.0	40.0	6.0	5.0		1.00	0.0	0.074
44	791003- 1	40.0	40.0	6.0	5.0		1.00	0.0	0.061
45	791127- 3	10.0	70.0	6.0	5.0		1.45	0.0	0.084
46	791127- 3	20.0	70.0	6.0	5.0		1.45	0.0	0.080
47	791127- 3	30.0	70.0	6.0	5.0		1.45	0.0	0.078
48	791004- 3	20.0	50.0	15.0	5.0		1.00	0.0	0.080
49	791004- 3	50.0	50.0	15.0	5.0		1.00	0.0	0.061
50	791004- 3	80.0	50.0	15.0	5.0		1.00	0.0	0.045
51	791103- 6	10.0	32.0	0.0	2.0		1.00	55.6	0.100
52	791103- 6	20.0	32.0	0.0	2.0		1.00	41.1	0.083
53	791103- 6	30.0	32.0	0.0	2.0		1.00	36.6	0.080
54	791103- 8	10.0	33.0	0.0	2.0		1.45	47.0	0.101
55	791103- 8	20.0	33.0	0.0	2.0		1.45	43.2	0.093

ORIGINAL PAGE IS
OF POOR QUALITY

56	791103- 8	30.0	33.0	0.0	2.0	1.45	40.9	0.087
57	791103- 7	30.0	32.0	0.0	2.0	1.00	35.6	0.081
58	791103- 9	30.0	33.0	0.0	2.0	1.45	39.4	0.084
59	791115- 5	10.0	70.0	0.0	2.0	1.00	64.3	0.084
60	791115- 5	20.0	70.0	0.0	2.0	1.00	47.1	0.080
61	791115- 5	30.0	70.0	0.0	2.0	1.00	43.4	0.075
62	791115- 6	30.0	70.0	0.0	2.0	1.00	43.7	0.076
63	791115- 7	30.0	70.0	0.0	2.0	1.45	49.0	0.084
64	791115- 8	10.0	70.0	0.0	2.0	1.45	55.8	0.090
65	791115- 8	20.0	70.0	0.0	2.0	1.45	51.9	0.086
66	791115- 8	30.0	70.0	0.0	2.0	1.45	51.9	0.083
67	800523- 1	20.0	70.0	0.0	2.0	1.45	55.7	0.094
68	800526- 2	20.0	70.0	0.0	2.0	1.00	34.4	0.073
69	800526- 6	20.0	70.0	0.0	2.0	1.45	47.6	0.087
70	800526- 7	20.0	70.0	0.0	2.0	1.45	45.6	0.086
71	791103- 7	30.0	32.0	6.0	2.0	1.00	0.0	0.078
72	791103- 9	30.0	33.0	6.0	2.0	1.45	0.0	0.082
73	791115- 6	30.0	70.0	6.0	2.0	1.00	0.0	0.075
74	791115- 7	30.0	70.0	6.0	2.0	1.00	0.0	0.082
75	800523- 1	20.0	70.0	6.0	2.0	1.45	0.0	0.093
76	800526- 1	20.0	70.0	6.0	2.0	1.00	0.0	0.065
77	800526- 4	20.0	70.0	6.0	2.0	1.00	0.0	0.067
78	800526- 6	20.0	70.0	6.0	2.0	1.45	0.0	0.086
79	800526- 9	20.0	70.0	6.0	2.0	1.45	0.0	0.092
80	791119- 1	10.0	28.0	0.0	1.0	1.45	47.9	0.101
81	791119- 1	20.0	28.0	0.0	1.0	1.45	39.1	0.090
82	791119- 1	30.0	28.0	0.0	1.0	1.45	38.5	0.083
83	791119- 2	30.0	29.0	0.0	1.0	1.45	37.4	0.085
84	791119- 3	30.0	30.0	0.0	1.0	1.90	45.0	0.089
85	791119- 4	10.0	30.0	0.0	1.0	1.90	49.3	0.099
86	791119- 4	20.0	30.0	0.0	1.0	1.90	45.9	0.095
87	791119- 4	30.0	30.0	0.0	1.0	1.90	43.1	0.089
88	791120- 1	10.0	30.0	0.0	1.0	1.45	47.9	0.100
89	791120- 1	20.0	30.0	0.0	1.0	1.45	43.2	0.092
90	791120- 1	30.0	30.0	0.0	1.0	1.45	37.1	0.084
91	791120- 2	30.0	30.0	0.0	1.0	1.45	36.9	0.086
92	791120- 3	30.0	30.0	0.0	1.0	1.90	42.6	0.091
93	791120- 4	10.0	30.0	0.0	1.0	1.90	48.0	0.100
94	791120- 4	20.0	30.0	0.0	1.0	1.90	43.7	0.095
95	791120- 4	30.0	30.0	0.0	1.0	1.90	40.6	0.090
96	791120- 5	10.0	68.0	0.0	1.0	1.90	52.9	0.096
97	791120- 5	20.0	68.0	0.0	1.0	1.90	50.6	0.093
98	791120- 5	30.0	68.0	0.0	1.0	1.90	49.9	0.090
99	791120- 6	30.0	68.0	0.0	1.0	1.90	51.2	0.091
100	791130- 1	10.0	30.0	0.0	1.0	1.45	44.5	0.096
101	791130- 1	20.0	30.0	0.0	1.0	1.45	36.1	0.086
102	791130- 1	30.0	30.0	0.0	1.0	1.45	28.4	0.081
103	791130- 2	30.0	30.0	0.0	1.0	1.45	31.6	0.082
104	791130- 3	30.0	70.0	0.0	1.0	1.45	55.4	0.092
105	791130- 5	10.0	70.0	0.0	1.0	1.45	66.0	0.098
106	791130- 5	20.0	70.0	0.0	1.0	1.45	58.3	0.095
107	791130- 5	30.0	70.0	0.0	1.0	1.45	51.1	0.092
108	800514- 1	20.0	70.0	0.0	1.0	1.45	45.1	0.083
109	800514- 2	20.0	70.0	0.0	1.0	1.90	53.7	0.094
110	800514- 3	20.0	70.0	0.0	1.0	1.90	56.1	0.097
111	800514- 4	20.0	70.0	0.0	1.0	1.45	46.9	0.083
112	800514- 9	20.0	70.0	0.0	1.0	1.90	46.5	0.088
113	791103- 5	10.0	31.0	0.0	1.0	1.45	52.0	0.114
114	791103- 3	20.0	31.0	0.0	1.0	1.45	43.9	0.105
115	791103- 1	10.0	30.0	0.0	1.0	1.00	39.4	0.088

116	791103- 2	20.0	30.0	0.0	1.0	1.00	27.0	0.080
117	791130- 6	10.0	70.0	0.0	1.0	1.45	66.5	0.098
118	791130- 6	20.0	70.0	0.0	1.0	1.45	57.0	0.096
119	791130- 6	30.0	70.0	0.0	1.0	1.45	49.9	0.092
120	791119- 2	30.0	29.0	6.0	1.0	1.45	0.0	0.085
121	791119- 3	30.0	30.0	6.0	1.0	1.90	0.0	0.089
122	791120- 2	30.0	30.0	6.0	1.0	1.45	0.0	0.085
123	791120- 3	30.0	30.0	6.0	1.0	1.90	0.0	0.089
124	791120- 6	30.0	68.0	6.0	1.0	1.90	0.0	0.089
125	791130- 2	30.0	30.0	6.0	1.0	1.45	0.0	0.083
126	791130- 3	30.0	70.0	6.0	1.0	1.45	0.0	0.090
127	800514- 1	20.0	70.0	6.0	1.0	1.45	0.0	0.081
128	800514- 2	20.0	70.0	6.0	1.0	1.90	0.0	0.092
129	800514-10	20.0	70.0	6.0	1.0	1.90	0.0	0.069
130	800514-12	20.0	70.0	6.0	1.0	1.45	0.0	0.079
131	791103- 4	10.0	32.0	6.0	1.0	1.45	0.0	0.115
132	791103- 4	20.0	32.0	6.0	1.0	1.45	0.0	0.105
133	791113- 1	10.0	33.0	0.0	0.5	1.90	59.5	0.105
134	791113- 1	20.0	33.0	0.0	0.5	1.90	44.0	0.098
135	791113- 1	30.0	33.0	0.0	0.5	1.90	37.0	0.092
136	791113- 2	10.0	32.0	0.0	0.5	1.60	64.8	0.111
137	791113- 2	20.0	32.0	0.0	0.5	1.60	46.4	0.102
138	791113- 2	30.0	32.0	0.0	0.5	1.60	31.5	0.092
139	791113- 3	20.0	33.0	0.0	0.5	1.60	40.7	0.101
140	791113- 4	30.0	33.0	0.0	0.5	1.90	43.2	0.094
141	791115- 1	10.0	70.0	0.0	0.5	1.60	89.8	0.111
142	791115- 1	20.0	70.0	0.0	0.5	1.60	73.9	0.108
143	791115- 2	15.0	68.0	0.0	0.5	1.60	81.3	0.110
144	791115- 3	27.5	66.0	0.0	0.5	1.90	63.2	0.099
145	791115- 4	10.0	70.0	0.0	0.5	1.90	73.7	0.104
146	791115- 4	20.0	70.0	0.0	0.5	1.90	67.5	0.101
147	791115- 4	27.5	70.0	0.0	0.5	1.90	65.3	0.099
148	791113- 3	20.0	33.0	6.0	0.5	1.60	0.0	0.098
149	791113- 4	30.0	33.0	6.0	0.5	1.90	0.0	0.092
150	791115- 2	15.0	68.0	6.0	0.5	1.60	0.0	0.106
151	791115- 3	10.0	66.0	6.0	0.5	1.90	0.0	0.099
152	791115- 3	27.5	66.0	6.0	0.5	1.90	0.0	0.095

HIS CORRELATION, FOR UP TO 32 DEGREES OF FREEDOM, IS PERFORMED WITH RESPECT TO THE TRACTION COEFFICIENT.

THE NUMBER OF DEGREES OF FREEDOM FOR THIS CORRELATION IS; 32

THE COEFFICIENTS ARE

0.859E-01	-0.582E-03	-0.480E-02	0.581E-03
0.162E-01	0.211E-03	-0.601E-02	-0.542E-04
-0.102E-02	-0.353E-03	-0.136E-03	0.401E-03
-0.132E-02	-0.848E-03	-0.255E-02	0.103E-02
-0.137E-01	-0.585E-03	0.344E-02	0.143E-02
0.277E-02	-0.382E-02	0.141E-01	0.701E-02
0.177E-02	0.104E-03	-0.162E-02	-0.723E-03
-0.850E-04	0.791E-03	0.389E-03	-0.291E-02

	TEST NOS.	SPEED* (-)	TEMP* (-)	SKIN* (-)	ASPECT* (-)	PRESS.* (-)	TRACT. COEFF.	EST.		PERCENT ERROR
1	791103-10	-0.57	-0.34	-1.00	1.05	-0.29	0.095	0.087		9.307
2	791103-10	-0.13	-0.34	-1.00	1.05	-0.29	0.080	0.080		-0.074
3	791103-11	-0.57	-0.34	-1.00	1.05	0.03	0.096	0.092		3.783
4	791103-11	-0.13	-0.34	-1.00	1.05	0.03	0.090	0.087		3.596
5	791103-11	0.30	-0.34	-1.00	1.05	0.03	0.084	0.081		3.372
6	791128- 1	-0.57	-0.40	-1.00	1.05	0.03	0.090	0.092		-1.818
7	791128- 1	-0.13	-0.40	-1.00	1.05	0.03	0.083	0.086		-3.777
8	791128- 1	0.30	-0.40	-1.00	1.05	0.03	0.078	0.081		-3.451
9	791123- 1	-0.57	-0.40	-1.00	1.05	-0.29	0.095	0.087		9.302
10	791123- 1	-0.13	-0.40	-1.00	1.05	-0.29	0.085	0.080		5.991
11	791123- 1	0.30	-0.40	-1.00	1.05	-0.29	0.079	0.074		7.158
12	791130- 4	-0.57	0.39	-1.00	1.05	-0.29	0.083	0.087		-4.283
13	791130- 4	-0.13	0.39	-1.00	1.05	-0.29	0.077	0.080		-3.914
14	791130- 4	0.30	0.39	-1.00	1.05	-0.29	0.071	0.074		-3.482
15	791120- 7	-0.57	0.39	-1.00	1.05	-0.29	0.079	0.087		-9.234
16	791120- 7	-0.13	0.39	-1.00	1.05	-0.29	0.074	0.080		-7.896
17	791120- 7	0.30	0.39	-1.00	1.05	-0.29	0.069	0.074		-6.342
18	791120- 8	-0.57	0.39	-1.00	1.05	0.03	0.084	0.083		1.730
19	791120- 8	-0.13	0.39	-1.00	1.05	0.03	0.081	0.079		2.682
20	791120- 8	0.30	0.39	-1.00	1.05	0.03	0.078	0.075		3.717
21	791004- 2	1.17	-0.07	-1.00	1.05	-0.29	0.059	0.061		-3.053
22	791004- 4	-0.13	-0.01	-1.00	1.05	-0.29	0.079	0.080		-0.801
23	791004- 4	1.17	-0.01	-1.00	1.05	-0.29	0.064	0.065		-0.873
24	791004- 4	2.47	-0.01	-1.00	1.05	-0.29	0.050	0.049		1.033
25	800529- 1	-0.13	0.39	-1.00	1.05	-0.29	0.071	0.080		-12.055
26	800529- 3	-0.13	0.39	-1.00	1.05	-0.13	0.082	0.079		3.124
27	791004- 1	2.47	0.39	-1.00	1.05	-0.29	0.044	0.041		7.742
28	791103-10	-0.57	-0.34	-1.00	1.05	-0.29	0.095	0.087		9.307
29	791103-10	-0.13	-0.34	-1.00	1.05	-0.29	0.080	0.080		-0.074
30	791103-10	0.30	-0.34	-1.00	1.05	-0.29	0.070	0.074		-4.948
31	791127- 1	-0.57	-0.40	2.10	1.05	-0.29	0.086	0.087		-0.829
32	791127- 1	-0.13	-0.40	2.10	1.05	-0.29	0.079	0.080		-1.322
33	791127- 1	0.30	-0.40	2.10	1.05	-0.29	0.076	0.073		3.500
34	791127- 2	-0.57	-0.40	3.50	1.05	0.03	0.087	0.084		3.724
35	791127- 2	-0.13	-0.40	3.50	1.05	0.03	0.082	0.084		-2.200
36	791127- 2	0.30	-0.40	3.50	1.05	0.03	0.080	0.084		-4.674
37	791127- 3	-0.57	0.39	3.50	1.05	0.03	0.084	0.086		-1.969
38	791127- 3	-0.13	0.39	3.50	1.05	0.03	0.080	0.080		-0.443
39	791127- 4	-0.57	0.39	2.10	1.05	-0.29	0.089	0.087		2.534
40	791127- 4	-0.13	0.39	2.10	1.05	-0.29	0.084	0.080		4.799

41	791127- 4	0.30	0.39	2.10	1.05	-0.29	0.080	0.073	8.679
42	800529- 7	-0.13	0.39	2.78	1.05	-0.13	0.083	0.080	3.570
43	791003- 1	-0.13	-0.20	3.79	1.05	-0.29	0.074	0.080	-7.853
44	791003- 1	0.95	-0.20	3.79	1.05	-0.29	0.061	0.063	-3.577
45	791127- 3	-0.57	0.39	3.50	1.05	0.03	0.084	0.086	-1.969
46	791127- 3	-0.13	0.39	3.50	1.05	0.03	0.080	0.080	-0.443
47	791127- 3	0.30	0.39	3.50	1.05	0.03	0.078	0.075	3.870
48	791004- 3	-0.13	-0.01	10.84	1.05	-0.29	0.080	0.079	0.764
49	791004- 3	1.17	-0.01	10.84	1.05	-0.29	0.061	0.062	-1.539
50	791004- 3	2.47	-0.01	10.84	1.05	-0.29	0.045	0.045	1.110
51	791103- 6	-0.57	-0.36	-1.00	-0.18	-0.29	0.100	0.096	3.792
52	791103- 6	-0.13	-0.36	-1.00	-0.18	-0.29	0.088	0.087	1.052
53	791103- 6	0.30	-0.36	-1.00	-0.18	-0.29	0.080	0.078	2.687
54	791103- 8	-0.57	-0.34	-1.00	-0.18	0.03	0.101	0.100	0.866
55	791103- 8	-0.13	-0.34	-1.00	-0.18	0.03	0.093	0.092	0.971
56	791103- 8	0.30	-0.34	-1.00	-0.18	0.03	0.087	0.084	3.421
57	791103- 7	0.30	-0.36	-1.00	-0.18	-0.29	0.081	0.078	3.930
58	791103- 5	0.30	-0.34	-1.00	-0.18	0.03	0.084	0.084	-0.088
59	791115- 5	-0.57	0.39	-1.00	-0.18	-0.29	0.084	0.086	-2.614
60	791115- 5	-0.13	0.39	-1.00	-0.18	-0.29	0.080	0.082	-2.723
61	791115- 5	0.30	0.39	-1.00	-0.18	-0.29	0.075	0.078	-4.170
62	791115- 6	0.30	0.39	-1.00	-0.18	-0.29	0.076	0.078	-2.844
63	791115- 7	0.30	0.39	-1.00	-0.18	0.03	0.084	0.084	0.075
64	791115- 8	-0.57	0.39	-1.00	-0.18	0.03	0.090	0.092	-1.693
65	791115- 8	-0.13	0.39	-1.00	-0.18	0.03	0.086	0.088	-1.969
66	791115- 8	0.30	0.39	-1.00	-0.18	0.03	0.083	0.084	-1.122
67	800523- 1	-0.13	0.39	-1.00	-0.18	0.03	0.094	0.088	6.901
68	800526- 2	-0.13	0.39	-1.00	-0.18	-0.29	0.073	0.082	-11.907
69	800526- 5	-0.13	0.39	-1.00	-0.18	0.03	0.087	0.088	-0.843
70	800526- 7	-0.13	0.39	-1.00	-0.18	0.03	0.088	0.088	-1.999
71	791103- 7	0.30	-0.36	0.80	-0.18	-0.29	0.078	0.078	0.375
72	791103- 9	0.30	-0.34	1.61	-0.18	0.03	0.082	0.084	-2.038
73	791115- 6	0.30	0.39	0.80	-0.18	-0.29	0.075	0.076	-1.356
74	791115- 7	0.30	0.39	0.80	-0.18	-0.29	0.082	0.076	7.073
75	800523- 1	-0.13	0.39	1.61	-0.18	0.03	0.093	0.083	11.308
76	800526- 1	-0.13	0.39	0.80	-0.18	-0.29	0.065	0.080	-21.193
77	800526- 4	-0.13	0.39	0.80	-0.18	-0.29	0.067	0.080	-18.105
78	800526- 6	-0.13	0.39	1.61	-0.18	0.03	0.086	0.083	3.519
79	800526- 9	-0.13	0.39	1.61	-0.18	0.03	0.092	0.083	10.231
80	791119- 1	-0.57	-0.44	-1.00	-0.59	0.03	0.101	0.102	-0.711
81	791119- 1	-0.13	-0.44	-1.00	-0.59	0.03	0.090	0.093	-3.799
82	791119- 1	0.30	-0.44	-1.00	-0.59	0.03	0.085	0.085	-2.671
83	791119- 2	0.30	-0.42	-1.00	-0.59	0.03	0.085	0.085	-0.248
84	791119- 3	0.30	-0.40	-1.00	-0.59	0.35	0.089	0.091	-2.221
85	791119- 4	-0.57	-0.40	-1.00	-0.59	0.35	0.099	0.105	-6.150
86	791119- 4	-0.13	-0.40	-1.00	-0.59	0.35	0.095	0.098	-3.250
87	791119- 4	0.30	-0.40	-1.00	-0.59	0.35	0.089	0.091	-2.221
88	791120- 1	-0.57	-0.40	-1.00	-0.59	0.03	0.100	0.102	-2.082
89	791120- 1	-0.13	-0.40	-1.00	-0.59	0.03	0.092	0.094	-1.736
90	791120- 1	0.30	-0.40	-1.00	-0.59	0.03	0.084	0.088	-1.345
91	791120- 2	0.30	-0.40	-1.00	-0.59	0.03	0.086	0.085	0.593
92	791120- 3	0.30	-0.40	-1.00	-0.59	0.35	0.091	0.091	0.001
93	791120- 4	-0.57	-0.40	-1.00	-0.59	0.35	0.100	0.105	-5.144
94	791120- 4	-0.13	-0.40	-1.00	-0.59	0.35	0.095	0.098	-3.250
95	791120- 4	0.30	-0.40	-1.00	-0.59	0.35	0.090	0.091	-1.104
96	791120- 5	-0.57	0.39	-1.00	-0.59	0.35	0.096	0.103	-6.696
97	791120- 5	-0.13	0.39	-1.00	-0.59	0.35	0.093	0.098	-5.742
98	791120- 5	0.30	0.39	-1.00	-0.59	0.35	0.090	0.094	-4.507
99	791120- 6	0.30	0.39	-1.00	-0.59	0.35	0.091	0.094	-3.401
100	791130- 1	-0.57	-0.40	-1.00	-0.59	0.03	0.096	0.102	-6.118

101	791130- 1	-0.13	-0.40	-1.00	-0.59	0.03	0.086	0.094	-8.432
102	791130- 1	0.30	-0.40	-1.00	-0.59	0.03	0.081	0.085	-5.024
103	791130- 2	0.30	-0.40	-1.00	-0.59	0.03	0.082	0.085	-3.796
104	791130- 3	0.30	0.39	-1.00	-0.59	0.03	0.092	0.087	5.748
105	791130- 5	-0.57	0.39	-1.00	-0.59	0.03	0.098	0.095	3.606
106	791130- 5	-0.13	0.39	-1.00	-0.59	0.03	0.095	0.091	4.637
107	791130- 5	0.30	0.39	-1.00	-0.59	0.03	0.092	0.087	5.748
108	800514- 1	-0.13	0.39	-1.00	-0.59	0.03	0.083	0.091	-8.880
109	800514- 2	-0.13	0.39	-1.00	-0.59	0.35	0.094	0.098	-4.651
110	800514- 3	-0.13	0.39	-1.00	-0.59	0.35	0.097	0.098	-1.508
111	800514- 4	-0.13	0.39	-1.00	-0.59	0.03	0.083	0.091	-8.880
112	800514- 9	-0.13	0.39	-1.00	-0.59	0.35	0.088	0.098	-11.269
113	791103- 3	-0.57	-0.38	-1.00	-0.59	0.03	0.114	0.102	10.304
114	791103- 3	-0.13	-0.38	-1.00	-0.59	0.03	0.105	0.094	11.425
115	791103- 1	-0.57	-0.40	-1.00	-0.59	-0.29	0.088	0.099	-11.653
116	791103- 2	-0.13	-0.40	-1.00	-0.59	-0.29	0.080	0.089	-10.780
117	791130- 6	-0.57	0.39	-1.00	-0.59	0.03	0.098	0.095	3.606
118	791130- 6	-0.13	0.39	-1.00	-0.59	0.03	0.096	0.091	5.696
119	791130- 6	0.30	0.39	-1.00	-0.59	0.03	0.092	0.087	5.748
120	791119- 2	0.30	-0.42	0.62	-0.59	0.03	0.085	0.085	0.420
121	791119- 3	0.30	-0.40	1.12	-0.59	0.35	0.089	0.090	-1.224
122	791120- 2	0.30	-0.40	0.62	-0.59	0.03	0.085	0.085	0.360
123	791120- 3	0.30	-0.40	1.12	-0.59	0.35	0.089	0.090	-1.224
124	791120- 6	0.30	0.35	1.12	-0.59	0.35	0.089	0.086	3.886
125	791130- 2	0.30	-0.40	0.62	-0.59	0.03	0.083	0.085	-2.015
126	791130- 3	0.30	0.39	0.62	-0.59	0.03	0.090	0.083	8.459
127	800514- 1	-0.13	0.39	0.62	-0.59	0.03	0.081	0.087	-6.717
128	800514- 2	-0.13	0.39	1.12	-0.59	0.35	0.092	0.091	1.131
129	800514-10	-0.13	0.39	1.12	-0.59	0.35	0.069	0.091	-27.959
130	800514-12	-0.13	0.39	0.62	-0.59	0.03	0.079	0.087	-9.215
131	791103- 4	-0.57	-0.36	0.62	-0.59	0.03	0.115	0.107	7.371
132	791103- 4	-0.13	-0.36	0.62	-0.59	0.03	0.105	0.096	9.166
133	791113- 1	-0.57	-0.34	-1.00	-0.80	0.35	0.105	0.106	-1.297
134	791113- 1	-0.13	-0.34	-1.00	-0.80	0.35	0.098	0.099	-0.686
135	791113- 1	0.30	-0.34	-1.00	-0.80	0.35	0.092	0.091	1.117
136	791113- 2	-0.57	-0.36	-1.00	-0.80	0.14	0.111	0.105	5.924
137	791113- 2	-0.13	-0.36	-1.00	-0.80	0.14	0.102	0.096	6.039
138	791113- 2	0.30	-0.36	-1.00	-0.80	0.14	0.092	0.087	5.094
139	791113- 3	-0.13	-0.34	-1.00	-0.80	0.14	0.101	0.096	5.029
140	791113- 4	0.30	-0.34	-1.00	-0.80	0.35	0.094	0.091	3.269
141	791115- 1	-0.57	0.39	-1.00	-0.80	0.14	0.111	0.099	11.100
142	791115- 1	-0.13	0.39	-1.00	-0.80	0.14	0.103	0.095	12.708
143	791115- 2	-0.35	0.35	-1.00	-0.80	0.14	0.110	0.097	12.522
144	791115- 3	0.19	0.31	-1.00	-0.80	0.35	0.099	0.098	1.123
145	791115- 4	-0.57	0.39	-1.00	-0.80	0.35	0.104	0.106	-1.934
146	791115- 4	-0.13	0.39	-1.00	-0.80	0.35	0.101	0.101	-0.077
147	791115- 4	0.19	0.39	-1.00	-0.80	0.35	0.099	0.097	1.667
148	791113- 3	-0.13	-0.34	-0.00	-0.80	0.14	0.098	0.093	-0.490
149	791113- 4	0.30	-0.34	0.19	-0.80	0.35	0.092	0.091	1.569
150	791115- 2	-0.35	0.35	-0.00	-0.80	0.14	0.101	0.093	12.804
151	791115- 3	-0.57	0.31	0.19	-0.80	0.35	0.099	0.100	-0.634
152	791115- 3	0.19	0.31	0.19	-0.80	0.35	0.095	0.092	3.058

THE MEAN OF THE ERROR IS -0.186%
THE STANDARD DEVIATION OF THE ERROR IS 6.226%

THE MEAN VELOCITY IS; 23.076 M/SEC
THE MEAN PRESSURE IS; 1.406 GPA
THE MEAN TEMPERATURE IS; 50.296 DEGREES C
THE MEAN SKIN PARAMETER IS; 0.000639

```
THE MEAN ASPECT PARAMETER IS;    2.441

STATEMENTS EXECUTED=  428247

CORE USAGE        OBJECT CODE=     9464 BYTES,ARRAY AREA=    16356 BYTES,TOTAL ARE

DIAGNOSTICS         NUMBER OF ERRORS=        0, NUMBER OF WARNINGS=        0, NUMB

COMPILE TIME=      1.07 SEC,EXECUTION TIME=     31.58 SEC,      19.25.26     WEDNES

          C$STOP
```

APPENDIX IV

"Traction drive performance predictions for the Johnson and Tevaarwerk Traction Model"

NASA TP 1530.

NASA Technical Paper 1530

Traction Drive Performance Prediction for the Johnson and Tevaarwerk Traction Model

Joseph L. Tevaarwerk
Lewis Research Center
Cleveland, Ohio

National Aeronautics
and Space Administration

**Scientific and Technical
Information Branch**

1979

SUMMARY

The recently developed Johnson and Tevaarwerk fluid rheology model was used to investigate the traction behavior for typical traction drive contacts. Fluid shear modulus and limiting fluid shear strength were allowed to vary over the contact area in accordance with observed traction behavior. The influence of aspect ratio of the contact and the invariably present spin was investigated. Graphical solutions of the analysis are provided which allow for the design optimization of traction drives. Comparisons were made with the commonly used rigid-plastic analysis of Wernitz.

The influence of low spin values on traction was found to be negligible; therefore, the simple slip analysis with the elastic-plastic model is sufficient. At moderate values of spin the complete spin analysis with the elastic-plastic model is needed to give accurate traction predictions. At sufficiently high spin the Johnson and Tevaarwerk model may be simplified to the rigid-plastic model, and the elastic effects in the fluid may be neglected. Contacts with a low aspect ratio predict a superior performance in that they show less slip for the same degree of traction. Sideways forces due to the spin on the contact can be substantial and may reach 75 percent of the transmitted traction force. Also the effect due to spin is always deleterious to the traction efficiency.

INTRODUCTION

Typically the power transmission in continuously variable speed traction drives occurs in a small, elastically deformed region on the two elements. Due to the rolling motion and in the presence of a fluid, a thin layer of lubricant is drawn into this contact area, thus separating the two bodies.

Relative velocities between the two bodies in contact shears the lubricant. Its resistance to shear permits a transmission of force between the two bodies. The amount of force that can be transmitted for a given amount of slip has been the subject of many past and present investigations, many of them resulting in fluid models (refs. 1 to 5).

The fluid in the gap is subjected to very high pressure gradients and pressures for very short times. The common behavior to high pressures is an increase in the viscous shear resistance of the lubricant (refs. 6 and 7), however, due to the extremely short duration of the pressure, the situation is not at all clearly understood. This is because there are no simple experiments that will directly measure the shear properties

of the lubricants. It is known, however, that there are definite time delays in the response of these lubricant properties to sudden pressure changes (ref. 8), and it is thought that the lubricant behaves in a more elastic fashion at low deformation rates (ref. 5).

Due to the uncertainties in the shear response of the fluid, the past design techniques for analyzing traction drive contacts were based upon the rigid-plastic concept as used by Wernitz (ref. 9) and Magi (ref. 10). More recently a refined traction model was proposed and experimentally validated by Johnson and Tevaarwerk (ref. 5) which considers the lubricant behavior to be viscoelastic reducing to an elastic-plastic model at high pressures and shear strains.

The objective of this investigation is to (1) examine the traction behavior of a lubricant for a typical traction drive contact using the Johnson and Tevaarwerk model; (2) generate design charts for traction drive contacts using this model; (3) make a comparison between this new model and the Wernitz-Magi approach; and (4) establish design criteria for the application of either of these models.

SYMBOLS

A	contact area, m^2
a, b	Hertzian contact ellipse parameters; a is the semiaxis in the rolling direction; b is the semiaxis perpendicular to the rolling direction, m
e	speed pole location, m
$\dot{e}_{ij}$	rate of strain tensor, sec^{-1}
F_x, F_y	traction force in x- and y-direction, respectively, N
$F(\tau_e)$	dissipative strain rate function, sec^{-1}
$\overline{F}(Z_e)$	dimensionless strain rate function
G	elastic shear modulus, N/m^2
$\overline{G}$	average elastic shear modulus over contact area, N/m^2
G_c	compliance corrected shear modulus, N/m^2
G_s	elastic shear modulus of disk material, N/m^2
h	film thickness, m
J_1	dimensionless slip in rolling direction
J_3	dimensionless spin
J_4	dimensionless traction in rolling direction

J_5	dimensionless traction perpendicular to rolling direction
J_6	dimensionless spin torque
J_7	dimensionless power loss
k	aspect ratio of Hertzian contact, b/a, dimensionless
m	initial slope of experimental traction curves, dimensionless
m'	initial slope of traction curve for dry rolling bodies, dimensionless
N	normal force on contact, N
P	Hertzian pressure in contact, N/m^2
P_o	maximum Hertzian pressure in contact, N/m^2
T	spin torque on contact, N-m/rad
q	aspect ratio dependent constant, dimensionless
$U^{\pm}$	velocities in x-direction on upper and lower body, m/sec
ΔU	rolling velocity difference (slip), m/sec
$V^{\pm}$	velocities in y-direction on upper and lower body, m/sec
ΔV	velocity difference in y-direction, m/sec
ΔX	dimensionless spin pole offset
X, Y	dimensionless Cartesian coordinates
x, y, z	Cartesian coordinates, m
Z	dimensionless stress
δ_x	spin pole offset, m
ε	dimensionless speed pole location
μ	maximum traction coefficient from experimental traction curve, dimensionless
τ	shear stress, N/m^2
τ_c	reference stress for hyperbolic sinh, N/m^2
τ_o	limiting shear strength of fluid, N/m^2
$\bar{\tau}_o$	average limiting shear strength of fluid over contact area, N/m^2
φ	equivalent strain rate parameter
ω	angular velocity difference between contacting bodies normal to contact area, rad/sec

Subscripts:

e	equivalent
ij	tensor coordinates
x, y, z	Cartesian coordinates

THEORETICAL ANALYSIS

Typically the power transmission in variable speed traction drives occurs in highly stressed contact areas that operate in the elastohydrodynamic lubrication (EHL) regime. The traction characteristics of these drives therefore depend to a large extent on the fluid and material properties at the EHL conditions that prevail. At these conditions of pressure ($\simeq 10^9$ Pa), transit time, (10^{-3} sec), and temperature ($30^\circ \rightarrow 150^\circ$ C), Johnson and Tevaarwerk, in reference 5, found that the shear behavior of the lubricants examined was best described by the following constitutive equation:

$$\frac{d(\tau_{ij}, G)}{dt} + \frac{\tau_{ij}}{\tau_e} F(\tau_e) = 2\dot{e}_{ij} \tag{1}$$

where

τ_{ij}	stress tensor
$\dot{e}_{ij}$	rate of strain tensor
τ_e	equivalent stress, $\sqrt{(\tau_{ij} \cdot \tau_{ij})/2}$
$F(\tau_e)$	nonlinear viscous function to be specified later
G	elastic shear modulus of fluid

Equation (1) was formulated by the simple addition of elastic and viscous compliances to account for the total compliance of the fluid film. Its correctness in formulation was extensively tested and verified in reference 11 using a point-contact-type disk machine that permits the study of traction under both slip, spin, and slip and spin.

To obtain the tractive capacity for a typical traction drive contact, equation (1) has to be solved as a series of coupled differential equations with the proper use of the geometric boundary conditions and the applied rate of strain tensor.

A typical Hertzian contact as it occurs in many forms of traction drives is shown in figure 1 together with the nomenclature that is commonly used. For this simple geometry equation (1) reduces to the following:

$$\left.\begin{aligned} \frac{d(\tau_x/G)}{dt} + \frac{\tau_x}{\tau_e} F(\tau_e) &= 2\dot{e}_x \\ \frac{d(\tau_y/G)}{dt} + \frac{\tau_y}{\tau_e} F(\tau_e) &= 2\dot{e}_y \end{aligned}\right\} \qquad (2)$$

and

$$\tau_e = \sqrt{\tau_x^2 + \tau_y^2}$$

The system of shear stresses acting on the surface gives rise to tractive forces F_y and F_x.

Figure 2 shows the side view of the contact; the following assumptions have been made:

(1) Film thickness h is constant over the contact area.

(2) Pressure distribution is Hertzian and the displacement of the effective pressure center from the contact center is indicated by δ_x.

In most forms of traction drives, not all of the velocities occur at once and in most cases $\Delta V = V = 0$ and only slip in the rolling direction and spin are present.

The simplified contact is shown in figure 3 together with the shear strain rate distribution in the y-direction (fig. 3(b)) and in the x-direction (fig. 3(c)). From this figure it is clear that

$$\dot{e}_x = \frac{1}{2}\left(\frac{\Delta U - \omega y}{h}\right)$$

$$\dot{e}_y = \frac{1}{2}\left[\frac{\omega(x + \delta_x)}{h}\right]$$

The system of equations (2) may now be written as

$$\left.\begin{aligned} \frac{d(\tau_x/G)}{dt} + \frac{\tau_x}{\tau_e} F(\tau_e) &= \frac{\Delta U - \omega y}{h} \\ \frac{d(\tau_y/G)}{dt} + \frac{\tau_y}{\tau_e} F(\tau_e) &= \frac{\omega(x + \delta_x)}{h} \end{aligned}\right\} \qquad (3)$$

We may use the following substitutions to nondimensionalize the set of equations (3):

$$X = x/a \qquad Y = y/b \qquad \Delta X = \delta/a$$

$$Z_x = \tau_x/\bar{\tau}_o \qquad Z_y = \tau_y/\bar{\tau}_o \qquad Z_e = \tau_e/\bar{\tau}_o$$

where $\bar{\tau}_o$ is some reference stress to be defined later. From the kinematics it follows that $x = Ut$. Now, because U is constant, we obtain $dt = (a/U)\,dX$. Equation (3) may now be written in a simple nondimensional form as

$$\left.\begin{aligned} \frac{dZ_x(\bar{\tau}_o/G)}{dX} + \frac{Z_x}{Z_e} F(Z_e \cdot \bar{\tau}_o) \frac{a}{U} &= \frac{a}{U}\left(\frac{\omega\sqrt{ab}}{h}\right)\left(\frac{\Delta U}{\omega\sqrt{ab}} - Y\sqrt{k}\right) \\ \frac{dZ_y(\bar{\tau}_o/G)}{dX} + \frac{Z_y}{Z_e} F(Z_e \cdot \bar{\tau}_o) \frac{a}{U} &= \frac{a}{U}\left(\frac{\omega\sqrt{ab}}{h}\right)\frac{(X + \Delta X)}{\sqrt{k}} \end{aligned}\right\} \tag{4}$$

where $Z_e = \sqrt{Z_x^2 + Z_y^2}$ and $k \equiv b/a$ is the aspect ratio of the contact. The boundary conditions for this set of equations are

$$Z_x = Z_y = 0 \quad \text{at} \quad X = -\sqrt{1 - Y^2} \tag{5}$$

under the assumption that the shear stresses are zero in the inlet region.

NONLINEAR FUNCTION $F(\tau_e)$

With the knowledge of the nonlinear function $F(\tau_e)$, the set of equations (4) may be solved for the stresses and hence for the traction forces.

Various forms of the function $F(\tau_e)$ are possible. In reference 11 it was shown that a fairly general form of it is given by the hyperbolic sinh, namely,

$$F(\tau_e) = \frac{\tau_c}{\eta} \sinh \frac{\tau_e}{\tau_c} \tag{6}$$

where

η linear Newtonian viscosity

τ_c reference shear stress

For fluids under high pressure, such as those that occur in traction drive contacts, it is acceptable to use the limiting case of equation (6), also known as the limiting shear stress model. In mathematical form the function may be written as

$$F(\tau_e) = 0 \quad \text{for} \quad \tau_e < \tau_o$$

and

$$F(\tau_e) = \frac{2(\tau_{ij} \cdot \dot{e}_{ij})}{\tau_o} \quad \text{for} \quad \tau_e = \tau_o \tag{7}$$

where τ_o is the local limiting shear strength of the fluid.

The model was suggested in reference 1 and has been used extensively in the analysis of traction drive contacts. The advantage in using this form of the nonlinear function is that we now only have one disposable parameter. When this form of the limiting shear stress formulation is used, equations (1) reduce to the well known Prandtl-Reuss equations for elastic, perfectly plastic material.

Curves B and C in figure 4 (reproduced from ref. 11), compare actual and predicted traction behavior of a circular contact under combined spin and slip and using the elastic-plastic form of equation (1). The two parameters G and τ_o were obtained from the measured initial slope and peak traction coefficient of the zero spin traction curve A in figure 4. These were, combined with the kinematic information on the strain distribution, used to predict the combined spin and slip curves B and C. The results show that the elastic-plastic form of equation (1) indeed predicts the observed traction correctly.

VARIATION OF THE FLUID PROPERTIES WITH PRESSURE

In order to solve equations (4) we have to know something about the effect of pressure on the magnitude of both the shear modulus G and the limiting shear stress τ_o. A simple approach would be to ignore any variation of the G and τ_o due to pressure and to set $G = \overline{G}$ and $\tau_o = \overline{\tau}_o$ where the bar denotes average properties; however, it was shown in reference 5 that to a fair approximation both G and τ_o are linear functions of pressure and, therefore a better description of the two parameters over the contact area would be to let

$$\tau_o = \frac{3}{2} \tau_o \sqrt{1 - X^2 - Y^2}$$

and

$$G = \frac{3}{2} \bar{G} \sqrt{1 - X^2 - Y^2} \tag{8}$$

This latter type of variation of G and τ_o does not necessarily give the best predictions of traction as is shown in figure 5. Here both types of variations of G and τ_o are shown. It may be observed that for small values of spin, the traction is predicted better by the averaged properties τ_o and $\bar{G}$ over the contact area, while at the larger values of spin the property variation as shown in equation (8) gives better results. Also, it should be noted that the small strain results are predominantly elastic and hence governed by G, while the large strain results are mostly governed by the plastic properties τ_o of the liquid. Therefore the following variations of G and τ_o should be used if a better fit is wanted:

$$G = \bar{G}$$

$$\tau_o = \frac{3}{2} \bar{\tau}_o \sqrt{1 - X^2 - Y^2}$$

The main reason for the apparent contradiction in the experimental variation of G with pressure and the variation giving the best fit is thought to be caused by disk compliance which is discussed in appendix A. When the present analysis is used to predict the performance of traction drive contacts consisting of the lubricant and the disks, then the appropriate value of G to use is that for the system, not just the fluid. This system modulus $\bar{G}$ can be taken as the shear modulus of the lubricant to give nearly correct predictions.

The shear modulus $\bar{G}$ and the limiting shear stress $\bar{\tau}_o$ are parameters that are not readily available but can easily be obtained from experimental traction curves. The measured initial traction slope m and the peak traction coefficient μ (see fig. 6) from a pure slip traction curve can be used to calculate $\bar{G}$ and the limiting shear stress $\bar{\tau}_o$; thus,

$$\bar{G} = \frac{3}{8} m \left(\frac{Nh}{a^2 b}\right)$$

$$\bar{\tau}_o = \frac{\mu N}{\pi ab} \qquad (10)$$

It is important that these two parameters are obtained under identical operating conditions to those prevailing in the traction drive contacts, namely contact pressure, temperature and area, film thickness and speed. It is possible, however, to use data that was obtained at the same pressure, temperature and speed but at different contact area, aspect ratio and film thickness through the use of the analysis as outlined in appendix B.

For ease of notation, various nondimensional groups are introduced now. The nondimensional groups are expressed in both the fluid properties $\bar{G}$ and $\bar{\tau}_o$ and the traction curve parameters m and μ. They are

$$J_1 = \frac{\bar{G}\sqrt{ab}}{\bar{\tau}_o h} \frac{\Delta U}{U}$$

$$= \frac{3}{8} \pi \left(\frac{m}{\mu}\right) \cdot \left(\frac{\Delta U}{U}\right) \cdot \sqrt{k} \qquad \text{(dimensionless slip)} \qquad (11)$$

and

$$J_3 = \frac{\bar{G}\sqrt{ab}}{\bar{\tau}_o h} \cdot \frac{\omega \sqrt{ab}}{U}$$

$$= \frac{3}{8} \pi \left(\frac{m}{\mu}\right) \cdot \left(\frac{\omega \sqrt{ab}}{U}\right) \cdot \sqrt{k} \qquad \text{(dimensionless spin)} \qquad (12)$$

Equations (4) and (7) may now be written as

$$\left.\begin{aligned} \frac{dZ_x}{dX} &= \frac{J_3}{\sqrt{k}}\left(\frac{J_1}{J_3} - Y\sqrt{k}\right) - \left(\bar{F}(Z_e) \cdot \frac{Z_x}{Z_e}\right) \\ \frac{dZ_y}{dX} &= \frac{J_3}{k}(X + \Delta X) - \left(\bar{F}(Z_e) \cdot \frac{Z_x}{Z_e}\right) \end{aligned}\right\} \tag{13}$$

where

$$Z_e = \sqrt{Z_x^2 + Z_y^2}$$

and $\bar{F}(Z_e) = 0$ when $Z_e < \frac{3}{2}\sqrt{1 - X^2 - Y^2}$

or

$$\bar{F}(Z_e) = \frac{J_3}{Z_e\sqrt{k}}\left[\left(\frac{J_1}{J_3} - Y\sqrt{k}\right)Z_x + \frac{(X + \Delta X)Z_y}{\sqrt{k}}\right]$$

when

$$Z_e = \frac{3}{2}\sqrt{1 - X^2 - Y^2}$$

Equation (13) may be solved for Z_x and Z_y using various values of J_1, J_3, k, and ΔX. In the reported calculations ΔX has been kept zero.

RIGID-PLASTIC MODEL

A particularly interesting case exists for equation (13) when the shear modulus goes to irfinity and the constitutive equation reduces to that for a rigid-plastic model. The equations now represent the von Mises criteria for plastic flow. This model has been used quite frequently in traction drive analyses for example by Wernitz in reference 9 and more recently by Magi in reference 10. The resulting stress equations for this model are

$$\left.\begin{aligned} Z_x &= \frac{3}{2}\frac{\sqrt{1 - X^2 - Y^2}\ (\varepsilon - Y\sqrt{k})}{\varphi} \\ Z_y &= \frac{3}{2}\frac{\sqrt{1 - X^2 - Y^2}\ (X + \Delta X)}{\varphi\sqrt{k}} \end{aligned}\right\} \qquad (14)$$

where

$$\varphi \equiv \sqrt{(\varepsilon - Y\sqrt{k})^2 + \frac{(X + \Delta X)^2}{k}}$$

and

$$\varepsilon \equiv \frac{J_1}{J_3}$$

The parameter ε has a special meaning in traction drive analysis and is often referred to as the speed pole location. Its meaning is made clear by looking at figure 3(c) where e is given by $e = \Delta U/\omega$. If we now divide this by $\sqrt{ab}$, we obtain $e/\sqrt{ab} \equiv \varepsilon = \Delta U/\omega\sqrt{ab}$. So the speed pole location parameter ε is nothing more than the ratio of slip to spin in the contact. This speed pole parameter is identical to that used by Magi in reference 10. From the definition of J_1 and J_3 we find that $\varepsilon \equiv J_1/J_3$. Strictly speaking the parameter J_1 and J_3 should not be used for the rigid-plastic model because both contain the shear modulus, however, the ratio J_1/J_3 forms a convenient independent parameter that is consistent with the work of previous researchers. Equation (14) then, is a limiting form of equation (13) when the elastic effects are negligible with J_1/J_3 as one of the independent parameters.

TRACTION CALCULATIONS

Of real interest in traction drive design are the traction, the slip, and the total losses in the system. Also of concern is the degree of sophistication that should be used to obtain correct answers. The level of the analysis is dependent upon where the elastic properties of the fluid are important and when the plastic properties are more dominant. These questions may be answered by solving equation (13) for the traction parameters.

In terms of the nondimensional parameters we have for the traction forces

$$\left.\begin{aligned} F_x &= \int_A \tau_x dA = ab\bar{\tau}_o \int_A Z_x dX\, dY \\ &= \pi ab\bar{\tau}_o J_4 \end{aligned}\right\} \quad (15)$$

where

$$J_4 \equiv \frac{1}{\pi} \int_A Z_x dX\, dY = \text{nondimensional traction in the rolling direction}$$

$$= \frac{F_x}{\pi ab\bar{\tau}_o} = \frac{F_x}{\mu N}$$

Similarly,

$$J_5 \equiv \frac{F_y}{\pi ab\bar{\tau}_o} = \frac{F_y}{\mu N} = \text{nondimensional traction perpendicular to the rolling direction.}$$

For the torque on the spinning contact we have

$$T = \int_A (\tau_y \cdot x - \tau_x \cdot y) dA$$

or

$$\frac{T}{\bar{\tau}_o ab\pi \cdot \sqrt{ab}} = \frac{T}{\mu N \cdot \sqrt{ab}} = J_6 \quad (16)$$

where

$$J_6 \equiv \frac{\sqrt{k}}{\pi} \int_A (Z_y \cdot X - Z_x \cdot Y \cdot k) dX\, dY$$

The power dissipated in the contact can now be calculated in terms of these nondimensional parameters; namely,

$$J_7 = J_6 \cdot J_3 + J_4 \cdot J_1$$

or in terms of real power

$$J_7 = \frac{\bar{G}}{\pi\sqrt{ab}\,\bar{\tau}_o^2 hU} (T \cdot \omega + F_x \cdot \Delta U) \qquad (17)$$

or

$$J_7 = \frac{3\pi}{8U} \cdot \sqrt{k} \cdot \frac{m}{\mu^2 N} (T \cdot \omega + F_x \cdot \Delta U)$$

where the terms in parentheses are the individual components of the power loss due to spin and longitudinal slip.

The important information from the calculations to present are traction J_4, J_5, and torque J_6 as functions of slip J_1 and spin J_3. Any other quantity may be calculated from these five parameters. As an independent variable we may select slip J_1, based upon the elastic-plastic argument, or the speed pole location J_1/J_3 as found in the rigid-plastic analysis. For the traction in the rolling direction J_4 it was decided to present the data using both slip J_1 and speed pole locations J_1/J_3 as the independent variable since both types of graphs reveal significant information.

The zero spin traction curves for an elastic-plastic material at various aspect ratios are shown in figure 7. We observe that at any slip J_1 we obtain more traction J_4 with the lower aspect ratio contacts. The explanation of this behavior lies in the fact that the mean shear strain is directly proportional to the contact dimension in the X-direction. The lower aspect ratio contacts have their semimajor axis in the running direction and therefore see a larger mean shear strain and hence the mean shear stress is larger. The effect shows up in the traction.

It may be expected that, at high local strain rates, the elastic effects are not significant and that the rigid-plastic model may be used to solve for the tractions. Figure 8 shows the traction J_4 for the rigid-plastic model at various aspect ratios as a function of the speed pole location. Again lower aspect ratio contacts appear to have a slight edge on traction for the same speed pole parameter.

To observe the effect of spin J_3 on the traction J_4 for the elastic-plastic model, the traction J_4 was calculated with various values of spin J_3 present and the results are shown in figure 9. These results are also presented with the speed pole parameter as the independent parameter in figure 10. A simple comparison with figures 7 and 8 therefore will show the influence of both elastic effects and spin on the traction J_4. In each case the connected lines represent constant values of spin J_3.

Figure 11 shows the resulting side force traction J_5 for $k = 1$ when a contact is under spin. This force is the result of elastic behavior of the fluid under spin and slip. At low slip $J_1 < 1.0$, the side force J_5 starts at zero for zero spin, reaches a maximum and then decreases for increasing spin. When more slip J_1 is introduced, the behavior is altered somewhat and the maximum value diminishes. Figure 12 shows the variation of the maximum value of the side force J_5 as a function of the aspect ratio k. Generally when k is small, there are larger side forces. As can be seen from figure 12 the side force J_5 can be an appreciable fraction of the traction J_4.

Figure 13 shows the values of nondimensional torque J_6 as a function of speed pole locations of J_1/J_3. Solid lines again indicate constant values of spin J_3. The resulting traction curves of J_4 versus slip J_1 (fig. 9) or speed pole location J_1/J_3 (fig. 10) show that in both cases the traction J_4 tends toward a limiting traction curve and appears to be independent of spin J_3. In figure 9 the lower spin value traction curves are indistinguishable from the zero spin traction curve. This suggests that below a certain value of spin J_3 the resulting value of traction J_4 is insensitive to spin and that the simple elastic-plastic model without spin predicts the correct tractions. From figure 10 it may be observed that for high values of spin J_3 the curves are indistinguishable from the traction curve for a rigid-plastic-like material. The suggestion here is that for values of spin J_3 above a certain threshold value the traction results J_4 are in fact independent of any elastic effects in the sheared material. This form of behavior with spin J_3 could have been predicted from the nature of the constitutive equation (13). For small values of spin J_3 the behavior would be almost elastic-like while for large values of spin J_3 the differential equations (13) become singular in nature. From all of the results in figures 9 and 10 it may be observed that the two threshold values are dependent on the ellipticity of the contact. In traction drives we are generally only interested in the traction range that lies somewhere near 75 percent of the maximum obtainable traction. For this traction value the various threshold values of spin J_3 as a function of the aspect ratio are shown in figure 14. The three regions of influence are indicated on figure 14. They are

Region I - elastic-plastic analysis without spin is sufficient

Region II - elastic-plastic analysis with spin is required

Region III - rigid-plastic analysis with spin is sufficient

The lines dividing the regions are the values of spin J_3 corresponding to a 5 percent increase in the slip traction level, compared to the master traction curves in figures 7 and 8.

LOSS FACTORS

Losses in the contacts of a traction drive are made up of two components (slip and spin losses) as was indicated in equation (17):

$$J_7 = (J_6 \times J_3 + J_4 \times J_1)$$

From the calculated results the power loss J_7 can be calculated from the individual components and we can establish curves of J_7 as a function of slip J_1 or speed pole location J_1/J_3. An example of J_7 versus J_1 is shown in figure 15 for $k = 1$.

It is, however, more convenient to define a loss factor LF which has a more direct meaning to us as follows:

$$(LF) \equiv \frac{J_7}{J_4}$$

$$= \frac{\bar{G}}{U\pi\sqrt{ab}\,\bar{\tau}_o^2 h}\,(T \cdot \omega + F_x \cdot \Delta U) \Big/ \frac{F_x}{\pi ab\bar{\tau}_o}$$

$$= \frac{\bar{G}\sqrt{ab}}{\bar{\tau}_o h}\left(\frac{\text{power loss}}{\text{power input}}\right)$$

$$= \frac{3\pi}{8}\sqrt{k}\,\frac{m}{\mu}\left(\frac{\text{power loss}}{\text{power input}}\right) \tag{18}$$

The loss factor may be thought of as an equivalent creep in the power transmission direction. It is interesting to note that, when the drive is idling (i.e., no net power output), then the loss factor is simply given by

$$(LF)_o = \frac{\bar{G}\sqrt{ab}}{\bar{\tau}_o h} \tag{19}$$

or in terms of traction curve parameters

$$(LF)_o = \frac{3\pi}{8} \sqrt{k} \frac{m}{\mu} \tag{20}$$

and we see that the idling losses are directly related to the traction curve parameters. Figure 16 shows the calculated loss factor curves as a function of the dimensionless transmitted traction J_4. This way of presenting the data is most useful since most forms of the traction drives employ a mechanism whereby the ratio of the normal load to the tractive force transmitted is maintained constant at values of 60 to 80 percent of the maximum obtainable traction coefficient. This feature means that these types of drives operate at essentially a constant value of J_4 much of the time, that is, along a vertical line at a constant value of J_4 in figure 16.

From the results in figure 16 it may be observed that the region of 60 to 80 percent of the maximum available traction, or $J_4 = 0.6$ to 0.8, is the most efficient when substantial spin is present, though this depends somewhat on the aspect ratio k. Also in this same region it may be observed that the loss factor is not affected by small values of spin and that it is the lowest for the contacts of low aspect ratio. The insensitivity to small values of spin indicates that the losses in the contact are predominantly due to creep for these small values of spin.

In figure 17 the loss factor at traction $J_4 = 0.75$ is plotted against the spin J_3 for the various aspect ratios considered in this work. From this figure it may be observed that the imposed spin has little or no influence on the loss factor at low values of spin.

From a practical point of view it can be concluded from figure 17 that a traction drive may be operated with values of spin J_3 up to approximately one without increasing the power losses in the contact.

Figure 18 shows the loss factor plotted as a function of J_1/J_3 at constant values of spin J_3 for $k = 1$. This figure indicates that the minimum value of the loss factor occurs at approximately constant values of the speed pole location ε or J_1/J_3 independent of the amount of spin present. This may be useful information in the design of angular contact bearings to minimize their losses.

CONCLUSIONS

The elastic-plastic approximation of the Johnson and Tevaarwerk fluid traction model was used to analyze the traction behavior of typical traction drive contacts. The two required fluid properties, shear modulus and limiting fluid shear strength, were allowed to vary over the contact area in accordance with observed traction behavior.

This investigation was particularly aimed at the role that both contact configuration and spin play in longitudinal traction. Graphical solutions of the analysis are provided which allow for the design optimization of traction drive contacts. Comparisons were made between the full Johnson and Tevaarwerk solutions and those which can be arrived at by using the commonly used rigid-plastic analysis due to Wernitz.

The most important conclusions drawn from the analysis are the following:

1. Under conditions of slip and spin several simplifications in the analysis may be used; they are (a) The influence of low spin values is negligible on the traction. Simple slip analysis with the elastic-plastic model is sufficient. (b) At moderate values of spin the complete analysis of spin with the elastic-plastic model is needed to give accurate traction predictions. (c) At high values of spin the elastic effects in the fluid may be neglected and the simple rigid-plastic analysis due to Wernitz may be used.

2. Traction improves with contacts whose major axis is in the rolling direction.

3. Sideways forces due to the spin on the contact can be a substantial fraction of the transmitted traction.

4. The effect of spin is always deleterious to traction efficiency.

Lewis Research Center,
National Aeronautics and Space Administration,
Cleveland, Ohio, July 11, 1979,
511-58.

APPENDIX A

CORRECTIONS FOR DISK COMPLIANCE

One of the implicit assumptions made in the present analysis is that the two contacting bodies are infinitely stiff in the plane of contact. This is not so in many practical situations. The effect of disk compliance may be studied by the following very simple model. Consider the layer of film between the two "contacting" disks. The combination disk, film, disk form a sandwich of three deformable elements and relative velocities between the two disks is accommodated by shear in all three elements. When the film is thin and stiff, most of the shear may in fact take place in the disks. This is certainly the case when the disks roll together without a lubricant. For two bodies that roll together without a lubricant film it has been shown in references 12 and 13 that the following creep due to the transmitted traction force F occurs:

$$\left(\frac{\Delta U}{U}\right)_{dry} = q\left(\frac{F}{\pi a b G_s}\right) \tag{A1}$$

where

G_s shear modulus of disk material

q constant depending on aspect ratio (given in appendix B).

For an elastic lubricant film of thickness h under shear due to the transmitted traction force F the creep is given by

$$\left(\frac{\Delta U}{U}\right)_{film} = \frac{32}{9\pi}\frac{h}{a}\left(\frac{F}{\pi a b \bar{G}}\right) \tag{A2}$$

where it was assumed that

$$G = \frac{3}{2}\bar{G}\sqrt{1 - X^2 - Y^2} \tag{8}$$

The total creep for the sandwich under the imposed traction F is given by the sum of the disk creep and the film creep, namely,

$$\left(\frac{\Delta U}{U}\right)_{total} = \frac{F}{\pi a b}\left(\frac{q}{G_s} + \frac{32}{9\pi}\frac{h}{a}\frac{1}{G}\right) \tag{A3}$$

The parameter q covers the range of $q = 0.4$ for $k = 0.2$ to $q = 0.93$ for $k = 5$ (longitudinal creep only). For commonly used traction drives operating at pressures above 1.2 gigapascals, $h/a \simeq 10^{-3}$ and steel is generally employed as the disk material. When these values are used in equation (A3) together with a fluid shear moduli $\bar{G}$ of about 10^9 pascals, as found experimentally, then it is observed that most of the creep in the sandwich in the small slip region takes place in the disks, not in the fluid film. Reported shear moduli, as obtained from disk machine experiments have to be corrected for this effect (see, for example, refs. 5, 11, 14, and 15) for compliance corrected shear moduli.

If, in the region of operation of traction drives, most of the elastic effects are caused by the disk material, then we are justified in using the shear modulus as a constant over the contact area since G_s is not affected to any extent by the normal pressure.

APPENDIX B

CORRECTIONS FOR CONTACT AREA, ASPECT RATIO, AND FILM THICKNESS

Frequently traction data is available for a fluid at the same speed, temperature, and pressure but not at the same contact area because the roller geometry may have been different. From the analysis in the text it is clear that roller compliance and contact area play a significant role in the determination of the traction slope. An exact analysis for the correction of these terms is not yet possible; however, we can attempt the following simplified procedure.

If we let m' be the slope of the traction curve for dry rolling bodies, then it follows that the compliance corrected modulus for the fluid is approximately

$$G_c = \bar{G}\left(1 - \frac{m}{m'}\right)^{-1} \tag{B1}$$

where

G_c compliance corrected modulus

$\bar{G}$ apparent modulus

m wet slope for contact

m' dry slope for contact

From the main text we have an expression for the apparent modulus equation

$$G = \frac{3}{8} m\left(\frac{Nh}{a^2 b}\right) \tag{10}$$

Also from equation (A1), we have for the dry slope that

$$\frac{F}{N}\Big/\frac{\Delta U}{U} \equiv m' = \frac{\pi a b G_s}{qN} \tag{B2}$$

Now because $N = (2/3)\pi a b P_o$ we can simplify this equation a bit further to

$$m' = \frac{3}{2}\frac{G_s}{qP_o} \tag{B3}$$

where q is aspect ratio dependent. Also equation (10) may be put in a slightly simpler form by this method

$$\overline{G} = \frac{\pi}{4} m \frac{P_o h}{a} \tag{B4}$$

If we now assume that the compliance correction according to equation (B1) is good to a fair degree, then for different measurements at the same pressure, speed, and temperature we might at least expect that the compliance corrected modulus would be the same; or if the * parameters refer to one set of experiments and the nonsuperscripted parameters to another set, then we may write under the aforementioned assumptions the following:

$$G_c = G_c^*$$

By using equations (B1) and (B4) this becomes

$$\frac{\pi}{4} m \frac{P_o h}{a} \left(1 - \frac{m}{m'}\right)^{-1} = \frac{\pi}{4} \frac{m^* h^*}{a^*} P_o \left(1 - \frac{m^*}{m'^*}\right)^{-1} \tag{B5}$$

The comparison is made at the same pressure P_o so we can simplify the aforementioned expression to

$$\frac{m^* h^* a}{m h a^*} = \left[1 + \frac{m}{m'} \left(\frac{a^* h m'}{m'^* h^* a} - 1\right)\right]^{-1} \tag{B6}$$

From equation (B3) for the same material and contact pressure we can write $m'/m'^* = q^*/q$ so that the final form of equation (B6) is

$$\frac{m^* h^* a}{m h a^*} = \left[1 + \frac{2}{3} \frac{m q P_o}{G_s} \left(\frac{a^* h q^*}{a q h^*} - 1\right)\right]^{-1} \tag{B7}$$

Equation (B7) now relates the unknown slope m^* to the other known parameters.

We do need the parameters q (the Kalker coefficients). These may be obtained from reference 13, and are plotted for both longitudinal traction measurements q_x and side slip traction measurements q_y in figure 19.

Equation (B7) is plotted in figure 20 for a common range of variables.

REFERENCES

1. Clark, O. H.; Woods, W. W.; and White, J. R.: Lubrication at Extreme Pressure with Mineral Oil Films. J. Appl. Phys., vol. 22, no. 4, Apr. 1951, pp. 474-483.

2. Smith, F. W.: The Effect of Temperature in Concentrated Contact Lubrication. ASLE Trans., vol. 5, no. 1, Apr. 1962, pp. 142-148.

3. Crook, A. W.: The Lubrication of Rollers, IV: Measurement of Friction and Effective Viscosity. Phil. Trans. Roy. Soc. (London), Series A, vol. 255, 1963, pp. 281-312.

4. Johnson, K. L.; and Cameron, R.: Shear Behavior of Elastohydrodynamic Oil Films at High Rolling Contact Pressures. Proc. Inst. Mech. Eng. (London), vol. 182, pt. I, no. 14, 1967, pp. 307-319.

5. Johnson, K. L.; and Tevaarwerk, J. L.: Shear Behavior of Elastohydrodynamic Oil Films. Proc. Roy. Soc. (London), Series A, vol. 356, no. 1685, Aug. 24, 1977, pp. 215-236.

6. Bridgeman, P. W.: Effect of Pressure on the Viscosity of 43 Pure Liquids. Proc. Am. Acad. Arts Sci., vol. 61, 1926, pp. 57-99.

7. Pressure Viscosity Report, Vols. 1 and 2. American Society of Mechanical Engineers, 1953.

8. Fein, R. S.: Effects of Lubricants on Transition Temperatures. ASLE Trans., vol. 8, no. 1, Jan. 1965, pp. 59-68.

9. Wernitz, W.: Friction at Hertzian Contact with Combined Roll and Twist. Rolling Contact Phenomena, J. B. Bidwell, ed., Elsevier Publ. Co., Inc., 1962, pp. 132-156.

10. Magi, Mart: On Efficiencies of Mechanical Coplanar Shaft Power Transmissions. Chalmers University of Technology, Gothenburg, 1974.

11. Tevaarwerk, J. L.: The Shear of Elastohydrodynamic Oil Films. Ph. D. Dissertation, Univ. of Cambridge, 1976.

12. Johnson, K. L.: The Effect of Spin Upon the Rolling Motion of an Elastic Sphere on a Plane. J. Appl. Mech., vol. 25, no. 3, Sep. 1958, pp. 332-338.

13. Kalker, J. J.: On the Rolling Contact of Two Elastic Bodies in the Presence of Dry Friction. Ph. D. Dissertation, Technische Hogeschool, Delft, 1967.

14. Johnson, K. L.; and Roberts, A. D.: Observations of Viscoelastic Behavior of an Elastohydrodynamic Lubricant Film. Proc. Roy. Soc. (London), Series A, vol. 337, no. 1609, Mar. 19, 1974, pp. 217-242.

15. Johnson, K. L.; Nayak, L.; and Moore, A. J.: Determination of Elastic Shear Modulus of Lubricants from Disc Machine Tests. Presented at the 5th Leeds-Lyon Symposium on Tribology: "Elastohydrodynamics and Related Topics," (Leeds, England), Sep. 19-22, 1978, Paper 21.

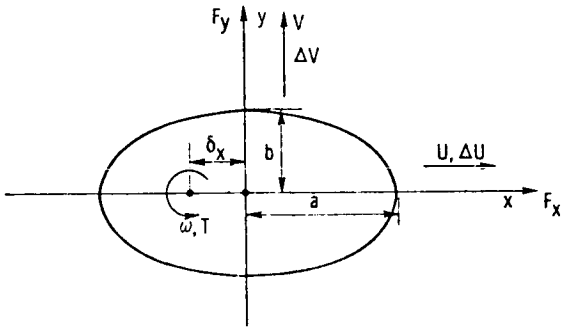

Figure 1. - Plan view of typical EHL contact indicating major variables; x is rolling direction. (The semimajor and minor axis are calculated from Hertzian theory.)

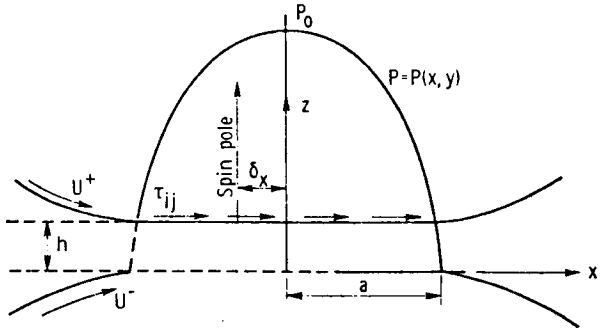

Figure 2. - Sideview of typical EHL contact with constant separation between two contacting bodies. Pressure distribution in contact area is assumed to be Hertzian.

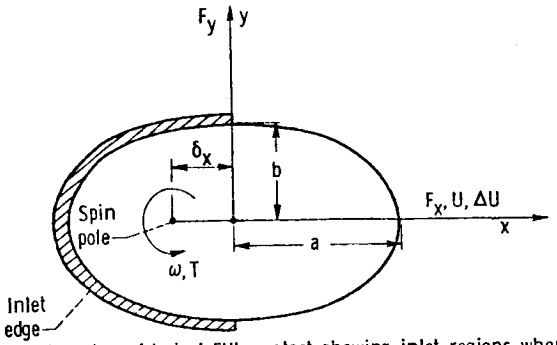

(a) Plan view of typical EHL contact showing inlet regions where shear stresses are assumed to be zero.

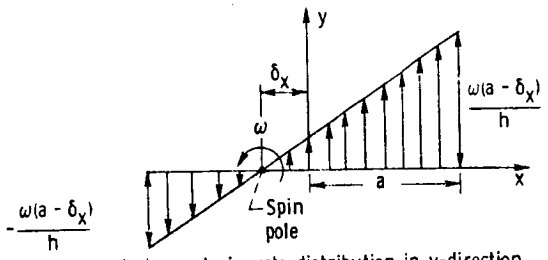

(b) Assumed shear strain rate distribution in y-direction along x-axis to spin and spin pole offset.

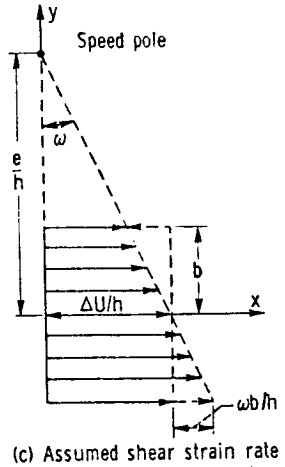

(c) Assumed shear strain rate distribution along y-axis in rolling direction due to spin and slip. Note location of speed pole $e \cong \Delta U/\omega$.

Figure 3. - Plan view of typical EHL contact with its associated center line strain rate distribution due to slip, spin, and spin pole offset.

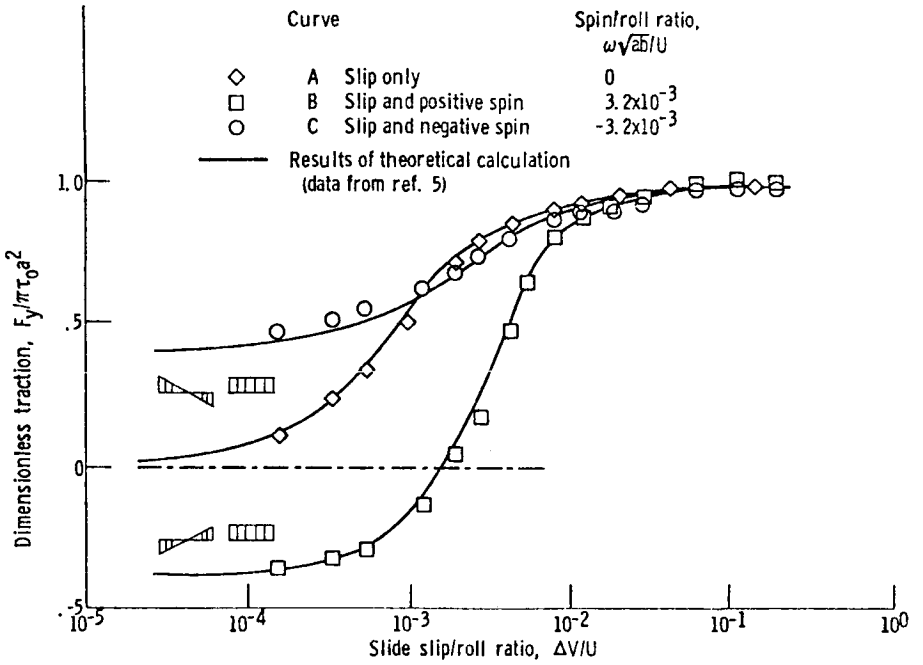

Figure 4. - Tests on hydratorque medium fluid in combined side slip and spin. Velocity in x-direction U = 1.9 meters per second; maximum Hertzian pressure in contact P_0 = 1.3 gigapascals; inlet temperature, 17° C. Elastic-plastic theory fitted to experimental results.

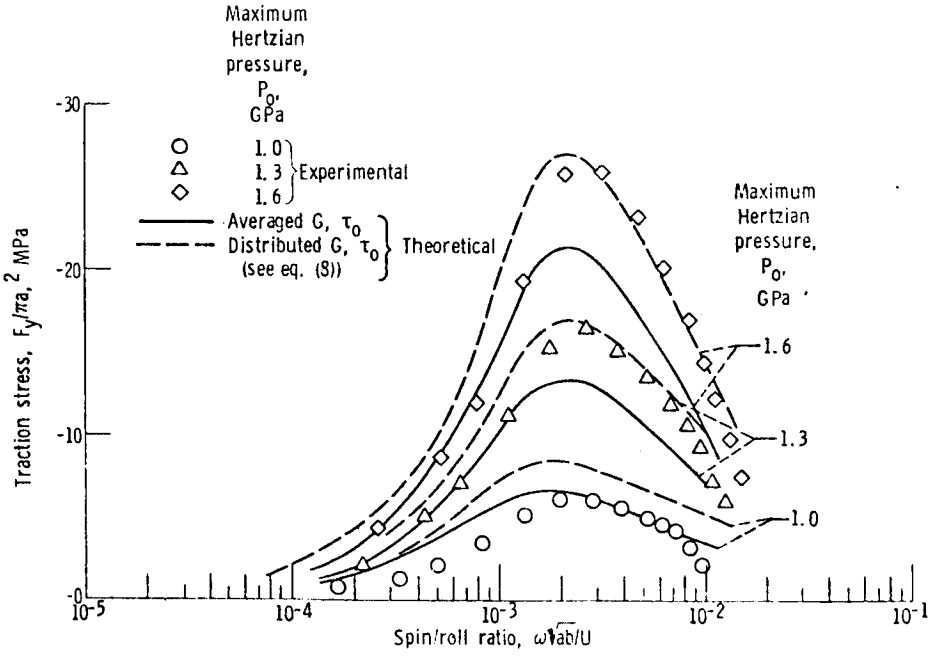

Figure 5. - Influence of average and pressure dependent shear properties G and τ_0 on spin fraction prediction (data from ref. 5). Fluid, Turbo 33; velocity in x-direction U = 1.2 meters per second; inlet temperature, 30° C.

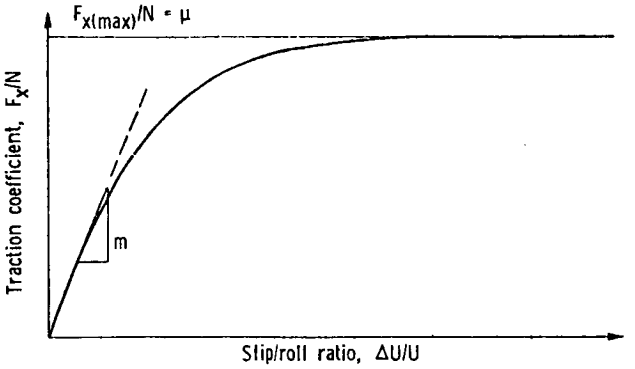

Figure 6. - Typical traction curve showing maximum traction coefficient μ and traction slope m.

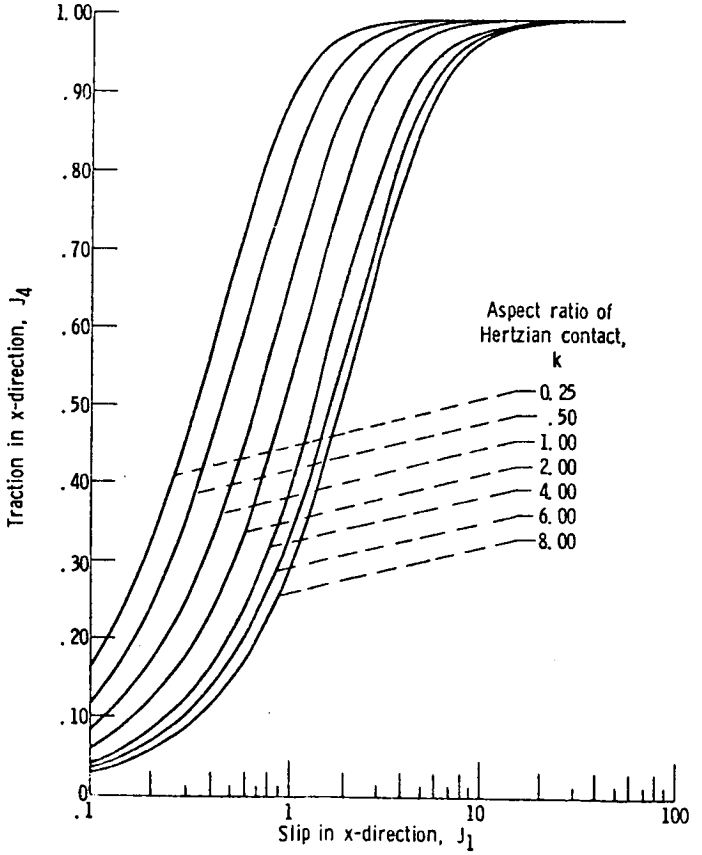

Figure 7. - Traction J_4 versus slip J_1 for various aspect ratios. Elastic-plastic theory is used. Dimensionless spin $J_3 = 0$; dimensionless spin pole offset $\Delta x = 0$.

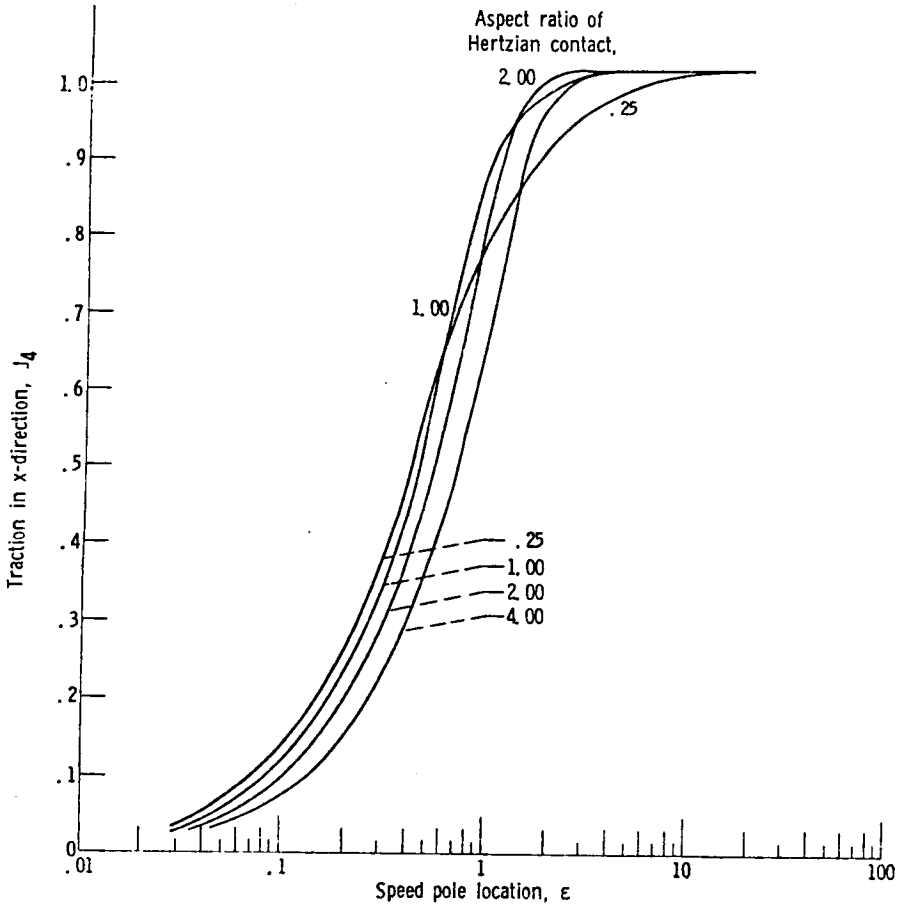

Figure 8. - Traction J_4 versus speed pole location for various aspect ratios. Rigid perfect plastic theory is used. Dimensionless spin pole offset $\Delta x = 0$.

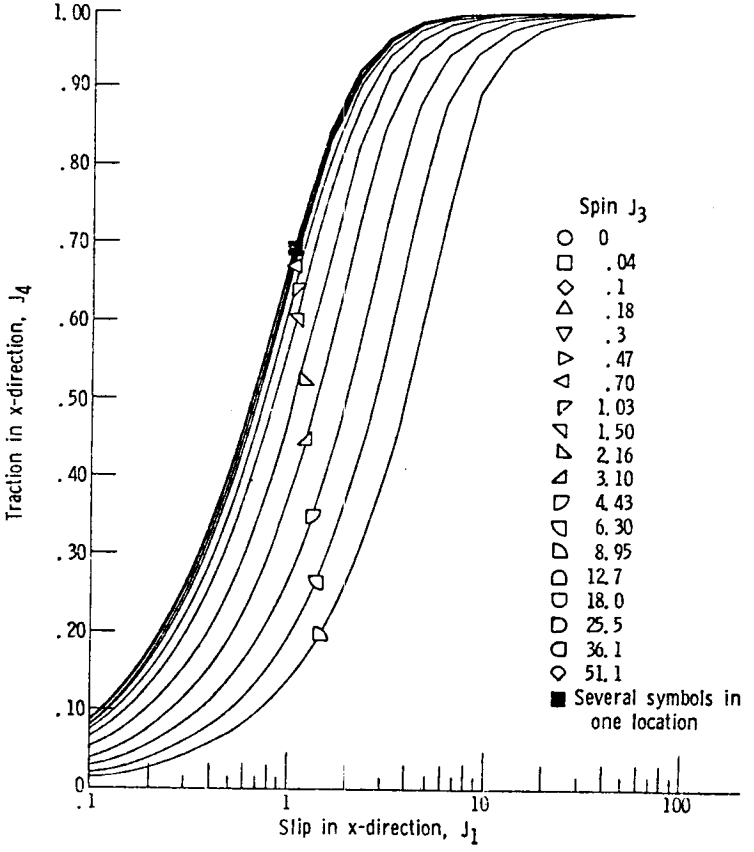

(a) Aspect ratio of Hertzian contact $k = 1.00$.

Figure 9. - Traction J_4 versus slip J_1 at various spin J_3 values.

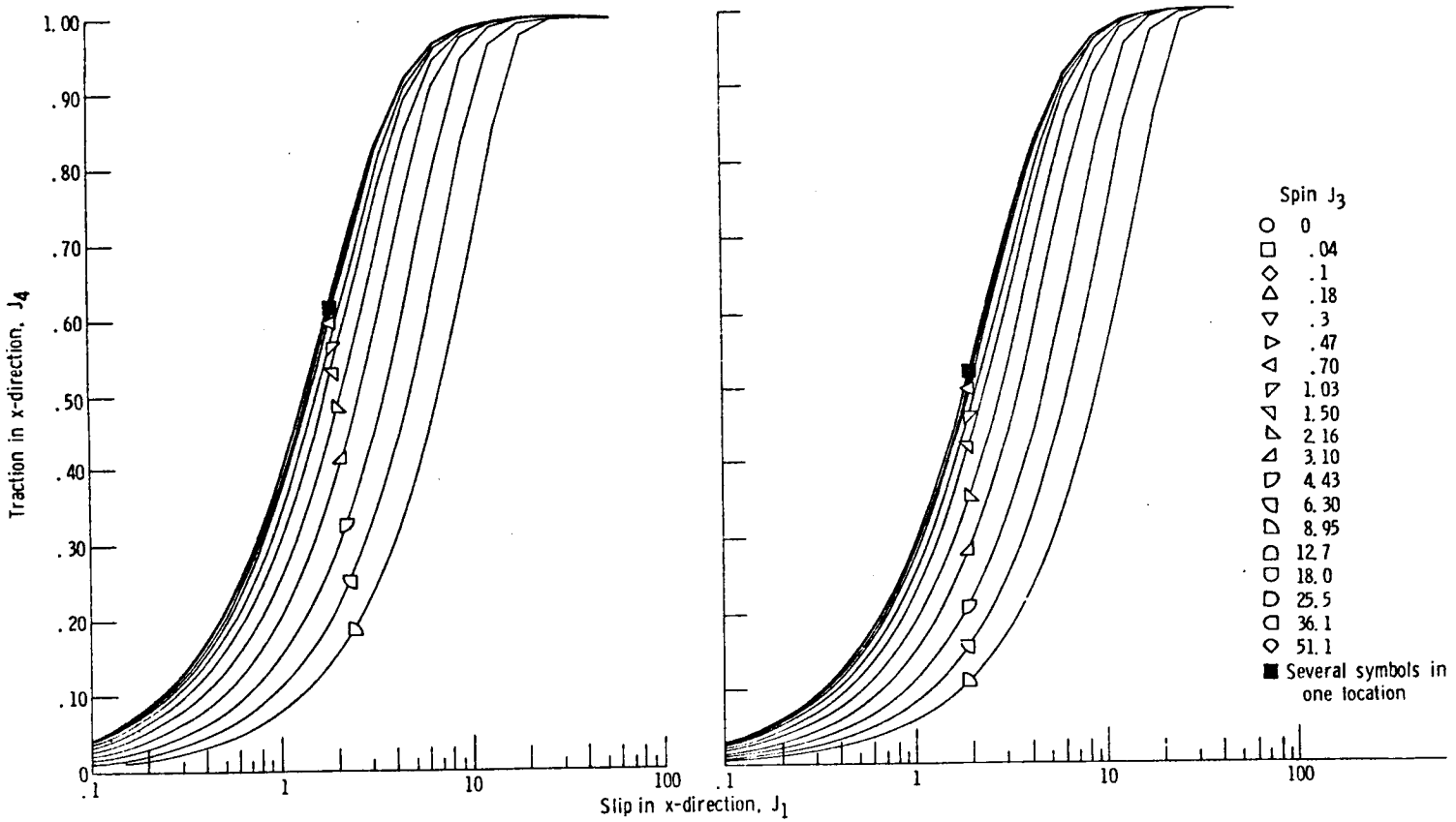

(b) Aspect ratio of Hertzian contact k = 4.00.

(c) Aspect ratio of Hertzian contact k = 8.00.

Figure 9. - Concluded.

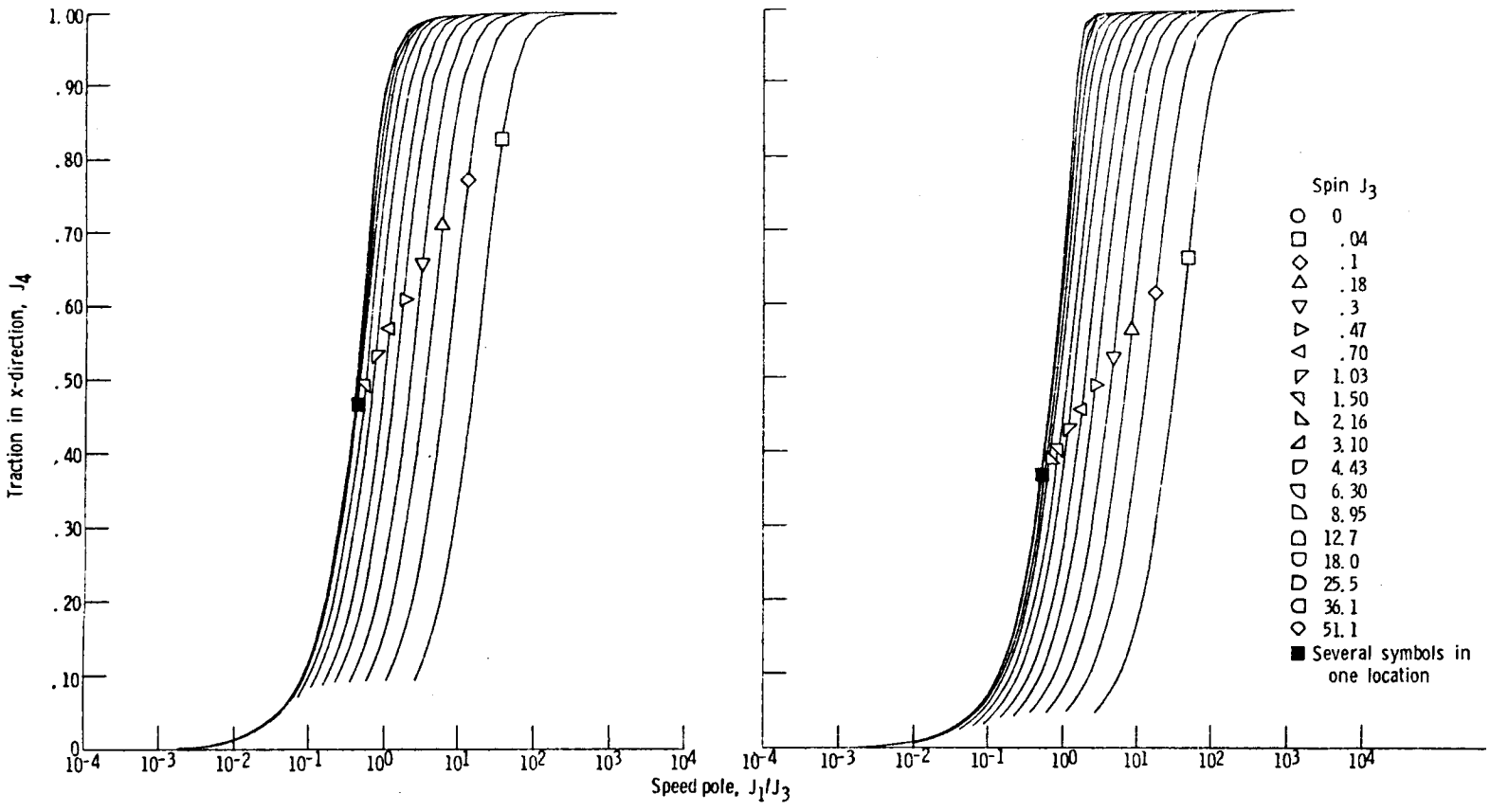

(a) Aspect ratio of Hertzian contact k = 1.00.

(b) Aspect ratio of Hertzian contact k = 4.00.

Figure 10. - Traction J_4 versus speed pole location ε, (J_1/J_3) at various spin values.

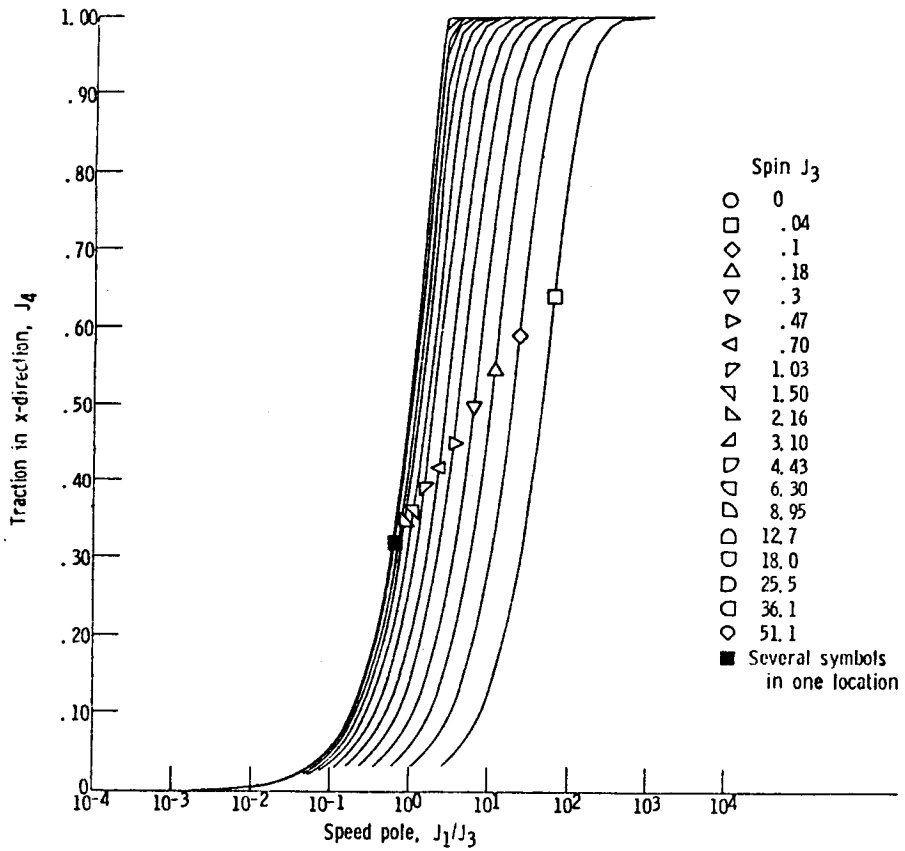

(c) Aspect ratio of Hertzian contact k = 8.00.

Figure 10. - Concluded.

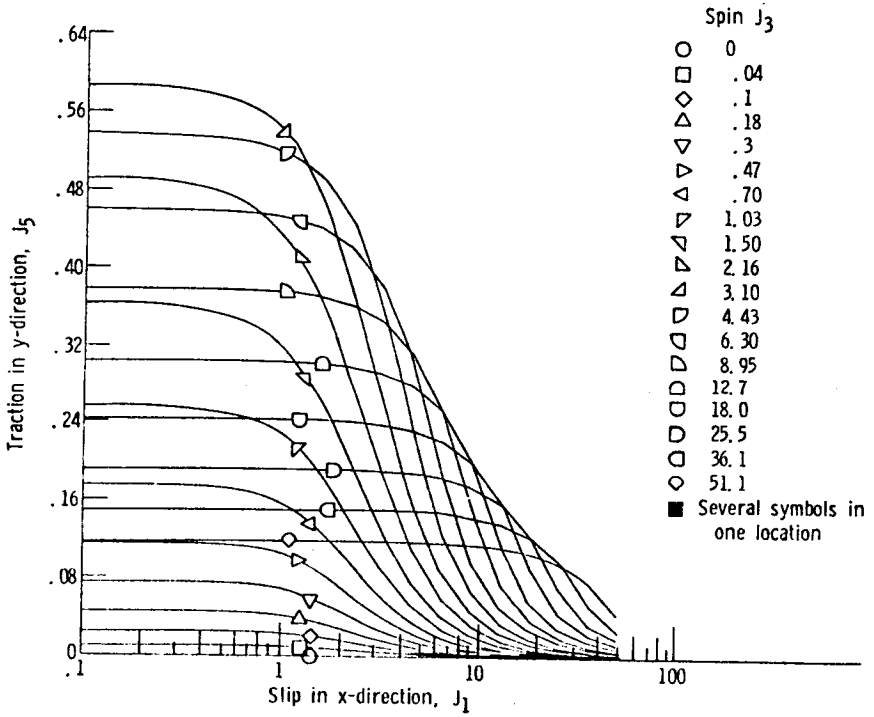

Figure 11. - Traction J_5 versus slip J_1 at various values of spin J_3. Aspect ratio of Hertzian contact k = 1.00.

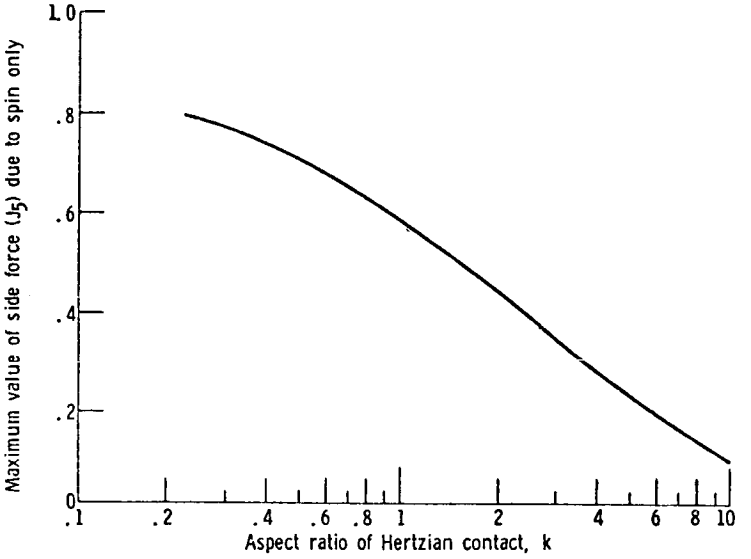

Figure 12. - Variation of maximum side force (J_5) with aspect ratio for contact under spin only.

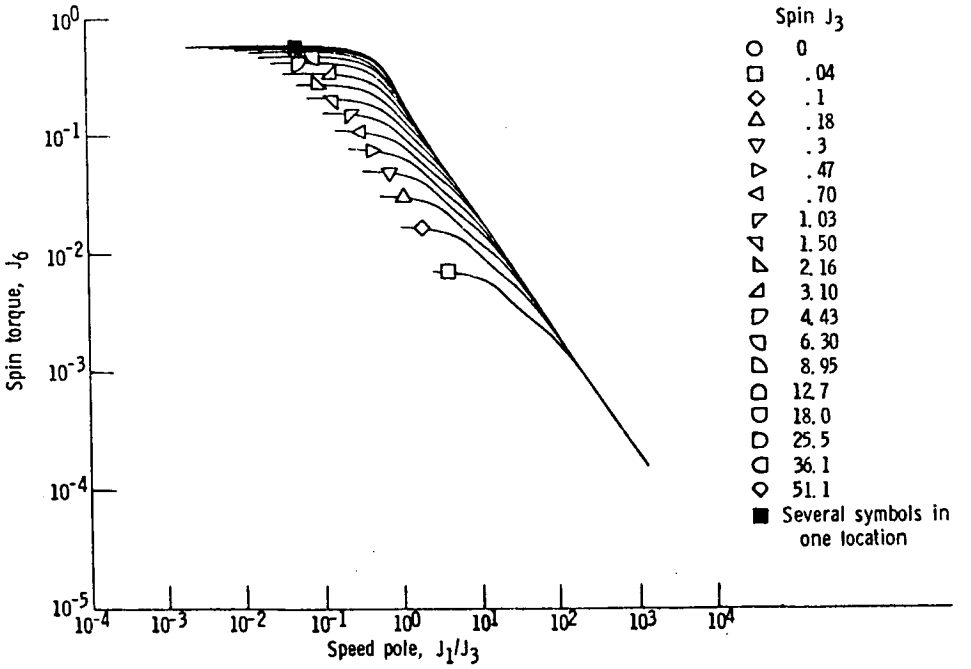

(a) Aspect ratio of Hertzian contact k = 1.00

Figure 13. - Dimensionless spin torque J_6 versus the speed pole location J_1/J_3 at various spin J_3 values.

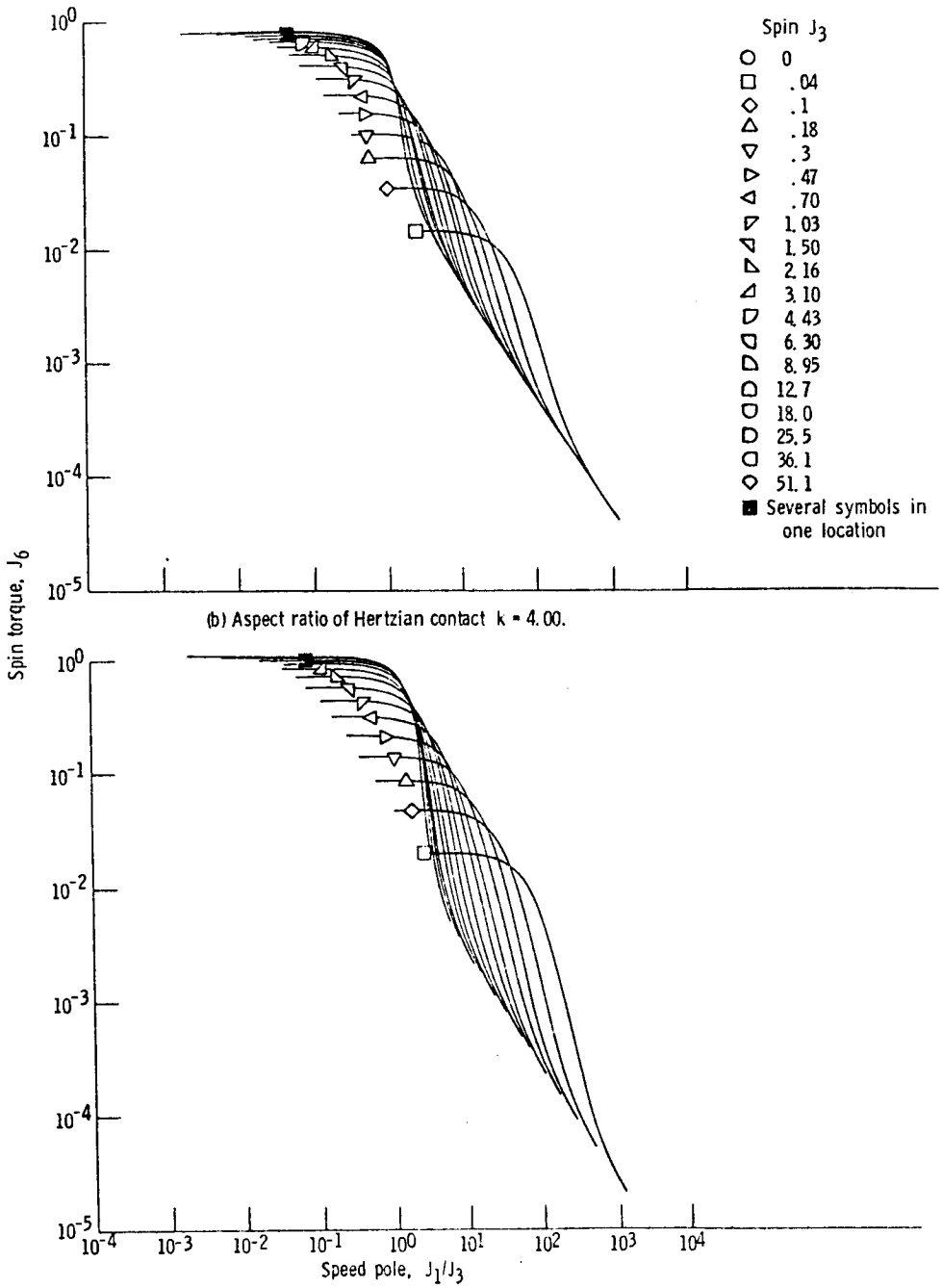

(b) Aspect ratio of Hertzian contact k = 4.00.

(c) Aspect ratio of Hertzian contact k = 8.00.

Figure 13. - Concluded.

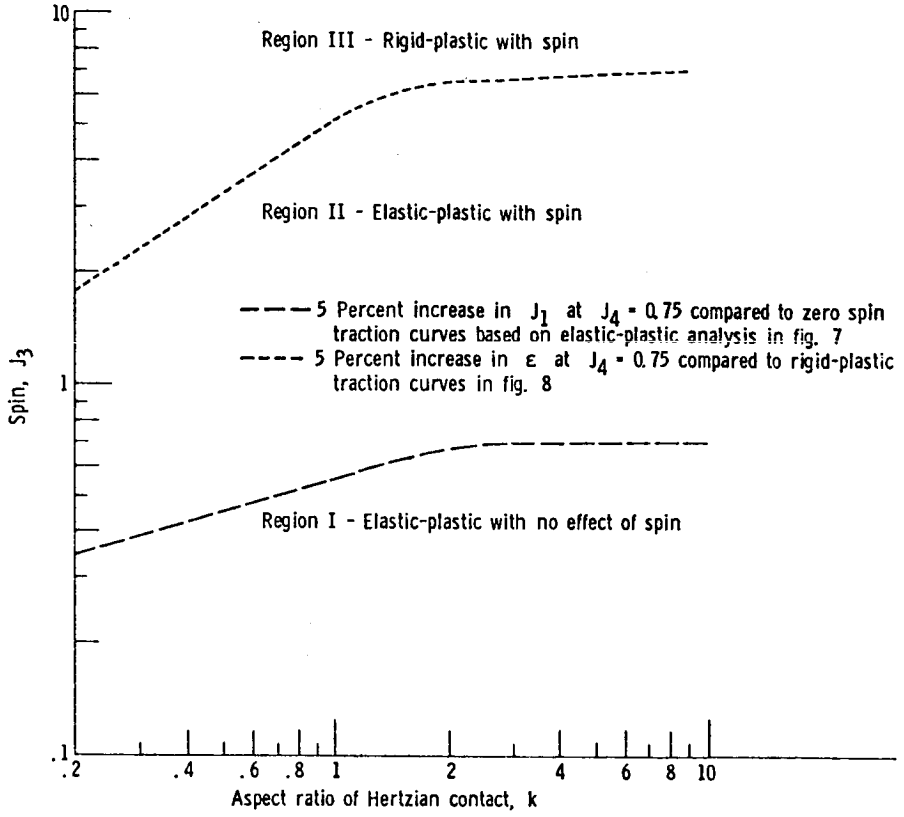

Figure 14. - Regions of influence of elastic and spin effects on slip J_1 at constant traction value J_4 = 0.75.

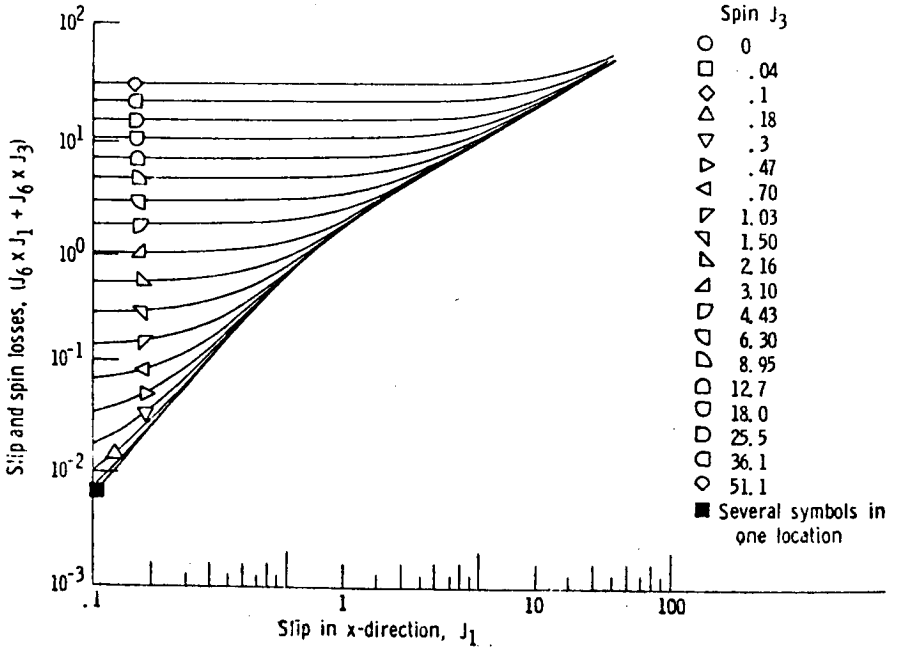

Figure 15. - Variation of $J_7 = (J_4 \times J_1 + J_6 \times J_3)$ with slip J_1 for aspect ratio of Hertzian contact k = 1.00.

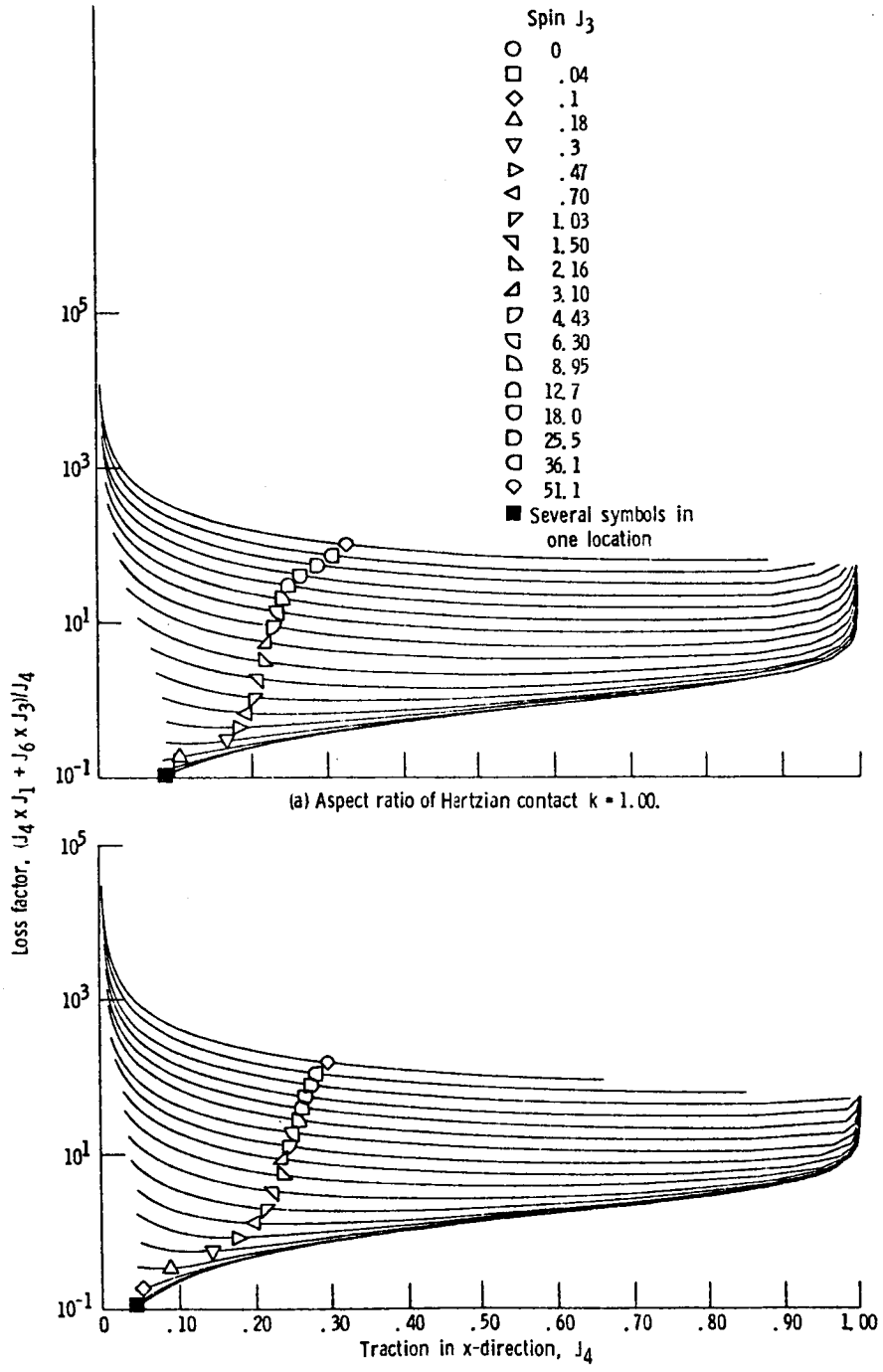

(a) Aspect ratio of Hertzian contact k = 1.00.

(b) Aspect ratio of Hertzian contact k = 4.00.

Figure 16. - Loss factor as function of traction J_4 at various spin J_3 values.

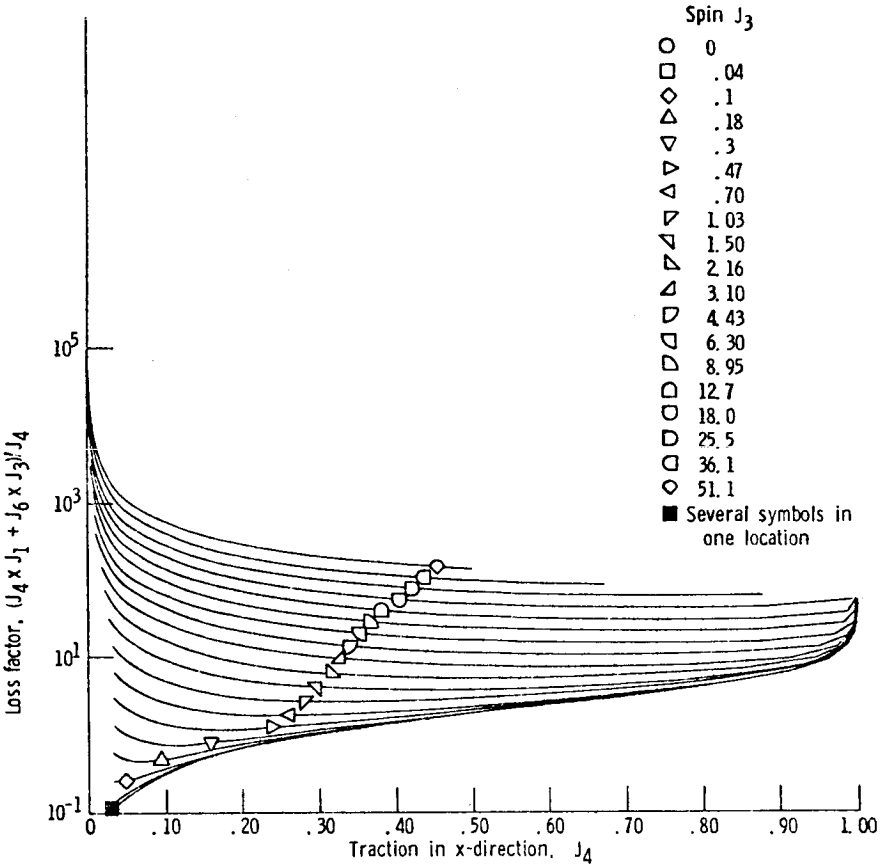

(c) Aspect ratio of Hertzian contact k = 8.00.

Figure 16. - Concluded.

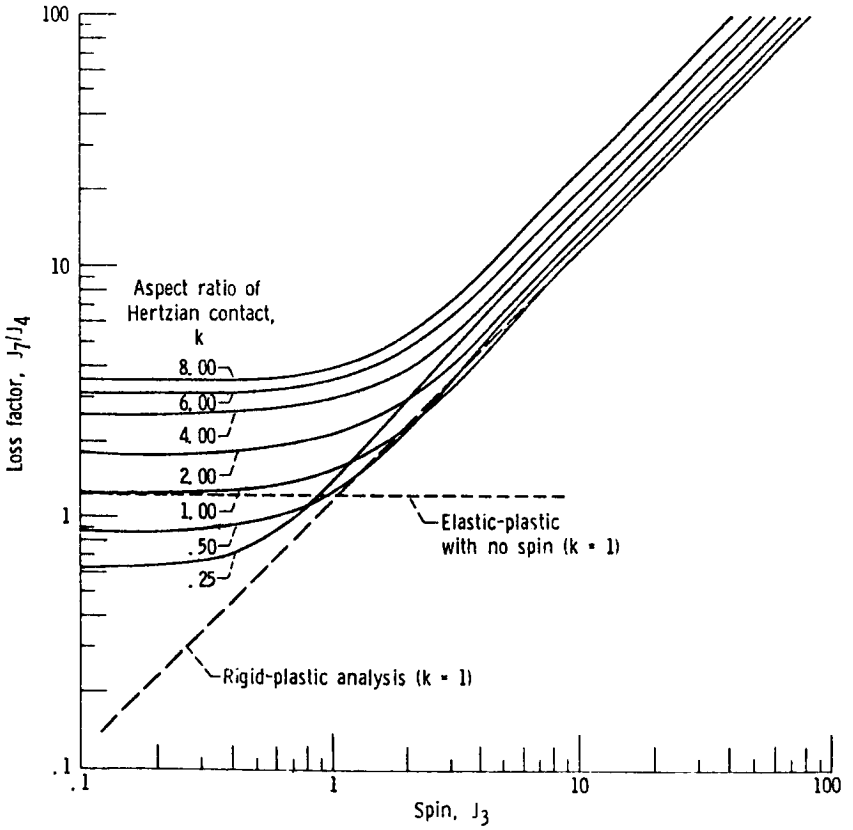

Figure 17. - Loss factor as a function of J_3 spin at various aspect ratios for J_4 = 0.75.

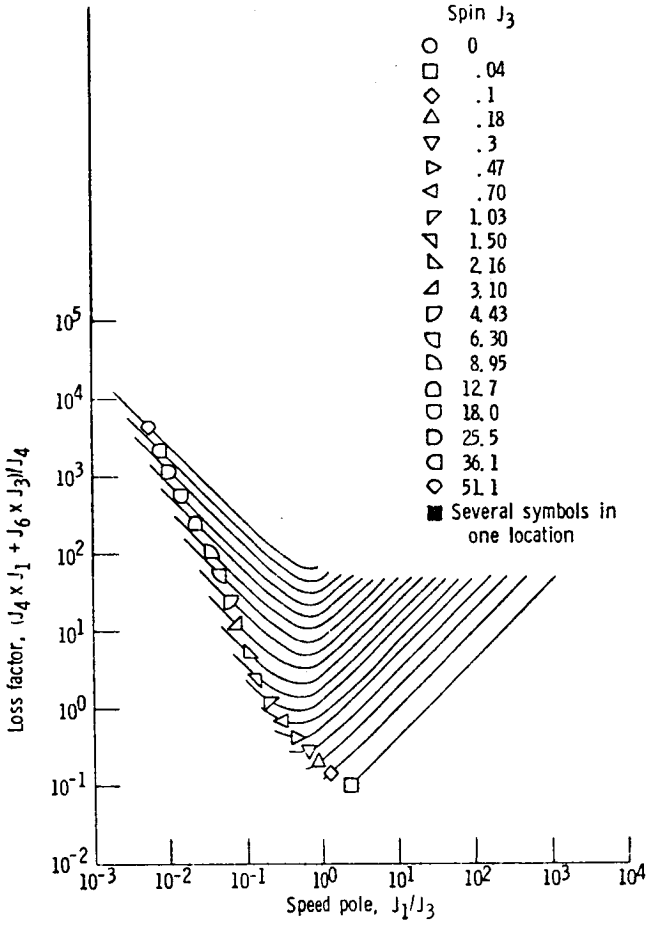

Figure 18. - Loss factor as function of ε speed pole location for at various values of spin J_3 for aspect ratio of Hertzian contact k = 1.00.

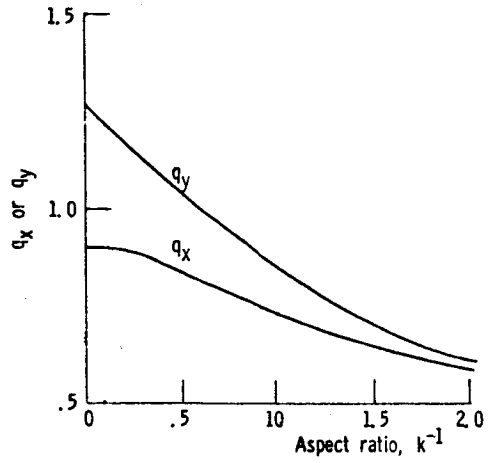

Figure 19. - Kalker coefficients q_x, q_y as function of aspect ratio k.

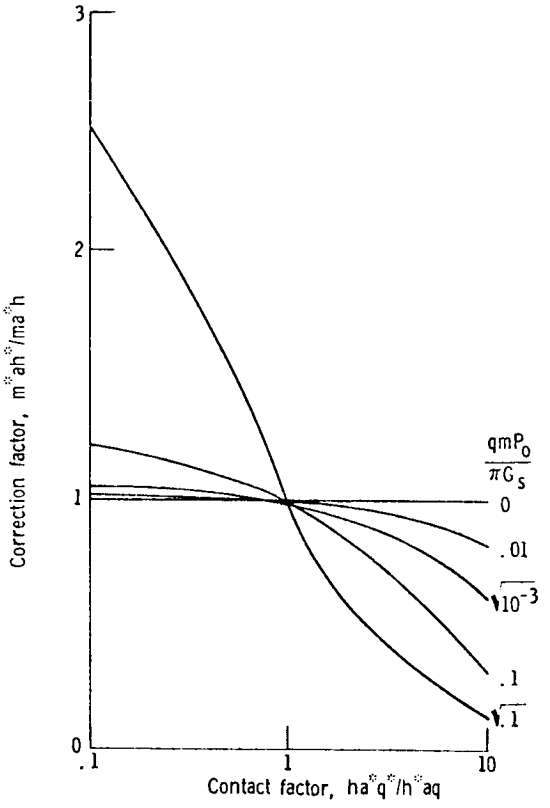

Figure 20. - Correction factors to convert slope m to m'.

APPENDIX V

The influence of fluid Rheology on the performance of Traction Drives

ASME Paper 78 Lub 10

J. L. Tevaarwerk
University of Waterloo,
Waterloo, Ontario, Canada

K. L. Johnson
Cambridge University
Engineering Laboratory, Cambridge, England

The Influence of Fluid Rheology on the Performance of Traction Drives

The performance of traction drives depends to a large extent on the rheological properties of the fluid in the EHL contact. Through the use of the recently proposed J + T constitutive equation, the influence of elastic effects in the fluids is examined. The results were compared with those obtained from conventional analysis. It is shown that essentially three regions of influence exist. For small values of spin and side slip the elastic effects in the fluid dominate and no consideration of the spin and side slip is required. At higher values of spin and side slip the elastic effect still exists but slip is influenced by the spin and slide slip. At still higher values of side slip and spin, the elastic effects in the fluid may be neglected. The various boundaries of the regions of influence depend on the aspect ratio of the contact.

1 Introduction

Continuously variable traction drives employing metal surfaces in rolling line or point contact require a lubricating fluid for satisfactory operation. Traction is transmitted between the rolling surfaces through an EHD fluid film. The performance of the drive therefore depends to a large extent on the rheological properties of the fluid in the EHD contact.

Conventional analysis ignores the rheology of the film and assumes that traction is related to slip in the "contact" area by the Coulomb law of friction where the local shear stress is proportional to the local pressure and acts in the direction opposite to the local slip. See for example Wernitz [1] and more recently Magi [2]. However, recent research into the shear behavior of EHD lubricant films makes it possible to examine the role of the fluid rheology in a rolling contact drive in a more fundamental way and perhaps shed some light on the fluid parameters which control the performance.

2 Rheology of Lubricants

Typically the contact area in a traction drive is an ellipse of about 1 mm^2. The fluid passes through the zone in about 1 msec during which it is subjected simultaneously to a pressure pulse of order 1.0 GPa and to a shear pulse arising from relative velocities between the two "contact" surfaces of the rolling elements. The way in which the fluid responds to these severe and highly transient conditions is not fully understood, but a fairly coherent picture is now emerging. The viscosity of lubricating fluids increases approximately exponentially with pressure so that in the contact of a traction drive the viscosity of the fluid is increased by many orders of magnitude. At these high viscosities the fluid responds to the transient shear in the manner of a viscoelastic solid. The shear modulus G of such materials is of order 1.0 GPa. The relaxation time of a viscoelastic material is given by the ratio of the viscosity to the shear modulus. When the viscosity exceeds 1.0 MPas the relaxation time exceeds the mean time of passage of fluid through the contact. At these conditions the lubricant behaves in a solid like manner. Some doubt has been expressed whether the viscosity reaches its equilibrium value given by the exponential relationship in the short times for which the pressure is applied, see for example Fein [3] and more recently Harrison and Trachman [4]. No doubt there is some compressional delay in the contact but whether the actual viscosity is one or two orders below that predicted from the Barus equations does not matter, provided it is well above that required for elastic like behavior. There is substantial evidence by Johnson and Roberts [5], Hirst and Moore [6], and Johnson and Tevaarwerk [7] that the pressures and short transit times in an EHL contact are sufficient to bring about the viscoelastic response from the fluid in the contact region.

A further feature of the fluid behavior is all important: at sufficiently high shear stresses there is a marked nonlinear decrease in shear stress with shear rate. The onset of nonlinearity in highly loaded contacts led Clark, et al. [8] and later Smith [9] to speculate whether the fluid was yielding like a plastic solid.

The simplest constitutive equation for a fluid film in simple shear which includes both viscoelasticity and nonlinear stress strain behavior is obtained by adding a nonlinear viscoes element to a linear elastic element as suggested by Johnson and Tevaarwerk [7] viz,

$$\dot{\gamma}\text{elastic} + \dot{\gamma}\text{viscous} = \dot{\gamma}\,\text{total}$$

$$\frac{1}{G}\frac{d\tau}{dt} + F(\tau) = \dot{\gamma} \tag{1}$$

where

G = elastic shear modulus

τ = shear stress

$F(\tau)$ = relationship between viscous shear rate and shear stress.

Contributed by the Lubrication Division and presented at the ASME-ASLE Joint Lubrication Conference, Minneapolis, Minn., October 24–26, 1978, of THE AMERICAN SOCIETY OF MECHANICAL ENGINEERS. Manuscript received by the Lubrication Division, March 8, 1978, revised manuscript received June 8, 1978. Paper No. 78-Lub-10.

the elastic/plastic J+T model may be used with parameters derived by the new methods of Bair and Winer. This now provides a real tool to the Traction Drive designer because a closed form solution of the elastic/plastic J+T model for the traction is known for all aspect ratios (see for example Tevaarwerk 1976, Tevaarwerk 1978, and Paper 78-Lub-10 at the 1978 Lubrication Conference).

The remaining problem is now one of explaining what causes the difference between EHL shear moduli and limiting strength and those observed by the authors. For example for the best fit of the J+T elastic/plastic model (see the authors' Fig. 14) $J+T$ obtain $\bar{G} \cong .10$ GPa; $\bar{\tau}_L \cong .80$ GPa while at the same conditions the above authors obtain $\bar{G} \cong .15$ GPa; $\bar{\tau}_L \cong 0.092$ GPa. Some of the differences may in fact be due to compressional heating effects, as hinted at in the paper, and also compliance enters into the picture. The other problem may be one of time delay effects.

Additional References

22 Johnson, K. K., and Tevaarwerk, J. L., *Proc. R. Soc. London*, Series A 356, 1977, pp. 215–236.
23 Tevaarwerk, J. L., PhD dissertation, Cambridge, 1976.
24 Tevaarwerk, J. L., *Proceedings of I.C.F.T.*, M.I.T. press, Dec. 1978.

C. W. Allen[3]

The authors have extended their previous work on traction in the elastohydrodynamic region in an attempt to relate the traction coefficient to primary fluid data.

In reviewing the paper, however, it appears that the primary measurements are not easily obtained but require the apparatus and procedures outlined in the companion paper, ASME Paper No. 78-Lub-8. In many cases the traction data may be more easily obtained directly than by first measuring the primary data.

The equivalent viscosity versus pressure curve (Fig. 8) is somewhat similar in form to that presented by the discusser and his colleagues in reference [25]. In our model, however, the secondary part of the curve continues to increase with pressure. The authors show this secondary portion of the curve as being almost flat. Using the authors' Fig. 8 would probably result in a traction coefficient which would decrease with pressure at high pressures. This does not agree with much of the published data, for example, that given by Trachman and Cheng (reference [26]).

It would have been helpful if the authors would have published comparisons of their model with some of the experimental results mentioned in references [1, 13, 16, 17, 18, and 19]. The one comparison that is given (Fig. 14) shows fair agreement throughout the range of experimental values, but the experimental values continue to increase at the high slide/roll ratios whereas the authors' isothermal values remain constant above a slide/roll ratio of 5×10^{-3}. Presumably at the higher slide roll ratios, the heat generation would increase and result in higher temperature, therefore the authors' values corrected for temperature would appear to actually decrease.

It is hoped that the authors will extend this work, particularly in the area of obtaining primary data for a large number of lubricants and hence use these data to compare their model with the many traction experiments already published.

Additional References

25 Allen, C. W., Townsend, D. P., and Zaretsky, E. V., "New Generalized Rheological Model for Lubrication of a Ball Spinning in a Nonconforming Groove," NASA, TN D-7280, 1973.
26 Trachman, E. G., and Cheng, H. S., "The Rheological Effects on Friction in Elastohydrodynamic Lubrication," NASA, CR 2206, Mar. 1973.

[3] California State University, Chico, Calif. 95929.

Authors' Closure

The authors appreciate the discussions of Professors Tevaarwerk and Allen and believe that they contribute to the content of the paper.

We believe the difference in the G_∞ values between those measured in EHD experiments such as Tevaarwerk's and, on the other hand, those measured ultrasonically or by our techniques is mainly due to the extreme difficulty in evaluating and interpreting the results from the EHD experiments. It is well known that very small alignment difficulties, knowledge of film thickness, careful traction and speed measurements and adequate accounting for disk elastic compliance all contribute to the difficulty of inferring shear moduli from EHD measurements. I think these experimental difficulties are at the root of the difference in shear modulus values reported.

With respect to Professor Allen's comments, we have performed both traction and limiting shear stress measurements and have found the limiting shear stress to be much easier to determine. The measurement of primary material properties is not only desirable from the point of view of being able to generalize results, but also from the fact that very small samples are required. We believe that Professor Allen may have misinterpreted Figure 8. The ordinate is a log scale, and the effective viscosity nearly proportional to pressure for a given shear rate. Because of the log scale of the ordinate the small variation of effective viscosity with pressure is difficult to see. Since the presentation we have measured the limiting shear stress for three of the Johnson and Tevaarwerk fluids on samples received from them.

These measurements have indicated that the predicted maximum traction value is closer than that shown in this paper and no illusion to temperature is necessary. The limiting shear stress measurements on these fluids also very correctly ranks the fluids with respect to maximum traction coefficient.

Equation (1) is for simple unidirectional shear and a more general form in tensor form was presented by Johnson and Tevaarwerk [7] as

$$\frac{1}{G}\frac{d\tau_{ij}}{dt} + \frac{\tau_{ij}}{\tau_e}F(\tau_e) = \dot{\gamma}ij \tag{2}$$

where

$$\tau_e = \sqrt{1/2\,(\tau_{ij}\cdot\tau_{ij})}$$

The term τ_{ij}/τ_e is the application of the normality rule from plasticity theory for the partitioning of the resulting viscous shear strain in the ij directions. The viscous function $F(\tau_e)$ can be any function which is consistent with experiment but Johnson and Tevaarwerk [7] have found that a good fit with a wide range of lubricating fluids was obtained with

$$F(\tau_e) = \frac{\tau_0}{\eta}\sinh\,(\tau_e/\tau_0) \tag{3}$$

where

η is the viscosity at small shear stress

τ_0 is a representative stress at which nonlinear behavior becomes significant.

Equations (2) and (3) may now be combined to give an equation for the shear behavior of a fluid in an EHL contact. For a contact subjected to a simple linear velocity difference in the rolling direction (slip) the shear strain is given by

$$\dot{\gamma}_x = \frac{\Delta U}{h} \tag{4}$$

where h is the film thickness separating the two surfaces. A suitable measure of time in such a contact is given by

$$t = \frac{Xa}{U} \tag{5}$$

a = contact dimension in rolling direction

U = rolling velocity

$X = x/a$ nondimensional coordinate in the rolling direction.

Combining this information gives the following equation for simple slip

$$\frac{d\tau_{x/\tau_0}}{dX} + \frac{Ga}{\eta U}\sinh\,(\tau_{x/\tau_0}) = \frac{G}{\tau_0}\frac{\Delta U}{h}\frac{a}{U} \tag{6}$$

This equation can be solved for the shear stress τ_x and this in turn may be integrated over the contact area to give the resulting traction as a function of the applied shear rate and a simple nondimensional parameter $\eta U/Ga$ known as the Deborah number D. The Deborah number is the ratio of the relaxation time of the fluid η/G to the mean transit time of the fluid through the contact a/U. Nondimensional traction curves for a number of Deborah numbers are shown in Fig. 1 taken from Tevaarwerk [10]. These curves were obtained for an aspect ratio $k = b/a = 1$ and under the assumption that the fluid properties η, G, and τ_0 were constant over the contact area.

There are several regions on this dimensionless traction chart that deserve attention. For low Deborah numbers the elastic effects in the fluid are negligible and the traction curve follows the viscous sinh law. First at low slip there is a linear newtonian increase in traction with slip giving way to more and more nonlinear behavior at higher values of slip.

For medium to large Deborah numbers the traction curves have a common linear elastic region in the small slip region giving way to the nonlinear viscous response according to the sinh law.

For large Deborah numbers the small slip behavior is still linear elastic but the nonlinear traction becomes less and less dependent upon the slip in an elastic-pastic like manner. Experimental evidence in support of this model for the fluid behavior under EHL conditions is included in Fig. 1.

3 Simplification in the Rheological Model for Purposes of Traction Drive Analysis

One of the selection criteria for a traction drive designers is the maximum obtainable traction coefficient for a given fluid. High values

Nomenclature

a,b = Hertzian contact dimensions (a is in the x direction), m

A = Hertzian contact area (πab), m^2

D = Deborah number ($\eta U/Ga$)

E = composite elastic modulus of the contact system, N·m^{-2}

F = dissipative strain rate function, s^{-1}

Fx, Fy = traction force in the x and y direction, N

G = local elastic shear modulus of the fluid, N·m^{-2}

$\bar{G}$ = average elastic shear modulus of the fluid over the contact area, N·m^{-2}

g_1', g_2' = Johnson viscosity and elasticity parameters

h = mean separation of the contact planes, m

J_1 = dimensionless longitudinal slip ($\bar{G}\sqrt{ab}\cdot\Delta U/\bar{\tau}_c h\cdot U$)

J_2 = dimensionless side slip ($\bar{G}\sqrt{ab}\cdot\Delta V/\bar{\tau}_c h\cdot U$)

J_3 = dimensionless spin on the contact ($\bar{G}\cdot ab\omega/\bar{\tau}_c h\cdot U$)

J_4 = dimensionless traction in x direction ($F_x/\pi ab\bar{\tau}_c$)

J_5 = dimensionless traction in y direction ($F_y/\pi ab\bar{\tau}_c$)

J_6 = dimensionless torque on the contact ($T/\pi ab\bar{\tau}_c\sqrt{ab}$)

J_7 = dimensionless losses ($J_1\times J_4 + J_2\times J_5 + J_3\times J_6$) ($\bar{G}\cdot[F_x\cdot\Delta U + F_y\cdot\Delta V + T\cdot\omega]/\bar{\tau}_c{}^2\sqrt{ab}\cdot hU$)

k = aspect ratio (b/a)

LF = loss factor ($J_7/J_4 = \bar{G}\sqrt{ab}\cdot[\Delta U\cdot F_x + \omega\cdot T + F_y\cdot\Delta V]/h\bar{\tau}_c\cdot UF_x$)

m = initial slope of the experimental traction curves

N = normal load on the contact, N

R = effective radius of the roller system, m

S = dimensionless slip parameter

t = time, s

T = spin torque on the contact, N·m

T_r = rolling torque, N·m

U^+, U^- = velocity in the x direction on the upper(+) and lower(−) body, m·s^{-2}

ΔU = velocity difference in x direction ($U^+ - U^-$), m·s^{-2}

U = rolling velocity, m·s^{-2}

V^+, V^- = velocity in the y direction, m·s^{-2}

ΔV = velocity difference in y direction ($V^+ - V^-$), m·s^{-2}

x, y, z = Cartesian coordinates, m

X, Y, Z = dimensionless Cartesian coordinates

$\dot{\gamma}$ = local shear strain rate, s^{-1}

$\dot{\gamma}_{ij}$ = local shear strain rate tensor, s^{-1}

$\dot{\gamma}_x, \dot{\gamma}_y$ = local shear strain rate in the x and y direction, s^{-1}

$\dot{\gamma}_e$ = local equivalent shear strain rate ($\sqrt{\dot{\gamma}_{ij}\cdot\dot{\gamma}_{ij}/2}$), s^{-1}

ϵ = speedpole location ($\epsilon = J_1/J_3 = \Delta U/\omega\sqrt{ab}$)

η = local fluid viscosity, N·sm^{-2}

τ = local shear stress, N·m^{-2}

τ_{ij} = local shear stress tensor, N·m^{-2}

τ_e = local equivalent shear stress, ($\sqrt{\tau_{ij}\cdot\tau_{ij}/2}$), N·m^{-2}

τ_0 = local representative shear stress, N·m^{-2}

τ_c = local critical plastic shear stress, N·m^{-2}

$\bar{\tau}_c$ = average critical plastic shear stress over the contact, N·m^{-2}

τ_x, τ_y = local shear stress in the x and y direction, N·m^{-2}

ϕ, ψ = dimensionless traction function

Terminology

speedpole = location where the EHL contact is in pure rolling

spinpole = point about which the spin takes place

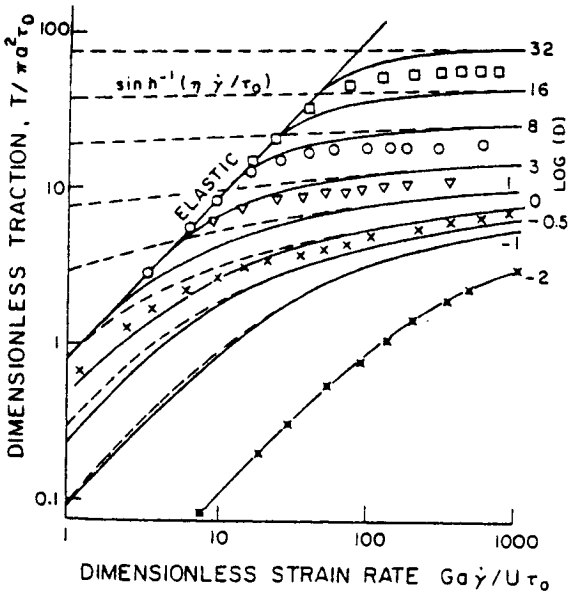

Fig. 1 Theoretical nondimensional traction curves for varying Deborah numbers $D(=\eta U/Ga)$. Experimental results at $\bar{P}$ = .67 GPa and θ = 35 C □, 5P4E; ○, LVI 260; ▽, Vit 79; X, Turbo 33; and ⊗, Turbo 33 at .47 GPa. Figure taken from Johnson and Tevaarwerk [7].

of the traction coefficient mean that lower contact stresses can be used or a reduced physical size of the traction drive for a given output. When typical traction curves are examined, it is found that those fluids which have high traction coefficients also have a rather low shear rate dependence in the nonlinear region. This suggests that an elastic/plastic type model may be sufficient for an overall analysis of traction drive performance.

The nonlinear function $F(\tau e)$ in equation (2) may be selected such that this equation represents elastic/plastic behavior of the fluid film. It should have the following form.

$$F(\tau_e) = 0 \quad \text{for} \quad \tau_e < \tau_c$$

$$F(\tau_e) = (\tau_{ij} \cdot \dot{\gamma}_{ij})/\tau_c \quad \text{for} \quad \tau_e = \tau_c \tag{7}$$

Where τ_c now is the limiting shear strength of the fluid. When equation (2) is used with equation (7) it becomes the well known Prandtl-Reuss equation for elastic/perfectly plastic flow as used in plasticity theory. This relationship was used by Tevaarwerk [10] to correctly predict the traction behavior of a circular contact under combined slip and spin. A similar type of model was used by Lingard [11], and more recently by Gaggermeier [12], however their model uses a viscous element instead of an elastic element. This is counter to the notion here that plastic like behavior only takes place at high Deborah numbers i.e. when the small strain results are *elastic*, not *viscous*.

A further simplification in the suggested constitutive equation is possible when the elastic shear strain rate forms a very small part of the total shear strain rate in the contact. This would be the case when large total shear strain rates exist nearly everywhere such as in contacts under severe conditions of spin or slip. The elastic shear strain rate component in equation (2) may now be neglected and this equation for a perfectly plastic dissipative function $F(\tau e)$ reduces to the following:

$$\tau_{ij} = \tau_c \, \dot{\gamma}_{ij}/\dot{\gamma}_e$$

where

$$\dot{\gamma}_e = \sqrt{\tfrac{1}{2} \, \dot{\gamma}_{ij} \cdot \dot{\gamma}_{ij}} \tag{8}$$

This type of model was used by Wernitz [1] and more recently by Magi [2] and it is an expression for the Coulomb law of friction.

This type of model may be referred to as a rigid/plastic model in that an infinite shear modulus G used in equation (2) together with equation (7) would produce the same result.

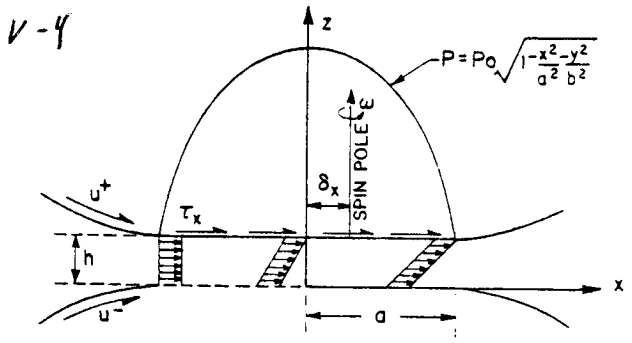

Fig. 2(*a*) Idealized EHL contact showing a film of oil under shear

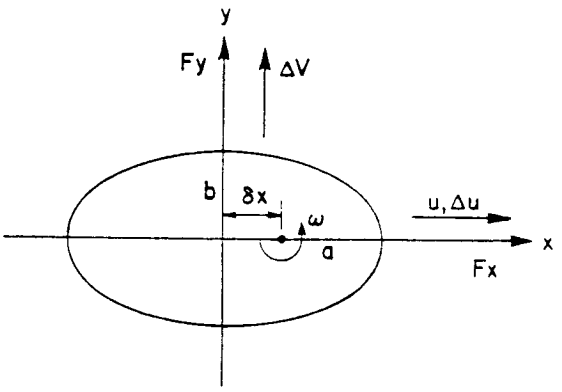

Fig. 2(*b*) Top view of the idealized EHL contact showing the various velocities as occurring in traction drives

4 Kinematics of Traction Drives

Fig. 2 shows a typical "contact" area similar to those occurring in traction drives. The combined rolling action $(U^+ + U^-)$ of the two "contacting" disk draws fluid into the contact zone and a thin layer of fluid is established between the two rolling element and by virtue of the relative velocity between the surfaces of the rollers, shear forces are transmitted through the film. The pressure in the small "contact" area is several orders of magnitude above ambient which strongly influences the rheological properties of the fluid.

Shear forces are transmitted through the film by virtue of a small relative velocity between the rolling surfaces. Relative velocity can arise in three different ways (see Fig. 2(*b*)):

(i) ΔU = slip = $U^+ - U^-$ = relative velocity in the rolling direction known as slip (occurs whenever any power is transmitted in a traction drive).

(ii) ΔV = side slip = $V^+ - V^-$ = relative velocity perpendicular to the rolling direction known as side slip (occurs in traction drives due to misalignments in shafts and when changing ratios. It may also be inherent in some designs).

(iii) ω = spin = relative angular velocity normal to the "contact" area known as spin (ω is the by-product of the kinematics of variable speed traction drives).

The velocity differences ΔU and ΔV are constant over the contact area. The spin takes place about a line joining the centers of the contacting disk. This line is referred to as the spin pole. (Note that this is different from the spin pole and speed pole concept of Wernitz [1].) This spin pole is chosen deliberately not to coincide with the center of the "contact" area.

It is usual to assume that the size and elliptical plane form of the film and the pressure in the film are given by the Hertz theory of dry contact. The thickness of the film h is taken to be uniform and compliance of rollers themselves in the tangential direction is neglected. In reality these conditions are only approximately met. The pressure distribution rises more gently at entry and falls more steeply at exit than the Hertz distribution so that the center of pressure is displaced towards the leading edge by a distance δ, which depends upon the conditions of speed and viscosity of the fluid. Johnson [13] suggested

that the pressure distribution was controlled principally by the nondimensional parameter $(N^4/\eta^3U^3ER^5)^{2/3}$ and recent detailed calculations by Hamrock [14] lead to the expression

$$\delta/a = 4.25(g_1')^{.022}(g_3')^{-.35}k^{.91} \tag{9}$$

This forward displacement of the center of pressure accounts for the hydrodynamic resistance to pure rolling (the so-called rolling traction). The rolling torque T_r is given by;

$$T_r = \delta \times N$$

where N is the total normal load on the contact. The effect only becomes significant at high speed.

We shall take account of the non-Hertzian pressure distribution, to a first approximation, by assuming that it remains Hertzian in shape acting on the "dry" elliptical area, but that the center of that area is shifted forward relative to the line of centers of the rollers by a displacement δ given by equation (9).

Optical interferometry has revealed that the film is thinner at the edges and the rear of the contact area than in the center, but the variation is not very great and will be ignored.

The shear strain rate at any point (x, y) in the fluid is then given by

$$\dot{\gamma}_x = \frac{\Delta U - \omega y}{h}$$

$$\dot{\gamma}_y = \frac{\Delta V + \omega(x - \delta)}{h} \tag{10}$$

5 Application of Constitutive Law to a General Contact

For a general traction drive contact under shear the constitutive equation (2) reduces to the following two coupled differential equations.

$$\frac{U}{Ga}\frac{d\tau_x}{dX} + \frac{\tau_x}{\tau_e}F(\tau_e) = \frac{\Delta U - \omega y}{h}$$

$$\frac{U}{Ga}\frac{d\tau_y}{dX} + \frac{\tau_y}{\tau_e}F(\tau_e) = \frac{\Delta V + \omega(x - \delta)}{h}$$

$$\tau_e = \sqrt{\tau_x^2 + \tau_y^2} \tag{11}$$

where dt has been replaced with $a/U\,dX$.

The boundary conditions to the above equations are

$$\tau_x = \tau_y = 0 \quad \text{when} \quad X = -\sqrt{1 - Y^2} \tag{12}$$

The subscripts x and y indicate the coordinate directions of the contact. For the *elastic/perfectly plastic* model the viscous functions $F(\tau_e)$ is given by,

$$F(\tau_e) = 0 \quad \text{when} \quad \tau_e < \tau_c$$

and

$$F(\tau_e) = \left[\tau_x\left\{\frac{\Delta U - \omega y}{h}\right\} + \tau_y\left\{\frac{\Delta V + \omega(x - \delta)}{h}\right\}\right] \Big/ \tau_c$$

$$\text{when} \quad \tau_e = \tau_c \tag{13}$$

While for a *rigid/perfectly* plastic model the stresses are given by;

$$\tau_x = \tau_c\{\Delta U - \omega y\}/\phi$$

$$\tau_y = \tau_c\{\Delta V + \omega(x - \delta)\}/\phi \tag{14}$$

where

$$\phi = \sqrt{(\Delta U - \omega y)^2 + (\Delta V + \omega(x - \delta))^2}$$

With the knowledge of the velocity differences over the contact area, the variation of G and τ_c over the contact area, and the initial boundary conditions, equation (11) or (14) may be solved for the shear stress distribution over the contact area. From these shear stresses one may obtain the traction in the rolling direction;

$$F_x = \int_A \tau_x dA, \quad \text{the traction perpendicular} \tag{15}$$

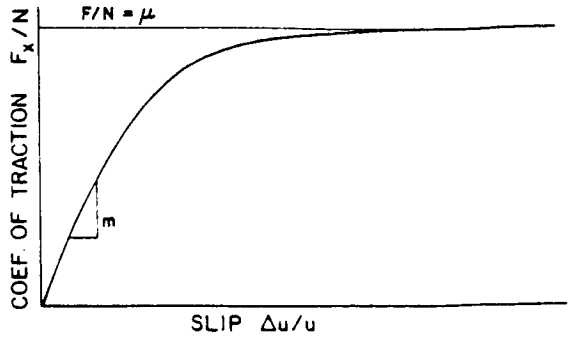

Fig. 3 General features of a traction curve obtained at moderate to high pressures

to the rolling direction;

$$F_y = \int_A \tau_y dA, \quad \text{and the resulting torque} \tag{16}$$

normal to the contact area;

$$T = \int_A \{\tau_y \cdot x - \tau_x \cdot y\} dA \tag{17}$$

6 Variation of the Fluid Properties Over the Contact Area

As indicated in the previous section, the variation of the shear modulus G and the limiting shear stress τ_c over the contact area need to be known before a solution to equation (11) or (14) is possible. The simplest would be to assume that G and τ_c are both constant over the contact area, however, experimental evidence (Johnson and Tevaarwerk [7]) indicates that both G and τ_c are approximately in direct proportion to the pressure.

A further complication arises in the specification of elastic modulus to use in equation (11). In the region of small slip where the elasticity of the fluid is significant, it is not adequate to ignore the elasticity of the rollers. An approach to separating the elastic compliance of the film from that of the rollers is discussed in some detail by Johnson and Roberts [5]. For practical purposes, however, a simple approach is suggested.

At present reliable independent measurements of the shear modulus of traction fluids is not available, so that useful practical data have to be obtained from rolling contact experiments. This being so, the procedure is greatly simplified if a mean effective modulus $\bar{G}$ is used which combines the elasticity of the rollers with that of the film. As far as the tangential compliance of the rollers is concerned this procedure implies that the roller surfaces deform tangentially like a simple elastic (Winkler) foundation, which Kalker [15] has shown to give reasonable results. The compliance of the rollers (i.e. the stiffness of the foundation) will be uniform throughout the "contact" area, while the compliance of the film varies with pressure. However, since the compliance of the rollers tends to outweigh that of the film under traction drive condition, it is good enough to take the effective modulus to be constant throughout the film. Its value may be found most conveniently from the linear slope of a simple traction-slip test as shown in Fig. 3 and given by:

$$\bar{G} = \frac{3}{8}m\bar{N}h/a^2b \tag{18}$$

In the case of the critical stress τ_c it is preferable to assume that it is everywhere proportional to the contact pressure, i.e.

$$\tau_c = \frac{2}{3}\bar{\tau}_c\sqrt{1 - X^2 - Y^2} \tag{19}$$

The value of the $\bar{\tau}_c$, is found from the maximum traction coefficient in a traction-slip experiment (Fig. 3) given by:

$$\bar{\tau}_c = \mu\bar{N}/\pi ab \tag{20}$$

In order to obtain reliable values of $\bar{G}$ and $\bar{\tau}_c$ in this way, it is necessary

to carry out the traction test at the same conditions of speed, pressure and temperature as obtained in the actual drive.

6 Dimensionless Traction Parameters

With the use of the average limiting shear stress $\bar{\tau}_c$ and the average shear modulus $\bar{G}$ over the "contact" area, the following dimensionless parameters are arrived at.

$$J_1 \equiv \frac{\bar{G}\sqrt{ab}}{\bar{\tau}_c h}\frac{\Delta U}{U} = \text{dimensionless slip}$$

$$J_2 \equiv \frac{\bar{G}\sqrt{ab}}{\bar{\tau}_c h}\frac{\Delta V}{U} = \text{dimensionless side-slip}$$

$$J_3 \equiv \frac{\bar{G}\sqrt{ab}}{\bar{\tau}_c h}\frac{\omega\sqrt{ab}}{U} = \text{dimensionless spin}$$

$$J_4 \equiv \frac{Fx}{\pi ab\bar{\tau}_c} = \text{dimensionless traction in the rolling direction}$$

$$J_5 \equiv \frac{Fy}{\pi ab\bar{\tau}_c}$$

= dimensionless traction perpendicular to the rolling direction

$$J_6 \equiv \frac{T}{\pi ab\bar{\tau}_c\sqrt{ab}}$$

= dimensionless torque normal to the contact area

$J_7 \equiv (J_1 \cdot J_4 + J_2 \cdot J_5 + J_3 \cdot J_6)$ Total dimensionless losses.

$$\equiv \frac{\bar{G}}{\pi\bar{\tau}_c{}^2\sqrt{ab}hU}\{Fx \cdot \Delta U + Fy \cdot \Delta V + T\cdot\omega\} \quad (21)$$

7 Computed Traction Results

With the knowledge of the variation of $\bar{G}$ and τ_c over the contact area, equations (11) may be integrated to find τ_x and τ_y throughout the contact and hence the resultant traction forces F_x, F_y, and moment T. Although for a number of special cases analytical solutions exist, the general situation of combined slip, side slip and spin was solved using digital techniques.

7.1 Traction Due to Slip. For simple slip J_1 on the contact of aspect ratio k the resulting traction J_4 is as follows

$$J_4 = \frac{1}{\pi}\left\{\frac{\pi}{2} - \sin^{-1}\left(\frac{1-S^2}{1+S^2}\right) + \frac{2S}{S^2+1}\right\} \quad (22)$$

where

$$S = \frac{2}{3}J_1/\sqrt{k}$$

The resulting J_4 as a function of J_1 and k is shown in Fig. 4(*a*). It may be observed from Fig. 4(*a*) that contacts of low aspect ratios have a superior performance in terms of traction at a given slip value. This is not a surprising result when it is remembered that the traction is strongly governed by the total strain in the contact. The average strain level in the contact is directly proportional to the applied slip and the contact length in the running direction. Low aspect ratio contacts therefore have a higher average strain level at identical slip values and hence show a higher traction. Whether this is so in practice needs to be investigated especially since compliance effects enter into the picture. The spin pole offset has no effect on J_4 under conditions of slip only.

7.2 Influence of Spin on Traction. For the combined action of slip and spin the resulting shear stresses are given by equation (11) by letting $\Delta V = 0$. The integration of the shear stresses produces the traction. No analytical solution is known to exist and the integrations were performed on a digital computer. The resulting traction curves are shown in Fig. 5 for an aspect ratio of $k = 1.0$. The influence of spin is to increase the slip, though this appears to be so only above a certain threshold value of spin. When the spin is sufficiently high it is expected that elastic strain may be neglected and the rigid/plastic model may be used.

The resulting traction due to the shear of a rigid/plastic like ma-

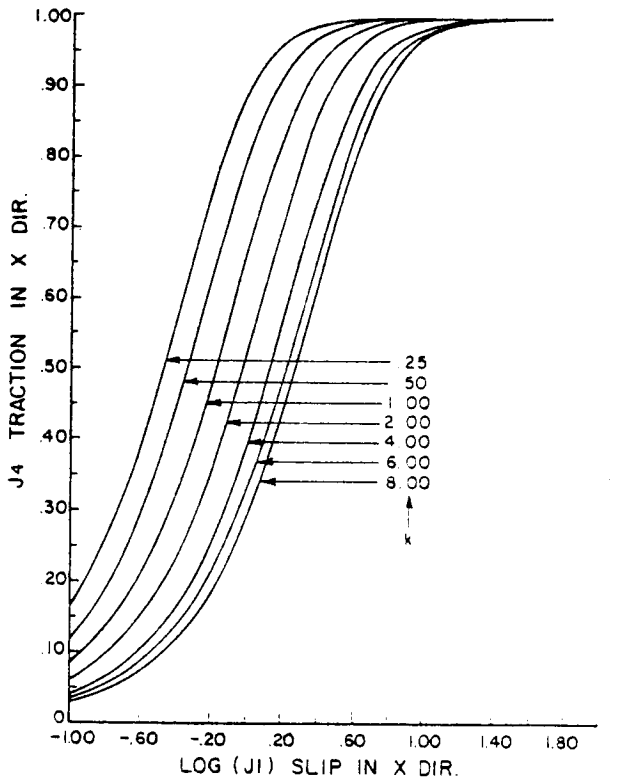

Fig. 4(*a*) Dimensionless traction curves for simple slip only at varying aspect ratios. These curves may be collapsed into one by dividing J_1 by $\sqrt{k}$. The elastic/plastic model is used here.

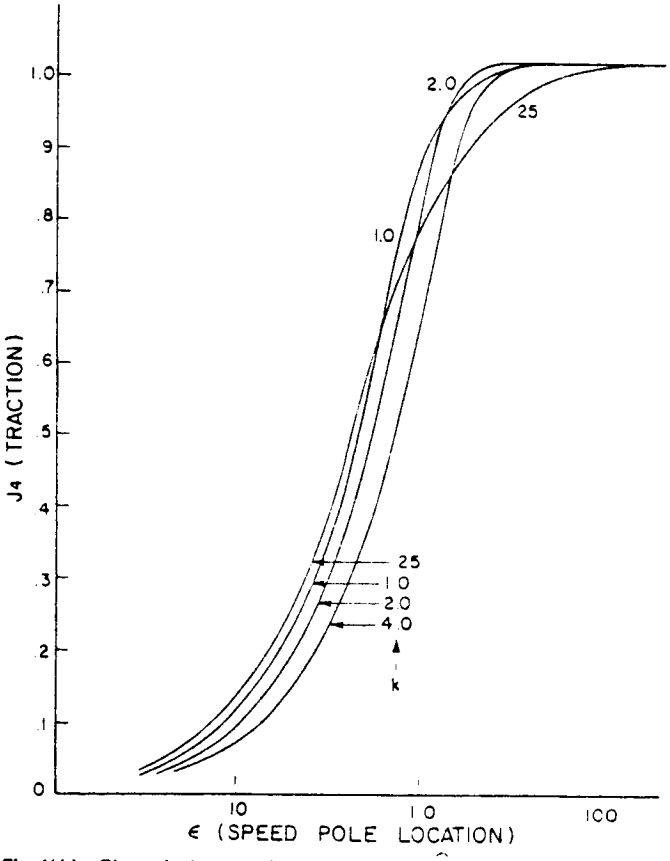

Fig. 4(*b*) Dimensionless traction curves as a function of the speed pole location (J_3/J_1) and at varying aspect ratios. The rigid/plastic model was used here.

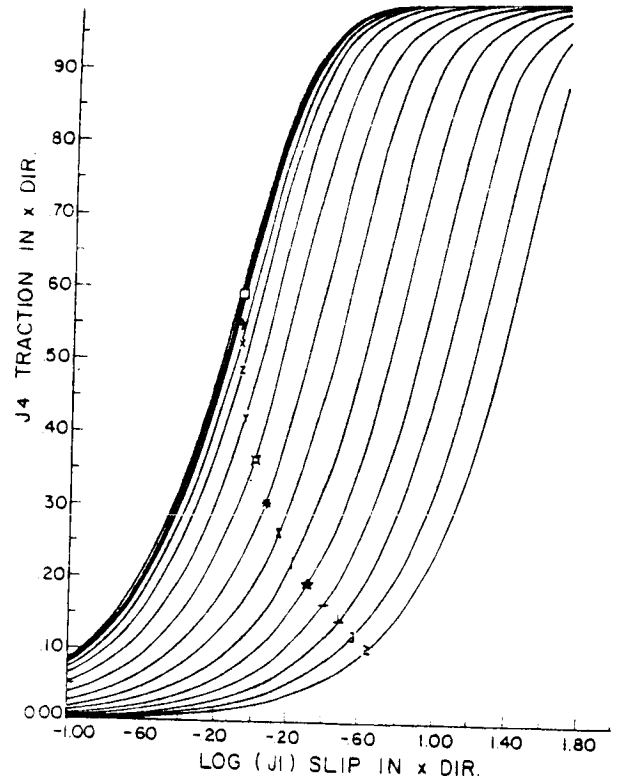

Fig. 5 Dimensionless traction curves for combined spin and slip for a contact with an aspect ratio of $k = 1$ and based on the elastic/plastic model. Spin J_3 = □, 0.0; ○, .04; △, .1; +, .18; ×, .3; ◇, .47; △, .70; ⊼, 1.03; Z, 1.50; Y, 2.16; ⌑, 3.10; ✳, 4.43; ⧖, 6.30; |, 8.95; ☆, 12.7; —, 18.0; ⊥, 25.5; |, 36.1; ⩾, 51.1.

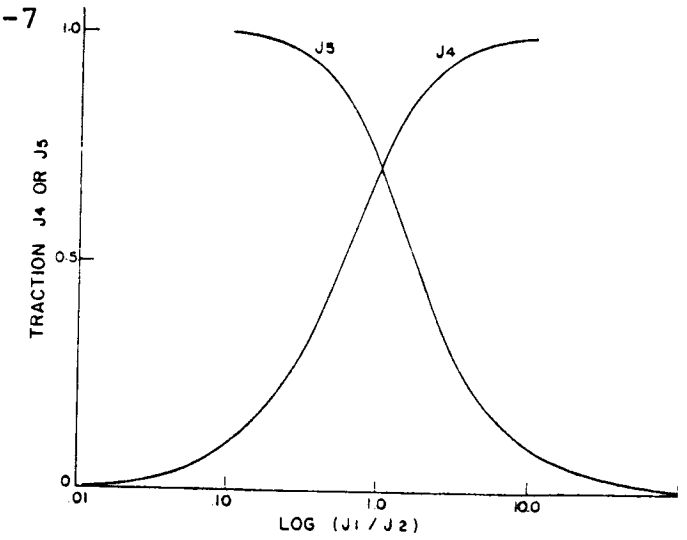

Fig. 6(*b*) Dimensionless traction curves for combined slip and side slip as a function of (J_1/J_2), based on the rigid/plastic model. These curves are valid for all aspect ratios.

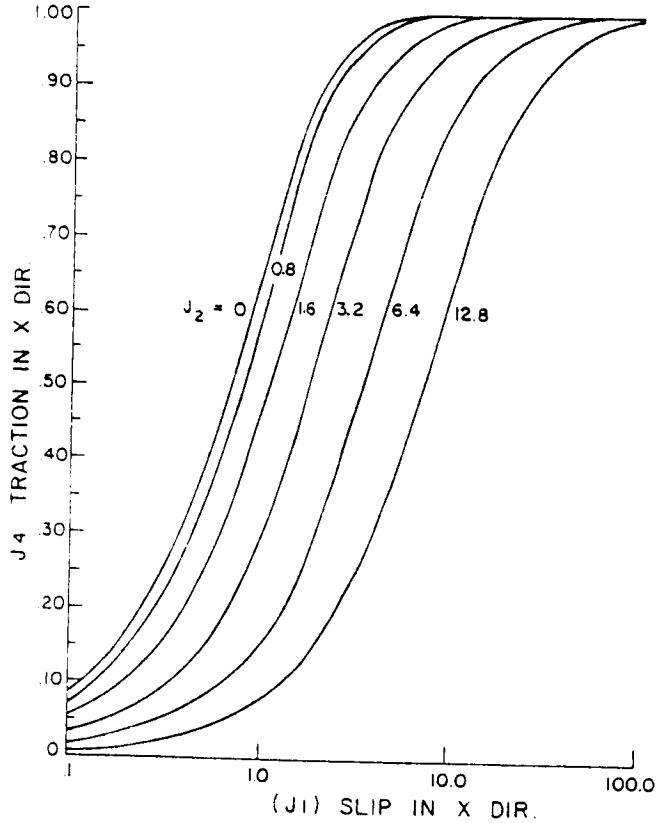

Fig. 6 Dimensionless traction curves for combined slip and side slip as a function of slip for an aspect ratio of $k = 1.0$

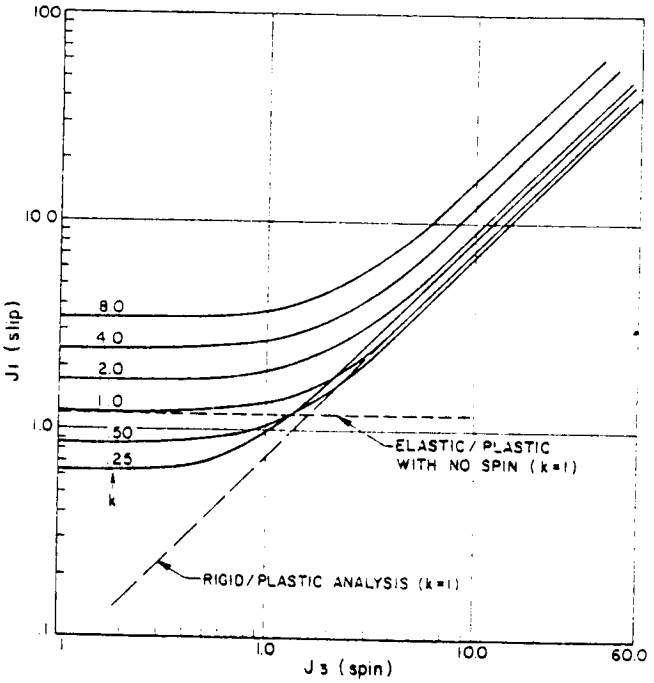

Fig. 7(*a*) Slip (J_1) as a function of spin (J_3) at a constant traction $J_4 = .75$ for the various aspect ratios. Included are the asymptotic results for $k = 1$ from the elastic/plastic and rigid/plastic analyses

terial in the contact is shown in Fig. 4(*b*). The independent parameters are the aspect ratio k and the speed pole location ϵ. The speed pole location parameter ϵ is identical to that used by Wernitz [1] and by Magi [2]. It is related to the dimensionless parameters used in this analysis as follows:

$$\epsilon = \frac{\Delta U}{\omega\sqrt{ab}} = J_1/J_3 \tag{26}$$

The use of either J_1 or J_3 is stricly speaking not correct here in the rigid/plastic analysis as both contain a shear modulus term, however, their ratio is independent of the shear modulus. The results in Fig. 4(*b*) were obtained by numerical integration of equation (14) over the contact area. Comparison with results obtained by Magi [2] showed complete agreement. In Fig. 4(*b*) the spin pole offset was kept zero.

7.3 Influence of Side Slip on Traction. For the combined action of slip and side slip the resulting tractions for an elastic/plastic model

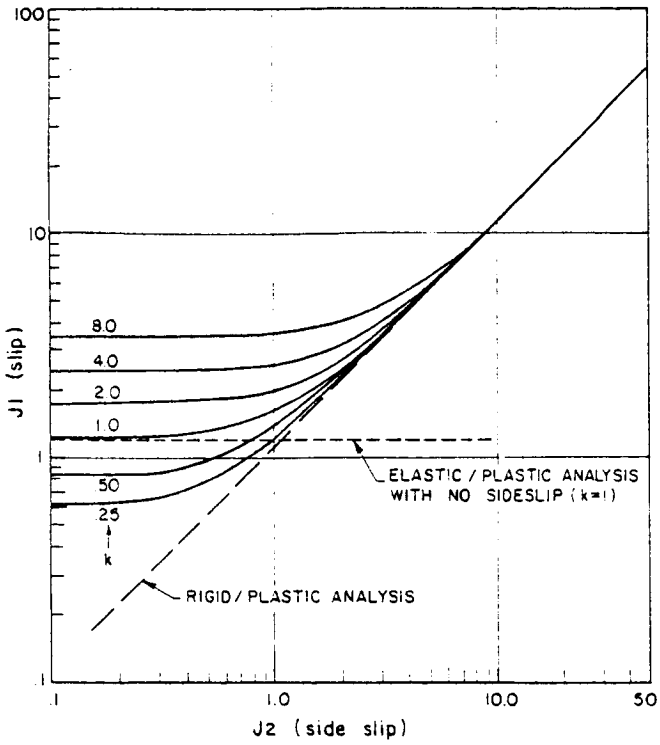

Fig. 7(*b*) Slip (J_1) as a function of side slip (J_2) at a constant traction J_4 = .75 for the various aspect ratios. Included are the asymptotic results for k = 1 from the elastic/plastic and rigid/plastic analyses

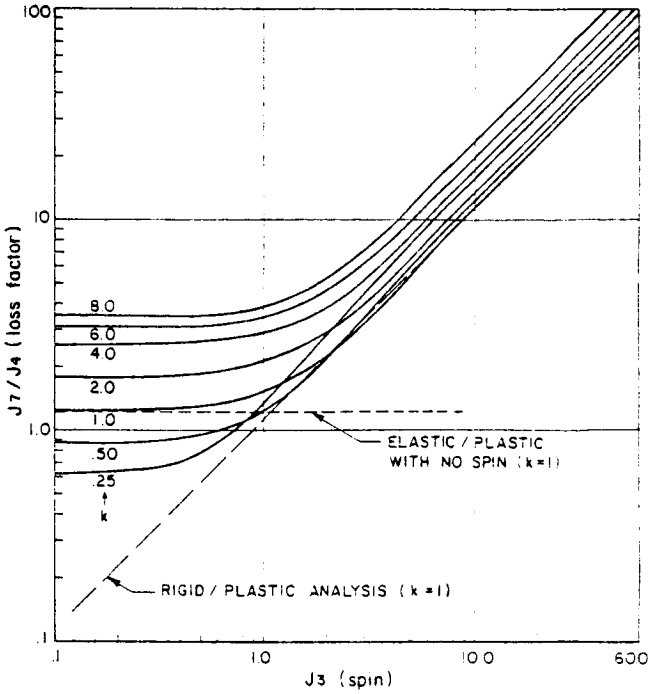

Fig. 9 Loss factor as a function of spin for the various aspect ratios. Included are the asymptotic results from the elastic/plastic and rigid/plastic analyses for k = 1.

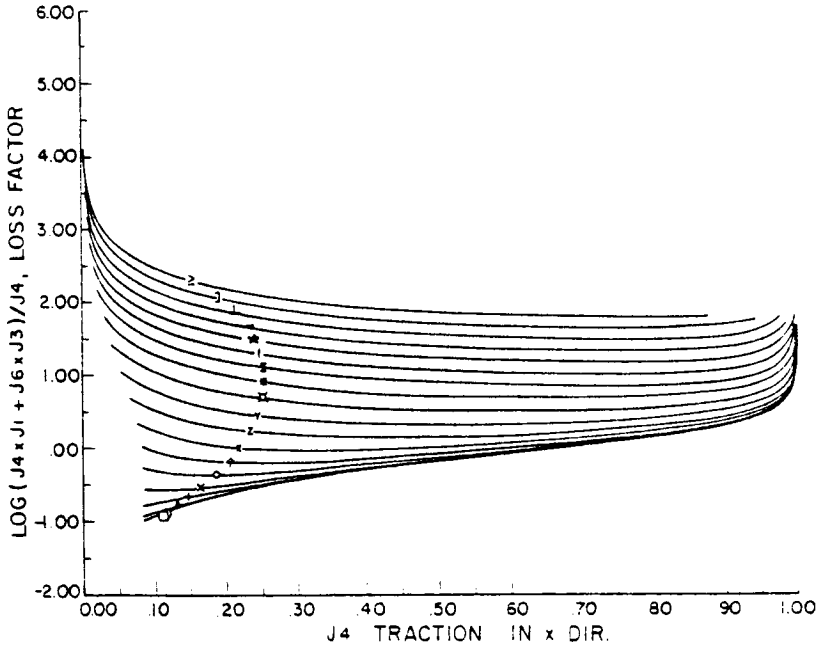

Fig. 8 Dimensionless losses as a function of the transmitted traction J_4 for various values of spin and an aspect ratio of k = 1. (For explanation of symbols, see Fig. 5.)

are given by

$$J_4 = \frac{2}{3} J_1 \psi / (S\sqrt{k})$$

$$J_5 = \frac{2}{3} J_2 \psi / (S\sqrt{k}) \tag{23}$$

where;

$$\psi = \frac{1}{\pi}\left[\frac{\pi}{2} - \sin^{-1}\left(\frac{1 - S^2}{1 + S^2}\right) + \frac{2S}{S^2 + 1}\right]$$

$$S = \frac{2}{3\sqrt{k}} \vee \overline{J_1^2 + J_2^2}$$

Fig. 6 shows J_4 as a function of J_1 at various values of J_2 for an aspect ratio of k = 1. The effect of J_2 is to reduce the obtained traction in the working range.

When the imposed side slip becomes sufficiently large, the elastic effects may be neglected and the traction can then be obtained by noting that $\psi = 1$ for large values of S.

Hence for the rigid-plastic model;

$$J_4 = \frac{J_1}{\sqrt{J_1^2 + J_2^2}}$$

$$J_5 = \frac{J_2}{\sqrt{J_1^2 + J_2^2}} \tag{24}$$

In Fig. 6(*b*) the resulting J_4 and J_5 are shown as a function of J_1/J_2, the longitudinal slip to side slip ratio. There is no effect of spin pole offset on the influence of side slip on traction.

8 Traction Results at Constant J_4

Many forms of the traction drives employ a mechanism to alter the normal load according to the magnitude of the torque transmitted. These mechanism are designed to operate the drive at a constant fraction of the maximum available traction, i.e. at a constant fraction of J_4 most commonly about 75 percent. Taking J_4 as a constant (=0.75), it is now possible to replot the results of all the traction calculations on two graphs: (i) The influence of spin on longitudinal slip (Fig. 7) and (ii) the influence of side slip on longitudinal slip (Fig. 7(*b*). These curves may be divided into three regions.

Region (i). Spin (J_3) and side slip (J_2) have a negligible effect on longitudinal slip (J_1). In this region the curves are asymptotic to the result given by equation (22) (Fig. 4)—shown by the elastic line to the left of Figs. 7—7(*b*).

Region (ii). A transition region in which a complete elastic-plastic analysis is required. The curves in this region are derived from the results given in Figs. 5 and 6.

Region (iii). A region in which elastic deformation is negligible so that the curves are asymptotic to the rigid-plastic analysis which gives a linear relationships between J_1 and J_3 and between J_1 and J_2. This is the region to which the analysis of Wernitz and Magi apply.

9 Losses in Traction Drives Under Spin

The total friction losses in the contact of a traction drive under spin consists of two components, the slip loss and the spin loss. Thus the nondimensional loss is defined by:

$$J_7 = J_1 \, x \, J_4 + J_3 \, x \, J_6 = \frac{\overline{G}}{\pi \sqrt{ab} U h \bar{\tau} c^2} (\Delta U \cdot F_x + \omega \cdot T)$$

The component in the brackets is the actual power loss in the contact. However the efficiency of the drives is better expressed by a loss factor proportional to the ratio of the power lost to the power transmitted

$$LF = \frac{\overline{G}\sqrt{ab}}{h\bar{\tau}_c} \left(\frac{\text{Power lost}}{\text{Power input}} \right) = \frac{\overline{G}\sqrt{ab}}{h\bar{\tau}_c} \left(\frac{\Delta U \cdot F_x + \omega \cdot T}{U \cdot F_x} \right) = J_7/J_4$$

The loss factor thus calculated as a function of slip traction J_4 is shown in Fig. 8 for an aspect ratio of $k = 1$ for various values of spin. It may be observed that the loss factor increases with increasing spin. When the spin is high the loss factor is a minimum at $J_4 \simeq .75$.

The loss factor may also be plotted for a constant traction value J_4. This is shown in Fig. 9 for the various aspect ratios and values of spin. At low values of spin the loss factor is constant and given by the slip J_1 corresponding to that aspect ratio and traction J_4 fraction. When the spin increases the loss factor increases until again it becomes asymptotic to the loss factor for the rigid/plastic analysis.

Conclusion

The work of Johnson and Tevaarwerk on the rheology of fluids in highly loaded EHD contacts suggests that typical traction fluids can be conveniently modelled for traction drive analysis as elastic-perfectly plastic solids. In this model the fluid is characterized by two independent parameters: its shear modulus G and its limiting or critical shear stress τ_c. The mean effective value of these parameters are best found by a traction test on a simple 2 disk machine at the appropriate conditions of speed, pressure and temperature. The traction transmitted by a rolling contact and the power dissipated in viscous heating are governed by not only the slip in the rolling direction (longitudinal slip) but also by the spin which is inevitable in variable speed drives and also by side slip when it arises. The elastic-plastic model has been used to derive traction and loss curves under various combinations of slip, spin and side spin. Three regions of behavior have been identified. If the spin or side slip is sufficiently small, as indicated in Figs. 7 and 7(*b*), the traction is independent of spin and side slip and depends upon the longitudinal slip only as given in Fig. 9. If the spin or side slip are sufficiently large, elastic effects in the fluid and also in the rollers can be neglected and the traditional method of analysis based on the Coulomb friction law (rigid-plastic model) is satisfactory. For moderate spin or side slip, elastic effects are not negligible as the results in this paper show.

For maximum efficiency i.e. for minimum loss factor the drive should transmit about 75 percent of its limiting traction.

Acknowledgment

One of the authors (JLT) would like to thank the Canadian National Research Council for support under grant number A4214.

References

1 Wernitz, W., *Rolling Contact Phenomena*, ed. Bidwell Elsevier, Amsterdam, 1962
2 Mägi, M., Chalmers University of Technology Gothenburg, 1974
3 Fein, R. S., ASME JOURNAL OF LUBRICATION TECHNOLOGY, Vol. 89, 1967, p. 127.
4 Harrison, G., and Trachman, E. G., ASME JOURNAL OF LUBRICATION TECHNOLOGY., Vol. 94, 1972, p. 306.
5 Johnson, K. L., and Roberts, A. D., *Proc. R. Soc. Lond.*, Series A 337, 1974, p. 217.
6 Hirst, W. and Moore, A. J., *Proc. R. Soc. Lond.*, Series A 337, 1974, p. 101.
7 Johnson, K. L., and Tevaarwerk, J. L., *Proc. R. Soc. Lond.*, Series A, Vol. 356, 1977, p. 215.
8 Clark, O. H., Woods, W. W., and White, J. R., *Journal of Applied Physics*, Vol. 22, No. 4, 1951, p. 474.
9 Smith, F. W., *Trans. ASLE* Vol. 5 1962, p. 142.
10 Tevaarwerk, J. L., PhD dissertation, Cambridge, 1976.
11 Lingard, S., *Tribology International*, 1974, p. 228.
12 Gaggermeier, H., PhD dissertation, Munich, 1977.
13 Johnson, K. L., *J. Mech. Engng Sci.*, Vol. 12, No. 1, 1970, p 9.
14 Hamrock, B. J., private communication, 1977.
15 Kalker, J. J. PhD dissertation, Delft, 1967.

DISCUSSION

S. H. Loewenthal[1]

The authors have made a timely and most welcome contribution to the understanding of lubricant behavior in power transmitting, traction contacts. Traction drives are currently the subject of renewed interest due to improvements in their power capacity through better lubricants and cleaner steels and their potential of reducing automotive fuel consumption. The solutions presented in this paper in graphical form to the authors' elastic-plastic model of traction will be of practical value in the design and optimization of contact geometry for these types of transmissions.

In the interest of independently verifying the accuracy of the proposed method, the discusser, for comparison purposes, has arbitrarily selected four sets of traction test data generated with a simple twin disk machine from the report of Gaggermeier [12]. In Gaggermeier's experiments, the effect of side slip under zero spin and the effect of spin under zero side slip on the traction-versus-slip curve was deter-

[1] NASA Lewis Research Center, Cleveland, Ohio.

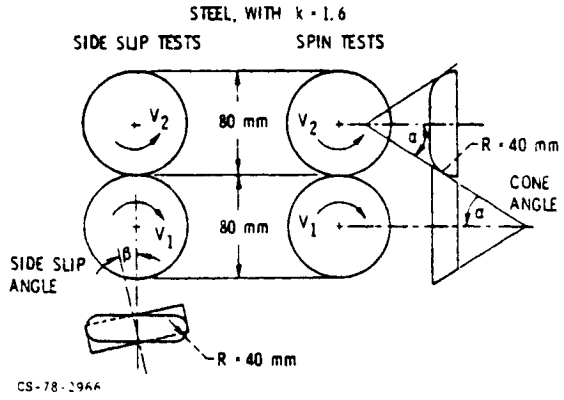

Fig. 9 Test disks for Gaggermeier's traction experiments [12]

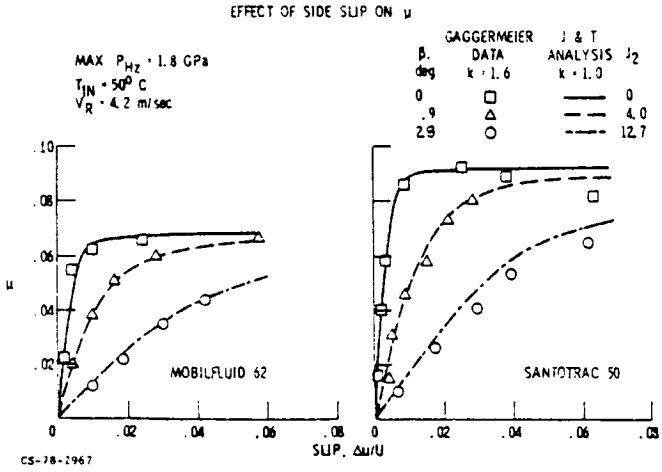

Fig. 10 Comparison of Johnson and Tevaarwerk analysis with test data

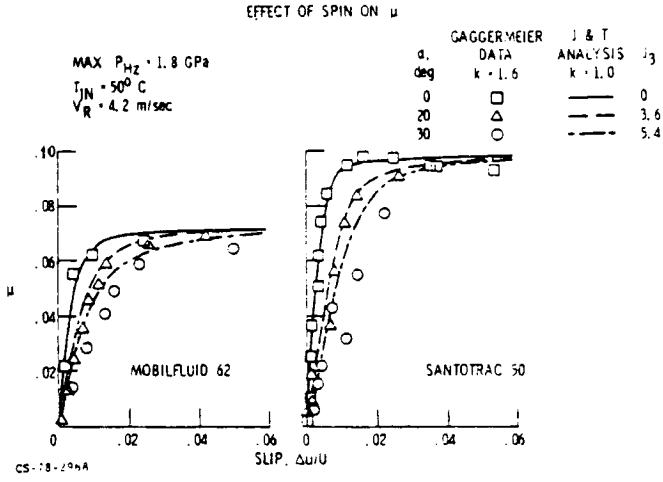

Fig. 11 Comparison of Johnson and Tevaarwerk analysis with test data

mined with the test disk geometry shown in Fig. 9. The data for these tests under one test operating condition with two lubricants appear in Figs. 10 and 11. Also shown on these figures are the predicted traction curves from the authors' analysis. The theoretical curves were generated by the discusser using the graphical solutions shown in Figs. 5 and 6. The values for $\overline{G}$ and $\overline{\tau}_c$ were found from equations (18) and (20) by measuring the initial slope m and peak traction coefficient μ_p from zero-spin/zero-side-slip-traction curve fitted through Gaggermeier's data.

As shown in Figs. 10 and 11, the predicted values of μ from the Johnson and Tevaarwerk analysis are in rather good agreement with the test data. This is despite the fact that the predictions were derived from Figs. 5 and 6 where the contact ellipticity ratio, $k = 1.0$, whereas the test disks had $k = 1.6$. As expected, the isothermal Johnson and Tevaarwerk analysis has a slight tendency to overpredict μ for the higher values of slip, side slip and spin as thermal effects become more pronounced. Thermal corrections to the theory would be helpful but are not essential from a design standpoint. This is because most traction drive contacts are designed to operate on the linear, isothermal portion of the traction curve and at the lowest possible values of side slip and spin.

It is apparent from the side slip data displayed in Fig. 10 that even a relatively small misalignment angle of 2.8 degrees causes a substantial reduction in μ, underscoring the need to maintain accurate alignment of roller components in traction drives. In contrast to this, the traction coefficient data with spin in Fig. 11 under the same operating conditions show surprisingly little adverse effect to spin even for disks with a relatively large cone angle of 30 degrees. Is there a physical explanation which the authors can give for the above observation?

Author's Closure

The authors would like to thank Dr. S. Loewenthal for his discussion and the comparison that he made between the results as published here and the experimental work by Gaggermeir [12].

In answer to the question at the end of the discussion it may be commented that slip angles and spin angles cannot be directly compared for their degree of influence on the traction. What is of importance is the degree of slip that results from these angles. In the case of the side slip experiment, the amount of side slip is given by $U\sin\beta$ while the average slip due to spin on the contact is given by $U\nu\overline{ab}\sin\alpha/r$, β is the sideslip angle and α is the spin angle. The reason for the smaller influence of the spin can be seen directly in that the term $\nu\overline{ab}/r$ is of order 10^{-1}, making the degree of slip due to spin quite a bit smaller than for the side slip experiment.

APPENDIX VI

This appendix contains the theoretical and experimental data for the experimental traction with spin curves shown in figure 2-12 to figure 2-19 and the theoretical prediction shown in figure 4-1 to figure 4-8.

TRACE NUMBER 79072704
ASPECT RATIO = 5
ZERO SPIN TRACTION SLOPE = 35
ZERO SPIN PEAK TRACTION COEFF.= .075
SPIN PEAK FRACTION COEFF.= .035
NORMAL LOAD (N) = 5000
HERTZ PRESSURE (GPA) = 1.45
INLET TEMPERATURE (C) = 73
SURFACE SPEED (M/S) = 80
SPIN ON THE CONTACT (-)= .021
DIMENSIONLESS SPIN J3 (-) = 25.8161723

POSITIVE ROLLING DIRECTION

*****EXPERIMENTAL*******		***********THEORETICAL**********			
DV/U	FY/FZ	J2	J5	J5*MU	J5*MS
0	-5.4E-03	0	-.160855094	-.0120641321	-5.62992935E-03
2.74E-03	3.15E-03	3.36839582	.045568033	3.41760248E-03	1.59488116E-03
5.48E-03	.01575	6.73679164	.266649446	.0199987085	9.33273063E-03
8.22E-03	.0234	10.1051875	.434597325	.0325947994	.0152109064
.01096	.02835	13.4735833	.553613791	.0415210344	.0193764827
.0137	.0315	16.8419791	.63696713	.0477725348	.0222938496
.01644	.0324	20.2103749	.696213333	.052216	.0243674667
.02192	.0324	26.9471666	.775413414	.058156006	.0271394695

NEGATIVE ROLLING DIRECTION

*****EXPERIMENTAL*******		***********THEORETICAL**********			
DV/U	FY/FZ	J2	J5	J5*MU	J5*MS
0	-5.4E-03	0	-.160855094	-.0120641321	-5.62992935E-03
-2.74E-03	-.0126	-3.36839582	-.322768135	-.0242076101	-.0112968847
-5.48E-03	-.0207	-6.73679164	-.444793634	-.0333595226	-.0155677772
-8.22E-03	-.0252	-10.1051875	-.538999143	-.0404249357	-.01886497
-.01096	-.0288	-13.4735833	-.61348722	-.0460115415	-.0214720527
-.0137	-.0306	-16.8419791	-.67214295	-.0504107213	-.0235250033
-.01644	-.0315	-20.2103749	-.718718279	-.0539038709	-.0251551399
-.02192	-.0324	-26.9471666	-.786521628	-.0589891221	-.027528257

ORIGINAL PAGE IS OF POOR QUALITY

TRACE NUMBER 79100403
ASPECT RATIO = 5
ZERO SPIN TRACTION SLOPE = 33.3
ZERO SPIN PEAK TRACTION COEFF.= .051
SPIN PEAK FRACTION COEFF.= .044
NORMAL LOAD (N) = 1500
HERTZ PRESSURE (GPA) = 1
INLET TEMPERATURE (C) = 50
SURFACE SPEED (M/S) = 80
SPIN ON THE CONTACT (-)= 7.1E-03
DIMENSIONLESS SPIN J3 (-) = 12.2123202

POSITIVE ROLLING DIRECTION

*****EXPERIMENTAL*******		**********	THEORETICAL	**********	
DV/U	FY/FZ	J2	J5	J5*MU	J5*MS
0	-.0142666667	0	-.201270212	-.0102647808	-8.8559893E-03
1.29E-03	5.70666666E-03	2.21885818	.0980186723	4.99895229E-03	4.31083159E-03
2.58E-03	.0214	4.43771635	.350749047	.0178882014	.0154330521
3.87E-03	.0313866667	6.65657452	.528909403	.0269743796	.0232720137
5.16E-03	.0370933333	8.8754327	.646405856	.0329666987	.0284419577
6.45E-03	.04066	11.0942909	.724737606	.0369616179	.0318884547
7.74E-03	.0428	13.313149	.778109233	.0396835709	.0342360043
.01032	.0428	17.7508654	.844553503	.0430722287	.0371607542
.0129	.0428	22.1885818	.882462591	.0450055921	.0388283754

NEGATIVE ROLLING DIRECTION

*****EXPERIMENTAL*******		**********	THEORETICAL	**********	
DV/U	FY/FZ	J2	J5	J5*MU	J5*MS
0	-.0142666667	0	-.201270212	-.0102647808	-8.8559893E-03
-1.29E-03	-.0214	-2.21885818	-.4173516	-.0212849316	-.0183634704
-2.58E-03	-.0328133333	-4.43771635	-.548151461	-.0279557245	-.0241186647
-3.87E-03	-.0370933333	-6.65657452	-.642933833	-.0327896255	-.0282890887
-5.16E-03	-.0413733333	-8.8754327	-.711122615	-.0362672534	-.0312893751
-6.45E-03	-.0435133333	-11.0942909	-.762061415	-.0388651322	-.0335307023
-7.74E-03	-.04494	-13.313149	-.800746625	-.0408390779	-.0352320515
-.01032	-.0456533333	-17.7508654	-.853960387	-.0435519798	-.0375743857
-.0129	-.0442266667	-22.1885818	-.887396482	-.0452572206	-.0390454451

**ORIGINAL PAGE IS
OF POOR QUALITY**

TRACE NUMBER 79100403
ASPECT RATIO = 5
ZERO SPIN TRACTION SLOPE = 46.9
ZERO SPIN PEAK TRACTION COEFF.= .081
SPIN PEAK FRACTION COEFF.= .08
NORMAL LOAD (N) = 1500
HERTZ PRESSURE (GPA) = 1
INLET TEMPERATURE (C) = 50
SURFACE SPEED (M/S) = 20
SPIN ON THE CONTACT (-)= 7.1E-03
DIMENSIONLESS SPIN J3 (-) = 10.8295884

POSITIVE ROLLING DIRECTION

*****EXPERIMENTAL******* DV/U	FY/FZ	********** J2	J5	THEORETICAL ********** J5*MU	J5*MS
0	-.0142666667	0	-.199909912	-.0161927029	-.015992793
1.29E-03	7.13333333E-03	1.96762943	.0921840652	7.46690928E-03	7.37472521E-03
2.58E-03	.0228266667	3.93525887	.340570214	.0275861873	.0272456171
3.87E-03	.0399466667	5.9028883	.519029307	.0420413738	.0415223445
5.16E-03	.0527866667	7.87051773	.639324023	.0517852458	.0511459218
6.45E-03	.0627733333	9.83814717	.719583303	.0582862475	.0575666642
7.74E-03	.0670533333	11.8057766	.775216906	.0627925694	.0620173525
.01032	.07276	15.7410355	.843982856	.0683626114	.0675196295
.0129	.07704	19.6762943	.882161258	.0714550619	.0705729006

NEGATIVE ROLLING DIRECTION

*****EXPERIMENTAL******* DV/U	FY/FZ	********** J2	J5	THEORETICAL ********** J5*MU	J5*MS
0	-.0142666667	0	-.199909912	-.0161927029	-.015992793
-1.29E-03	-.0313866667	-1.96762943	-.420926595	-.0340950542	-.0336741276
-2.58E-03	-.0456533333	-3.93525887	-.551923784	-.0447058265	-.0441539027
-3.87E-03	-.0542133333	-5.9028883	-.645440416	-.0522806737	-.0516352333
-5.16E-03	-.05992	-7.87051773	-.713421554	-.0577871459	-.0570737244
-6.45E-03	-.0642	-9.83814717	-.76359072	-.0618508483	-.0610872576
-7.74E-03	-.06848	-11.8057766	-.801792186	-.0649451671	-.0641433749
-.01032	-.07276	-15.7410355	-.85448599	-.0692133652	-.0683588792
-.0129	-.07704	-19.6762943	-.887683045	-.0719023267	-.0710146436

TRACE NUMBER 79072601
ASPECT RATIO = 1
ZERO SPIN TRACTION SLOPE = 53.5
ZERO SPIN PEAK TRACTION COEFF.= .083
SPIN PEAK FRACTION COEFF.= .084
NORMAL LOAD (N) = 3000
HERTZ PRESSURE (GPA) = 1.22
INLET TEMPERATURE (C) = 32.5
SURFACE SPEED (M/S) = 20
SPIN ON THE CONTACT (-)= 3E-03
DIMENSIONLESS SPIN J3 (-) = 2.27812588

POSITIVE ROLLING DIRECTION

*****EXPERIMENTAL*******		**********	THEORETICAL	**********	
DV/U	FY/FZ	J2	J5	J5*MU	J5*M9
0	-.0320833333	0	-.45793279	-.0380084216	-.0384663547
1.27E-03	-.01925	.964406623	.185143274	.0153668918	.0155520351
2.54E-03	3.85E-03	1.92881325	.595603863	.0494351207	.0500307245
3.81E-03	.0243833333	2.89321987	.804418599	.0667667438	.0675711623
5.08E-03	.04235	3.85762649	.897681394	.0745075557	.0754052371
6.35E-03	.0564666667	4.82203312	.938963869	.0779340011	.0788720965
7.62E-03	.0667333333	5.78643974	.957053542	.079435444	.0803924975
.01016	.077	7.71525299	.969832676	.0804961121	.0814659449
.0127	.0821333333	9.64406623	.972737956	.0807372504	.0817099803

NEGATIVE ROLLING DIRECTION

*****EXPERIMENTAL*******		**********	THEORETICAL	**********	
DV/U	FY/FZ	J2	J5	J5*MU	J5*M9
0	-.0320833333	0	-.45793279	-.0380084216	-.0384663547
-1.27E-03	-.04235	-.964406623	-.810581823	-.0672782913	-.0680999731
-2.54E-03	-.0539	-1.92881325	-.899598465	-.0746666726	-.075566271
-3.81E-03	-.0628833333	-2.89321987	-.938362979	-.0778841273	-.0788224901
-5.08E-03	-.0680166667	-3.85762649	-.953232441	-.0791182926	-.080071525
-6.35E-03	-.0718666667	-4.82203312	-.961063135	-.0797682402	-.0807293033
-7.62E-03	-.077	-5.78643974	-.965714323	-.0801542888	-.0811200031
-.01016	-.08085	-7.71525299	-.970666743	-.0805653397	-.0815360064
-.0127	-.0834166667	-9.64406623	-.973083478	-.0807659287	-.0817390121

TRACE NUMBER 79111902
ASPECT RATIO = 1
ZERO SPIN TRACTION SLOPE = 35.9
ZERO SPIN PEAK TRACTION COEFF.= .085
SPIN PEAK FRACTION COEFF.= .084
NORMAL LOAD (N) = 185
HERTZ PRESSURE (GPA) = 1.45
INLET TEMPERATURE (C) = 29
SURFACE SPEED (M/S) = 30
SPIN ON THE CONTACT (-)= 1.03E-03
DIMENSIONLESS SPIN J3 (-) = .512499589

POSITIVE ROLLING DIRECTION

*****EXPERIMENTAL*******		**********		THEORETICAL **********	
DV/U	FY/FZ	J2	J5	J5*MU	J5*MS
-2.1805E-04	-.0259459459	-.108495665	-.202695874	-.0172291493	-.0170214574
4.0495E-04	-2.16216216E-03	.20149195	.0637962702	5.42268297E-03	5.35099477E-03
1.02795E-03	.0172972973	.511479566	.311499829	.0264774954	.0261459854
1.65095E-03	.0367567568	.821467181	.508345197	.0432093417	.0427009365
2.27395E-03	.054054054	1.1314548	.653913421	.0555826408	.0549287274
2.89695E-03	.067027027	1.44144241	.754719459	.064151154	.0633944745
3.51995E-03	.0778378379	1.75143003	.824788897	.0701070563	.0692922473
4.76595E-03	.0864864865	2.37140526	.903551711	.0768018954	.0758983487

NEGATIVE ROLLING DIRECTION

*****EXPERIMENTAL*******		**********		THEORETICAL **********	
DV/U	FY/FZ	J2	J5	J5*MU	J5*MS
2.1805E-04	-.0108108108	.108495665	-.0160199986	-1.36169988E-03	-1.34567988E-03
-4.0495E-04	-.0367567568	-.20149195	-.282567585	-.0240182447	-.0237356771
-1.02795E-03	-.0583783784	-.511479566	-.529399063	-.0449989203	-.0444695213
-1.65095E-03	-.0735135135	-.821467181	-.701544349	-.0596312697	-.0589277253
-2.27395E-03	-.08	-1.1314548	-.806164133	-.0685239513	-.0677177072
-2.89695E-03	-.0843243243	-1.44144241	-.867047269	-.0736990179	-.0728319706
-3.51995E-03	-.0864864865	-1.75143003	-.904832483	-.0769107611	-.0760059286
-4.76595E-03	-.0864864865	-2.37140526	-.943086446	-.0801623479	-.0792192614

TRACE NUMBER 80051402
ASPECT RATIO = 1
ZERO SPIN TRACTION SLOPE = 59.6
ZERO SPIN PEAK TRACTION COEFF.= .098
SPIN PEAK FRACTION COEFF.= .091
NORMAL LOAD (N) = 416
HERTZ PRESSURE (GPA) = 1.9
INLET TEMPERATURE (C) = 70
SURFACE SPEED (M/S) = 20
SPIN ON THE CONTACT (-)= 1.35E-03
DIMENSIONLESS SPIN J3 (-) = .967241064

POSITIVE ROLLING DIRECTION

*****EXPERIMENTAL*******		**********		THEORETICAL **********	
DV/U	FY/FZ	J2	J5	J5*MU	J5*MS
-1.998E-04	-.0280769231	-.143151678	-.327419397	-.0320871009	-.0297951851
4.662E-04	7.01923077E-03	.334020581	.0719765075	7.05369774E-03	6.54986212E-03
1.1322E-03	.0333413462	.811192839	.400502866	.0392492809	.0364457603
1.7982E-03	.0526442308	1.2883651	.626047163	.061352622	.0569702919
2.4642E-03	.0684375	1.76553736	.760698611	.0745324639	.0692015771
3.1302E-03	.0772115385	2.24270961	.85238011	.0835332509	.0775655
3.7962E-03	.0824759615	2.71988187	.902492535	.0884442684	.0821240297
5.1282E-03	.0894951923	3.67422639	.940414664	.0921642371	.0855839744

NEGATIVE ROLLING DIRECTION

*****EXPERIMENTAL*******		**********		THEORETICAL **********	
DV/U	FY/FZ	J2	J5	J5*MU	J5*MS
1.998E-04	-.0105288462	.143151678	-.085420961	-8.37125418E-03	-7.77330745E-03
-4.662E-04	-.0403605769	-.334020581	-.484092259	-.0474410414	-.0440523995
-1.1322E-03	-.0684375	-.811192839	-.754856851	-.0739759714	-.0686919774
-1.7982E-03	-.0789663461	-1.2883651	-.865948799	-.0848629823	-.0788013407
-2.4642E-03	-.0859855769	-1.76553736	-.915527971	-.0897217412	-.0833130454
-3.1302E-03	-.0894951923	-2.24270961	-.940721445	-.0921907016	-.0856056515
-3.7962E-03	-.0894951923	-2.71988187	-.955398659	-.0936290686	-.0869413278
-5.1282E-03	-.09125	-3.67422639	-.969528673	-.0950138099	-.0882271883

TRACE NUMBER 80062306
ASPECT RATIO = 1
ZERO SPIN TRACTION SLOPE = 53.9
ZERO SPIN PEAK TRACTION COEFF.= .096
SPIN PEAK TRACTION COEFF.= .0955
NORMAL LOAD (N) = 416
HERTZ PRESSURE (GPA) = 1.9
INLET TEMPERATURE (C) = 70
SURFACE SPEED (M/S) = 20
SPIN ON THE CONTACT (-)= 1.35E-03
DIMENSIONLESS SPIN J3 (-) = .892960143

POSITIVE ROLLING DIRECTION

*****EXPERIMENTAL*******		**********		THEORETICAL **********	
DV/U	FY/FZ	J2	J5	J5*MU	J5*MS
-5.36E-04	-.0533653846	-.354538249	-.486535447	-.046707403	-.04664[illegible]
8.04E-04	.0142307692	.531807374	.237942065	.0228424382	.022733[illegible]
2.144E-03	.0622596154	1.418153	.685030626	.0657629401	.065[illegible]
3.484E-03	.0871634616	2.30449862	.867321732	.0832628863	.083[illegible]
4.824E-03	.0978365385	3.19084424	.934697377	.0897309482	.089[illegible]
6.164E-03	.101394231	4.07718986	.960183398	.0921776062	.091[illegible]
7.504E-03	.101394231	4.96353549	.970534737	.0931713347	.092[illegible]
.010184	.101394231	6.73622674	.976085702	.0937042274	.093[illegible]

NEGATIVE ROLLING DIRECTION

*****EXPERIMENTAL*******		**********		THEORETICAL **********	
DV/U	FY/FZ	J2	J5	J5*MU	J5*MS
5.36E-04	.0160096154	.354538249	.105525401	.0101304385	.010077[illegible]
-8.04E-04	-.0569230769	-.531807374	-.610393114	-.058597739	-.05829[illegible]
-2.144E-03	-.0889423077	-1.418153	-.881327564	-.0846074462	-.0841[illegible]
-3.484E-03	-.0978365385	-2.30449862	-.943109699	-.0905385312	-.0900[illegible]
-4.824E-03	-.0996153846	-3.19084424	-.96334545	-.0924811632	-.0919[illegible]
-6.164E-03	-.101394231	-4.07718986	-.973384957	-.0934449559	-.0929[illegible]
-7.504E-03	-.101394231	-4.96353549	-.97501877	-.093601802	-.0931[illegible]
-.010184	-.101394231	-6.73622674	-.976169155	-.0937122389	-.0932[illegible]

ORIGINAL PAGE IS
OF POOR QUALITY

TRACE NUMBER 80062801
ASPECT RATIO = 5
ZERO SPIN TRACTION SLOPE = 41.2
ZERO SPIN PEAK TRACTION COEFF.= .082
SPIN PEAK FRACTION COEFF.= .082
NORMAL LOAD (N) = 460
HERTZ PRESSURE (GPA) = 1
INLET TEMPERATURE (C) = 70
SURFACE SPEED (M/S) = 20
SPIN ON THE CONTACT (-)= 1.98E-03
DIMENSIONLESS SPIN J3 (-) = 2.62068202

POSITIVE ROLLING DIRECTION

*****EXPERIMENTAL*******		**********		THEORETICAL **********	
DV/U	FY/FZ	J2	J5	J5*MU	J5*MS
-3.9E-04	-.0176956522	-.516194944	-.26654215	-.0218564563	-.0218564563
9.1E-04	.0273478261	1.20445487	.264158195	.021660972	.021660972
2.21E-03	.0498695652	2.92510469	.624738407	.0512285494	.0512285494
3.51E-03	.0675652174	4.6457545	.802322228	.0657904227	.0657904227
4.81E-03	.0756086957	6.36640431	.88372253	.0724652475	.0724652475
6.11E-03	.078826087	8.08705413	.92338391	.0757174094	.0757174094
7.41E-03	.0804347826	9.80770394	.943483118	.0773656157	.0773656157
.01001	.0820434783	13.2490036	.961764483	.0788646874	.0788646874

NEGATIVE ROLLING DIRECTION

*****EXPERIMENTAL*******		**********		THEORETICAL **********	
DV/U	FY/FZ	J2	J5	J5*MU	J5*MS
3.9E-04	8.04347826E-03	.516194944	.0602346368	4.93924021E-03	4.93924021E-03
-9.1E-04	-.0386086956	-1.20445487	-.460353169	-.0377489599	-.0377489599
-2.21E-03	-.0595217391	-2.92510469	-.744008064	-.0610086612	-.0610086612
-3.51E-03	-.0707826087	-4.6457545	-.857775753	-.0703376117	-.0703376117
-4.81E-03	-.0756086957	-6.36640431	-.909405496	-.0745712507	-.0745712507
-6.11E-03	-.078826087	-8.08705413	-.935191171	-.076685676	-.076685676
-7.41E-03	-.0804347826	-9.80770394	-.950806329	-.077966119	-.077966119
-.01001	-.0820434783	-13.2490036	-.962382475	-.0789153629	-.0789153629

APPENDIX VII

This appendix contains the experimental and theoretical data for the traction traces with spin, side slip and longitudinal slip. It consists of the following sub-appendices.

APPENDIX	DESCRIPTION
VII-A	Side slip traces only.
VII-B	Side slip and longitudinal slip combined.
VII-C	Side slip and spin only.
VII-D	Side slip, spin and longitudinal slip.

Side Slip Traction Trace With 0^{o} Spin

The aspect ratio is; 0.5
The slope is; 64.06
The traction coefficient is; 0.0935
The Y factor/cm is; 0.0221052
The X factor/cm is; 0.0026052

∧V/U			Fy/N				
cm	∧V/U	J2	cm	Fy/N (act)	J5 (act)	Fy/N (thy)	J5 (thy)
0	0	0	0	0	0	0	0
0.25	0.0006	0.371	1.85	0.0408	0.437	0.0386	0.413
0.50	0.0013	0.743	2.95	0.0652	0.697	0.0643	0.688
0.75	0.0019	1.115	3.57	0.0789	0.844	0.0780	0.834
1.00	0.0026	1.486	3.85	0.0851	0.910	0.0847	0.906
1.25	0.0032	1.858	4.00	0.0884	0.945	0.0883	0.944
1.50	0.0039	2.230	4.05	0.0895	0.957	0.0901	0.964
2.00	0.0052	2.973	4.15	0.0917	0.981	0.0919	0.983
2.50	0.0065	3.717	4.20	0.0928	0.992	0.0927	0.991
3.00	0.0078	4.460	4.22	0.0932	0.997	0.0930	0.995
3.50	0.0091	5.204	4.22	0.0932	0.997	0.0932	0.997
4.00	0.0104	5.947	4.22	0.0932	0.997	0.0933	0.998
5.00	0.0130	7.434	4.20	0.0928	0.992	0.0934	0.999
6.00	0.0156	8.921	4.20	0.0928	0.992	0.0934	0.999
7.00	0.0182	10.408	4.20	0.0928	0.992	0.0935	1.000
8.00	0.0208	11.895	4.15	0.0917	0.981	0.0935	1.000

Side Slip Traction Trace With 0° Spin

The aspect ratio is; 1.0
The slope is; 57.60
The traction coefficient is; 0.0956
The Y factor/cm is; 0.0173485
The X factor/cm is; 0.0025669

$\Delta V/U$			Fy/N				
cm	$\Delta V/U$	J2	cm	Fy/N (act)	J5 (act)	Fy/N (thy)	J5 (thy)
0	0	0	0	0	0	0	0
0.25	0.0006	0.455	1.85	0.0320	0.335	0.0348	0.364
0.50	0.0012	0.911	3.50	0.0607	0.635	0.0602	0.630
0.75	0.0019	1.366	4.20	0.0728	0.762	0.0752	0.787
1.00	0.0025	1.822	4.80	0.0832	0.871	0.0836	0.874
1.25	0.0032	2.277	5.07	0.0879	0.920	0.0881	0.922
1.50	0.0038	2.733	5.22	0.0905	0.947	0.0907	0.949
2.00	0.0051	3.644	5.35	0.0928	0.970	0.0932	0.975
2.50	0.0064	4.555	5.40	0.0936	0.979	0.0944	0.987
3.00	0.0077	5.466	5.45	0.0945	0.989	0.0948	0.992
3.50	0.0089	6.377	5.50	0.0954	0.998	0.0951	0.995
4.00	0.0102	7.288	5.50	0.0954	0.998	0.0952	0.996
5.00	0.0128	9.110	5.52	0.0957	1.001	0.0954	0.998
6.00	0.0154	10.932	5.50	0.0954	0.998	0.0955	0.999
7.00	0.0179	12.754	5.50	0.0954	0.998	0.0955	0.999
8.00	0.0205	14.576	5.50	0.0954	0.998	0.0956	1.000

Side Slip Traction Trace With 0° Spin

The aspect ratio is; 2.0
The slope is; 54.40
The traction coefficient is; 0.100
The Y factor/cm is; 0.0145373
The X factor/cm is; 0.0025669

V/U			Fy/N				
cm	V/U	J2	cm	Fy/N (act)	J5 (act)	Fy/N (thy)	J5 (thy)
0	0	0	0	0	0	0	0
0.25	0.0006	0.581	2.00	0.0290	0.290	0.0332	0.332
0.50	0.0012	1.163	4.00	0.0581	0.581	0.0588	0.588
0.75	0.0019	1.744	5.15	0.0748	0.748	0.0750	0.750
1.00	0.0025	2.326	5.90	0.0857	0.857	0.0846	0.846
1.25	0.0032	2.908	6.32	0.0918	0.918	0.0902	0.902
1.50	0.0038	3.489	6.50	0.0944	0.944	0.0935	0.935
2.00	0.0051	4.653	6.70	0.0973	0.973	0.0968	0.968
2.50	0.0064	5.816	6.75	0.0981	0.981	0.0982	0.982
3.00	0.0077	6.979	6.80	0.0988	0.988	0.0989	0.989
3.50	0.0089	8.142	6.80	0.0988	0.988	0.0993	0.993
4.00	0.0102	9.306	6.80	0.0988	0.988	0.0995	0.995
5.00	0.0128	11.632	6.77	0.0984	0.984	0.0998	0.998
6.00	0.0154	13.959	6.75	0.0981	0.981	0.0999	0.999
7.00	0.0179	16.285	6.70	0.0973	0.973	0.0999	0.999
8.00	0.0205	18.612	6.65	0.0966	0.966	0.1000	1.000

Side Slip Traction Trace With 0° Spin

The aspect ratio is; 5.0
The slope is; 52.40
The traction coefficient is; 0.089
The Y factor/cm is; 0.0151398
The X factor/cm is; 0.0026248

ΔV/U			Fy/N				
cm	ΔV/U	J2	cm	Fy/N (act)	J5 (act)	Fy/N (thy)	J5 (thy)
0	0	0	0	0	0	0	0
0.25	0.0006	1.017	2.25	0.0340	0.382	0.0324	0.364
0.50	0.0013	2.035	3.75	0.0567	0.637	0.0561	0.630
0.75	0.0019	3.053	4.60	0.0696	0.782	0.0700	0.787
1.00	0.0026	4.071	5.10	0.0772	0.867	0.0778	0.874
1.25	0.0032	5.088	5.37	0.0813	0.913	0.0821	0.922
1.50	0.0039	6.106	5.55	0.0840	0.944	0.0845	0.949
2.00	0.0052	8.142	5.67	0.0858	0.964	0.0868	0.975
2.50	0.0065	10.177	5.75	0.0870	0.978	0.0878	0.987
3.00	0.0078	12.213	5.75	0.0870	0.978	0.0883	0.992
3.50	0.0091	14.248	5.80	0.0878	0.986	0.0886	0.995
4.00	0.0104	16.284	5.80	0.0878	0.986	0.0886	0.996
5.00	0.0131	20.355	5.87	0.0888	0.998	0.0888	0.998
6.00	0.0157	24.426	5.80	0.0878	0.986	0.0888	0.998
7.00	0.0183	28.497	5.75	0.0870	0.978	0.0889	0.999
8.00	0.0209	32.568	5.75	0.0870	0.978	0.0890	1.000

Longitudinal Traction Trace With 0° Spin including side slip

The aspect ratio is; 0.5
The slope is; 66.74
The traction coefficient is; 0.0935
The Y factor/cm is; 0.0168621
The X factor/cm is; 0.0089113

	U/U cm	ΔU/U	J1	Fx/N cm	Fx/N (act)	J4 (act)	F_x/N (thy)	J4 (thy)	J2
	0	0	0	0	0	0	0	0	0.152
	0.25	0.0022	1.32	5.70	0.096	1.027	0.082	0.876	0.152
	0.50	0.0044	2.64	6.37	0.107	1.148	0.091	0.975	0.152
	0.75	0.0066	3.97	6.75	0.113	1.217	0.093	0.991	0.152
	1.00	0.0089	5.29	6.90	0.116	1.244	0.093	0.996	0.152
A	1.25	0.0111	6.62	6.95	0.117	1.253	0.093	0.998	0.152
	1.50	0.0133	7.94	7.02	0.118	1.266	0.093	0.998	0.152
	2.00	0.0178	10.59	7.10	0.119	1.280	0.093	0.999	0.152
	2.50	0.0222	13.24	7.15	0.120	1.289	0.093	0.999	0.152
	3.00	0.0267	15.89	7.10	0.119	1.280	0.093	0.999	0.152
	4.00	0.0356	21.19	6.95	0.117	1.253	0.093	0.999	0.152
	0	0	0	0	0	0	0	0	1.516
	0.25	0.0022	1.32	4.50	0.075	0.811	0.059	0.627	1.516
	0.50	0.0044	2.64	5.75	0.096	1.036	0.080	0.854	1.516
	0.75	0.0066	3.97	6.25	0.105	1.127	0.087	0.928	1.516
	1.00	0.0089	5.29	6.55	0.110	1.181	0.090	0.958	1.516
B	1.25	0.0111	6.62	6.70	0.112	1.208	0.091	0.973	1.516
	1.50	0.0133	7.94	6.80	0.114	1.226	0.092	0.981	1.516
	2.00	0.0178	10.59	6.95	0.117	1.253	0.092	0.989	1.516
	2.50	0.0222	13.24	7.05	0.118	1.271	0.093	0.993	1.516
	3.00	0.0267	15.89	7.02	0.118	1.266	0.093	0.995	1.516
	4.00	0.0356	21.19	6.90	0.116	1.244	0.093	0.997	1.516
	0	0	0	0	0	0	0	0	5.306
	0.25	0.0022	1.32	1.72	0.029	0.310	0.023	0.241	5.306
	0.50	0.0044	2.64	3.00	0.050	0.541	0.042	0.445	5.306
	0.75	0.0066	3.97	4.08	0.068	0.735	0.056	0.598	5.306
	1.00	0.0089	5.29	4.80	0.080	0.865	0.066	0.705	5.306
C	1.50	0.0133	7.94	5.65	0.095	1.018	0.078	0.831	5.306
	2.00	0.0178	10.59	6.10	0.102	1.100	0.083	0.893	5.306
	2.50	0.0222	13.24	6.35	0.107	1.145	0.087	0.928	5.306
	3.00	0.0267	15.89	6.50	0.109	1.172	0.089	0.948	5.306
	4.00	0.0356	21.19	6.57	0.110	1.184	0.091	0.970	5.306
	5.00	0.0445	26.49	6.50	0.109	1.172	0.092	0.980	5.306
	0	0	0	0	0	0	0	0	10.764
	0.25	0.0022	1.32	0.85	0.014	0.153	0.011	0.122	10.764
	0.50	0.0044	2.64	1.75	0.029	0.315	0.022	0.238	10.764
	1.00	0.0089	5.29	3.00	0.050	0.541	0.041	0.441	10.764
	1.50	0.0133	7.94	4.00	0.067	0.721	0.055	0.593	10.764
D	2.00	0.0178	10.59	4.67	0.078	0.842	0.066	0.701	10.764
	3.00	0.0267	15.89	5.55	0.093	1.000	0.077	0.827	10.764
	4.00	0.0356	21.19	5.90	0.099	1.064	0.083	0.891	10.764
	5.00	0.0445	26.49	6.00	0.101	1.082	0.087	0.926	10.764
	6.00	0.0534	31.79	6.08	0.102	1.096	0.089	0.947	10.764
	7.00	0.0623	37.09	6.07	0.102	1.094	0.090	0.960	10.764

Longitudinal Traction Trace With 0° Spin including side slip

The aspect ratio is; 1.0
The slope is; 65.19
The traction coefficient is; 0.0956
The Y factor/cm is; 0.0146718
The X factor/cm is; 0.0109629

	△U/U			Fx/N				
	cm	△U/U	J1	cm	Fx/N (act)	J4 (act)	Fx/N (thy)	J4 (thy)	J2
	0	0	0	0	0	0	0	0	0.0001
	0.25	0.0027	2.20	5.30	0.077	0.813	0.087	0.915	0.0001
	0.50	0.0054	4.40	5.90	0.086	0.905	0.094	0.985	0.0001
	0.75	0.0082	6.60	6.07	0.089	0.931	0.095	0.995	0.0001
	1.00	0.0109	8.80	6.22	0.091	0.954	0.095	0.997	0.0001
A	1.25	0.0137	11.00	6.27	0.091	0.962	0.095	0.998	0.0001
	1.50	0.0164	13.21	6.32	0.092	0.969	0.096	0.999	0.0001
	2.00	0.0219	17.61	6.37	0.093	0.977	0.096	0.999	0.0001
	2.50	0.0274	22.01	6.40	0.093	0.982	0.096	0.999	0.0001
	3.00	0.0328	26.42	6.37	0.093	0.977	0.096	0.999	0.0001
	4.00	0.0438	35.22	6.27	0.091	0.962	0.096	0.999	0.0001
	0	0	0	0	0	0	0	0	0.892
	0.25	0.0027	2.20	5.00	0.073	0.767	0.082	0.860	0.892
	0.50	0.0054	4.40	5.72	0.083	0.877	0.092	0.966	0.892
	0.75	0.0082	6.60	6.00	0.088	0.920	0.094	0.986	0.892
	1.00	0.0109	8.80	6.20	0.090	0.951	0.095	0.992	0.892
B	1.25	0.0137	11.00	6.30	0.092	0.966	0.095	0.995	0.892
	1.50	0.0164	13.21	6.32	0.092	0.969	0.095	0.997	0.892
	2.00	0.0219	17.61	6.37	0.093	0.977	0.095	0.998	0.892
	2.50	0.0274	22.01	6.40	0.093	0.982	0.096	0.999	0.892
	3.00	0.0328	26.42	6.40	0.093	0.982	0.096	0.999	0.892
	4.00	0.0438	35.22	6.25	0.091	0.959	0.096	0.999	0.892
	0	0	0	0	0	0	0	0	4.855
	0.25	0.0027	2.20	2.70	0.039	0.414	0.039	0.409	4.855
	0.50	0.0054	4.40	4.00	0.058	0.613	0.064	0.668	4.855
	0.75	0.0082	6.60	4.85	0.071	0.744	0.077	0.803	4.855
	1.00	0.0109	8.80	5.23	0.076	0.802	0.084	0.874	4.855
C	1.50	0.0164	13.21	5.80	0.085	0.890	0.090	0.938	4.855
	2.00	0.0219	17.61	6.00	0.088	0.920	0.092	0.963	4.855
	2.50	0.0274	22.01	6.10	0.089	0.936	0.093	0.976	4.855
	3.00	0.0328	26.42	6.15	0.090	0.943	0.094	0.983	4.855
	4.00	0.0438	35.22	6.12	0.089	0.939	0.095	0.990	4.855
	5.00	0.0548	44.03	6.02	0.088	0.923	0.095	0.993	4.855
	0	0	0	0	0	0	0	0	14.170
	0.25	0.0027	2.20	1.00	0.014	0.153	0.014	0.153	14.170
	0.50	0.0054	4.40	1.77	0.025	0.271	0.028	0.296	14.170
	1.00	0.0109	8.80	3.10	0.045	0.475	0.050	0.527	14.170
	1.50	0.0164	13.21	4.02	0.058	0.616	0.065	0.681	14.170
D	2.00	0.0219	17.61	4.62	0.067	0.709	0.074	0.779	14.170
	3.00	0.0328	26.42	5.20	0.076	0.798	0.084	0.881	14.170
	4.00	0.0438	35.22	5.50	0.080	0.844	0.089	0.927	14.170
	5.00	0.0548	44.03	5.55	0.081	0.851	0.091	0.951	14.170
	6.00	0.0657	52.84	5.55	0.081	0.851	0.092	0.965	14.170
	7.00	0.0767	61.64	5.52	0.080	0.847	0.093	0.974	14.170

Longitudinal Traction Trace With 0° Spin including side slip

The aspect ratio is; 2.0
The slope is; 62.78
The traction coefficient is; 0.100
The Y factor/cm is; 0.0137539
The X factor/cm is; 0.0045806

	ΔU/U			Fx/N					
	cm	ΔU/U	J1	cm	Fx/N (act)	J4 (act)	Fx/N (thy)	J4 (thy)	J2
	0	0	0	0	0	0	0	0	0.0001
	0.25	0.0011	1.19	4.60	0.063	0.632	0.060	0.599	0.0001
	0.50	0.0022	2.39	6.20	0.085	0.852	0.085	0.854	0.0001
	0.75	0.0034	3.59	6.82	0.093	0.938	0.094	0.939	0.0001
	1.00	0.0045	4.79	7.10	0.097	0.976	0.097	0.970	0.0001
A	1.25	0.0057	5.98	7.25	0.099	0.997	0.098	0.983	0.0001
	1.50	0.0068	7.18	7.30	0.100	1.004	0.099	0.990	0.0001
	2.00	0.0091	9.58	7.37	0.101	1.013	0.099	0.995	0.0001
	2.50	0.0114	11.97	7.37	0.101	1.013	0.100	0.997	0.0001
	3.00	0.0137	14.37	7.37	0.101	1.013	0.100	0.998	0.0001
	4.00	0.0183	19.16	7.32	0.100	1.006	0.100	0.999	0.0001
	0	0	0	0	0	0	0	0	1.768
	0.25	0.0011	1.19	3.25	0.044	0.447	0.046	0.460	1.768
	0.50	0.0022	2.39	5.10	0.070	0.701	0.073	0.729	1.768
	0.75	0.0034	3.59	5.97	0.082	0.821	0.086	0.855	1.768
	1.00	0.0045	4.79	6.50	0.089	0.894	0.091	0.914	1.768
B	1.25	0.0057	5.98	6.80	0.093	0.935	0.095	0.945	1.768
	1.50	0.0068	7.18	6.97	0.095	0.958	0.096	0.962	1.768
	2.00	0.0091	9.58	7.15	0.098	0.983	0.098	0.979	1.768
	2.50	0.0114	11.97	7.22	0.099	0.993	0.099	0.987	1.768
	3.00	0.0137	14.37	7.25	0.099	0.997	0.099	0.991	1.768
	4.00	0.0183	19.16	7.25	0.099	0.997	0.099	0.995	1.768
	0	0	0	0	0	0	0	0	7.072
	0.25	0.0011	1.19	1.10	0.015	0.151	0.017	0.165	7.072
	0.50	0.0022	2.39	2.05	0.028	0.281	0.032	0.317	7.072
	1.00	0.0045	4.79	3.40	0.046	0.467	0.056	0.557	7.072
	1.50	0.0068	7.18	4.65	0.063	0.639	0.071	0.710	7.072
C	2.00	0.0091	9.58	5.37	0.073	0.738	0.080	0.802	7.072
	3.00	0.0137	14.37	6.17	0.084	0.848	0.090	0.896	7.072
	4.00	0.0183	19.16	6.55	0.090	0.900	0.094	0.937	7.072
	5.00	0.0229	23.95	6.72	0.092	0.924	0.096	0.958	7.072
	6.00	0.0274	28.74	6.77	0.093	0.931	0.097	0.970	7.072
	7.00	0.0320	33.53	6.77	0.093	0.931	0.098	0.978	7.072
	0	0	0	0	0	0	0	0	16.797
	1.00	0.0045	4.79	1.70	0.023	0.233	0.027	0.274	16.797
	2.00	0.0091	9.58	3.00	0.041	0.412	0.050	0.495	16.797
	3.00	0.0137	14.37	4.02	0.055	0.552	0.065	0.649	16.797
	4.00	0.0183	19.16	4.65	0.063	0.639	0.075	0.751	16.797
D	5.00	0.0229	23.95	5.20	0.071	0.715	0.082	0.818	16.797
	6.00	0.0274	28.74	5.50	0.075	0.756	0.086	0.863	16.797
	7.00	0.0320	33.53	5.67	0.077	0.779	0.089	0.894	16.797
	8.00	0.0366	38.32	5.77	0.079	0.793	0.092	0.915	16.797
	9.00	0.0412	43.12	5.85	0.080	0.804	0.093	0.931	16.797
	12.00	0.0549	57.49	5.90	0.081	0.811	0.096	0.959	16.797

Longitudinal Traction Trace With 0° Spin including side slip

The aspect ratio is; 5.0
The slope is; 61.10
The traction coefficient is; 0.089
The Y factor/cm is; 0.0128688
The X factor/cm is; 0.0023956

	ΔU/U		Fx/N					
	cm	ΔU/U	J1	cm	Fx/N (act)	J4 (act)	Fx/N (thy)	J4 (thy)	J2
	0	0	0	0	0	0	0	0	0.0001
	0.25	0.0005	1.08	3.35	0.043	0.484	0.034	0.385	0.0001
	0.50	0.0011	2.16	4.80	0.061	0.694	0.058	0.655	0.0001
	0.75	0.0017	3.24	5.50	0.070	0.795	0.072	0.808	0.0001
	1.00	0.0023	4.33	5.90	0.075	0.853	0.079	0.888	0.0001
A	1.25	0.0029	5.41	6.30	0.081	0.910	0.083	0.931	0.0001
	1.50	0.0035	6.49	6.40	0.082	0.925	0.085	0.956	0.0001
	2.00	0.0047	8.66	6.60	0.084	0.954	0.087	0.979	0.0001
	2.50	0.0059	10.83	6.65	0.085	0.961	0.088	0.988	0.0001
	3.00	0.0071	12.99	6.75	0.086	0.976	0.088	0.993	0.0001
	4.00	0.0095	17.32	6.80	0.087	0.983	0.089	0.998	0.0001
	0	0	0	0	0	0	0	0	2.560
	0.25	0.0005	1.08	2.00	0.025	0.289	0.026	0.293	2.560
	0.50	0.0011	2.16	3.60	0.046	0.520	0.047	0.528	2.560
	1.00	0.0023	4.33	5.35	0.068	0.773	0.070	0.791	2.560
	1.50	0.0035	6.49	6.00	0.077	0.867	0.080	0.896	2.560
B	2.00	0.0047	8.66	6.37	0.081	0.921	0.084	0.941	2.560
	3.00	0.0071	12.99	6.37	0.081	0.921	0.087	0.974	2.560
	4.00	0.0095	17.32	6.80	0.087	0.983	0.088	0.986	2.560
	5.00	0.0119	21.66	7.00	0.090	1.012	0.088	0.991	2.560
	6.00	0.0143	25.99	7.00	0.090	1.012	0.088	0.994	2.560
	7.00	0.0167	30.32	7.00	0.090	1.012	0.089	0.995	2.560
	0	0	0	0	0	0	0	0	10.832
	1.00	0.0023	4.33	2.10	0.027	0.303	0.033	0.367	10.832
	2.00	0.0047	8.66	3.85	0.049	0.556	0.055	0.621	10.832
	3.00	0.0071	12.99	4.95	0.063	0.715	0.068	0.765	10.832
	4.00	0.0095	17.32	5.55	0.071	0.802	0.075	0.846	10.832
C	5.00	0.0119	21.66	5.95	0.076	0.860	0.079	0.893	10.832
	6.00	0.0143	25.99	6.30	0.081	0.910	0.082	0.922	10.832
	7.00	0.0167	30.32	6.40	0.082	0.925	0.084	0.941	10.832
	8.00	0.0191	34.65	6.50	0.083	0.939	0.085	0.954	10.832
	9.00	0.0215	38.99	6.55	0.084	0.947	0.086	0.963	10.832
	12.00	0.0287	51.98	6.60	0.084	0.954	0.087	0.978	10.832
	0	0	0	0	0	0	0	0	27.965
	1.00	0.0023	4.33	0.90	0.011	0.130	0.014	0.152	27.965
	2.00	0.0047	8.66	1.67	0.021	0.241	0.026	0.295	27.965
	3.00	0.0071	12.99	2.37	0.030	0.342	0.037	0.421	27.965
	4.00	0.0095	17.32	3.00	0.038	0.433	0.047	0.526	27.965
D	5.00	0.0119	21.66	3.50	0.045	0.506	0.054	0.612	27.965
	6.00	0.0143	25.99	3.92	0.050	0.566	0.061	0.680	27.965
	7.00	0.0167	30.32	4.25	0.054	0.614	0.065	0.734	27.965
	8.00	0.0191	34.65	4.55	0.058	0.657	0.069	0.778	27.965
	9.00	0.0215	38.99	4.72	0.060	0.682	0.072	0.812	27.965
	12.00	0.0287	51.98	5.12	0.065	0.740	0.078	0.880	27.965

Side Slip Traction Trace With 6° Spin

The aspect ratio is; 0.5

The traction coefficient is; 0.0935
The Y factor/cm is; 0.0216799
The X factor/cm is; 0.0026052

V/U cm	V/U	J2	Fy/N cm	Fy/N (act)	J5 (act)	Fy/N (thy)	J5 (thy)	J3
0	0	0	-1.55	-0.034	-0.359	-0.027	-0.285	0.6044
0.25	0.0007	0.372	0.00	0.000	0.000	0.012	0.126	0.6044
0.50	0.0013	0.744	1.73	0.038	0.401	0.041	0.443	0.6044
0.75	0.0020	1.115	2.74	0.059	0.635	0.061	0.657	0.6044
1.00	0.0026	1.487	3.48	0.075	0.807	0.074	0.792	0.6044
1.25	0.0033	1.859	3.95	0.086	0.916	0.082	0.872	0.6044
1.50	0.0039	2.230	4.25	0.092	0.985	0.086	0.920	0.6044
2.00	0.0052	2.974	4.50	0.098	1.043	0.090	0.965	0.6044
2.50	0.0065	3.717	4.60	0.100	1.067	0.092	0.982	0.6044
3.00	0.0078	4.461	4.60	0.100	1.067	0.092	0.989	0.6044
3.50	0.0091	5.204	4.65	0.101	1.078	0.093	0.993	0.6044
4.00	0.0104	5.947	4.65	0.101	1.078	0.093	0.995	0.6044
5.00	0.0130	7.437	4.60	0.100	1.067	0.093	0.997	0.6044
6.00	0.0156	8.921	4.55	0.099	1.055	0.093	0.998	0.6044
7.00	0.0182	10.405	4.55	0.099	1.055	0.093	0.998	0.6044
8.00	0.0208	11.894	4.50	0.098	1.043	0.093	0.998	0.6044
0	0	0	-1.55	-0.034	-0.359	-0.027	-0.285	-0.6044
0.25	0.0007	0.372	-2.90	-0.063	-0.672	-0.063	-0.676	-0.6044
0.50	0.0013	0.744	-3.90	-0.085	-0.904	-0.080	-0.855	-0.6044
0.75	0.0020	1.115	-4.25	-0.092	-0.985	-0.086	-0.922	-0.6044
1.00	0.0026	1.487	-4.45	-0.096	-1.032	-0.089	-0.953	-0.6044
1.25	0.0033	1.859	-4.50	-0.098	-1.043	-0.091	-0.969	-0.6044
1.50	0.0039	2.230	-4.55	-0.099	-1.055	-0.091	-0.978	-0.6044
2.00	0.0052	2.974	-4.60	-0.100	-1.067	-0.092	-0.988	-0.6044
2.50	0.0065	3.717	-4.60	-0.100	-1.067	-0.093	-0.992	-0.6044
3.00	0.0078	4.461	-4.60	-0.100	-1.067	-0.093	-0.995	-0.6044
3.50	0.0091	5.204	-4.60	-0.100	-1.067	-0.093	-0.996	-0.6044
4.00	0.0104	5.947	-4.60	-0.100	-1.067	-0.093	-0.997	-0.6044
5.00	0.0130	7.437	-4.57	-0.099	-1.060	-0.093	-0.998	-0.6044
6.00	0.0156	8.921	-4.55	-0.099	-1.055	-0.093	-0.998	-0.6044
7.00	0.0182	10.405	-4.50	-0.098	-1.043	-0.093	-0.998	-0.6044
8.00	0.0208	11.894	-4.50	-0.098	-1.043	-0.093	-0.998	-0.6044

Side Slip Traction Trace With 6° Spin

The aspect ratio is; 1.0

The traction coefficient is; 0.0956
The Y factor/cm is; 0.0169199
The X factor/cm is; 0.0026052

V/U cm	V/U	J2	Fy/N cm	Fy/N (act)	J5 (act)	Fy/N (thy)	J5 (thy)	J3
0	0	0	-1.00	-0.017	-0.177	-0.024	-0.254	1.0832
0.25	0.0007	0.462	0.85	0.014	0.150	0.010	0.100	1.0832
0.50	0.0013	0.925	2.65	0.045	0.469	0.037	0.390	1.0832
0.75	0.0020	1.387	3.65	0.062	0.646	0.057	0.598	1.0832
1.00	0.0026	1.849	4.40	0.074	0.779	0.071	0.739	1.0832
1.25	0.0033	2.312	5.00	0.085	0.885	0.079	0.830	1.0832
1.50	0.0039	2.774	5.50	0.093	0.973	0.085	0.887	1.0832
2.00	0.0052	3.698	5.80	0.098	1.027	0.090	0.946	1.0832
2.50	0.0065	4.623	5.90	0.100	1.044	0.093	0.971	1.0832
3.00	0.0078	5.548	5.93	0.100	1.049	0.094	0.983	1.0832
3.50	0.0091	6.472	5.95	0.101	1.053	0.095	0.989	1.0832
4.00	0.0104	7.396	6.00	0.102	1.062	0.095	0.992	1.0832
5.00	0.0130	9.249	6.00	0.102	1.062	0.095	0.995	1.0832
6.00	0.0156	11.094	5.95	0.101	1.053	0.095	0.996	1.0832
7.00	0.0182	12.947	5.95	0.101	1.053	0.095	0.997	1.0832
8.00	0.0208	14.793	5.80	0.098	1.027	0.095	0.997	1.0832
0	0	0	-1.00	-0.017	-0.177	-0.024	-0.254	-1.0832
0.25	0.0007	0.462	-3.10	-0.052	-0.549	-0.056	-0.591	-1.0832
0.50	0.0013	0.925	-4.50	-0.076	-0.796	-0.075	-0.788	-1.0832
0.75	0.0020	1.387	-5.20	-0.088	-0.920	-0.084	-0.877	-1.0832
1.00	0.0026	1.849	-5.50	-0.093	-0.973	-0.088	-0.922	-1.0832
1.25	0.0033	2.312	-5.75	-0.097	-1.018	-0.091	-0.947	-1.0832
1.50	0.0039	2.774	-5.80	-0.098	-1.027	-0.092	-0.962	-1.0832
2.00	0.0052	3.698	-5.90	-0.100	-1.044	-0.093	-0.978	-1.0832
2.50	0.0065	4.623	-5.95	-0.101	-1.053	-0.094	-0.986	-1.0832
3.00	0.0078	5.548	-5.95	-0.101	-1.053	-0.095	-0.990	-1.0832
3.50	0.0091	6.472	-5.95	-0.101	-1.053	-0.095	-0.993	-1.0832
4.00	0.0104	7.396	-5.95	-0.101	-1.053	-0.095	-0.994	-1.0832
5.00	0.0130	9.249	-5.90	-0.100	-1.044	-0.095	-0.996	-1.0832
6.00	0.0156	11.094	-5.85	-0.099	-1.035	-0.095	-0.997	-1.0832
7.00	0.0182	12.947	-5.85	-0.099	-1.035	-0.095	-0.997	-1.0832
8.00	0.0208	14.793	-5.80	-0.098	-1.027	-0.095	-0.997	-1.0832

Side Slip Traction Trace With 6° Spin

The aspect ratio is; 2.0

The traction coefficient is; 0.100
The Y factor/cm is; 0.0156251
The X factor/cm is; 0.0026446

V/U cm	ΔV/U	J2	Fy/N cm	Fy/N (act)	J5 (act)	Fy/N (thy)	J5 (thy)	J3
0	0	0	-0.83	-0.013	-0.130	-0.017	-0.169	1.4603
0.25	0.0007	0.599	1.10	0.017	0.172	0.015	0.145	1.4603
0.50	0.0013	1.198	2.70	0.042	0.422	0.041	0.407	1.4603
0.75	0.0020	1.797	3.60	0.056	0.563	0.060	0.601	1.4603
1.00	0.0026	2.397	4.45	0.070	0.653	0.073	0.733	1.4603
1.25	0.0033	2.996	5.10	0.080	0.797	0.082	0.820	1.4603
1.50	0.0040	3.595	5.47	0.085	0.855	0.088	0.876	1.4603
2.00	0.0053	4.794	5.90	0.092	0.922	0.094	0.937	1.4603
2.50	0.0066	5.993	6.07	0.095	0.948	0.096	0.964	1.4603
3.00	0.0079	7.191	6.17	0.096	0.964	0.098	0.977	1.4603
3.50	0.0093	8.389	6.20	0.097	0.969	0.098	0.984	1.4603
4.00	0.0106	9.589	6.25	0.098	0.977	0.099	0.989	1.4603
5.00	0.0132	11.982	6.25	0.098	0.977	0.099	0.993	1.4603
6.00	0.0159	14.384	6.25	0.098	0.977	0.100	0.995	1.4603
7.00	0.0185	16.777	6.25	0.098	0.977	0.100	0.996	1.4603
8.00	0.0212	19.178	6.25	0.098	0.977	0.100	0.997	1.4603
0	0	0	-0.83	-0.013	-0.130	-0.017	-0.169	-1.4603
0.25	0.0007	0.599	-2.95	-0.046	-0.461	-0.047	-0.473	-1.4603
0.50	0.0013	1.198	-4.10	-0.064	-0.641	-0.069	-0.687	-1.4603
0.75	0.0020	1.797	-4.80	-0.075	-0.750	-0.081	-0.808	-1.4603
1.00	0.0026	2.397	-5.35	-0.084	-0.836	-0.087	-0.874	-1.4603
1.25	0.0033	2.996	-5.55	-0.087	-0.867	-0.091	-0.913	-1.4603
1.50	0.0040	3.595	-5.75	-0.090	-0.898	-0.094	-0.938	-1.4603
2.00	0.0053	4.794	-6.00	-0.094	-0.938	-0.096	-0.964	-1.4603
2.50	0.0066	5.993	-6.10	-0.095	-0.953	-0.098	-0.977	-1.4603
3.00	0.0079	7.191	-6.20	-0.097	-0.969	-0.098	-0.984	-1.4603
3.50	0.0093	8.389	-6.25	-0.098	-0.977	-0.099	-0.988	-1.4603
4.00	0.0106	9.589	-6.30	-0.098	-0.984	-0.099	-0.991	-1.4603
5.00	0.0132	11.982	-6.30	-0.098	-0.984	-0.099	-0.994	-1.4603
6.00	0.0159	14.384	-6.30	-0.098	-0.984	-0.100	-0.996	-1.4603
7.00	0.0185	16.777	-6.25	-0.098	-0.977	-0.100	-0.996	-1.4603
8.00	0.0212	19.178	-6.25	-0.098	-0.977	-0.100	-0.997	-1.4603

Side Slip Traction Trace With 6° Spin

The aspect ratio is; 5.0

The traction coefficient is; 0.089
The Y factor/cm is; 0.0153200
The X factor/cm is; 0.0026648

ΔV/U			Fy/N					
cm	ΔV/U	J2	cm	Fy/N (act)	J5 (act)	Fy/N (thy)	J5 (thy)	J3
0	0	0	-0.75	-0.011	-0.129	-0.012	-0.140	3.7003
0.25	0.0007	1.033	0.62	0.009	0.107	0.011	0.126	3.7003
0.50	0.0013	2.067	1.85	0.028	0.318	0.032	0.358	3.7003
0.75	0.0020	3.100	2.90	0.044	0.499	0.048	0.535	3.7003
1.00	0.0027	4.133	3.65	0.056	0.628	0.059	0.663	3.7003
1.25	0.0033	5.166	4.23	0.065	0.728	0.067	0.752	3.7003
1.50	0.0040	6.199	4.65	0.071	0.800	0.072	0.814	3.7003
2.00	0.0053	8.267	5.10	0.078	0.878	0.079	0.887	3.7003
2.50	0.0067	10.333	5.37	0.082	0.924	0.082	0.925	3.7003
3.00	0.0080	12.399	5.45	0.083	0.938	0.084	0.947	3.7003
3.50	0.0093	14.466	5.50	0.084	0.947	0.085	0.959	3.7003
4.00	0.0107	16.533	5.57	0.085	0.959	0.086	0.966	3.7003
5.00	0.0133	20.659	5.62	0.086	0.967	0.087	0.974	3.7003
6.00	0.0160	24.800	5.62	0.086	0.967	0.087	0.978	3.7003
7.00	0.0187	28.926	5.60	0.086	0.964	0.087	0.980	3.7003
8.00	0.0213	33.067	5.57	0.085	0.959	0.087	0.983	3.7003
0	0	0	-0.75	-0.011	-0.129	-0.012	-0.140	-3.7003
0.25	0.0007	1.033	-2.05	-0.031	-0.353	-0.035	-0.388	-3.7003
0.50	0.0013	2.067	-3.30	-0.051	-0.568	-0.051	-0.575	-3.7003
0.75	0.0020	3.100	-3.95	-0.061	-0.680	-0.062	-0.695	-3.7003
1.00	0.0027	4.133	-4.40	-0.067	-0.757	-0.069	-0.773	-3.7003
1.25	0.0033	5.166	-4.70	-0.072	-0.809	-0.074	-0.827	-3.7003
1.50	0.0040	6.199	-4.95	-0.076	-0.852	-0.077	-0.864	-3.7003
2.00	0.0053	8.267	-5.22	-0.080	-0.899	-0.081	-0.911	-3.7003
2.50	0.0067	10.333	-5.35	-0.082	-0.921	-0.083	-0.937	-3.7003
3.00	0.0080	12.399	-5.47	-0.084	-0.942	-0.085	-0.953	-3.7003
3.50	0.0093	14.466	-5.52	-0.085	-0.950	-0.086	-0.964	-3.7003
4.00	0.0107	16.533	-5.60	-0.086	-0.964	-0.086	-0.971	-3.7003
5.00	0.0133	20.659	-5.60	-0.086	-0.964	-0.087	-0.979	-3.7003
6.00	0.0160	24.800	-5.60	-0.086	-0.964	-0.087	-0.983	-3.7003
7.00	0.0187	28.926	-5.57	-0.085	-0.959	-0.088	-0.986	-3.7003
8.00	0.0213	33.067	-5.55	-0.085	-0.955	-0.088	-0.988	-3.7003

Longitudinal Traction Trace With 6° Spin including side slip

The aspect ratio is; 0.5

The traction coefficient is; 0.0935
The Y factor/cm is; 0.0136310
The X factor/cm is; 0.0090103

	cm	ΔU/U	J1	Fx/N cm	Fx/N (act)	J4 (act)	Fx/N (thy)	J4 (thy)	J2
	0	0	0	0	0	0	0	0	0.0001
	0.25	0.0023	1.34	5.65	0.077	0.824	0.081	0.864	0.0001
	0.50	0.0045	2.68	6.45	0.088	0.940	0.091	0.969	0.0001
	0.75	0.0068	4.02	6.70	0.091	0.977	0.092	0.987	0.0001
	1.00	0.0090	5.36	6.90	0.094	1.006	0.092	0.988	0.0001
A	1.25	0.0113	6.70	7.00	0.095	1.021	0.092	0.989	0.0001
	1.50	0.0135	8.04	7.10	0.097	1.035	0.092	0.989	0.0001
	2.00	0.0180	10.72	7.25	0.099	1.057	0.093	0.990	0.0001
	2.50	0.0225	13.40	7.30	0.100	1.064	0.093	0.990	0.0001
	3.00	0.0270	16.07	7.25	0.099	1.057	0.093	0.990	0.0001
	4.00	0.0360	21.43	7.10	0.097	1.035	0.093	0.990	0.0001
	0	0	0	0	0	0	0	0	1.338
	0.25	0.0023	1.34	4.80	0.065	0.700	0.065	0.700	1.338
	0.50	0.0045	2.68	5.95	0.081	0.867	0.083	0.892	1.338
	0.75	0.0068	4.02	6.40	0.087	0.933	0.088	0.944	1.338
	1.00	0.0090	5.36	6.67	0.091	0.972	0.090	0.964	1.338
B	1.25	0.0113	6.70	6.85	0.093	0.999	0.091	0.973	1.338
	1.50	0.0135	8.04	6.95	0.095	1.013	0.091	0.978	1.338
	2.00	0.0180	10.72	7.12	0.097	1.038	0.092	0.983	1.338
	2.50	0.0225	13.40	7.12	0.097	1.038	0.092	0.986	1.338
	3.00	0.0270	16.07	7.10	0.097	1.035	0.092	0.987	1.338
	4.00	0.0360	21.43	7.02	0.096	1.023	0.092	0.988	1.338
	0	0	0	0	0	0	0	0	5.353
	0.25	0.0023	1.34	1.65	0.022	0.241	0.023	0.246	5.353
	0.50	0.0045	2.68	3.00	0.041	0.437	0.042	0.451	5.353
	0.75	0.0068	4.02	4.05	0.055	0.590	0.056	0.602	5.353
	1.00	0.0090	5.36	4.75	0.065	0.693	0.066	0.706	5.353
C	1.50	0.0135	8.04	5.67	0.077	0.827	0.077	0.827	5.353
	2.00	0.0180	10.72	6.22	0.085	0.907	0.083	0.888	5.353
	2.50	0.0225	13.40	6.40	0.087	0.933	0.086	0.921	5.353
	3.00	0.0270	16.07	6.57	0.090	0.958	0.088	0.940	5.353
	4.00	0.0360	21.43	6.72	0.092	0.980	0.090	0.961	5.353
	5.00	0.0451	26.79	6.65	0.091	0.970	0.091	0.971	5.353
	0	0	0	0	0	0	0	0	12.416
	0.25	0.0023	1.34	0.80	0.011	0.117	0.010	0.107	12.416
	0.50	0.0045	2.68	1.55	0.021	0.226	0.020	0.210	12.416
	1.00	0.0090	5.36	2.70	0.037	0.394	0.037	0.394	12.416
	1.50	0.0135	8.04	3.75	0.051	0.547	0.050	0.540	12.416
D	2.00	0.0180	10.72	4.40	0.060	0.641	0.061	0.648	12.416
	3.00	0.0270	16.07	5.23	0.071	0.762	0.073	0.785	12.416
	4.00	0.0360	21.43	5.73	0.078	0.835	0.080	0.857	12.416
	5.00	0.0451	26.79	5.92	0.081	0.863	0.084	0.899	12.416
	6.00	0.0541	32.15	6.25	0.085	0.911	0.086	0.924	12.416
	7.00	0.0631	37.50	6.20	0.085	0.904	0.088	0.940	12.416

Longitudinal Traction Trace With 6° Spin including side slip

The aspect ratio is; 1.0

The traction coefficient is; 0.0956
The Y factor/cm is; 0.0124639
The X factor/cm is; 0.0110232

	ΔU/U			Fx/N				
	cm	ΔU/U	J1	cm	Fx/N (act)	J4 (act)	Fx/N (thy)	J4 (thy)	J2
	0	0	0	0	0	0	0	0	0.0001
	0.25	0.0028	2.21	6.40	0.080	0.834	0.085	0.891	0.0001
	0.50	0.0055	4.43	7.00	0.087	0.913	0.093	0.976	0.0001
	0.75	0.0083	6.64	7.25	0.090	0.945	0.094	0.988	0.0001
	1.00	0.0110	8.85	7.35	0.092	0.958	0.095	0.989	0.0001
A	1.25	0.0138	11.07	7.42	0.092	0.967	0.095	0.990	0.0001
	1.50	0.0165	13.28	7.50	0.093	0.978	0.095	0.990	0.0001
	2.00	0.0221	17.71	7.52	0.094	0.980	0.095	0.990	0.0001
	2.50	0.0276	22.14	7.45	0.093	0.971	0.095	0.990	0.0001
	3.00	0.0331	26.57	7.35	0.092	0.958	0.095	0.990	0.0001
	4.00	0.0441	35.42	7.12	0.089	0.928	0.095	0.990	0.0001
	0	0	0	0	0	0	0	0	1.204
	0.25	0.0028	2.21	5.85	0.073	0.763	0.079	0.830	1.204
	0.50	0.0055	4.43	6.90	0.086	0.900	0.091	0.953	1.204
	0.75	0.0083	6.64	7.20	0.090	0.939	0.093	0.976	1.204
	1.00	0.0110	8.85	7.35	0.092	0.958	0.094	0.982	1.204
B	1.25	0.0138	11.07	7.42	0.092	0.967	0.094	0.985	1.204
	1.50	0.0165	13.28	7.50	0.093	0.978	0.094	0.986	1.204
	2.00	0.0221	17.71	7.55	0.094	0.984	0.094	0.988	1.204
	2.50	0.0276	22.14	7.53	0.094	0.982	0.095	0.989	1.204
	3.00	0.0331	26.57	7.40	0.092	0.965	0.095	0.989	1.204
	4.00	0.0441	35.42	7.22	0.090	0.941	0.095	0.990	1.204
	0	0	0	0	0	0	0	0	4.777
	0.25	0.0028	2.21	2.75	0.034	0.359	0.041	0.425	4.777
	0.50	0.0055	4.43	4.75	0.059	0.619	0.065	0.683	4.777
	0.75	0.0083	6.64	5.85	0.073	0.763	0.078	0.811	4.777
	1.00	0.0110	8.85	6.32	0.079	0.824	0.084	0.875	4.777
C	1.50	0.0165	13.28	6.85	0.085	0.893	0.089	0.933	4.777
	2.00	0.0220	17.71	7.10	0.088	0.926	0.091	0.957	4.777
	2.50	0.0276	22.14	7.17	0.089	0.935	0.093	0.968	4.777
	3.00	0.0331	26.57	7.17	0.089	0.935	0.093	0.975	4.777
	4.00	0.0441	35.42	7.05	0.088	0.919	0.094	0.982	4.777
	5.00	0.0551	44.28	6.87	0.086	0.896	0.094	0.985	4.777
	0	0	0	0	0	0	0	0	14.150
	0.25	0.0028	2.21	1.00	0.012	0.130	0.015	0.154	14.150
	0.50	0.0055	4.43	2.10	0.026	0.274	0.028	0.297	14.150
	1.00	0.0110	8.85	3.75	0.047	0.489	0.050	0.527	14.150
	1.50	0.0165	13.28	4.85	0.060	0.632	0.065	0.679	14.150
D	2.00	0.0221	17.71	5.50	0.069	0.717	0.074	0.775	14.150
	3.00	0.0331	26.57	6.15	0.077	0.802	0.084	0.875	14.150
	4.00	0.0441	35.42	6.35	0.079	0.828	0.088	0.920	14.150
	5.00	0.0551	44.28	6.37	0.079	0.831	0.090	0.944	14.150
	6.00	0.0661	53.13	6.35	0.079	0.828	0.091	0.957	14.150
	7.00	0.0772	61.99	6.27	0.078	0.817	0.092	0.966	14.150

Longitudinal Traction Trace With 6° Spin including side slip

The aspect ratio is; 2.0

The traction coefficient is; 0.100
The Y factor/cm is; 0.0138367
The X factor/cm is; 0.0046666

	△U/U			Fx/N				
	cm	△U/U	J1	cm	Fx/N (act)	J4 (act)	Fx/N (thy)	J4 (thy)	J2
	0	0	0	0	0	0	0	0	0.0001
	0.25	0.0012	1.22	3.50	0.048	0.484	0.050	0.504	0.0001
	0.50	0.0023	2.44	5.50	0.076	0.761	0.080	0.802	0.0001
	0.75	0.0035	3.66	6.30	0.087	0.872	0.092	0.919	0.0001
	1.00	0.0047	4.88	6.70	0.093	0.927	0.096	0.960	0.0001
A	1.25	0.0058	6.10	6.77	0.094	0.937	0.098	0.976	0.0001
	1.50	0.0070	7.32	6.92	0.096	0.958	0.098	0.983	0.0001
	2.00	0.0093	9.76	7.03	0.097	0.973	0.099	0.989	0.0001
	2.50	0.0117	12.21	7.10	0.098	0.982	0.099	0.990	0.0001
	3.00	0.0140	14.64	7.17	0.099	0.992	0.099	0.990	0.0001
	4.00	0.0187	19.53	7.17	0.099	0.992	0.099	0.990	0.0001
	0	0	0	0	0	0	0	0	2.037
	0.25	0.0012	1.22	2.55	0.035	0.353	0.040	0.404	2.037
	0.50	0.0023	2.44	4.40	0.061	0.609	0.068	0.684	2.037
	0.75	0.0035	3.66	5.50	0.076	0.761	0.083	0.831	2.037
	1.00	0.0047	4.88	6.05	0.084	0.837	0.090	0.900	2.037
B	1.25	0.0058	6.10	6.40	0.089	0.886	0.094	0.935	2.037
	1.50	0.0070	7.32	6.60	0.091	0.913	0.095	0.952	2.037
	2.00	0.0093	9.76	6.82	0.094	0.944	0.097	0.971	2.037
	2.50	0.0117	12.21	6.95	0.096	0.962	0.098	0.978	2.037
	3.00	0.0140	14.64	7.05	0.098	0.976	0.098	0.981	2.037
	4.00	0.0187	19.53	7.05	0.098	0.976	0.099	0.985	2.037
	0	0	0	0	0	0	0	0	8.150
	0.25	0.0012	1.22	1.00	0.014	0.138	0.015	0.147	8.150
	0.50	0.0023	2.44	1.85	0.026	0.256	0.028	0.284	8.150
	1.00	0.0047	4.88	3.30	0.046	0.457	0.051	0.511	8.150
	1.50	0.0070	7.32	4.32	0.060	0.598	0.067	0.665	8.150
C	2.00	0.0093	9.76	5.05	0.070	0.699	0.076	0.763	8.150
	3.00	0.0140	14.64	5.92	0.082	0.819	0.087	0.867	8.150
	4.00	0.0187	19.53	6.32	0.087	0.875	0.092	0.915	8.150
	5.00	0.0233	24.40	6.52	0.090	0.902	0.094	0.940	8.150
	6.00	0.0280	29.29	6.60	0.091	0.913	0.095	0.954	8.150
	7.00	0.0327	34.17	6.60	0.091	0.913	0.096	0.964	8.150
	0	0	0	0	0	0	0	0	18.696
	1.00	0.0047	4.88	1.55	0.021	0.215	0.025	0.251	18.696
	2.00	0.0093	9.76	2.80	0.039	0.387	0.046	0.459	18.696
	3.00	0.0140	14.64	3.80	0.053	0.526	0.061	0.611	18.696
	4.00	0.0187	19.53	4.47	0.062	0.619	0.072	0.716	18.696
D	5.00	0.0233	24.40	4.97	0.069	0.688	0.079	0.787	18.696
	6.00	0.0280	29.29	5.30	0.073	0.733	0.084	0.835	18.696
	7.00	0.0327	34.17	5.50	0.076	0.761	0.087	0.869	18.696
	8.00	0.0373	39.05	5.62	0.078	0.778	0.089	0.894	18.696
	9.00	0.0420	43.93	5.72	0.079	0.792	0.091	0.911	18.696
	12.00	0.0560	58.57	5.83	0.081	0.807	0.094	0.944	18.696

Longitudinal Traction Trace With 6° Spin including side slip

The aspect ratio is; 5.0

The traction coefficient is; 0.089
The Y factor/cm is; 0.0125408
The X factor/cm is; 0.0095925

	cm	ΔU/U	J1	Fx/N cm	Fx/N (act)	J4 (act)	Fx/N (thy)	J4 (thy)	J2
	0	0	0	0	0	0	0	0	0.0001
	0.25	0.0024	4.34	4.65	0.058	0.655	0.056	0.627	0.0001
	0.50	0.0048	8.67	6.45	0.081	0.909	0.083	0.932	0.0001
	0.75	0.0072	13.01	6.97	0.087	0.982	0.087	0.982	0.0001
	1.00	0.0096	17.35	7.10	0.089	1.000	0.088	0.989	0.0001
A	1.25	0.0120	21.68	7.17	0.090	1.010	0.088	0.990	0.0001
	1.50	0.0144	26.02	7.22	0.091	1.017	0.088	0.990	0.0001
	2.00	0.0192	34.71	7.22	0.091	1.017	0.088	0.990	0.0001
	2.50	0.0240	43.37	7.15	0.090	1.008	0.088	0.990	0.0001
	3.00	0.0288	52.05	7.10	0.089	1.000	0.088	0.990	0.0001
	4.00	0.0384	69.39	6.85	0.086	0.965	0.088	0.990	0.0001
	0	0	0	0	0	0	0	0	3.614
	0.25	0.0024	4.34	4.00	0.050	0.564	0.049	0.555	3.614
	0.50	0.0048	8.67	5.97	0.075	0.841	0.076	0.858	3.614
	1.00	0.0096	17.35	6.90	0.087	0.972	0.086	0.969	3.614
	1.50	0.0144	26.02	7.10	0.089	1.000	0.087	0.981	3.614
B	2.00	0.0192	34.71	7.15	0.090	1.008	0.088	0.985	3.614
	3.00	0.0288	52.05	7.05	0.088	0.993	0.088	0.988	3.614
	4.00	0.0384	69.39	6.85	0.086	0.965	0.088	0.989	3.614
	5.00	0.0480	86.74	6.62	0.083	0.933	0.088	0.990	3.614
	6.00	0.0576	104.10	6.45	0.081	0.909	0.088	0.990	3.614
	7.00	0.0672	121.44	6.25	0.078	0.881	0.088	0.990	3.614
	0	0	0	0	0	0	0	0	13.012
	1.00	0.0096	17.35	5.75	0.072	0.810	0.070	0.783	13.012
	2.00	0.0192	34.71	6.75	0.085	0.951	0.082	0.926	13.012
	3.00	0.0288	52.05	6.78	0.085	0.955	0.086	0.961	13.012
	4.00	0.0384	69.39	6.73	0.084	0.948	0.087	0.973	13.012
C	5.00	0.0480	86.74	6.47	0.081	0.912	0.087	0.979	13.012
	6.00	0.0576	104.10	6.35	0.080	0.895	0.087	0.983	13.012
	7.00	0.0672	121.44	6.15	0.077	0.867	0.088	0.985	13.012
	8.00	0.0767	138.78	6.00	0.075	0.845	0.088	0.986	13.012
	9.00	0.0863	156.13	5.82	0.073	0.820	0.088	0.987	13.012
	12.00	0.1151	208.16	5.35	0.067	0.754	0.088	0.989	13.012
	0	0	0	0	0	0	0	0	35.904
	1.00	0.0096	17.35	2.85	0.036	0.402	0.038	0.427	35.904
	2.00	0.0192	34.71	4.45	0.056	0.627	0.061	0.686	35.904
	3.00	0.0288	52.05	5.15	0.065	0.726	0.072	0.814	35.904
	4.00	0.0384	69.39	5.40	0.068	0.761	0.078	0.879	35.904
D	5.00	0.0480	86.74	5.45	0.068	0.768	0.081	0.915	35.904
	6.00	0.0576	104.10	5.42	0.068	0.764	0.083	0.936	35.904
	7.00	0.0672	121.44	5.35	0.067	0.754	0.085	0.950	35.904
	8.00	0.0767	138.78	5.25	0.066	0.740	0.085	0.959	35.904
	9.00	0.0863	156.13	5.13	0.064	0.723	0.086	0.965	35.904
	12.00	0.1151	208.16	4.90	0.061	0.690	0.087	0.976	35.904

APPENDIX VII-E

This appendix contains the traction coefficient and traction slope obtained under conditions of spin,side slip and longitudinal slip. All the data reported was obtained at a surface velocity of 20 m/sec and an inlet temperature of 70'C. Four different side slip values were imposed for each test and the exact value of side slip is indicated below each corresponding traction coefficient. The initial traction slope m that is indicated is for the zero spin ond zero side slip test. The spin values indicated are in degrees tilt of the toroidal axis with respect to the axis of the disc.

COMBINED LONGITUDINAL AND SIDE SLIP TEST RESULTS FOR SANTOTRAC-50 AT 20 M/SEC AND 70 'C. ALL RESULTS WERE OBTAINED ON THE LOW SPEED MACHINE.

TEST #	Po	k spin m	Traction Coefficient.
80081202	2.4	.5 0.0 36.1 side slip(%)	.118 .111 .107 .095 0.0 .142 .591 1.67
80081302	2.4	.5 6.0 --- side slip(%)	.101 .100 .098 .089 0.0 .163 .656 1.73
80081304	2.4	.5 0.0 41.3 side slip(%)	.100 .099 .095 .086 0.0 .177 .654 1.80
80081308	2.53	.5 0.0 37.4 side slip(%)	.142 .141 .131 .121 0.0 .285 .920 1.86
80081310	2.53	.5 6.0 --- side slip(%)	.119 .118 .109 .099 0.0 .241 .933 2.17
80062303	1.45	1 0.0 33.7 side slip(%)	.093 .092 .089 .085 0.0 .164 .820 1.69
80062305	1.45	1 6.0 --- side slip(%)	.097 .097 .092 .083 0.0 .153 .727 1.77
80062308	1.90	1 0.0 54.8 side slip(%)	.095 .095 .090 .083 0.0 .142 .668 1.75
80062310	1.90	1 6.0 --- side slip(%)	.096 .098 .092 .083 0.0 .095 .655 1.75
80062602	1.90	1 6.0 --- side slip(%)	.094 .094 .090 .080 0.0 .164 .641 1.94
80062609	1.00	2 6.0 --- side slip(%)	.088 .087 .083 .074 0.0 .164 .846 2.01
80062611	1.00	2 0.0 48.4 side slip(%)	.097 .097 .091 .080 0.0 .145 .754 2.06
80062614	1.45	2 6.0 --- side slip(%)	.095 .094 .088 .077 0.0 .224 .899 2.06
80062616	1.45	2 0.0 88.0 side slip(%)	.098 .096 .090 .078 0.0 .207 .827 1.94
80062618	1.00	5 0.0 66.8 side slip(%)	.090 .090 .084 .070 0.0 .150 .685 1.95
80062702	1.22	5 0.0 78.3 side slip(%)	.089 .089 .085 .073 0.0 .180 .741 1.89

80062804	1.22	5 6.0 ---	.091	.090	.086	.069
		side slip(%)	0.0	.192	.720	2.00
80062802	1.00	5 6.0 ---	.086	.085	.078	.060
		side slip(%)	0.0	.221	.964	2.16

C-3

COMBINED LONGITUDINAL AND SIDE SLIP TEST RESULTS FOR TDF-88 AT 20 M/SEC AND 70 'C. ALL RESULTS WERE OBTAINED ON THE LOW SPEED MACHINE.

TEST #	Po (GPa)	k spin m	Traction Coefficient			
80053103	2.1	.5 0.0 54.6	.093	.092	.087	.080
		side slip(%)	0.0	.228	.911	1.93
80053105	2.1	.5 6.0 ---	.095	.094	.088	.080
		side slip(%)	0.0	.131	.709	1.78
80060302	1.90	1 0.0 53.2	.095	.093	.087	.078
		side slip(%)	0.0	.144	.708	1.94
80060304	1.90	1 6.0 ---	.091	.090	.085	.078
		side slip(%)	0.0	.110	.591	1.52
80051407	1.45	1 0.0 31.6	.088	.088	.083	.076
		side slip(%)	0.0	.121	.663	1.61
80051411	1.90	1 6.0 ---	.093	.092	.086	.080
		side slip(%)	0.0	.155	.703	1.40
80051413	1.45	1 6.0 ---	.091	.090	.086	.080
		side slip(%)	0.0	.142	.639	1.46
80052603	1.00	2 0.0 16.4	.084	.080	.074	.058
		side slip(%)	0.0	.264	1.16	2.59
80052605	1.00	2 6.0 ---	.084	.082	.076	.064
		side slip(%)	0.0	.364	1.13	2.28
80052608	1.45	2 0.0 87.8	.090	.089	.082	.070
		side slip(%)	0.0	.226	.964	2.13
80052610	1.45	2 6.0 ---	.092	.090	.083	.067
		side slip(%)	0.0	.287	1.09	2.45
80052902	1.00	5 0.0 35.8	.077	.077	.072	.058
		side slip(%)	0.0	.078	.599	2.01
80052904	1.22	5 0.0 83.7	.082	.079	.076	.064
		side slip(%)	0.0	.130	.755	2.01
80052906	1.00	5 6.0 ---	.080	.078	.072	.058
		side slip(%)	0.0	.208	1.02	2.19
80052908	1.22	5 6.0 ---	.087	.086	.079	.062
		side slip(%)	0.0	.268	1.17	2.55